Linear optimization models for the simultaneous design of mass and heat networks of an eco-industrial park

Sami Ghazouani

THÈSE DE DOCTORAT

de l'Université de recherche Paris Sciences et Lettres
PSL Research University

Préparée à MINES ParisTech

Modèles linéaires d'optimisation pour la conception simultanée de réseaux de matière et de chaleur d'un écoparc industriel
Linear optimization models for the simultaneous design of mass and heat networks of an eco-industrial park

École doctorale n°432

SCIENCES ET MÉTIERS DE L'INGÉNIEUR

Spécialité ÉNERGÉTIQUE ET PROCÉDÉS

COMPOSITION DU JURY :

M Jean-Michel RENEAUME
Professeur
Université de Pau, Président

M Mahmoud EL HALWAGI
Professeur
Texas A&M, Rapporteur

M Ludovic MONTASTRUC
Maître de conférence
ENSIACET, Rapporteur

Mme Solène LE BOURDIEC
Ingénieure de recherche
EDF, Examinatrice

M Didier MAYER
Professeur
Mines ParisTech, Examinateur

M Assaad ZOUGHAIB
Maître-Assistant HDR
Mines ParisTech, Examinateur

Soutenue par **Sami GHAZOUANI**
le 05 Décembre 2016

Dirigée par **Assaad Zoughaib**

MINES ParisTech | PSL RESEARCH UNIVERSITY PARIS

Remerciements

Tout d'abord, j'aimerais remercier chaleureusement mon directeur de thèse Pr. Assaad Zoughaib pour ses longues discussions qui ont façonné le contenu de cette thèse et qui m'ont énormément apporté en tant que jeune chercheur. Grâce à sa convivialité (et ses très bonnes blagues), ce travail s'est déroulé dans la bonne humeur. Grâce à son ambition pour ce travail et son écoute attentive, il m'a véritablement poussé à toujours aller plus loin. Je n'aurais pas pu souhaiter de meilleur mentor.

Ensuite je voudrais remercier sincèrement Dr. Solène Le Bourdiec pour son aide, ses conseils et sa disponibilité tout au long de ses trois années de thèse. Par sa pertinence et sa motivation, Solène m'a permis de valoriser grandement ces travaux dans la communauté scientifique et au sein de l'entreprise EDF. J'ai vraiment hâte que l'on continue de travailler ensemble dans les années qui viennent.

Je remercie Pr. Mahmoud El Halwagi et Dr. Ludovic Montastruc pour m'avoir fait l'honneur d'accepter d'être les rapporteurs de ma thèse ainsi que pour l'attention qu'ils ont porté à mon travail et la qualité de leurs remarques. Je remercie tout particulièrement Pr. El Halwagi pour sa grande hospitalité lors de ma venue pendant mois dans son laboratoire à l'université Texas A&M aux Etats-Unis. Ce fut l'un des moments forts de ces trois années de travail et une expérience mémorable. Mes remerciements vont egalement à Pr. Jean-Michel Reneaume pour avoir accepter de faire partie et de présider mon jury de thèse. De même, je remercie Pr. Didier Mayer pour avoir pris le temps de participer à mon jury thèse.

Je tiens à exprimer ma grande reconnaissance à Mai Riche pour son appui dans la recherche ce sujet de thèse et pour m'avoir permis de travailler avec elle durant cette période d'incertitude. Je remercie aussi Bernard Maestrali pour sa confiance et son soutien avant, pendant et après ma thèse et pour m'avoir aidé à intégrer l'entreprise EDF. Je remercie Romain Farel et PS2E pour leur grande participation dans le démarrage de cette thèse. Je remercie les collègues de l'équipe E26 d'EDF pour leur coopération (surtout Sandrine et Thuy-An) et la bonne ambiance dans l'équipe. Enfin, je remercie vivement EDF pour m'avoir donner l'opportunité de faire cette thèse et de l'avoir financée.

Je remercie également les membres du CES de Mines ParisTech pour leur accueil chaleureux et leur assistance lors de ces trois années, en particulier Rocio, Joëlle et Stéphanie. Je souhaite remercier vivement les doctorants, post-docs, chercheurs et stagiaires du laboratoire pour les grandes discussions qui ont pu animer les repas du midi (en particulier Afif et Karim), la convivialité, les échanges et l'entre-aide qui ont rendu le travail quotidien de ces trois années de thèse plus agréable et enrichissant que je n'aurais pu l'imaginer. Je remercie tout particulièrement Alaa, Fabien, Sahar et Toan pour cela.

Je remercie aussi les étudiants et collaborateurs du Pr. El Halwagi (Debalina, Erfika, Marc, Kevin, Chi) pour leur accueil et pour les soirées texanes. Mes remerciements vont au Dr. Esmael Said pour sa contribution à la réalisation de l'étude sur la TMD présentée dans le chapitre IV lors de mon passage aux Etats-Unis.

Enfin, je voudrais remercier chaleureusement ma mère, ma sœur et ma famille portugaise pour m'avoir soutenu et motivé tout au long de ma vie. Je remercie la belle famille pour ses encouragements lors de cette dernière année assez compliquée que l'on a vécu et le très bon champagne de ma soutenance. Je tiens à remercier mes amis Noémie, Faustine, Félix et Arnaud d'être venus assister à ma soutenance. Et je remercie profondément ma compagne Laure pour son support quotidien depuis tant d'années sans lequel je n'aurais sûrement pas mené à bien tous ces accomplissements. Petite dédicace à notre petite famille féline.

Contents

List of Figures

List of Tables

Introduction

Sustainability is a notion that is taking a greater importance in industrial process engineering, as low-cost energy supplies and high quality natural resources, such as clean water, are getting scarcer and scarcer. Moreover, environmental and quality regulations are getting more restrictive, which implies substantial investments in waste treatment units. Industries are looking for innovative ways to maintain or gain a competitive edge while facing new economic and environmental challenges.

Process effluents recovery can be a tremendous source of revenue as well as a smart way to reduce their environmental footprint for industrial processes. Reusing effluents for heating purposes or reducing resource consumption can lead to substantial operating costs savings. Moreover, actual synergies between several companies sharing resources and wastes can be sources of new untapped potentials for reducing resources needs and environmental footprint while improving the economic competitiveness of several industrial partners on a larger scale. This type of cooperation between industrial companies is called an eco-industrial park (EIP).

Therefore, technical solutions to reach these objectives must be designed to be cost-effective and meet modern ecological standards. The method developed to find these solutions must be applicable at different scales: from the process to the territorial level.

The main motivation of this thesis is to help industrial actors (or groups of them resulting in an eco-industrial park) to reduce their consumption of resources and energy, and limit their environmental footprint, without modifying the design of unitary operations within the process. The objective is to find the best economical solution to recycle waste effluents generated by industrial processes and use them as resources to supply heat and matter to the process simultaneously. Thus, limiting the amount of wastes to be treated and discarded back to the environment as well as reducing its dependency to energy suppliers and the swift price variations.

Mass and heat integration must be considered at once because every operation within the process requires matter and energy to accomplish its defined tasks. Matter may be used to transport energy. Energy may be transformed to produce matter. Finding ways to use waste effluents as mass and energy resources can lead to substantial operating costs savings and complying more easily with strict environmental regulations.

Few works have tried to consider these two aspects in a single model, especially when the unitary operations of a given process are modeled as sinks (entry of the unit) and sources (exit of the unit) with available or required fixed flow rates, respectively. Moreover, the research on eco-industrial parks structures is quite recent and has really taken off in the last decade. Solving this kind of optimization problem is quite complex because it involves different companies, with different objectives and mutually shared structures (such as pipelines, treatment units, utilities,...). Mathematical optimization techniques are the most appropriate to address this type of problem. Among them, linear formulation seems more relevant than non-linear because, even though non-linear approaches are the most studied optimization techniques due to their easy set up, they require an initial guess and can be stuck in a local optimum, if they converge at all. Linear formulation can be demanding in computational power and time, but their resolution is more steady and reliable. Therefore, using a linear formulation of the problem, while avoiding losing accuracy, is a challenging task with an interesting advantage when it comes to solving the problem.

The main contributions produced in the presented work are summarized as follows:

- **Three systematic and systemic linear models** have been developed to optimize the mass and heat requirements of an heat integrated mass allocation network within any industrial process. Mass streams are characterized by their composition and properties. Several external sources of fresh matter or heating utilities contribution can be considered and optimized in a single problem. The opportunity of non-isothermal mixing is readily available in the model linear formulation to further reduce energy needs.

- The last presented model allow minimizing the operating and capital costs of the optimal mass allocation and heat exchanger networks (MAHEN) **simultaneously**.

- A generic and simple formulation representing **regeneration units** can be used in order to integrate them in the design of mass allocation and heat exchanger network.

- The three developed models can be applied at **various scales** designing local and global heat and mass networks. A few additional notions (sites, clusters, intermediate heat and mass networks) are added to represent the possibilities of sharing resources between companies when addressing an EIP design problem. But, the same models are used to address the problem at each scale.

- A spatial representation of industrial sites are taken into account in an EIP design problem. The distance and the position of each site are considered in the cost of the intermediate networks connecting sites together to transport heat and matter.

The models developed as well as the methodology to use them are presented in the following chapters:

- The first chapter of this manuscript describes the societal, environmental and industrial issues that motivate this work. A literature review of the various approaches regarding process integration is presented. It helps explaining the scientific objectives defined for this work. Finally, the solving methodology is presented.

- The second chapter introduces the general features of the heat and mass integration problem. A first linear model (M1) allows solving solely the mass allocation network constraints to find the minimum fresh resource consumption. Then a second linear model (M2) presents a new superstructure that allows considering the mass and heat aspects of the problem simultaneously. This model aims at targeting the minimum operating cost considering mass and energy related costs. The models are tested on two literature case studies to show the advantage of simultaneous optimization of both heat and mass requirements over a sequential approach. Several sensitivity analyses on different parameters are carried out to evaluate their influence on the optimal solution.

- The third chapter presents the third linear model (M3) which allows designing the optimal mass allocation and heat exchanger networks simultaneously. The objective function of this problem is the total annualized cost considering operating and capital costs. The model introduces new objects (mixer and splitter units) to further reduce the number of heat exchangers in the HEN and consequently its cost. The two previous case studies are used to illustrate the performances of the proposed model compared to literature results and show the capacity of the mixer and splitter units to improve the solution.

- The fourth chapter adds to the three previous models the possibility to use objects named regeneration units that allows modifying properties of mass streams in order to further improve the recycling of waste effluents. A study of the integration of two different technologies (a thermal membrane distillation unit to produce fresh water from salted water and available excess heat, and a liquid-liquid extraction unit to comply with environmental regulations) in on the two previous case studies (the phenol production case) is presented illustrating the possibilities offered by this regeneration unit model and evaluating the influence on the MAHEN design.

- The fifth chapter presents a new linear model (M4) expanding the applicability of the three previous models to larger scales by introducing new concepts (sites, clusters, and indirect heat and mass networks between entities) which allow finding the optimal design an eco-industrial park. A case study is developed to illustrate how is applied the extended model as well as different optimization strategies that can be applied to such problem.
- The last chapter presents the conclusions and proposes perspectives of necessary future developments after this work.

Chapter 1

Context and Challenges

In this chapter, contextual elements are presented to show the link between world systemic constraints (demographic and economic growths), resources consumption (focusing mainly on energy and water) and environmental issues (climate change and upcoming resources scarcity) related to the current production and consumption patterns.

The concepts of circular economy and industrial ecology are introduced as they represent new potential practices that can help current societies making the shift towards true sustainability. They argue that wastes produced by human activities, particularly in the industry, can be considered as readily available and economical resources.

One industrial application of these concepts is the eco-industrial park (EIP) in which various industrial partners share resources and wastes to improve their economic and environmental performances. Two illustrative examples are provided to demonstrate the potential of EIP and the motivations of the thesis are presented.

A state of the art review of the theoretical notions of heat and mass integration as well as coupled mass/heat integration is realized to understand the basic notions that will be use as a framework for the presented work.

Finally, the scientific challenges this work is trying to meet regarding the simultaneous design of mass and heat recovery networks as well as the synthesis of EIP are presented. The developed models and methodology to tackle these challenges are described.

1.1 General overview

1.1.1 Systemic constraints

Since the industrial revolution, the world population has grown exponentially from 1 billion around 1850 to 7.4 billion today (Fig.1.1). It increases at a staggering rate of 80 millions people per year. This expansion can be easily associated with technological innovations; in particular, with the rise and mastering of energy provided by fossil fuels.

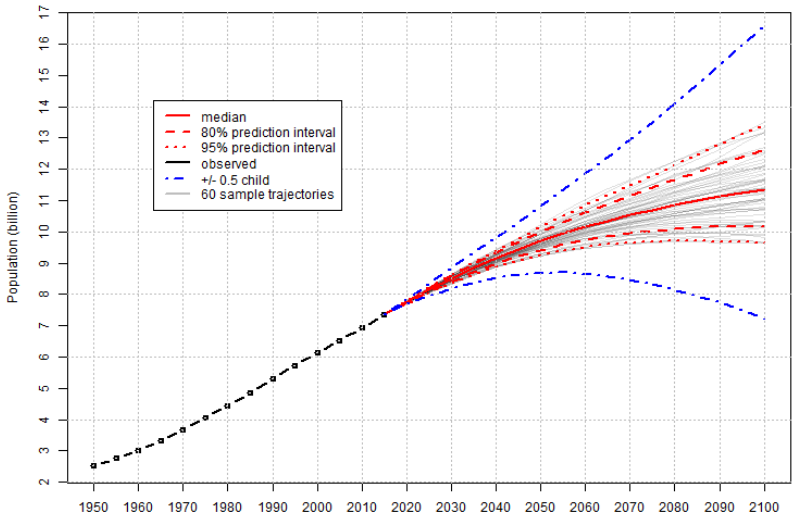

Figure 1.1: World population since the Industrial Revolution and its possible variations [113]

It has resulted in a tremendous period of prosperity for human civilization unprecedented in History (Fig.1.2). The exponential growth of the world's gross domestic product (GDP) from the 1850s is evidence of it.

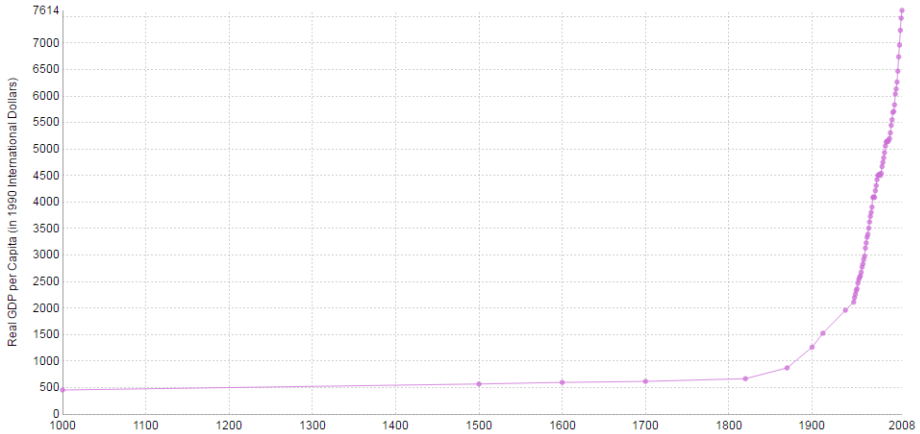

Figure 1.2: World GDP over the last thousand years[1]

However, this population and economic growth put a great and steady pressure on the environment since more and more natural resources are consumed as well as wastes and pollutions are generated. Indeed, in the prevailing linear economic model, resources are extracted and transformed to produce goods and services which are then consumed producing wastes that are more or less discarded as they are to environment.

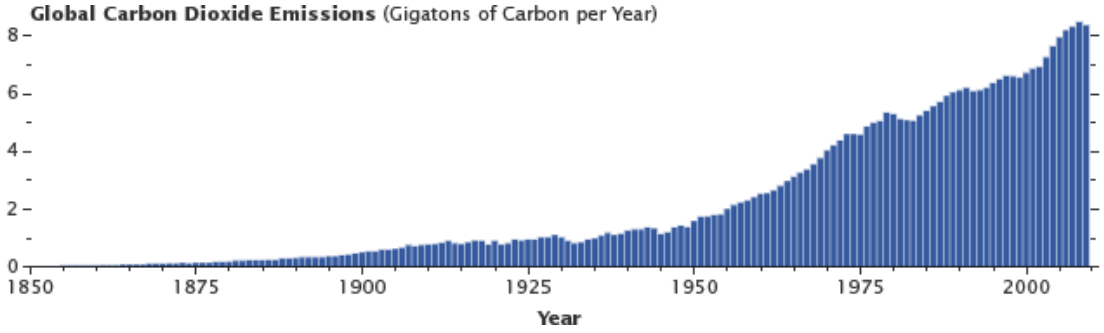

Figure 1.3: CO_2 emissions since the Industrial revolution[2]

Unfortunately, the human activities has been profoundly linked to an increase in greenhouse gases emissions and pollutions around the world (Fig.1.3). It results in dramatic changes in the climate and environment with significant consequences on human lives (natural disasters, health issues, political conflicts) which may worsen if the current conditions remain identical. Knowing that in order to limit global warming to $2°C$, a maximum CO_2 emissions of approximately 3 000 gigatons (Gt), of which two thirds have already been emitted [38] should not be exceeded. This suggests that the current economic model is not sustainable for the planet as well as for its inhabitants.

A steadily increasing proportion of the population in developing countries (basically countries which are not OECD[3] members), particularly in China and India where one third of the world's population lives, are demanding higher living and working standards; driven by the globalization of markets, information and culture. Therefore, building infrastructures is necessary to provide a more reliable access to food, water and energy as well as all goods and services that the modern economy of developed countries offers to its inhabitants. For that purpose, their industrial sector will consume more and more natural resources and energy (in particular fossil fuels as shown in Fig.1.4) to meet the growing demands.

The world population is expected to reach 9 billion people around 2050 (Fig.1.1). More and more people will live in cities (by 2050, nearly 70% of the world population will live in urban areas [87]) and will have access to all goods that the economy can offer (cars, computers, Internet, smart phones,...).

[1]https://ourworldindata.org/gdp-growth-over-the-last-centuries/
[2]Graph by Robert Simmon, using data from the *Carbon Dioxide Information Analysis Center*
[3]Organization for Economic Co-operation and Development

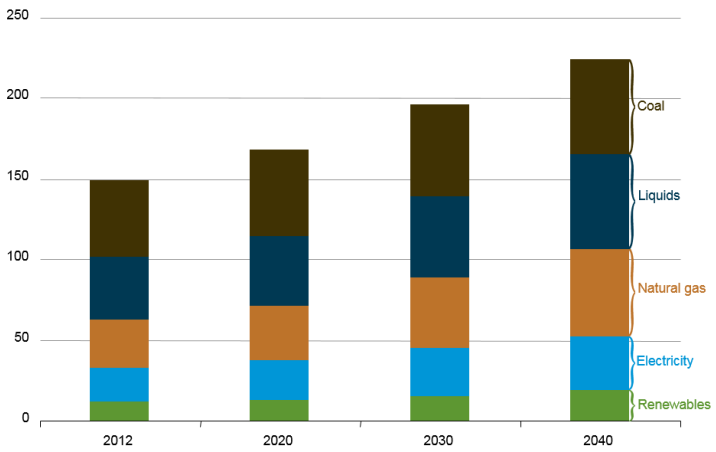

Figure 1.4: Non OECD industrial sector energy consumption forecasts ($\times 10^{15}$ Btu) [30]

This will create a strong competition for land (between agriculture, industry and housing) and resources (especially in water stress regions between drinking water for people and water necessary for manufacturing goods). Therefore, new ways of producing and consuming must be found to sustain the rising population and its needs while avoiding environmental damages and resources scarcity.

1.1.2 Energy consumption and production

Currently, the world consumes on average 150 000 TWh of primary energy per year. It more than doubled over the last 40 years (Fig.1.5). Fossil fuels (coal, oil, gas) represent the main energy source with 78% of the world primary energy consumption. They are also the main source of greenhouse gases (GHG) emissions.

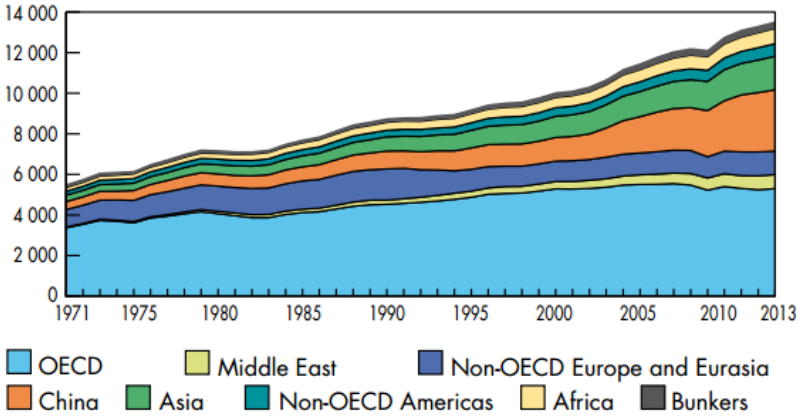

Figure 1.5: World total primary energy consumption from 1971 to 2013 by fuel (Mtoe) [35]

The world final energy consumption is roughly divided between residential (20%), transport (25%) and industry (55%) mainly provided by fossil fuels [35]. As shown in Fig.1.6, industrial activities account for more than 50% of world GHG emissions (32 Gt in 2014) and its share has been growing rapidly in non-OECD countries (mostly China and India) related to their economic growth. In OECD countries, relocation of industrial activities as well as measures to improve the energy efficiency helped controlling the level of emissions in the last 25 years. However, the global GHG emissions have increased by around 50%.

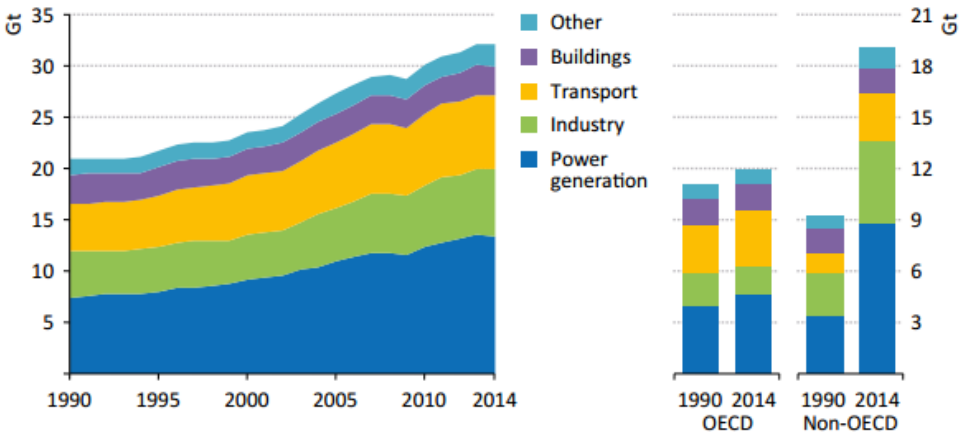

Figure 1.6: CO_2 emissions between 1990 and 2014 [38]

By 2050, the world economy is expected to be four times larger than it is currently [87]. The energy needs will be 80% higher than today if no changes are implemented by then, whether on technical, cultural, political, economic or social levels. Even though the part of renewable energies in the world energy mix is likely to grow faster than any other types of energy source, fossil fuels will remain the most important one (Fig.1.7).

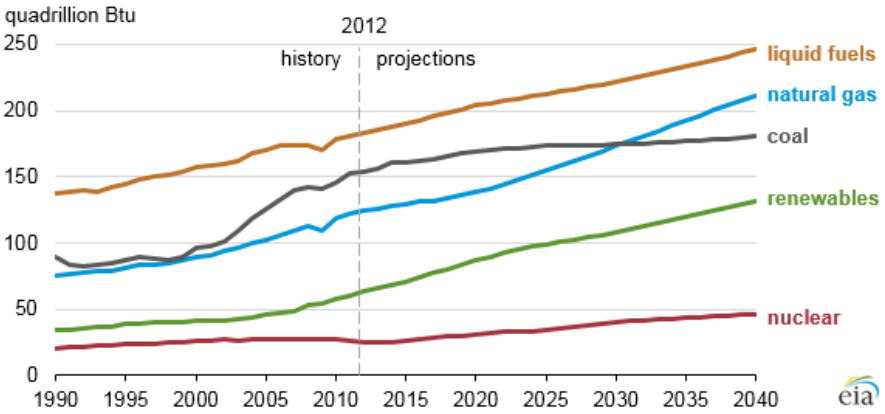

Figure 1.7: Projection of world's final energy consumption by fuel by 2040 ($\times 10^{15}$ Btu) [30]

Even though their integration and management on the electrical grid remain a complex problem to be solved due to their intermittent nature, renewable energies are the future of world energy supply. One complementary solution that can help answering current environmental and economic issues would be reducing energy needs by improving radically the efficiency of existing urban and industrial processes. Indeed, energy efficiency aims at reducing energy requirements to produce the same output. In Fig.1.8, it represents around 40% of the total potential for GHG emissions reduction. In particular, it accounts for more than two thirds of the industry potential.

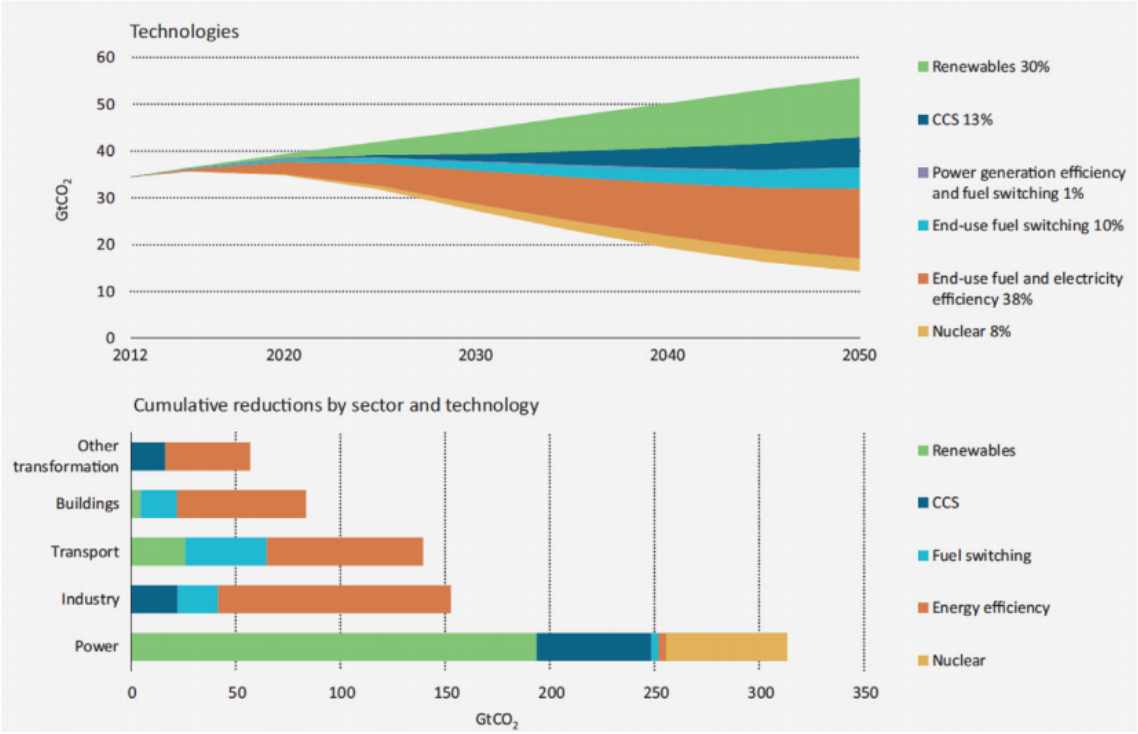

Figure 1.8: Technical solutions to limit CO_2 emissions and their potential [37]

Energy efficiency has various economical advantages at different scales. For a company, it can increase a product profitability and reduce the dependency towards energy suppliers. For a country, it helps avoiding energy importations, controlling its trade balance and it will have deep political implications for its geopolitical strategies and budget allocations (see Fig.1.9).

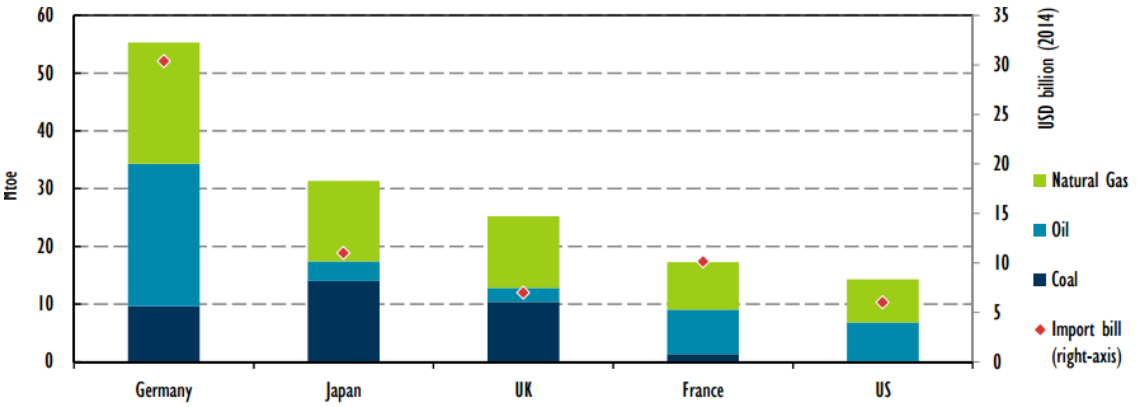

Figure 1.9: Avoided volume and value of energy imports from efficiency investments in IEA (2014) [36]

As shown previously, fossil fuels are likely to remain the main energy source for this century and since the beginning of it, oil and gas markets have experienced significant price volatility (Fig.1.10).

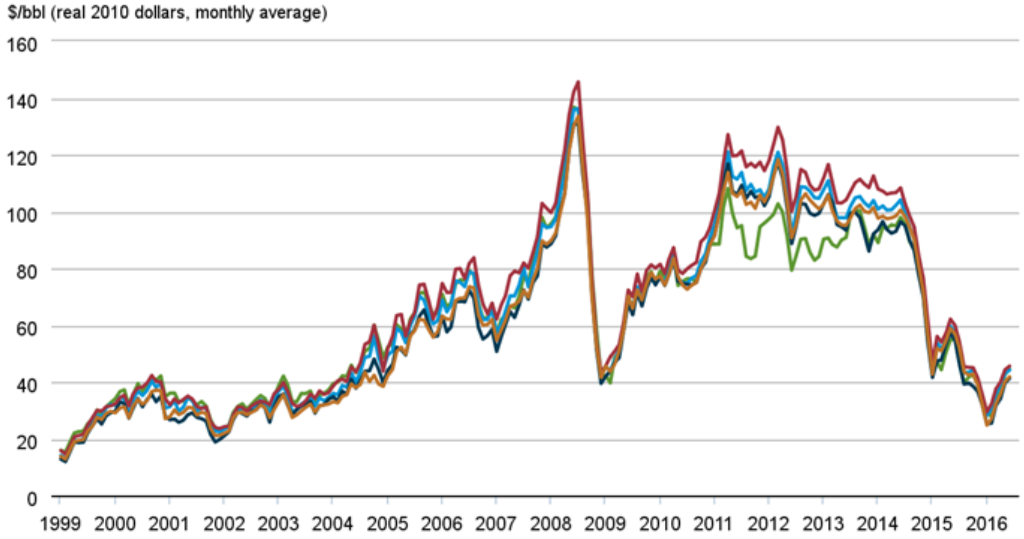

Figure 1.10: Crude oil prices variations since the beginning of the century[4]

The causes of these variations are often rooted in political turmoil (wars in Iraq, Syria and Libya), world economic crisis (sub-primes crisis in 2008) or technical uncertainties (supposed oil peak occurrence, US shale gas potential). These variations influence greatly social and environmental policies as well as profitability of investments. Therefore, reducing energy needs can and will limit the economic impact of swift variations in fuel prices that are likely to occur in the decades ahead.

[4]Bloomberg, Thomas Reuters. Published by U.S. Energy Information Administration

1.1.3 Water consumption

Over the last few decades, the soaring demand for freshwater, combined with substantial decline in available resources have led to water-supply issues around the world. In addition to water demand for drinking, urban, and agricultural purposes, water is an essential commodity in many industries. The world consumes approximately 4000 km^3 each year [112]. Its consumption increases by 1.6% each year. However, there are important disparities in resources and consumption: a small number of countries share more than half of all fresh water resources while few countries consume a consequent part of these resources (mostly USA, China, India) [87]. This situation can exacerbate tensions in water stress areas (for instance, conflict between Israel and Palestine over Jordan River). Moreover, environmental disasters may worsen (for instance, droughts in Africa or China, wildfires in USA) due to the combination of human activities development, poor water management and climate change. This reinforces the idea that natural resources such as water must be managed more efficiently.

Currently, water consumption is divided mainly into three sectors: domestic (10%), industrial (20%) and agricultural (70%) uses. However, these proportions change substantially between countries as shown in Fig.1.11. Depending on how their economy is structured, the water use (apart from domestic use) will be directed towards the agriculture or the industry. If developing countries are using most of their water for agricultural purposes, one can argue that as they shift towards the structure of rich-income countries, industrial water use will grow quite strongly in the next decades, quite similarly as the energy demand.

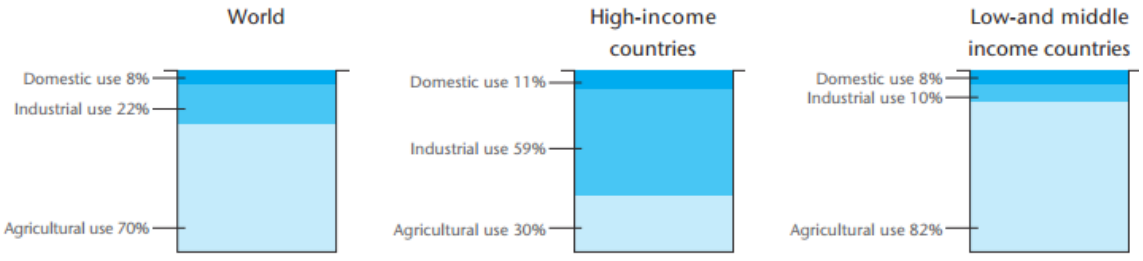

Figure 1.11: Water consumption by sector [111]

Sustainable industrial development must involve cost-effective strategies for managing water consumption and treatments to conserve water resources and reduce the negative environmental impact associated with discharging wastewater into the environment. Water is used in various ways: washing operations, transport, solvent, raw material and steam utility network. Even if its overall consumption is relatively small, the industry has a significant environmental footprint because wastewater effluents can contain various toxic pollutants and lack of regulations or controls may lead to environmental pollution.

Therefore, designing cost-efficient and performing water networks is a major challenge in the industry. European regulations [5] aim at driving industrial actors towards zero liquid waste, ideally around 2020. Reusing and recycling as well as developing efficient production or treatment technologies are becoming essential. These operations and processes often require huge amount of energy. As well as energy production or transportation require substantial amount of water. Therefore, finding ways to take advantage of the link between energy and water use (and more generally natural resources) can help tackle the various problems exposed previously.

1.1.4 Current and future regulations - Constraints on industrial actors

Political actions have been taken at different scales (international, regional or national) to improve resources use efficiency and limit environmental footprint of human activities.

In the early 90s, the Kyoto protocol set targets to signing partners to reduce their CO_2 emissions levels by 2010. In march 2007, the European Union adopted new environmental targets even more ambitious than that of the Kyoto Protocol for 2020[6]: 20% in renewable energies in its energy mix, 20% of energy consumption saved by increasing energy efficiency, 20% reduction of GHG emissions based on 1990 levels. Recently, countries met at COP 21 conference and agreed on new objectives for the next 30 years.

In order to reach the objectives in terms of energy efficiency, France decided to base its strategy on energy and fuel suppliers such as EDF, TOTAL or ENGIE [20]. These companies are expected to reduce their energy consumption or their clients' by a given amount set over a period of time. For instance, the objective was set at 345 TWh cumac (cumulated and actualized) over the period of 2011-2014. EDF was in charge of 40% of the total[7]. In case the target is not met, the companies would be compelled to pay fines. Therefore, companies like EDF are looking for new and innovative ways to improve the energy efficiency of their clients.

Regarding natural resources such as water, environmental standards concerning their use and their disposal once transformed vary a lot from one country to another. But more and more regulations are tightened around the world since sustainability and pollution protection and prevention have become predominant in political actions.

In France, several laws[8] and decrees[9] control the use of water on the national territory. In particular, they impose temperature, concentrations and physical and chemical limitations to wastewater effluents as well as specific locations for their restitution to the environment.

[5] 2455/2001/CE, 2000/60/CE

[6] ec.europa.eu/clima/policies/strategies/2020/

[7] travaux.edf.fr/construction-et-renovation/demarches-on-vous-guide/les-certificats-d-economies-d-energie

[8] Loi n°64-1245, Loi n°92-3, Loi n°2006-1772

[9] Arrêté du 02 février 1998, Arrêté du 5 juillet 2014

These regulations push industrial actors innovating to keep up with them and to keep their edge with respect to their competitors. One of the most promising solutions is to improve the efficiency of existing processes. One way to do so is to consider wastes no longer as liabilities but as resources with great potential.

In summary, the abundant and easy access to energy sources thanks to fossil fuels started an era in human history that led through unprecedented economic and demographic growth. Unfortunately, the massive consumption of fossil fuels, as well as natural resources, has had major consequences on the environment. Now, since the economic and demographic trends are more than likely to keep moving in the same direction and an important part of the world's population will need and want easy access to utilities and commodities, there is a critical need to shift our production and consumption habits. Moreover, focusing on the industry, companies must face new and necessary environmental regulations acting on their economic performances. Therefore, technical solutions must be designed to be cost-effective and meet modern ecological standards. One interesting solution is improving resources use efficiency of industrial processes. In order to achieve this objective, reusing and recycling waste effluents (heat or mass) allow creating new internal resources and reducing needs for external supplies. This idea is developed in the concepts of circular economy as well as industrial ecology which are the premises of the work presented in this thesis.

1.2 Circular Economy and Industrial Ecology

"A circular economy is restorative and regenerative by design and aims to keep products, components, and materials at their highest utility and value at all times. The concept distinguishes between technical and biological cycles. It is a continuous positive development cycle that preserves and enhances natural capital, optimizes resource yields, and minimizes system risks by managing finite stocks and renewable flows. It works effectively at every scale".[10]

Circular economy is a concept that seeks to design every human activity as part of closed-looped processes rather than linear open lines. Instead of exploiting resources and discarding them once transformed, consumed and treated, by-product and wastes can undergo transformations and re-enter the processes to avoid the consumption of new resources and limit the impact on its environment. The European Commission adopted the *Circular Economy Package*[11] in December 2015 to help its members make the transition towards this type of economy by setting targets for reduction of waste and establish an ambitious and credible long-term plan for waste management and recycling.

[10] www.ellenmacarthurfoundation.org
[11] Directive 94/62/EC, Directive 2008/98/EC

In the same philosophy, the concept of industrial ecology can be seen as a particular application of the circular economy concepts. On a given area, industrial partners look for synergies between their processes in order to share resources and wastes that can help all actors to reduce globally their environmental footprint and improve their economic performances. One of the most promising applications of this concept is the development of eco-industrial parks. However, early partial applications appeared with the effort to recycle wastes.

1.2.1 Wastes to Resources

The development of bio-fuels is a good illustration of the interest of giving wastes a new purpose. At first, bio-fuels were and still are produced using agricultural products such as beet-roots or sugar cans for ethanol, or soya, colza or wheat for bio-diesel. However, these crops create a competition with the ones used for feeding people, require new lands, water, energy and chemicals to be produced. These drawbacks limit the interest for these new fuels as they defeat their purposes of being more environmental friendly than fossil fuels. However, the second generation of bio-fuels are based on using agricultural wastes [18]. These new resources do not require any extra use of energy, water or chemicals. They can provide additional revenues for farmers and they are economical for fuel producer. Actually, there are more and more processes developed to transform biomass wastes into fuels and bio-gas such as waste wood [84], wastewater [48] and several other industrial or agricultural wastes [11, 85].

These examples are simple illustrations of the circular economy and industrial ecology concepts as wastes from one industry can become a resource for another one; reducing the environmental footprint and improving the profitability of both processes. However, these opportunistic exchanges can be expanded and organized on a larger scale to increase the synergies and reach even greater environmental and economic performances. This organization between several industrial sites is called an eco-industrial park.

1.2.2 Eco-Industrial Park

Chertow [21] defines Industrial Symbiosis as *"engaging traditionally separate entities in a collective approach to competitive advantage involving physical exchange of materials, energy, water, and by-products"*. An Eco-Industrial Park (EIP) is *"a community of manufacturing and service businesses located together on a common property. Members seek enhanced environmental, economic, and social performance through collaboration in managing environmental and resource issues"* [79]. Many projects have emerged in last 40 years around this concept and it gains more and more attention recently since it brings an appealing solution to the many economic, social and environmental issues that have been mentioned previously.

Kalundborg (Denmark) is one of the first successful examples of eco-industrial park. It includes nine public and private companies including a power station (Asnaes), oil refinery (Statoil) and the municipality (Fig.1.12).

It started in 1972 when the oil refinery accepted to provide excess gas to a gypsum board producer (Gyproc). The integration between companies gradually evolved over times as they negotiated (without any state intervention) to share water supply, waste heat and other materials over the last 40 years.

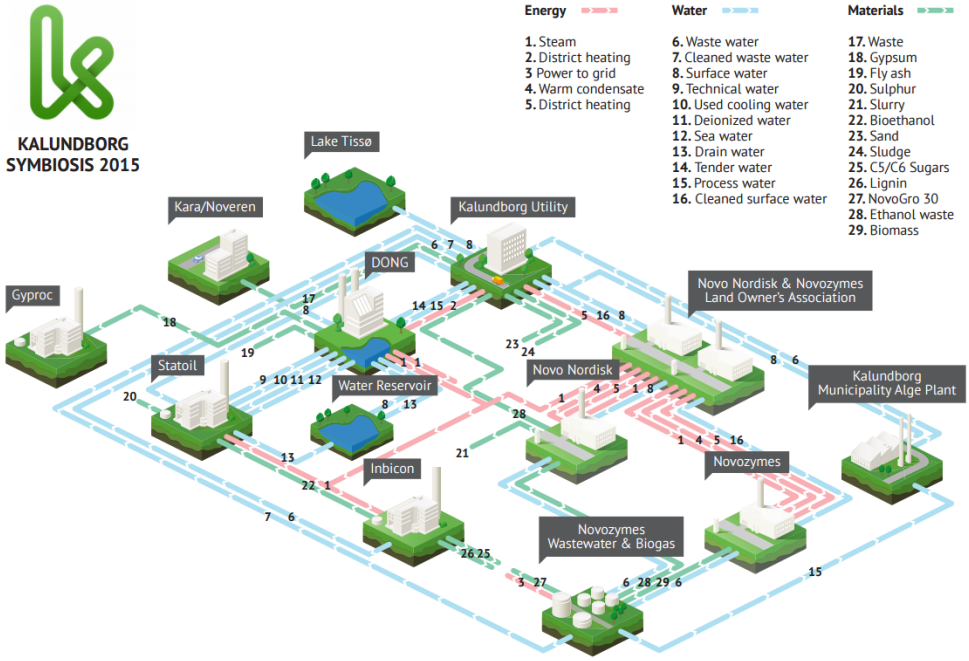

Figure 1.12: Eco-Industrial park of Kalundborg, Denmark[12]

Substantial savings are realized for the different partners: 1.2 million cubic meters of freshwater for Statoil, 30 000 tons of coal for Asnaes, the urban heating network is completely supplied by the power station waste heat, and much more other kind of savings. Overall, the industrial symbiosis avoid 275 000 tons of CO_2 emissions per year [95].

Countries around the world are trying to set a legal framework and financial aids to boost the creation of such structures, in particular in China, Japan, the Netherlands and South Korea. The Ulsan eco-industrial park started in much the same way than Kalundborg, around 1985 when regulations were getting tighter in South Korea because severe episodes of environmental pollution. In 2005, it was selected to be part of the governmental program called *"Korean EIP Master Plan"* launched to develop 8 national EIPs between 2005 and 2020.

[12]http://www.symbiosis.dk/en

It regroups various types of industries as shown in Fig.1.13. The presented structure realized 68.52 millions of dollars of profits in 2012 with a payback time estimated between few months to less than 4 years for the connections implemented. Every year, the EIP CO_2 emissions are reduced by 227 ktons [12] compared to the non integrated situation.

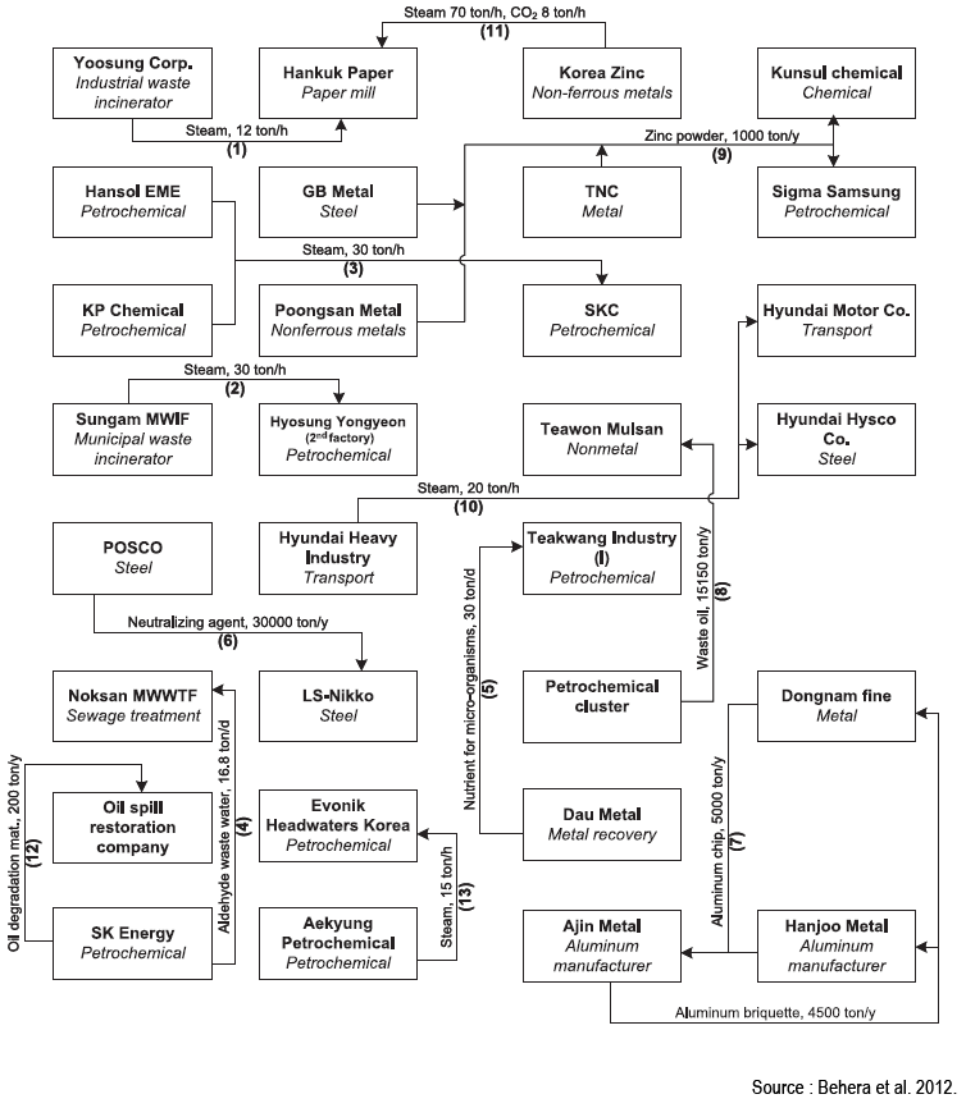

Figure 1.13: Eco-Industrial park of Ulsan, South Korea [12]

Obviously, EIP implementation is a complex matter since it may involve many industrial partners and the idea that each company could depend on others can really hinder its deployment or at least slow it down. However, the results of existing structures motivate the study and optimization of future industrial symbioses to reach even greater performances.

These two examples illustrate well the important gains that can result from industrial symbiosis regarding cost-effectiveness, CO_2 emissions reductions and overall resources use efficiency. The approaches took to build and set up eco-industrial parks are really specific to each case. No systemic and systematic methodology exists to search optimal synergies between industrial sites. The development of models and tools dedicated to EIP design would facilitate the dialog between potential industrial partners by testing various scenarios to find the most appropriate design and encourage strongly the implementation of such structures.

1.2.3 Motivations of the thesis

The main motivation of this thesis is to help industrial actors (or groups of them such as in an EIP) to reduce their consumption of resources and energy, and limit their environmental footprint. The objective is to recycle waste effluents generated by industrial processes and use them as resources to supply heat and matter to the process. Thus, limiting the amount of waste to be treated and discharged back to the environment as well as reducing the dependency of industrial companies to energy suppliers and to swift price variations.

The scientific objective of this work is to develop a methodology that helps designing optimal networks to reallocate, regenerate and treat waste effluents (mainly liquids) as well as heat exchange networks to recover and take advantage of their heat content. Much of the interest of this work focuses on improving existing processes design, not to transform them because most of the potentials can be found in existing structures and industrial companies are often reluctant to modify drastically their processes. The methodology must lead to economically interesting solutions since it is one of the main conditions for an industrial company to implement changes on its process to be more competitive.

The methodology must be based on a systemic approach as it should be able to look at the full resource efficiency potential of the studied system. The approach must be applicable at different scales (process, site, EIP). It should be able to look for further synergies and take into account characteristics constraints and opportunities at each scale. The methodology must also be systematic because it must adapt to any type of industrial processes (refinery, petrochemical, food, paper, metal, chemical industries,...) and be studied with the same approach to be able to compare results with one another. That is why the starting point of this work will relies on the state of the art review of **Process Integration** methodologies. This research area is looking for approaches to optimize resources consumption in industrial processes meeting all the criteria mentioned previously.

1.3 Process Integration

Process integration is a *"holistic approach to process design, retrofitting and operation that emphasizes the unity of the process"* [39]. It is a concept used for improving industrial process resources consumption. The methodology is based on a systemic and systematic approach. Every operation requires energy and matter as inputs and can produce them as outputs; therefore, looking globally at a process, synergies can be found internally in order to reduce the need for external resources. The main idea is to realize mass and energy balances considering all inlet and outlet streams at once; rather than focusing on each unit composing the process. A recent state of the art review has been realized by Klemes et al. [71].

The main objectives of process integration are:

- Evaluating minimal resources consumption (mass or heat) based on preliminary design of process units ahead of the complete and final process design. This is called *targeting*.
- Reducing resources consumption and waste generation (mass or heat) by recovering waste heat or matter looking for matches throughout the whole process.
- Lowering operating and capital costs (OPEX and CAPEX).

By adding constraints (for instance, forbidding heat exchange between two particular heat streams), modifying operating conditions or changing which streams are considered, different integration patterns can be generated. The strength of this methodology is to be able to look at various solutions (depending on costs/benefits analysis or operating constraints) without having to design precisely any elements in the process (such as heat exchangers, reactors, separators,...). Moreover, it allows its application to a variety of process: refinery [29, 108], chemistry [33, 66], paper [63], food [70].

Research on this topic started during the 70's with works on **heat integration**. Afterwards, during the late 80's, **mass integration** was introduced as an extension of the previous research on heat recovery. Finally, in the early 2000's, research began to focus on a coupled mass/heat problem.

1.3.1 Heat integration

During the oil crisis throughout the 70's, improving energy efficiency in the industry became a topic of interest. The fundamental idea is to seek out every internal need for heating and cooling, and try to match them as well as possible using heat exchangers. Heat loads that cannot be provided or extracted with internal streams are taken care of by external utilities. The evaluation of what could be the Minimum external Energy Requirements (MER), Linhoff et al. [76] introduced the concept of **Pinch Analysis**. Since

then, various approaches have been to tackle the optimization problems of energy requirements, heat exchanger network (HEN) design or utilities and thermodynamic conversion systems sizing (such as heat pumps or Rankine cycles).

Pinch Analysis is a graphical method that consists of evaluating the minimum external energy requirements for a given set of heat streams characterized by their heat loads and their inlet and outlet temperatures. Given a minimum temperature difference ΔT_{min}, which characterizes the balance between heat recovery efficiency and cost-effectiveness, composite curves can be built to show the MER of the design. The main information drawn from this curve is the pinch temperature and heating and cooling targets. The pinch temperature defines two independent problems: above the pinch, where there is a shortage of heat, and below the pinch, where there is an excess of heat.

Once targets have been evaluated, a more detailed study is led to synthesize a network of heat exchangers capable of reaching heating and cooling targets. Moreover, different objectives (utility cost, GHG emissions, number of heat exchangers or capital costs) may be targeted; therefore, moving away for minimum energy consumption. The results of such studies are to design cost-effective networks resulting in a decrease of energy consumption. Multiple strategies were developed from the pinch analysis [76, 77] towards mathematical optimization techniques [10, 92, 117] to reach a more optimal design [61, 94] as well as integrated more realistic constraints.

Regarding energy integration at territorial scale, it was initially developed under the name of '*"Total site analysis (TSA)"* by Dhole et al. [29] which was further explained by Klemeš et al. [69]. By then, the methodologies developed tried to extend the pinch analysis to multiple sites as well as including the design of energy conversion systems such as co-generation and heat pumps between several sites. Several recent works are still based on graphical approaches [65, 114].

Rodera et al. [97] developed an MILP model based on pinch analysis to distribute directly or indirectly available heat through several plants optimizing the heating and cooling requirements as well as the optimum location of the intermediate fluid circuits. Several works followed improving this initial one and keeping the same overall procedure [7, 8, 98].

Recently, Farhat et al. [45] proposed a methodology based on the exergy optimization for selecting network temperature and then optimizing in the operating and capital costs including the heat exchanger cost with heating network as well as the length, diameter and pressure losses within the pipes.

1.3.2 Mass Integration

Similarly to heat integration, the objectives of mass integration are to look for internal opportunities to avoid using external resources and reduce waste generation (sent to costly treatment units or the surroundings of the plant subjected to strict regulations). These objectives can be reached by allocating waste streams (sources) towards process units (sinks or demands) that may require specific amount of matter with particular features (i.e. composition or properties).

Indeed, for operating or safety reasons, limitations can be set at the inlet of every process unit. This will translate by defining allowable composition and property ranges. Therefore, the resulting composition and properties of the mixture entering a given process unit must be within the set boundaries. And as heat integration, mass integration first works were based on insights given by composite curves diagram as it is shown in following paragraphs.

Different types of mass integration problem exist depending on what transformations matter can undergo [41]:

- Direct Reuse: Waste streams are used as they are
- Recycle: Waste streams can be treated (with regeneration units) to be either recycled within the process or discharged to the environment
- Reactor network: Waste streams can be transformed and generate new streams with different contents

The work presented in this thesis will focus on the reuse and recycle of waste streams. The definition of the basic reuse/recycle problem can be of two types: **fixed pollutant load** or **fixed flow rate**.

1.3.2.1 Fixed pollutant load

Process units considered are the ones where a pollutant load is transferred to a solvent (mainly water). In this kind of process, only the composition is considered. Each process unit is characterized by a fixed pollutant load and limitations in terms of inlet and outlet maximum allowable composition. Inlet and outlet streams are related to each other. The problem is defined as mono-pollutant or multi-pollutant [116].
The objectives of this type of problem are:

- Determining the optimal flow rates to go through each process unit
- Finding the optimal inlet and outlet composition
- Establishing the amount of fresh resource required
- Designing the optimal network topology

Based on an analogy with heat integration composite curves, Wang et al. [116] built water pinch diagram which plots pollutant load versus maximum concentration (Fig.1.14). Similarly to classical composite curves, targets can be identified from this diagram concerning the minimum fresh water requirements as well as the minimum waste discharge. Note that this representation is mostly associated with water network design. Sev-

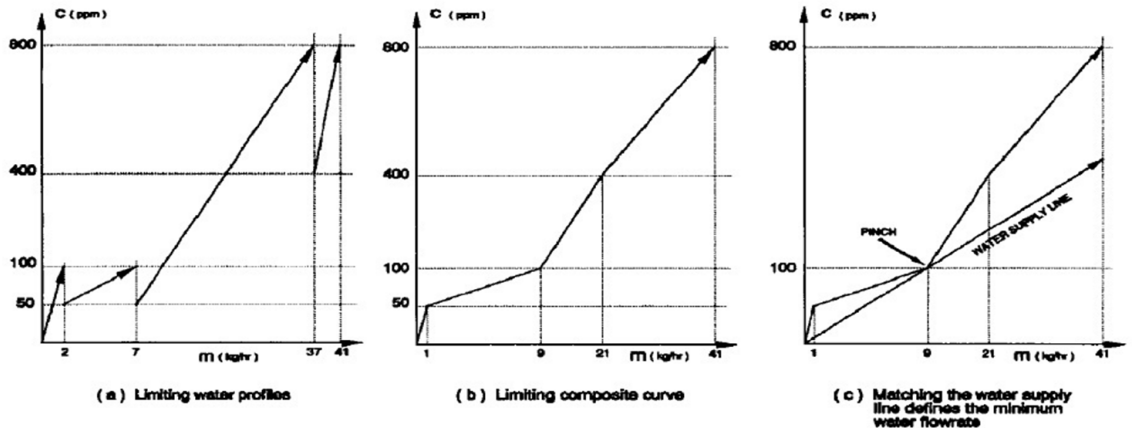

Figure 1.14: Water Pinch diagram [116]

eral conceptual [32, 55] and mathematical models [6, 101, 102, 108] have been developed in order to minimize water consumption in industrial processes for single or multi contaminant cases. Some of these works included treatment units to further reduce the water consumption [15, 46, 59, 66, 72].

The main drawback of this problem definition is that process units are defined by one or several mass loads to be removed; discarding several other types of units such as reactors that can generate or consume materials. Moreover, their characterization are limited to the stream composition (and no other physical or chemical properties such as pH or COD) and the design of each unit is variable. Therefore, for preexisting processes where unitary operations designs are fixed, it is interesting to consider *"fixed flow rate"* problem definition.

1.3.2.2 Fixed flow rate

In this approach, process units can be of any kind as long as they produce or consume a specific matter: mass exchanger, reactors, separators or coolers. They are designated as sources and sinks. The design of each process unit is not considered.

Sources are waste streams with a fixed flow rate and fixed composition and properties. **Sinks** are process units requiring a fixed amount of matter characterized by composition and properties that are included within acceptable range. Inlet and outlet streams are not bound, rather there may not be an inlet and an outlet streams to consider for each operation.

The objectives are:

- What amount of fresh resource is required?
- What is the topology of the network?

Similarly to the previous problem, graphical approaches based on the pinch analysis were developed to target minimum fresh resource consumption and waste generation by plotting sources and sinks composite curves on a cumulated mass load versus cumulated flow rate diagram (Fig.1.15).

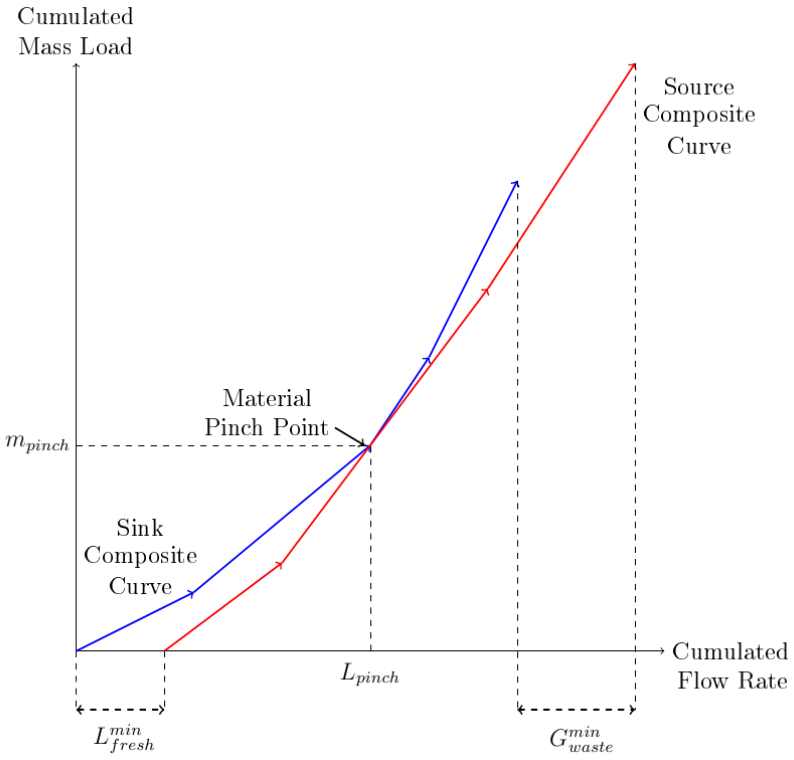

Figure 1.15: Mass composite curves

As the complexity of this problem grows, graphical methodologies can no longer be efficient because they cannot account for all the dimensions of the problem; therefore, mathematical approaches have been developed to address this problem more easily. The characteristic quality can refer to a single contaminant composition [42, 49], multiple contaminants composition [40] or properties [43, 67, 68, 86, 93].

This problem definition is more appropriate when trying to build an add-on recycling network rather than make the process fit such network. Moreover, it seems more likely that an eco-industrial park will be built from existing processes which can thus be decomposed into sources and sinks.

1.3.2.3 EIP mass integration

The research on Eco-Industrial Parks structures is quite recent and has really taken off in the last decade. Solving the problem of EIP optimization is complex because it involves different companies, with different objectives and mutually shared structures (such as pipelines, treatment units, utilities,...).

An extensive literature review was realized by Boix et al. [14] showed that among all the EIP optimization studies, most of them focused on optimizing the sharing of a particular resource. This resource is often water or energy. Fewer studies proposed approaches for other specific resources such as H_2 which are more case related [56, 75, 106].

EIP water networks were extensively studied using both kinds of mass integration problems (fixed flow rate and fixed pollution load). This problem is tackled by mathematical programming problems with mostly economic or environmental objective functions. The main differences lay in the problem definition and the modeling of the objectives. There are two types of definition that can be incorporated within the same problem: **direct inter-plant integration** where plants exchanges water stream directly between them and **indirect inter-plant network** where mass streams can go through regeneration units before being distributed [24].

Early studies based their methodologies on graphical approaches [47, 88, 89, 107] but their limitation to single contaminant problem and the need to get and optimize the EIP design had led towards mathematical optimization techniques. Intermediate procedure were developed such as the one proposed by Chew et al. [22] where they used a graphical approach coupled with mathematical programming. In this study, an automated produced allows targeting minimum fresh water flow rate, followed by a linear programming approach to design a detailed water network.

Chew et al. [24] introduced the concepts of direct versus indirect inter-plant water integration. The indirect integration allows the use of intermediate entities which were either a storage tank or a regeneration unit (or both). Depending on the selected strategy (direct or indirect integration), the formulation of the model was an MILP (direct integration) or an MINLP (indirect integration). The objective was to minimize the fresh water consumption. Lovelady et al. [78] proposed to add an intermediate layer where several interception units could be used to modify the composition of streams prior to being allocated to EIP sinks. The objective function was the total annualized cost which included the use of interception units. Based on a similar problem, Rubio-Castro et al. [99] developed an MINLP model that included the possibility of retrofitting existing inner and outer water networks from multiple plants and designing a shared water treatment plant.

Boix et al. [16] introduced a multi-objective model in which the fresh water, regenerated water flow rates and the number of connections are minimized reducing optimizing the operating costs related to water consumption and the complexity of the water network. Thus, resulting in a cost-efficient and likely-to-be-built structure for the EIP. The result

is a Pareto front in which a lot of optimal solutions are available from which depending on various and different criteria a solution can be selected. Alnouri et al. [5] proposed an optimization approach to design water networks within industrial cities testing centralized or decentralized strategies for the placement of water treatment interceptors. One of the interesting innovations of the developed MINLP model is that it took into account in its formulation the design of the piping across sites locations and the installation constraints based on the industrial city layout.

In the last decade, approaches based on game theory were developed to select an optimal solution for direct integration schemes [23]. Chew et al. [25] generated several network structures with pinch techniques which were then analyzed and selected using a game theory approach depending on the strategy (cooperative versus non-cooperative) on which the EIP was to be built. Ramos et al. [96] developed a very promising approach to synthesize a water nexus in an EIP solving a multi-leader-follower problem. Base on game theory, the model is formulated as a Nash game where an EIP authority is looking to minimizing the EIP freshwater consumption and each company participating in the EIP wants to minimize its total annualized cost. With this formulation, they were able to conclude that the solution found represents most of the times an equilibrium satisfying fairly all involved partners.

1.3.3 Coupled Heat/Mass Integration

Furthermore, in reality, mass and heat integration must be considered at once because every operation within the process requires matter and energy to accomplish the defined tasks. Matter is used to transport energy. Energy is used to transform and produce matter. Therefore, considering the energy aspect of waste streams reuse can improve substantially the relevance of it. The inlet and outlet of every process unit are characterized by a temperature. Therefore, mass streams connecting two units are considered either hot or cold. Reusing or recycling waste streams imply to choose which flow rate each mass stream will have; therefore, it also implies to define the heat load it will transport or will need. Thus, heat exchanges can occur between them in the same way described for a heat integration problem.

Efficient management of raw materials is essential to improve economic and environmental performances of industrial processes. Waste effluents can be considered as mass and energy resources; therefore, finding ways to reuse or recycle them may allow reducing operating costs and complying more easily with strict environmental regulations. However, those solutions may imply additional capital expenditures. Thus, an economic optimum must be found considering reducing energy and resources consumption, waste generation and extra capital costs related to mass and heat recovery. So, over the last decade, the focus has been primarily on creating methodologies to tackle the problem of **Mass Allocation Network (MAN) and Heat Exchangers Network (HEN)** designs. Several

methods and models can be found to tackle this coupled integration problem. They can be sorted into two main categories: **Graphical approaches and Mathematical programming models**.

1.3.3.1 Graphical approaches

From the fixed load problem definition, many works have looked to optimize both fresh water and the energy consumptions. Savulescu et al. [105] developed an approach to simplify the HEN design of already designed water networks using their ability to mix and split. Based on the analysis of the classical composite curves, a temperature versus flow rate diagram called *"source–demand energy composite curves"* is built. This diagram presents the surplus or deficit of each source with respect to the demands. Therefore, multiple mixing scenarios can be tested resulting in a new HEN design. Building upon this work, Savulescu et al. [103, 104] presented the *"two dimensional grid diagram"* allows to find a water network design that minimizes the use of water and energy before designing the HEN. In a similar approach, Martínez-Patiño et al. [81,82] introduced "temperature versus concentration diagram" and sequentially synthesizes water networks and direct and indirect heat exchange networks. Hou et al. [58] introduced Temperature and Concentration Order Composite Curves (TCOCC) which is employed to guide the design of appropriate water networks for heat recovery.

For the fixed flow rate problem, source-demand energy composite curves [80, 115] or Modified Problem Table Algorithm [9] have been introduced.

Graphical approaches are used to give useful insight on performances that can be expected of the process in the best case scenario. These techniques have the main advantage to give quick insights but they are limited to single contaminant and small sized problems. Moreover, the resulting design are not economically optimal. That is why mathematical optimization techniques have been developed to tackle such problems and obtain more relevant designs.

1.3.3.2 Mathematical approaches

Mathematical programming techniques are used to tackle more complex problems in a more systematic way. Any physical problem is decomposed into a set of equations that describes the constraints that characteristic variables of the studied system are subjected to. Interesting features of the system are selected and included in an objective function that is optimized. There are several mathematical techniques; but most of them can be classified along one defining feature: **Linear** or **Non-linear**.

Linear Programming (LP) model are described by a set of linear equations and a linear objective function. If some variables are integer the model is called Mixed Integer Linear Programming (MILP). Most of physical systems are described by non-linear equa-

tions. Therefore, the difficulty relies upon linearizing some equations, which can result in losing information while solving the problem, adding a significant number of variables and overall lengthening the computation time. However, its solving is mostly based on an algorithm called *simplex* that guarantees its convergence and the optimality of its solution.

Now, addressing the solving of problems described with non-linear equations can be realized with two main techniques: **Stochastic** or **Deterministic**.

Stochastic formulations implement a probabilistic algorithm to initialize several parameters and iteratively solve the problem, selecting interesting solutions along the way modifying the parameters values until it reaches the optimal criteria on the ultimate solution. The probabilistic layer is often based on a natural process such as neuronal networks, ant colony algorithm or particle swarm optimization. There are easy to implement but if the problem becomes too complex, iterations can take a long time to converge.

Deterministic formulations are classified depending on the use of integer variable the model: Non-Linear Programming (NLP) or Mixed Integer Non-Linear Programming (MINLP). There are the most studied optimization techniques because their set up is easy; however, most of them require an initial guess and can be stuck in a local optimum, if they converge at all.

Regarding the coupled heat/mass integration problem, the problem definition and the objective function selected can vary:

For fixed load problems, sequential solving strategies were implemented in order to keep each problem size relatively small to synthesize Water Allocation and Heat Exchange Networks (WAHEN). Basically, a first model is used to synthesize promising Water Allocation Networks (WAN) targeting minimum fresh and energy consumption [8], or promising heat exchange matches estimating HEN costs [74], or multi-objectives such as fresh water consumption, energy consumption, interconnection number and number of heat exchangers [17, 27]. Then, another model is used to design the HEN based on the WAN structure found during the previous step. This approach facilitates solving this problem and can be economically interesting as items related to operating costs are optimized. Therefore, solutions obtained are always valuable if you are looking at a long-term investment. However, it does not take into account possible rearrangement that can occur to balance operating and capital costs if you want to make your investment more profitable more rapidly. It can overlook economically interesting solutions.

Simultaneous approaches have been implemented to consider multiple objectives at once, even though they are more demanding in terms of computation time. They often first solve a simplified model to obtain good initial guesses, and then solve a more complex superstructure based model to determine the design of the WAHEN simultaneously. Over the last decade, this approach have been well studied and gain in complexity to include

more realistic features of the problem [3,13,73] and possibilities for heat exchanges [2,60] or regeneration units [4,31]. Most of the methodologies are non-linear models.

For fixed flow rate problems, fewer works were presented in the last five years. Sahu et al. [100] presented three LP models for targeting minimum fresh water and energy consumption, and synthesizing heat integrated resource allocation network (HIRAN) considering isothermal and non-isothermal mixing. Iterations are realized on all potential pinch points to identify the minimum energy consumption. George et al. [50] introduced a discontinuous non-linear programming (DNLP) model to optimize the total operating costs of the HIRAN, taking into account non-isothermal mixing. Tan et al. [110] proposed a MINLP formulation based on the floating pinch concept [109] to design a HIRAN with minimum operating costs, for multiple contaminants and considering other properties. The authors limit the study to isothermal mixing cases. HEN is designed afterwards.

Jimenez et al. [64] presented a model for designing heat integrated water networks considering mass and properties. It includes contaminants and properties interception units dedicated to each stream. The methodology is based on a mixed-integer non linear programming (MINLP) model and the objective function to minimize is the total annual cost. A superstructure is proposed, with a first stage HEN before mixing mass streams is designed, then mass streams can enter interception units, and finally a second HEN is designed after mixing all mass streams allocated to a specific sink.

Few models were presented to solve this type of problems, and even fewer are linear and simultaneous.

1.3.3.3 EIP mass and heat integration

Overall, very few studies tried to tackle these different aspects within a single methodology. Pan et al. [91] pointed it out in their work and proposed a general methodology going from unit operations to processes, plants and industrial networks. At each level, each system is studied and optimized, then surrogate models are built to be implemented in the upper layer of the problem. In their article, they present a case study related to the inter-plant mass exchange design; and they will work on integrating the other aspects previously mentioned in future works.

1.3.4 Synthesis of the state of the art

The literature review presented in the previous paragraphs shows that the research regarding process integration takes on ever greater importance because the issues related to sustainability and cost-effectiveness are critical for industrial companies. Moreover, the need for integrating accurately several features and indicators of performances in the same approach has led to the use of mathematical programming over graphical approaches.

At a process scale, several models have been developed to tackle mass or energy integration problems; however, fewer have tried to addressed the two issues *simultaneously*. The ones who tried developed mostly *non-linear* models which are the most studied optimization techniques because their set up is easy; however, most of them require an initial guess and can be stuck in a local optimum, if they converge at all. Moreover, these models often used *fixed pollutant load* formulation of the mass integration problem, whose main drawback is that process units are defined by one or several mass loads to be removed; discarding several other types of units such as reactors that can generate or consume materials. Additionally, the design of each unit considered is variable. Therefore, for preexisting processes where unitary operations designs are fixed and industrial actors are reluctant to change their process, it can limit the applicability of such models.

At a territorial scale, the research on eco-industrial parks structures is quite recent and has really taken off in the last decade. Solving the problem of EIP optimization is quite complex because it involves different companies, with different objectives and mutually shared structures (such as pipelines, treatment units, utilities,...). EIP optimization studies are still in their infancy. Water and energy exchanges between industrial sites have been studied separately at least to a certain extent. A model incorporating these two aspects and addressing them simultaneously has yet to be developed.

1.4 Scientific ambitions and methodology presentation

According to the previous analyses of the current environmental and economic issues faced by the industry and state of the art, the main objective of this doctoral dissertation is to develop models capable of designing cost-effective mass allocation and heat exchanger networks in order to reduce resources consumption (mass and energy) as well as waste and pollution generation, from the process to the territorial scale.

To reach the scientific objectives of this work, the developed models must integrate the following features:

- The **economic criteria** is one of the most relevant for industrial actors when deciding whether or not to go through an investment decision or participating in an eco-industrial park.
- To further improve the results of the mass and heat integration, the optimization will occur **simultaneously**.
- The reference configuration for the mass integration problem will be a **fixed flow rate formulation** as it interferes less with the process units design and it can be more flexible on the features of the sources and sinks (regarding quality).

- The model must adapt to **different scales** (process, site and industrial area) to look for further opportunities of resource recovery. It actually reinforces the first choice, as it seems less likely that, within an eco-industrial park, local operations will be modified in case it is better for the EIP.

- The model formulation will be **linear** leading to a more steady and reliable solving.

The proposed methodology consists of solving three consecutive models of increasing difficulty in order to have a better understanding of the several parameters and constraints on the solution at a process level, then a fourth model is used to design a collaborative eco-industrial park:

- A first MILP model (M1) is solved using only the mass related equations. Its objective is to minimize the global mass resources consumption. Sources and sinks are characterized by a range of selected properties. Multiple fresh sources and waste sinks can be tested at once. This model is described in Chapter II.

- A second MILP model (M2) is developed to take into account the heating and cooling potential of each generated mass stream. A transshipment model is used to realize the heat integration and evaluate the heating and cooling needs. Process heat streams can be included in the problem definition. Multiple utility streams differentiated by their temperatures and costs can be evaluated simultaneously. The objective function is the annual operating costs that include the cost for fresh sources, waste sinks and heating and cooling utilities. The result of the first step can be used to define a range over the global resource consumption in order to reduce the search space of the problem. This model is presented in Chapter II.

- A third MILP model (M3) finally optimizes that the total annualized cost (TAC) including the operating and capital costs of the mass allocation and heat exchangers networks. This model is developed in Chapter III. An alternate version of M2 (M2') has been developed to select mathematical objects called mixer and splitter units that are able to further reduce the cost of the HEN structure. This additional model is presented in Chapter III.

- In Chapter IV, process units used to treat mass streams and change their physical and chemical properties are modeled based on previously introduced objects and integrated to the three previous models. Their purpose is to increase the possibilities of internal recovery of matter and heat.

- A fourth MILP model (M4) is presented as an extension of the three previous models to design a collaborative eco-industrial park thanks to the notions of sites, clusters (groups of sites that can have direct heat and mass exchanges) and intermediate

networks (heat or mass networks that allow indirect exchanges between clusters). These notions are introduced and illustrated in Chapter V.

Chapter 2

Heat integrated resource allocation network design

This chapter presents a new approach to design networks used to recover heat and mass from available waste streams and reuse them within the process. The objective is to design an heat-integrated resource allocation networks with a minimum total annualized cost. Two linear models are introduced for targeting the economically optimal fresh resource consumption and heat requirements simultaneously. These two models are based on works published in two articles [53, 54].

A first MILP model (M1) describes the mass related constraints of the problem in order to determine the minimum fresh resource flow rate necessary to satisfy all them. The model takes into account multi-contaminants and multi-properties of the mass streams. It also includes the possibility to use several fresh resources (with different characteristics) and several waste sinks (with different limitations).

A second MILP (M2) model is used to design an optimal heat integrated resource allocation network. It includes the equations developed in the M1 model. Heat integration is realized with a modified transshipment model, where a temperature scale is built with a set of discrete values for the temperature in order to account for non-isothermal mixing in a linear model. The objective function includes fresh resource, waste discharge and utilities costs. The result of the M1 model is used to bind the global resource consumption of the problem in the M2 problem.

The models M1 and M2 are able to consider technical restrictions that can occur on-site, such as limitations on fresh supplies, on waste treatment units or on certain allocations due to available space, security or operability. Including them allows the models to provide more realistic solutions.

The methodology is tested on two literature case studies to show the advantage of simultaneous optimization of both heat and mass requirements over a sequential approach. Several sensitivity analyses on different parameters are carried out to evaluate their influence on the optimal solution.

2.1 Problem statement

An industrial process can be decomposed into successive unitary operations, each one consuming and producing raw materials and energy to achieve their purpose. Some of these requirements can be fulfill by costly external matter sources and utilities, and waste effluents, whether mass or heat, must be dealt with to comply with environmental standards. Therefore, it would be cost-effective to reuse these effluents to meet some of the process requirements in terms of mass and energy. For that purpose elements of the process of modeled as follows focusing on one specific material.

Process sources ($j \in J_p$) are effluents created by process units with a given mass flow rate (L_j) which can be reused instead of being discarded to the environment with potentially costly treatments. **Fresh sources** ($j \in J_f$) are available to satisfy the need of process units (sinks) by providing a mass flow rate for a given cost to be determined (L_j^f). They are both characterized by their composition ($(y_{j,k})_{k \in K}$) and properties ($(p_{j,m})_{p_m \in P}$).

Process sinks ($i \in I_p$) require a specific mass flow rate (G_i), at the desired temperature, with limitations on the composition ($(z_{i,k}^{min}, z_{i,k}^{max})_{k \in K}$) and properties ($(p_{i,m}^{min}, p_{i,m}^{max})_{p_m \in P}$) of their feeding stream. **Waste sinks** ($i \in I_w$) represent the discharge points of the process where not reusable effluents are sent to be treated and discarded. They are particular sinks with no predefined mass flow rate (G_i^w).

Since they can have different temperatures (T_j for the sources and T_i for the sinks), connecting sources and sinks create mass streams which are also heat streams with undetermined heat requirements a priori. These heat streams can be integrated together to lower the minimum heating cooling requirements. Hence, the mass allocation network can be optimized by minimizing energy and fresh resources needs as well as the generation of waste effluents.

In addition to heating and cooling needs of mass streams, **process heat streams** ($h_p \in H_p$), which are streams characterized by a fixed heat load (q_{h_p}), inlet and outlet temperatures ($T_{h_p}^{in}$, $T_{h_p}^{out}$) and a mass flow rate (L_{h_p}), are also considered in the whole system heat integration.

Residual heating and cooling needs can be fulfilled by **utility heat streams** ($h_u \in H_u$). They are characterized by the same attributes as the ones of process heat streams ($T_{h_u}^{in}$, $T_{h_u}^{out}$, L_{h_u}); except that their output (q_{h_u}) is variable and a cost is associated with their use.

Fig.2.1 summarizes all the elements characteristics and notations.

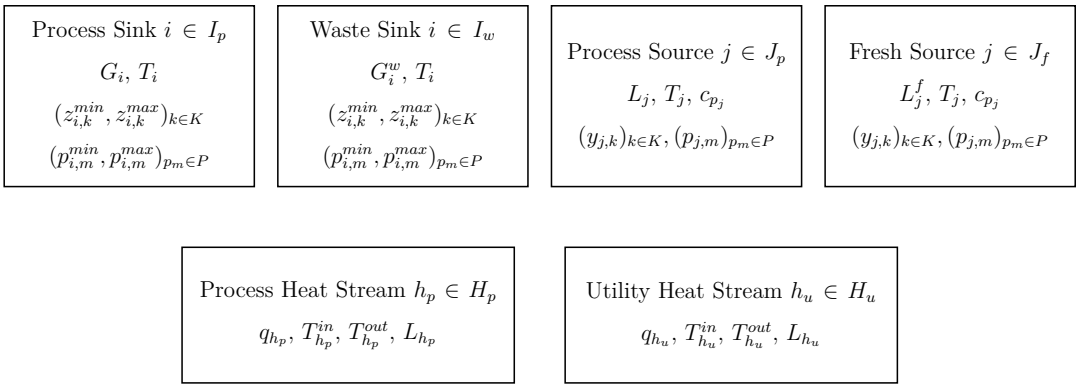

Figure 2.1: Elements and notations of the M1 and M2 models

The objective is to design an optimal direct reuse network while targeting the minimal total annual operating cost of such a network, considering the cost of fresh resource and heating and cooling requirements (given the total operating hours). Fig.3.5 presents the superstructure of the problem with its elements and their interactions:

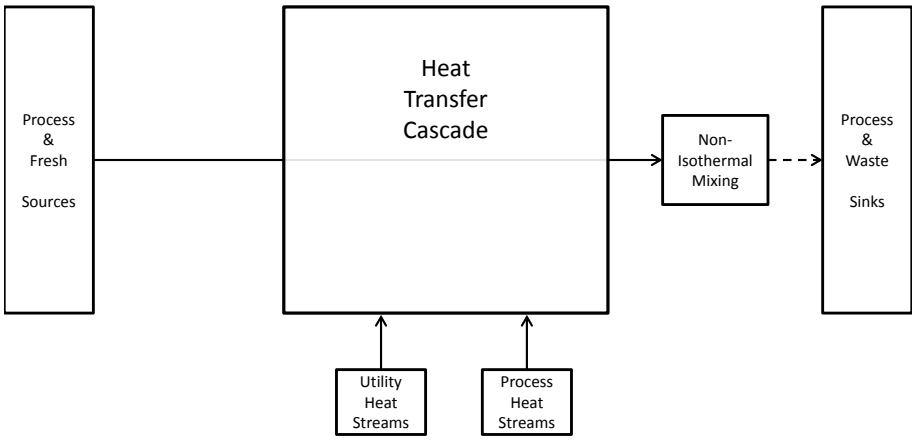

Figure 2.2: Schematic representation of interactions between mass and heat streams

Note that the heat exchanger network (HEN) is not designed at this point.

Moreover, technical restrictions can occur on-site, such as limitations on fresh supplies, on generated waste or on certain allocations due to available space, security or operability. The proposed model includes a more accurate characterization of mass and heat streams and allows constraining the solution search space so that it is more likely to be implemented on site.

2.2 Model Formulation

2.2.1 1^{st} MILP: Targeting the minimum fresh consumption (M1)

In this first model, the objective is to determine the minimum fresh consumption (L^{min}_{fresh}) feasible to comply with all the following constraints that include mass balances, property limitations and technical restrictions (such as forbidden allocations).

2.2.1.1 Mass balance and property constraints

For each process sink $i \in I_p$, the mass flow rate requirement (G_i) has to be met by a linear combination of all sources (L_{ij}) mass flow rates, while never exceeding the maximum allowable mass load ($z^{max}_{i,k}$) for each contaminant $k \in K$ and reaching the minimum load imposed ($z^{min}_{i,k}$ which is often null):

$$\forall i \in I_p, \sum_{j \in J_p \cup J_f} L_{ij} = G_i \tag{2.1}$$

$$f\forall i \in I_p, \forall k \in K,\ G_i \times z^{min}_{i,k} \leq \sum_{j \in J_p \cup J_f} L_{ij} \times y_{j,k} \leq G_i \times z^{max}_{i,k} \tag{2.2}$$

For each waste sink $i \in I_w$, the total mass flow rate (G^w_i) treated by the sink, which is a result of the optimization, is equal to a linear combination of all sources mass flow rates:

$$\forall i \in I_w, \sum_{j \in J_p \cup J_f} L_{ij} = G^w_i \tag{2.3}$$

$$\forall i \in I_w, \forall k \in K,\ G^w_i \times z^{min}_{i,k} \leq \sum_{j \in J_p \cup J_f} L_{ij} \times y_{j,k} \leq G^w_i \times z^{max}_{i,k} \tag{2.4}$$

Similar equations are used for properties. Each property $p_m \in P$ is characterized by a mixing rule defined by a function ϕ_m [40, 57, 86, 93]. The resulting value of the property p_m must be within the range defined for each sink. Assuming that ϕ_m is an increasing function, the following equations are obtained:

$$\forall i \in I_p, \forall p_m \in P,\ G_i \times \phi_m(p^{min}_{i,m}) \leq \sum_{j \in J_p \cup J_f} L_{ij} \times \phi_m(p_{j,m}) \leq G_i \times \phi_m(p^{max}_{i,m}) \tag{2.5}$$

$$\forall i \in I_w, \forall p_m \in P,\ G^w_i \times \phi_m(p^{min}_{i,m}) \leq \sum_{j \in J_p \cup J_f} L_{ij} \times \phi_m(p_{j,m}) \leq G^w_i \times \phi_m(p^{max}_{i,m}) \tag{2.6}$$

Moreover, for each process source $j \in J_p$, the sum of stream mass flow rates allocated to each sink (process and waste) must be equal to its total mass flow rate (L_j):

$$\forall j \in J_p, \sum_{i \in I_p \cup I_w} L_{ij} = L_j \tag{2.7}$$

Similarly, for each fresh source $j \in J_f$, the total mass flow rate (L_j^f) provided by j, which is a result of the optimization, must be:

$$\forall j \in J_f, \sum_{i \in I_p \cup I_w} L_{ij} = L_j^f \tag{2.8}$$

As previously mentioned, the objective of this first model is to minimize the total fresh consumption (L_{fresh}) which is defined as the sum of all the fresh sources mass flow rates:

$$\sum_{j \in J_f} L_j^f = L_{fresh} \tag{2.9}$$

2.2.1.2 Technical restrictions on mass flow rates

Allocations can be limited, forbidden or imposed, due to space, safety or operability restrictions on site. The following equations present how these restrictions are handled in the proposed model. This particular aspect was presented in [54].

Binary variables ($\gamma_{L_{ij}}$) are introduced to establish the existence of an allocation between sink i and source j, and define the acceptable range for the mass flow rate that transits between them:

$$\forall i \in I_p \cup I_w, \forall j \in J_p \cup J_f, L_{ij} - L_{ij}^{max} \times \gamma_{L_{ij}} \leq 0 \tag{2.10}$$

$$\forall i \in I_p \cup I_w, \forall j \in J_p \cup J_f, L_{ij} - L_{ij}^{min} \times \gamma_{L_{ij}} \geq 0 \tag{2.11}$$

In case specific bounds are not imposed for a given allocation, extreme values can be given to L_{ij}^{min} and L_{ij}^{max} in order for the equations to still be valid.

If the connection is imposed, then the value of L_{ij} is set to the corresponding specific value L_{ij}^{exist}:

$$L_{ij} = L_{ij}^{exist} \tag{2.12}$$

In particular, if the connection is forbidden, $L_{ij}^{exist} = 0$.

Restrictions can not only be imposed on specific connections but also on a set of connections. More specifically, the total available mass flow rate of a particular fresh source can be limited as well as the one sent to a given waste sink L_j^f:

$$L_j^f \leq L_{j,max}^f \, G_i^w \leq G_{i,max}^w \tag{2.13}$$

Or, the number of connections for each source can be restricted to a maximum N_j^{max} to avoid to limit the complication of the process flow sheet:

$$\sum_{i \in I_p \cup I_w} \gamma_{L_{ij}} \leq N_j^{max} \tag{2.14}$$

These restrictions are useful to obtain a more realistic solution.

2.2.1.3 Objective function

The objective of this first model is to minimize the global fresh resources consumption:

$$minimize\ L_{fresh}$$

The result of this first problem is used in the following model to bind the search space of the total fresh source consumption as the second MILP model objective is to target the minimum annualized operating costs including mass and heat aspects of the studied process.

2.2.2 2^{nd} MILP: Targeting the minimum annualized operating cost (M2)

The second MILP model M2 optimizes the global fresh resource and the energy consumption simultaneously. It takes into account non-isothermal mixing. The first MILP M1 is not necessary to do a total cost optimization, however it gives useful insights on preferential allocations considering only mass related constraints. Moreover, it allows reducing the search space for the global fresh resource consumption, which can speed up the resolution.

2.2.2.1 Limitations of the fresh resource consumption search space

The result of the M1 model gives the value of the lower bound for the global fresh resource search space:

$$\sum_{j \in J_f} L_j^f = L_{fresh} \geq L_{fresh}^{min} \tag{2.15}$$

An upper bound is defined by the user relatively to L_{fresh}^{min} thanks to a parameter ΔL_{fresh}^{max}:

$$\sum_{j \in J_f} L_j^f = L_{fresh} \leq L_{fresh}^{min} \times (1 + \Delta L_{fresh}^{max}) \tag{2.16}$$

Setting the fresh resource flow rate to its minimum does not guarantee to obtain the minimum cost for the network, since it does not take into account the effect on utility targets. Therefore, being able to define a range for the fresh resource consumption helps finding a solution more or less resource-intensive.

2.2.2.2 Heat integration

Heat integration aims at reducing the heating and cooling demands of the process. Heat integration model used is based on the classic transshipment model. As explained previously, mass streams connecting sources and sinks are heat streams with undetermined heat loads. A mass stream (ms) can be characterized as hot or cold whether its inlet temperature is superior or inferior to its outlet temperature, respectively. Mass streams allocated to a given sink are mixed prior to entering the sink and the resulting temperature must be equal to the sink temperature. To reach this temperature, mass streams can either be heated up or cooled down through indirect heat exchange to the desired temperature (isothermal-mixing), or they can be mixed at different temperatures (non-isothermal mixing). In a non-isothermal case, a stream can be split into a number of other streams at various temperatures (between T_j and T_i). Therefore, the equation modeling the heat given or required by a stream, depending on its nature (hot or cold) is non-linear:

$$q_{ij} = L_{ij} \times c_{pj}(T) \times (T_{ij}^{int} - T_j)$$

where T_{ij}^{int} is a temperature between T_j and T_i, and $c_{pj}(T)$ depends on the temperature.

As several variables (L_{ij}, T_{ij}^{int} and $c_{pj}(T)$) are multiplied, the problem is no longer linear. To overcome this issue, a temperature scale is built where the intermediate temperature levels at which the splits can occur or the heat transfer can stop are predefined. The heat capacity function $c_{pj}(T)$ is used to calculate $c_{pj,n}$ which is an average value for each interval n as explained in Eq.2.25 . The remaining variables to be optimized are the mass flow rates L_{ij}; therefore, the set of equations are linear.

First of all, a primary shifted temperature scale $\{T_n^*\}_{n\in[1,N]}$ is built, assuming that all sources and sinks are connected, and that all heat streams, which are created by the connections between sources and sinks, take part in the indirect heat exchange. N represents the number of distinct shifted temperatures obtained with Eq.2.17 and Eq.2.18. They create $N-1$ intervals in an ascending scale so that $\forall n \in [1, N-1], T_n < T_{n+1}$:

For hot streams:

$\forall i \in I_p \cup I_w, \forall j \in J_p \cup J_f,\ T_j > T_i,\ \exists (n,m) \in [1,N]^2,$

$$\begin{aligned} T_j^{h*} &= T_j - \Delta T_{min}/2 = T_n^* \\ T_i^{h*} &= T_i - \Delta T_{min}/2 = T_m^* \end{aligned} \tag{2.17}$$

For cold streams:

$\forall i \in I_p \cup I_w, \forall j \in J_p \cup J_f,\ T_j < T_i,\ \exists (n,m) \in [1,N]^2,$

$$\begin{aligned} T_j^{c*} &= T_j + \Delta T_{min}/2 = T_n^* \\ T_i^{c*} &= T_i + \Delta T_{min}/2 = T_m^* \end{aligned} \tag{2.18}$$

With this simple temperature scale, matter extractions can only occur at few temperature levels. Therefore, to add more possibilities and improve the accuracy of the solution, the temperature scale is divided into smaller temperature intervals. A new parameter (ΔT_{step}^{max}) is introduced for this purpose.

The new temperature scale $\{T_n^{'*}\}_{n\in[1,N']}$ is obtained by dividing the previous temperature scale $\{T_n^*\}_{n\in[1,N]}$ so that a gap between two consecutive temperatures is smaller than ΔT_{step}^{max}. If two consecutive temperatures on the initial temperature scale $\{T_n^*\}_{n\in[1,N]}$ are separated by an interval strictly greater than ΔT_{step}^{max}, then this interval is divided into smaller ones, such as they all are shorter than ΔT_{step}^{max}:

$$\forall n \in [1, N'-1],\ T_{n+1}^{'*} - T_n^{'*} \leq \Delta T_{step}^{max} \tag{2.19}$$

More specifically, the final temperature scale $\{T_n^{'*}\}_{n\in[1,N']}$ is determined as follows:
Let's note Q_n and r_n, respectively, the quotient and the rest of the division between $T_{n+1}^* - T_n^*$ and ΔT_{step}^{max}. Let's note I_n, the number of temperature intervals between T_n^* and T_{n+1}^*.

If $T_{n+1}^* - T_n^* \leq \Delta T_{step}^{max}$ then

$$I_n = 1 \tag{2.20}$$

If $T_{n+1}^* - T_n^* > \Delta T_{step}^{max}$ and $r_n = 0$ then

$$I_n = Q_n \tag{2.21}$$

If $T_{n+1}^* - T_n^* > \Delta T_{step}^{max}$ and $r_n \neq 0$ then

$$I_n = Q_n + 1 \tag{2.22}$$

Note that $N^{'}$, which indicates the number of temperature levels on the new scale, is equal to:

$$N^{'} = 1 + \sum_n I_n \tag{2.23}$$

The following temperatures indicate the level, on the temperature scale $\{T_n^{'*}\}_{n\in[1,N']}$, at which a heat stream begins and finishes, depending on its nature(hot or cold). Let n $\in [1, N^{'}]$,

$$\begin{aligned} T_n^{'*} &= T_i^{*h},\ n = N_i^h \\ T_n^{'*} &= T_i^{*c},\ n = N_i^c \\ T_n^{'*} &= T_j^{*h},\ n = N_j^h \\ T_n^{'*} &= T_j^{*c},\ n = N_j^c \end{aligned} \tag{2.24}$$

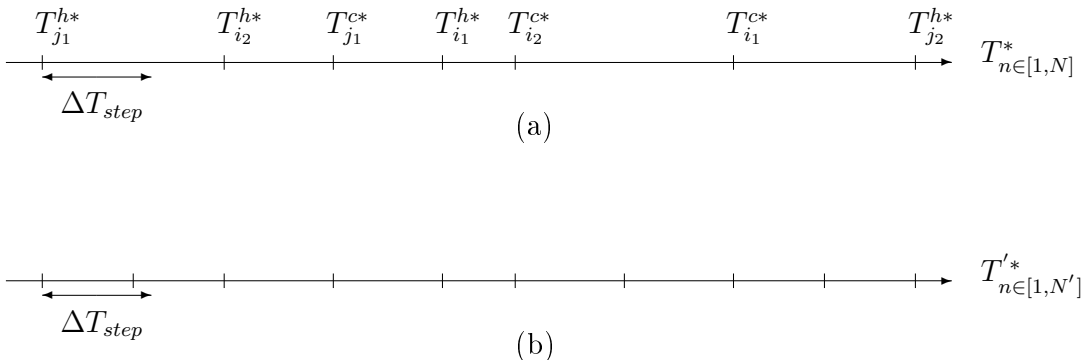

Figure 2.3: (a) Initial temperature scale - (b) Final temperature scale

Once the final temperature scale is determined, it is possible to address the issue of the temperature dependence of the heat capacity. It is approximated by an average value within each temperature interval. This value is calculated beforehand for each interval as follows: Let n $\in [1, N^{'} - 1]$,

$$c_{pj,n} = \frac{c_{pj}(T_{n+1}^{'*}) + c_{pj}(T_n^{'*})}{2} \tag{2.25}$$

To determine the quantity extracted from a stream, going from source j to sink i, at a temperature level $T_n^{'*}$, $L_{ij,n}$ are introduced as shown in Fig.3.8.

Let's consider a stream going from source j to sink i. This stream will be referred to as the main stream. At each temperature level $T_n^{'*}$ (between T_j^{c*} and T_i^{c*}), for cold streams, or, between T_j^{h*} and T_i^{h*}, for hot streams), the main stream can be split. Part of the main stream $L_{ij,n}$, which can be the entire stream, is extracted at a temperature level $T_n^{'*}$ and is directly sent to sink i, to be mixed with the other streams allocated to it.

The remaining part of the main stream ($\widetilde{L}_{ij,n}$), if there is still one, indirectly exchanging heat between $T_n^{'*}$ and $T_{n-1}^{'*}$ for a hot stream (descending order), or between $T_n^{'*}$ and $T_{n+1}^{'*}$ for a cold stream (ascending order).

Note that two consecutive splits can be seen as a single split at an intermediate temperature in between the two extreme values of the interval. This property will be exploited in the Chapter III.

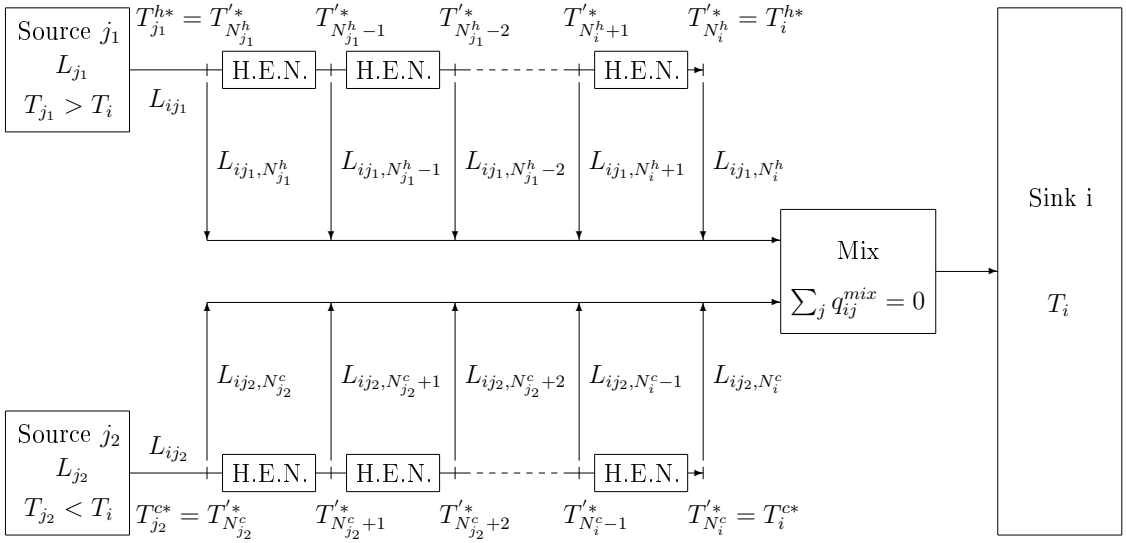

Figure 2.4: Superstructure for mass/heat integration through non-isothermal mixing

The extracted mass flow rate at each temperature level cannot exceed the allocation mass flow rate:

$$\forall i \in I_p \cup I_w, \forall j \in J_p \cup J_f, \forall n \in [N_{ij}^{min}; N_{ij}^{max}], L_{ij,n} \leq L_{ij} \tag{2.26}$$

The sum of all extractions mass flow rates is equal to the allocation mass flow rate:

$$\forall i \in I_p \cup I_w, \forall j \in J_p \cup J_f, \sum_n L_{ij,n} = L_{ij} \tag{2.27}$$

The existence of an extraction at a given temperature level is identified with a binary variable (γ_L):

$$\forall i \in I_p \cup I_w, \forall j \in J_p \cup J_f, \forall n \in [N_{ij}^{min}; N_{ij}^{max}], L_{ij,n} - \gamma_{L_{ij,n}} \times L_{ij}^{max} \leq 0 \tag{2.28}$$

Thus, the number of extractions can be restrained (N_{split}^{max}) to manage the complexity of the optimal configuration and potentially the computation time:

$$\forall i \in I_p \cup I_w, \forall j \in J_p \cup J_f, \sum_n \gamma_{L_{ij,n}} \leq N_{split}^{max} \tag{2.29}$$

Note that N_{split}^{max} has to be superior to 1.

Fig.2.5 shows a theoretical example where the number of extractions is limited to 1. This restriction forces matter to be extracted all at once.

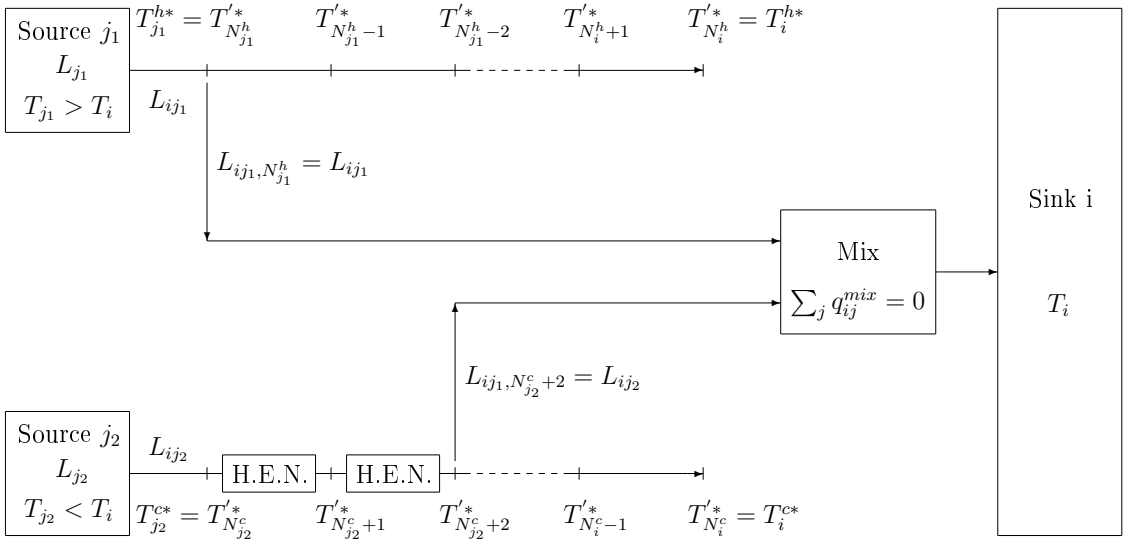

Figure 2.5: Non-isothermal mixing example - $N^{max}_{split} = 1$

The model formulation also allows the analysis of isothermal cases as shown in Fig.2.6.

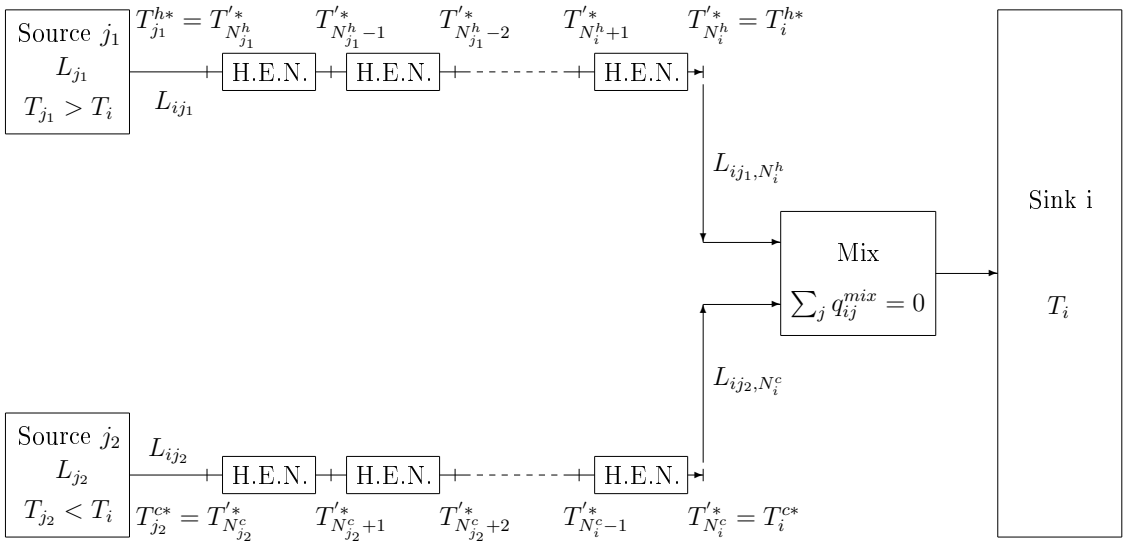

Figure 2.6: Particular case of the isothermal mixing

In the case of isothermal mixing, splits only occur at the sink temperature level:

For hot streams:

$$\forall i \in I_p \cup I_w, \forall j \in J_p \cup J_f, \forall n \in [N_{ij}^{min}+1; N_{ij}^{max}], L_{ij,n} = 0 \tag{2.30}$$

For cold streams:

$$\forall i \in I_p \cup I_w, \forall j \in J_p \cup J_f, \forall n \in [N_{ij}^{min}; N_{ij}^{max}-1], L_{ij,n} = 0 \tag{2.31}$$

Each extraction at a temperature level n is sent to the sink i. Let's note N_{ij}^{out} the index on the temperature scale of the sink temperature (which is different depending on whether the mass stream is hot or cold). The resulting temperature must be equal to the sink temperature. Therefore, the heat balance for the mix after the indirect heat exchanges is:

$$\forall i \in I_p \cup I_w, \sum_{j \in J_p \cup J_f} \sum_{n=N_{ij}^{min}}^{N_{ij}^{max}} L_{ij,n} \times cp_{j,n} \times (T'^{*}_{N_{ij}^{out}} - T'^{*}_{n}) = 0 \tag{2.32}$$

The remaining part of the stream after each extraction ($\widetilde{L}_{ij,n}$) exchanging heat is:

For hot mass streams:

$$\forall i \in I_p \cup I_w, \forall j \in J_p \cup J_f, \forall n \in [N_{ij}^{min}; N_{ij}^{max}-1], L_{ij} - \sum_{k=n+1}^{N_{ij}^{max}} L_{ij,k} = \widetilde{L}_{ij,n} \tag{2.33}$$

For cold mass streams:

$$\forall i \in I_p \cup I_w, \forall j \in J_p \cup J_f, \forall n \in [N_{ij}^{min}; N_{ij}^{max}], L_{ij} - \sum_{k=N_{ij}^{min}}^{n} L_{ij,k} = \widetilde{L}_{ij,k} \tag{2.34}$$

The indirect heat transferred, in each temperature interval, is defined as follows:

$$\begin{aligned} \forall i \in I_p \cup I_w, \forall j \in J_p \cup J_f, \forall n \in [N_{ij}^{min}; N_{ij}^{max}-1], \\ \widetilde{L}_{ij,n} \times cp_j \times (T'^{*}_{n+1} - T'^{*}_{n}) = q_{ij,n} \geq 0 \end{aligned} \tag{2.35}$$

Moreover, heat streams (process $h_p \in H_p$ or utility $h_u \in H_u$) are included in the overall heat balance. The heat capacity for heat streams are defined as:

$$\forall h_p \in H_p, \forall n \in [N_{h_p}^{min}; N_{h_p}^{max} - 1], CP_{h_p} = q_{h_p}/(T_{N_{h_p}^{max}}^{'*} - T_{N_{h_p}^{min}}^{'*}) \tag{2.36}$$

$$\forall h_u \in H_u, \forall n \in [N_{h_u}^{min}; N_{h_u}^{max} - 1], CP_{h_u} = q_{h_u}/(T_{N_{h_u}^{max}}^{'*} - T_{N_{h_u}^{min}}^{'*}) \tag{2.37}$$

Therefore,

$$\forall h_p \in H_p, \forall n \in [N_{h_p}^{min}; N_{h_p}^{max} - 1], CP_{h_p} \times (T_{n+1}^{'*} - T_n^{'*}) = q_{h_p,n} \geq 0 \tag{2.38}$$

$$\forall h_u \in H_u, \forall n \in [N_{h_u}^{min}; N_{h_u}^{max} - 1], CP_{h_u} \times (T_{n+1}^{'*} - T_n^{'*}) = q_{h_u,n} \geq 0 \tag{2.39}$$

Binary variables ($\gamma_{q_{h_u}}$) are introduced to indicate if the output of a given utility heat stream h_u is not null:

$$\forall h_u \in H_u, q_{h_u} - \gamma_{q_{h_u}} \times q_{h_u}^{max} \leq 0 \tag{2.40}$$

Thus, the total heat provided (q_n^h) or required (q_n^c) at the n^{th} temperature interval is:

$$\begin{aligned} &\forall n \in [0, N^{'} - 1], \\ &\sum_{i \in I_p \cup I_w} \sum_{j \in J_p \cup J_f} q_{ij,n} + \sum_{h_p \in H_p} q_{h_p,n} + \sum_{h_u \in H_u} q_{h_u,n} = \\ &\qquad \begin{cases} q_n^h \geq 0 & \text{for all hot mass and heat streams} \\ -q_n^c \geq 0 & \text{for all cold mass and heat streams} \end{cases} \end{aligned} \tag{2.41}$$

The classic transshipment model is used to calculate the overall heating and cooling requirements Fig.2.7. The energy balance at the n^{th} temperature interval is:

$$R_n = q_n^h + q_n^c + R_{n+1} \tag{2.42}$$

where $R_n \geq 0$ represents the residual heat provided by the n^{th} temperature interval. Note that since the utilities are taken into account in q_n^{hot} and q_n^{cold}, the whole system is closed:

$$R_{N'} = R_0 = 0 \tag{2.43}$$

Finally, the global heating and cooling utility loads are defined as follows:

$$Q_{heating} = \sum_{h_u \in H_u \cap H_{hot}} q_{h_u} \tag{2.44}$$

$$Q_{cooling} = \sum_{h_u \in H_u \cap H_{cold}} q_{h_u} \tag{2.45}$$

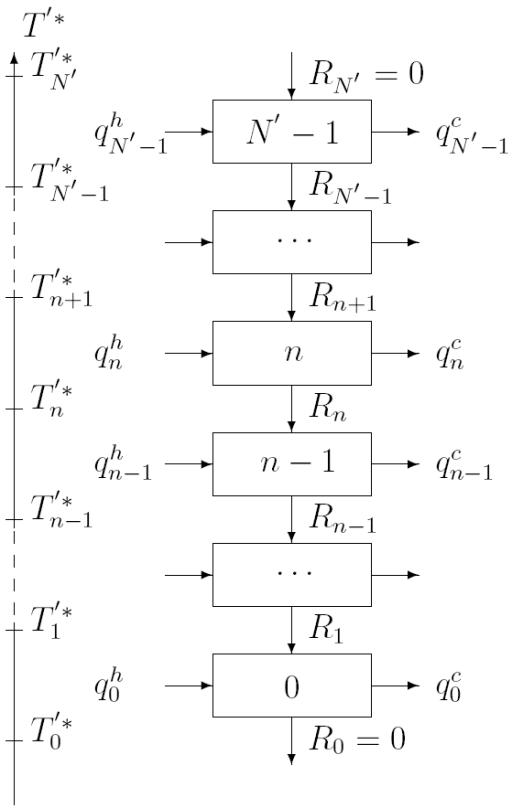

Figure 2.7: Heat Cascade Diagram

The models presented in this work have the advantage of remaining linear while taking into account mass and energy aspects of the mass allocation network simultaneously. However, the possible drawback of this model is that the computation time may become important, depending on the value of ΔT^{max}_{step}, N_{split} and the number of sources and sinks.

2.2.3 Objective function

The objective function representing the annual operating costs (AOC) is minimized to obtain an optimal heat-integrated mass allocation network.

$$minimize\ AOC$$

Assuming a nominal cost of fresh source j (C^f_j), waste sink i (C^w_i) and utility heat stream h_u (C_{h_u}), the AOC for a given total of operating hours (h_{op}) is expressed as follows:

$$AOC = h_{op} \times \left(\sum_{j \in J_f} C^f_j \times L^f_j + \sum_{i \in I_w} C^w_i \times G^w_i + \sum_{h_u \in H_u} C_{h_u} \times q_{h_u} \right) \tag{2.46}$$

2.3 Case studies

Two case studies from the literature have been selected to validate the relevance of simultaneous mass/heat optimization as well as evaluate the influence of several parameters on the optimal solution.

The first case study (ammonia (NH_3) recovery) is presented to validate the results obtained by the two models M1 and M2 in comparison with the ones found in the literature. Several sensitivity analyses are used to test the relative importance on the solution of different parameters introduced in the models (ΔL_{fresh}^{max}, ΔT_{min}, N_{split}^{max}, ΔT_{step}^{max}).

The second case study (phenol production process) is a multi-properties case used to illustrate how to model real on-site constraints and their influence on the optimal solution.

For these case studies, the MILP models M1 and M2 were implemented and solved with GLPK solver (GLPK version: 4.60 - Processor: Intel© CORE™ i7 - 2760QM CPU @ 2.40GHz - RAM: 8Go - OS: Windows© 7).

2.3.1 Mono-contaminant case: Ammonia Recovery

The first case study deals with ammonia (NH_3) recovery. Ammonia is needed in some parts of the process plant (sour gas absorption column, dust-cleaning agent) and produced in others (calcium chloride production section of the plant). It has to be treated due to its hazardous characteristics.

It is a mono-contaminant case which illustrates the influence of several parameters introduced in the models on the optimal targets. This case study appears in many articles [100, 110, 115] which allows comparing performances. The economic and thermodynamic data are taken from Tan et al. [110].

The purpose of the study is to determine the amount of NH_3 that can be recovered and how it should be allocated to reduce the amount of fresh ammonia to be bought, to be treated and the minimum energy required.

The process data are given in Table 2.1. Note that the heat capacity is supposed constant for each source.

	Flow rate ($kg.s^{-1}$)	Comp. in impurities (ppm)	Temperature ($°C$)
Sink			
Sink1	350	0 - 0	30
Sink2	677	0 - 40	187
Sink3	126	0 - 75	55
Sink4	202	0 - 100	98
Waste		0 - 500	40
Source			
Source1	530	30	21
Source2	68	150	43
Source3	1130	300	130
Source4	36	500	35
Fresh		0	30

Heat capacity = $2.19 kJ.kg^{-1}.K^{-1}$

Table 2.1: Ammonia recovery case - Process Data

The economic data and selected parameters are given in Table 2.2:

Economic data		*Parameters*	
C_{fresh}	500 €$.ton^{-1}$	h_{op}	8000 hours
C_{waste}	0 €$.ton^{-1}$	ΔL_{fresh}^{max}	900 %
C_{hot}	0.01 €$.kWh^{-1}$	ΔT_{min}	35 $°C$
C_{cold}	0.0025 €$.kWh^{-1}$	ΔT_{step}^{max}	5 $°C$
		N_{split}^{max}	50

Table 2.2: Ammonia recovery case - Economic Data and Calculation Parameters

2.3.1.1 Comparison with literature results

Table 2.3 shows the results given by articles found in the literature and the results obtained by the introduced methodology:

Model	Sahu et al. (2012)	Tan et al. (2014)	Models M1 & M2
L_{fresh} $(kg.s^{-1})$	655	654.9	654.9
Q_h (kW)	132 925.5	132 927.0	132 927.0
Q_c (kW)	79 224.5	79 228.0	79 228.0

(a) Isothermal case

Sahu et al. (2012)	Models M1 & M2
655	654.9
131 882.4	131 883.3
78 181.4	78 184.5

(b) Non-isothermal case

Table 2.3: Comparison with literature results - $\Delta T_{min} = 35°C$

Sahu et al. [100] presented a linear sequential methodology, which determines first L^{min}_{fresh}, and then minimizes the utility targets. The results are similar to the ones obtained with the proposed methodology for both isothermal and non-isothermal cases. The rounding up done on L^{min}_{fresh} by Sahu et al. [100] has a strong influence on the AOC, since the fresh resource cost is outweighing the thermal utilities cost by several orders of magnitude. This explains why both linear methodologies do not get the same optimal configuration and targets.

Tan et al. [110] presented a non-linear simultaneous model to synthesize the HIRAN by optimizing the AOC. The results obtained are exactly the same for the targets as well as the mass allocation network. Fig.2.8 shows the heat integrated mass allocation network designed with the presented model for the non-isothermal case. Note that the mass allocation is the same for isothermal and non-isothermal cases; the only difference comes from the heat requirements, which are reduced in the latter case.

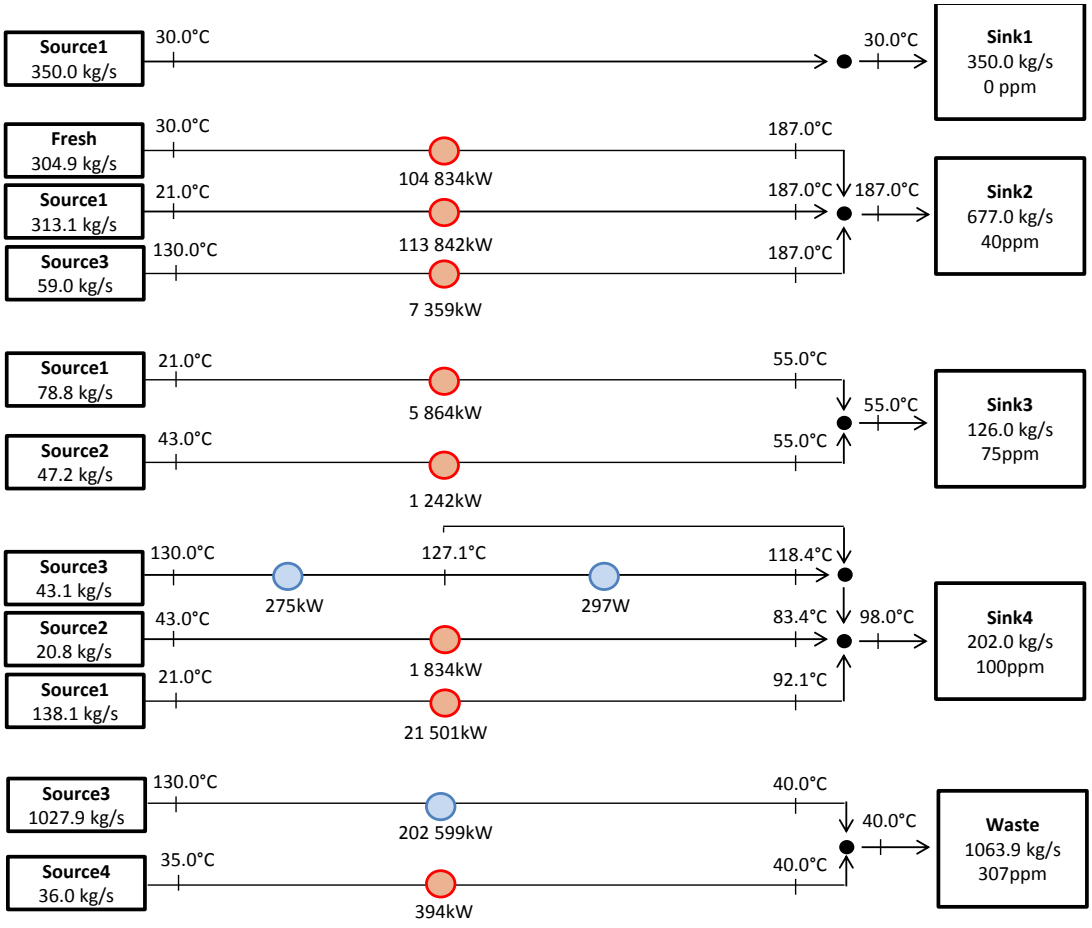

Figure 2.8: Optimal HIRAN for ammonia recovery case - $\Delta T_{min} = 35°C$

Wan Alwi et al. [115] used the same case study to illustrate their graphical method (that considers isothermal mixing), but they changed ΔT_{min} to a value of $10°C$. In Table 2.4, the results obtained by Wan Alwi et al. [115] and by the introduced model are presented in the case of isothermal mixing.

	Wan Alwi et al. (2011)	Model M2
L_{fresh} $(kg.s^{-1})$	655.0	654.9
Q_h (kW)	96 572	98 045.2
Q_c (kW)	71 869	44 346.4

Table 2.4: Comparison with literature results - $\Delta T_{min} = 10°C$

These results show that the proposed model M2 based on a mathematical approach is more optimal compared to the graphical approach [115]. Indeed, the latter reduced too much the hot utility and missed the configuration that can dramatically cut down the cold utility requirement. Fig.2.9 shows the optimal HIRAN design obtained by M2.

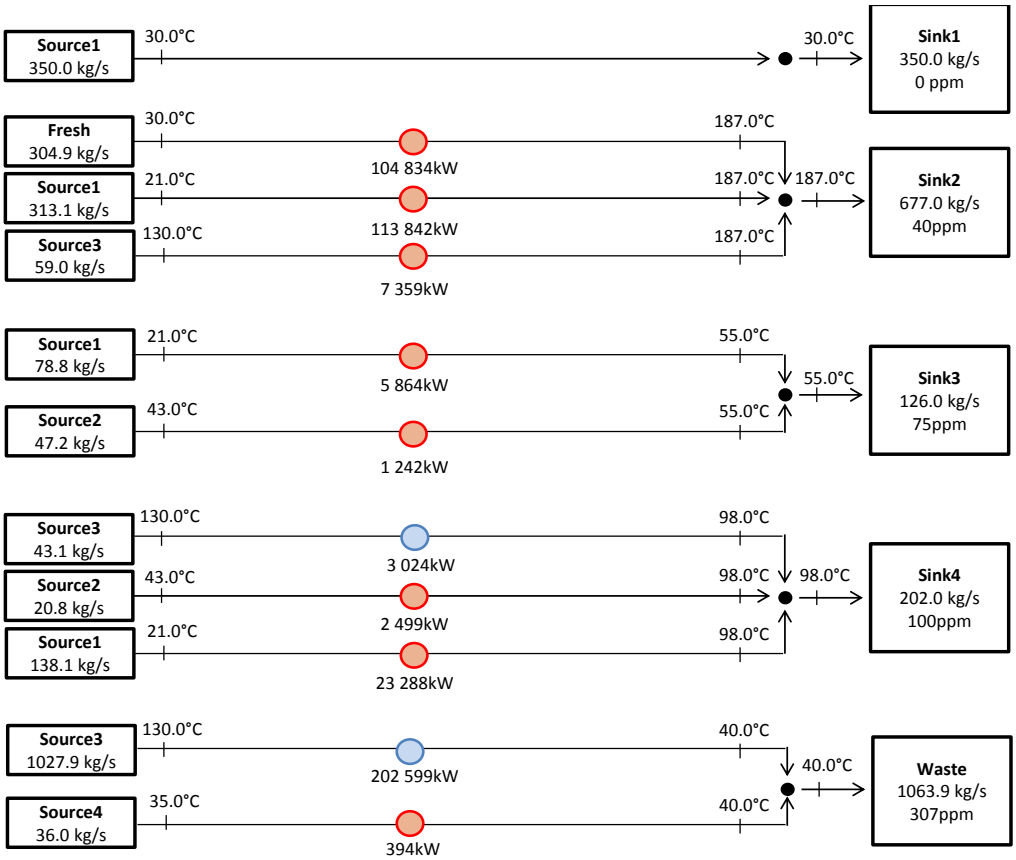

Figure 2.9: Optimal HIRAN for ammonia recovery case - $\Delta T_{min} = 10°C$

The non-isothermal case was not addressed by Wan Alwi et al. [115]. However, it is possible to compare the results obtained by M2 model between both isothermal and non-isothermal mixing. In this case, they both give the same results regarding utility targets and cost. This can be explained by the fact that as ΔT_{min} gets smaller, heat integration is more efficient and utility targets are lowered. Therefore, when ΔT_{min} decreases, non-isothermal mixing provide less and less extra savings compared to isothermal mixing.

However, if the capital cost of heat exchangers (related to their existences and their exchange surfaces) was taken into account, it may have an effect on cost.

So far, the models M1 and M2 proved to be as accurate as the others found in the literature. The choice to favor non-isothermal mixing is justified by the results obtained because extra energy savings can be made, or at least have the same results as isothermal mixing. It certainly will provide extra savings in capital costs as it is an equivalent to heat exchangers with no surface, i.e., free heat exchangers.

2.3.1.2 Sensitivity analyses

To have a better understanding of the influence of several introduced parameters in the models M1 and M2, sensitivity analyses are realized. These analyses study the influence of C_{fresh}, ΔL^{max}_{fresh}, ΔT_{min}, N^{max}_{split} and ΔT^{max}_{step} in the ammonia recovery case.

- **Sensitivity to C_{fresh} and ΔL^{max}_{fresh}**

In the ammonia recovery case study, the fresh resource cost is overwhelming to highlight properly the potential bargain between energy and fresh resource costs. Indeed, the fresh resource cost represents about 99.9 % of the total operating cost. That discriminates in favor of network configurations requiring a minimum of fresh resources. To illustrate the relevance of the M2 model, it is necessary to curb the fresh resource cost so that energy and mass costs become comparable.

From a cost optimization perspective, fixing the value of L_{fresh} to its minimum may overlook network configurations that overall minimize the operating cost by increasing fresh source flow rate and reducing thermal utilities. For instance, imagine a sink that has to be supplied at $50°C$. To do so, one can either use a process source at $10°C$ or the fresh source at $20°C$. Clearly, the energy requirement will be higher when using the process source. Thus, if the hot utility cost is higher than the fresh resource cost, it will be more efficient to use more fresh resources. So first, the sensitivity of the solution to the fresh resource nominal cost (C_{fresh}) is studied assuming that $\Delta L^{max}_{fresh} = 900\%$.

Fig.2.10 shows the evolution of the total annual operating cost and fresh resource flow rate depending on C_{fresh}.

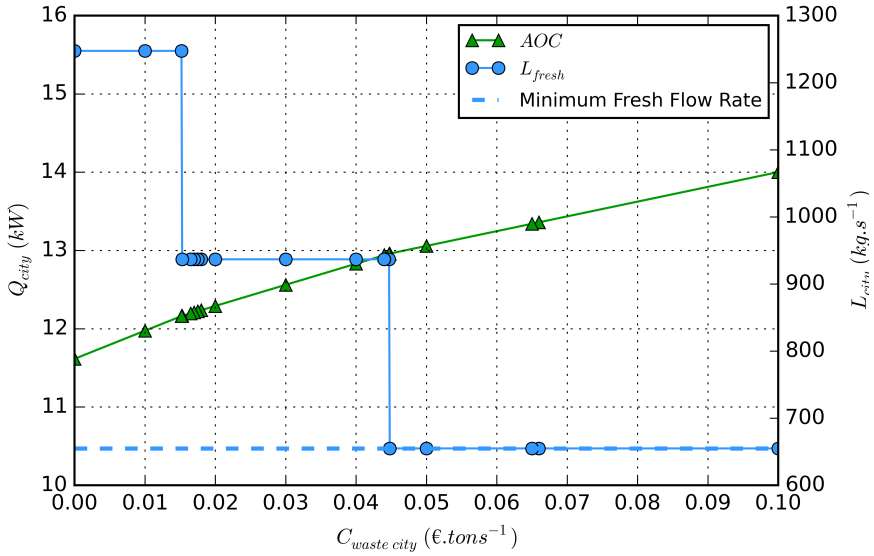

Figure 2.10: Sensitivity analyses of AOC and L_{fresh} to C_{fresh}

Fig.2.11 represents the variation of cold and hot utility targets as well as fresh resource flow rate depending on C_{fresh}.

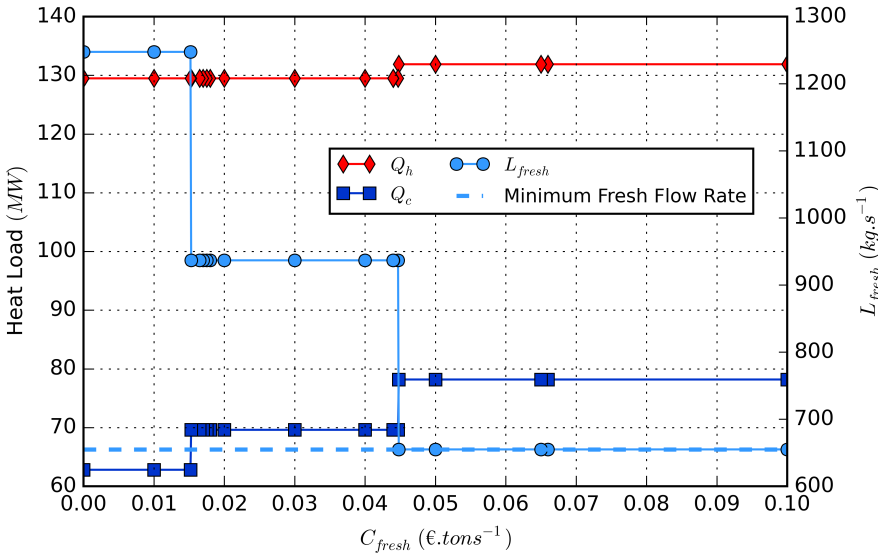

Figure 2.11: Sensitivity analyses of Q_h, Q_c and L_{fresh} to C_{fresh}

It can be deduced from Fig.2.10 and Fig.2.11 that optimal configurations depending on the cost structure of the problem are obtained while L_{fresh} does not reach its minimum. In fact, using more fresh resources may entail consequent reductions of energy requirements. This shows that $DeltaL_{fresh}^{max}$ can have a considerable influence on the optimal solution.

The following discussion examines the modifications in the network configuration depending on C_{fresh}. Allocation changes occur when the rise in fresh resource consumption becomes cost efficient. It implies that the cutback in the utility cost outweighs the fresh resource cost increase. At each change in Fig.2.11, the allocation network is modified to be more cost efficient. It adopts a new structure defining mass streams with new heat requirements. Two optimal heat integrated mass allocation networks, for three different values of C_{fresh} (0.09, 0.03 and 0.01€.ton^{-1}) are presented in Fig.2.12 to Fig.2.14.

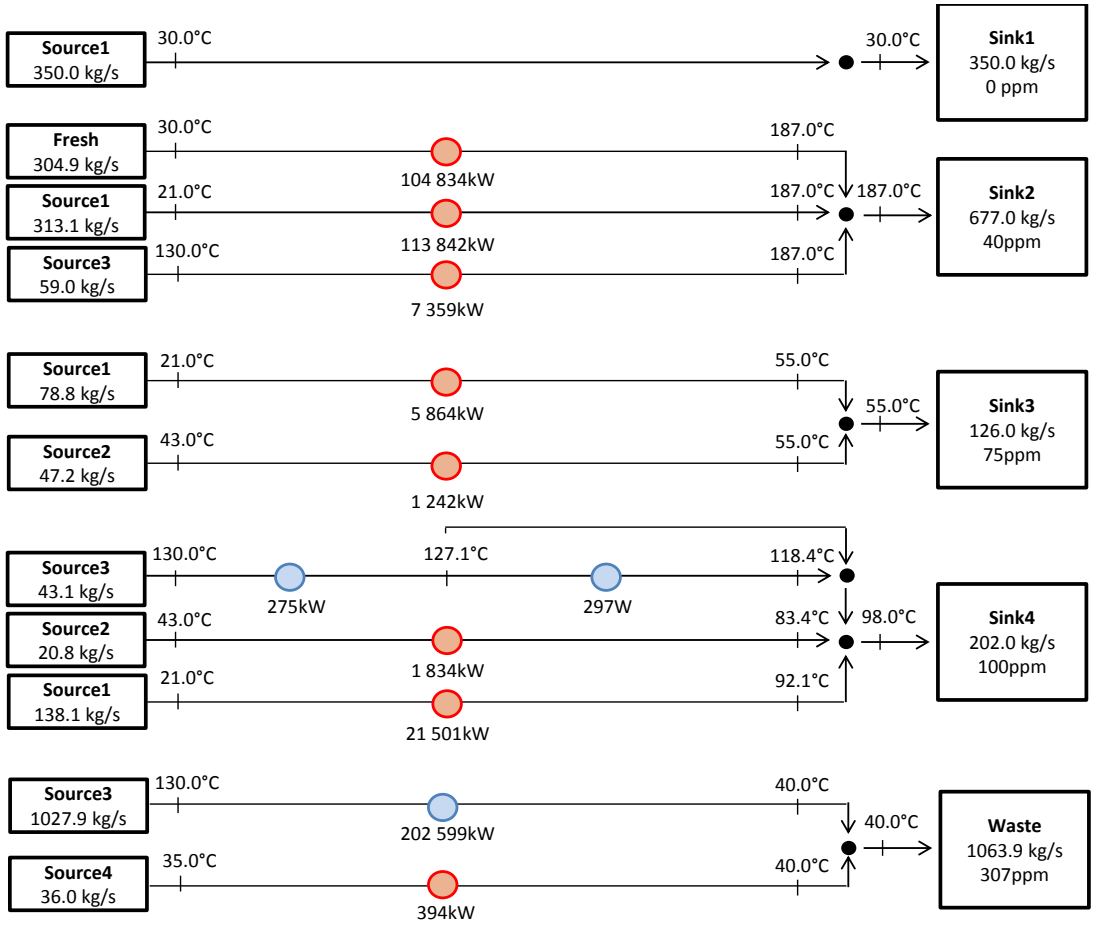

Figure 2.12: Optimal HIRAN configuration when $C_{fresh} = 0.09€.ton^{-1}$

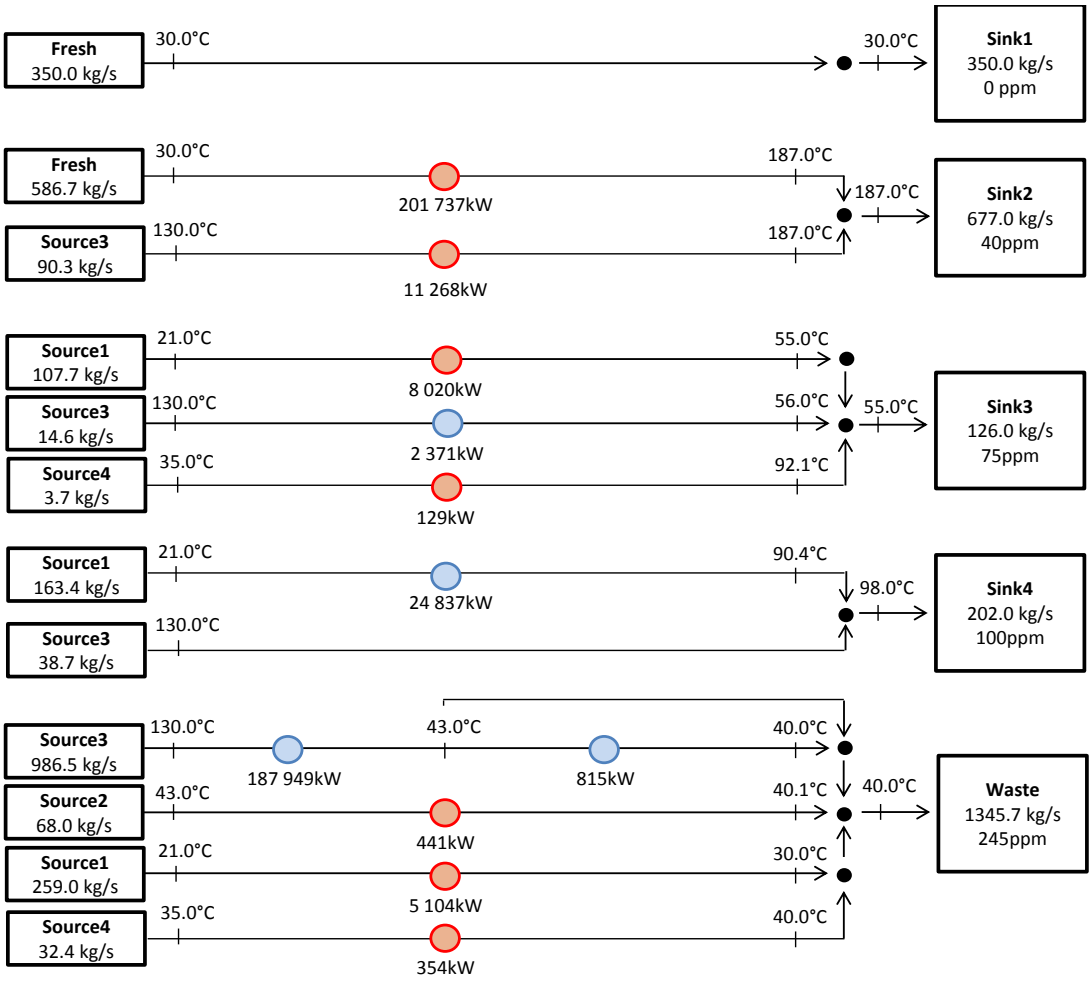

Figure 2.13: Optimal HIRAN configuration when $C_{fresh} = 0.03€.ton^{-1}$

Starting from the initial fresh resource nominal cost ($500€.ton^{-1}$), the design of the optimal HIRAN remains the same as shown in Fig.2.12 until it reaches $0.044€.ton^{-1}$ (Fig.2.11). At this point, the main change in the HIRAN design compared to the initial structure concerns $Source1$ allocated to $Sink2$ (Fig.2.13). This connection creates an important need for heating, from a very low temperature ($21°C$) to a very high temperature ($187°C$). Since the fresh resource has a temperature superior to $Source1$ temperature, the hot utility requirement will be reduced if $Sink2$ is fed with more fresh resource.

The last change in structure occurs when $C_{fresh} = 0.015€.ton^{-1}$. In this new structure shown in Fig.2.14, a fraction of $Source1$ has to be reallocated and it appears that the best choice is to send $Source1$ to the waste unit (at $40°C$).

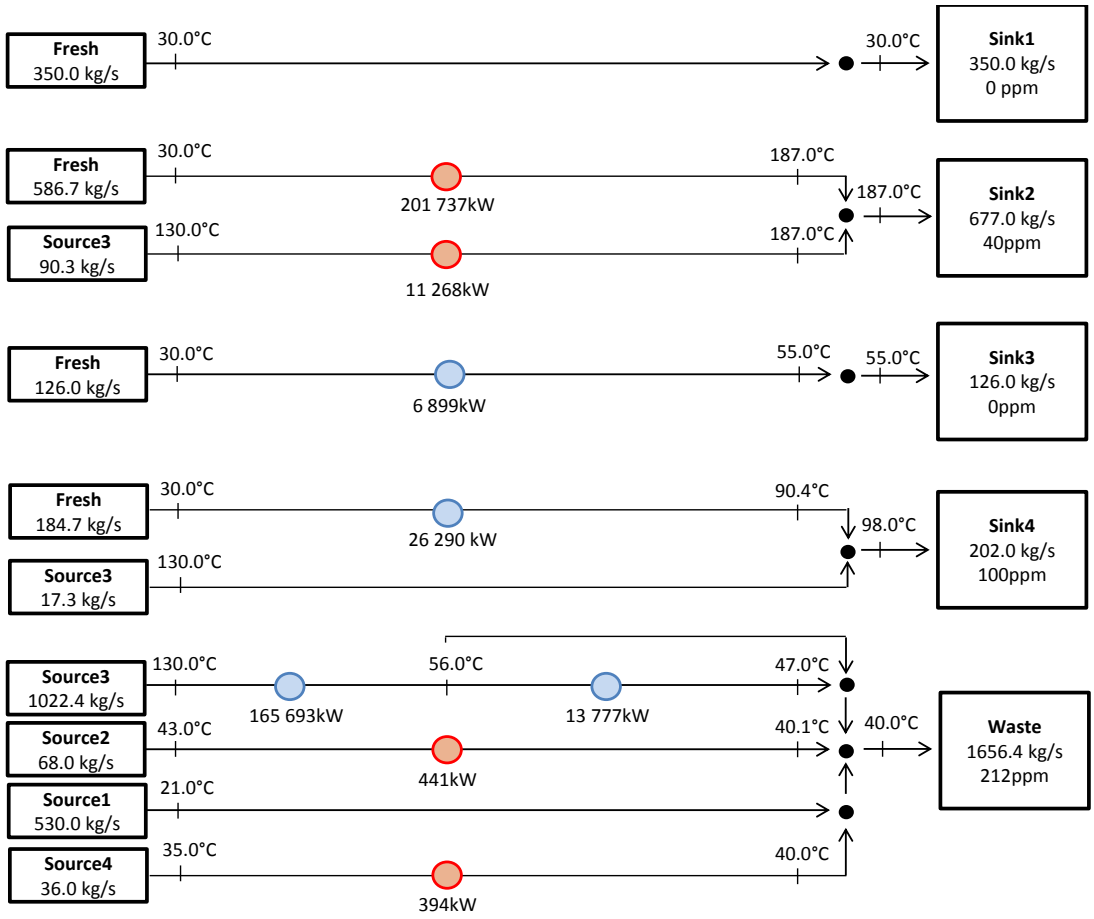

Figure 2.14: Optimal HIRAN configuration when $C_{fresh} = 0.01€.ton^{-1}$

This new allocation creates an important cold stream that can be used for cooling purposes and reducing cold utility. This rise in fresh resource consumption is now cost efficient, since the cutback in the utility cost outweighs the raise of fresh resource cost.

This sensitivity analysis validates the fact that if the objective is to reach a global optimum designing an heat-integrated mass allocation network, it is fundamental to optimize fresh resource and thermal utilities simultaneously. The introduced parameter ΔL^{max}_{fresh} (Eq.2.16) allows the relative extension of L_{fresh} search space with the possibility to limit its boundaries.

• **Sensitivity to ΔT_{min}**

The previous study shows that the parameter ΔL_{fresh}^{max} characterizes a compromise between mass and heat integration. This balance can also be modified with the parameter ΔT_{min}.

It is known that the smaller ΔT_{min} is, the smaller the utility targets are. By changing the value of ΔT_{min} and widening the search space for L_{fresh}, the mass allocation network and heat integration are both modified. Note that, even if it is not included in the objective function of M2 model, the overall heat exchangers area required to transfer it between streams will increase when ΔT_{min} decreases.

The influence of ΔT_{min} on both the energy requirements and fresh resource flow rate can be tested for a few nominal costs of fresh resource. Three cases are studied for different values of C_{fresh} (0.05, 0.025 and 0.015€.ton^{-1}). ΔT_{min} varies from $1°C$ to $60°C$ for each case. Results are shown in Fig.2.15, 2.16 and 2.17.

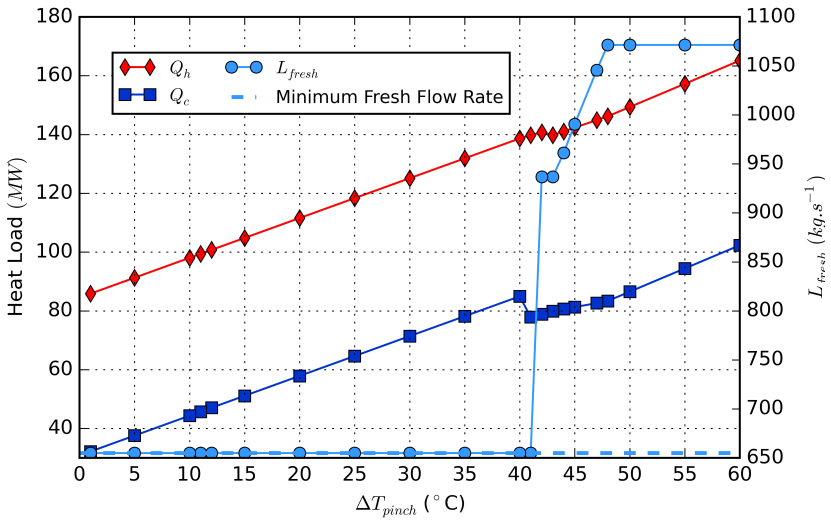

Figure 2.15: Sensitivity analyses of Q_h, Q_c and L_{fresh} to ΔT_{min} - $C_{fresh} = 0.05€.ton^{-1}$

The evolution of the fresh resource flow rate (and the HIRAN design) with ΔT_{min} depends on the cost of the fresh source. As long as C_{fresh} remains high enough (here above 0.015€.ton^{-1}), L_{fresh} is equal to its minimum value L_{fresh}^{min} when ΔT_{min} is small. When ΔT_{min} increases, it reaches values where L_{fresh} starts to rise and the mass allocation network changes ($\Delta T_{min} \geq 40°$ when $C_{fresh} = 0.05€.ton^{-1}$, $\Delta T_{min} \geq 10°$ when $C_{fresh} = 0.025€.ton^{-1}$). This implies that as long as the internal heat recovery allows having relatively low external energy requirements (for low values of ΔT_{min}), it is unnecessary to consume more fresh resources.

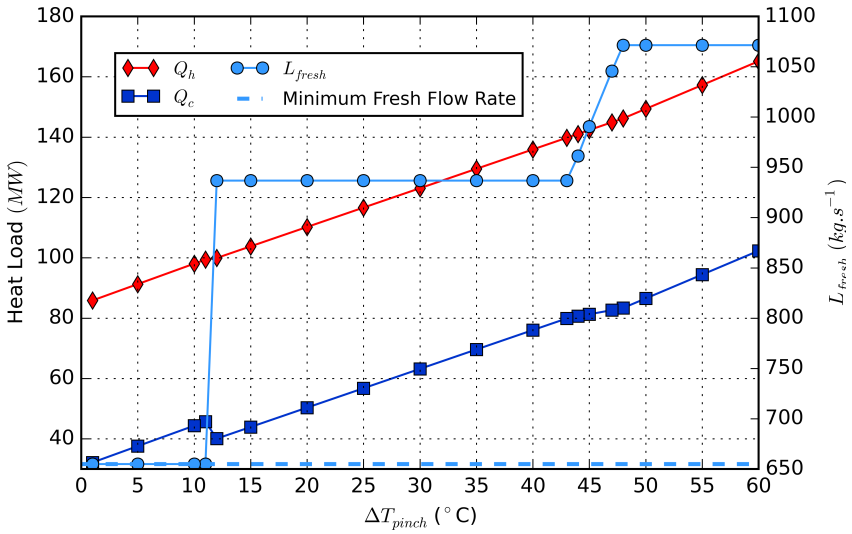

Figure 2.16: Sensitivity analyses of Q_h, Q_c and L_{fresh} to ΔT_{min} - $C_{fresh} = 0.025€.ton^{-1}$

However, at one point, depending on C_{fresh} and ΔL_{fresh}, the previous mass allocation network will no longer be the most efficient energy-wise and an adjustment of L_{fresh} will result in a downturn in utility targets and a reduction of the operating cost (Fig.2.15 and Fig.2.16).

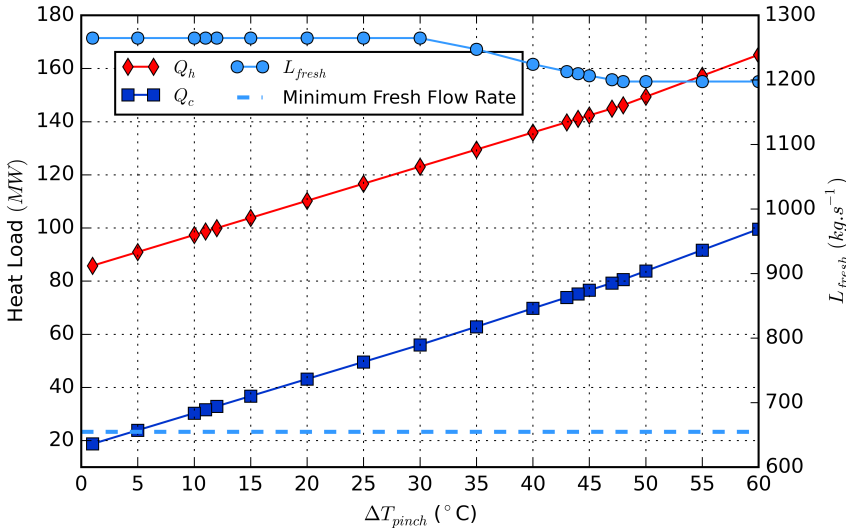

Figure 2.17: Variation of Q_h, Q_c and L_{fresh} - $C_{fresh} = 0.015€.ton^{-1}$

The situation is different when C_{fresh} drops low enough (below $0.015€.ton^{-1}$) as shown in Fig.2.17. Even when ΔT_{min} becomes very small, the fresh resource cost is so low that it is economically more relevant to allocate fresh resources to process sinks and process sources to the waste treatment unit.

The overall cost is optimized; but, the energy consumption of the network is more significant. When ΔT_{min} increases, heat integration is no longer optimized and a downward adjustment of the fresh resource flow rate L_{fresh} needs to be done (Fig.2.17).

In every case, the annual operating cost decreases with ΔT_{min} because the opportunities of internal heat recovery are more important; however, as previously mentioned, the capital costs will also increase. Therefore, the optimal structure of the HIRAN must take into account the capital investments required to realize the heat exchanges within the process. The model M3 able to address this problem is presented in Chapter III.

- **Sensitivity to N_{split}^{max} and ΔT_{step}^{max}**

N_{split}^{max} defines how streams can be split in non-isothermal cases. In this example, its variation has no direct effect on the optimum values of L_{fresh}, Q_h, Q_c and the total cost, since many configurations are able to achieve minimum mass and energy requirements. The only measurable effect is on the computation time (t_{comp}).

Table 2.5 gives the computation times depending on the values of C_{fresh} and N_{split}^{max}.

C_{fresh} (€.ton^{-1})	N_{split}^{max} -	Q_h (MW)	Q_c (MW)	L_{fresh} ($kg.s^{-1}$)	t_{comp} (sec)
0.09	1 - 50	131.9	78.2	1063.9	6.30 - 0.20
0.03	1 - 50	129.5	69.6	1345.7	0.10 - 0.20
0.01	1 - 50	129.5	62.8	1656.4	0.01

Table 2.5: Optimal targets and computation time depending on N_{split}^{max} and C_{fresh} with $\Delta T_{step}^{max} = 5°C$

For the cases tested, the computation time ranges from 0.01 and 6.30 seconds, depending on N_{split}^{max} value. Longer computation times are necessary when N_{split}^{max} has a small value (1 or 2), and when the ratio between fresh resource and cold utility costs are closed because there are no main driver for the solution. Note that in most of cases, the HIRAN remains identical as N_{split}^{max} varies because. This parameter will take a greater importance when the capital costs will be included in the objective function because it will influence the heat exchangers design.

Table 2.6 illustrates the influence of ΔT_{step}^{max} on the computation time and the variables number (binary (N_{binary}) and continuous ($N_{non-zeros}$)).

N_{split}^{max}	1				10			
ΔT_{step}^{max} $(°C)$	1	5	10	35	1	5	10	35
$N^{'}$	207	57	42	34	207	57	42	34
t_{comp} (s)	0.9	≤0.1	≤0.1	≤0.1	0.3	≤0.1	≤0.1	≤0.1
$N_{constraints}$	1 762	570	478	467	1 758	569	466	455
$N_{continuous}$	1 084	326	260	246	1 084	326	260	246
$N_{binaries}$	1 434	404	306	275	1 418	401	283	256
$N_{non-zeros}$	25 434	3 552	2 598	2 522	25 405	3 549	2 525	2 451

Table 2.6: Computation statistics depending on N_{split}^{max} and ΔT_{step}^{max} with $C_{fresh} = 0.09€.ton^{-1}$

In this particular case, ΔT_{step}^{max} has no influence on the optimal targets, but, like N_{split}^{max}, it affects the computation time and the variables number. As it increases, the computation time and the number of variables decrease. In addition, for a given ΔT_{step}^{max}, if N_{split}^{max} increases, the number of variables will remain roughly the same, but the computation time will be shortened. It shows that, in this case, stricter constraints have a stronger effect on the computation time than on the variables number.

N_{split}^{max} will have an effect on the optimal network configuration if capital costs are taken into account in the objective function with the operation costs simultaneously. Indeed, it will strongly influence the number of heat exchangers needed, the size of their areas, and consequently the total cost.

Obviously, these conclusions are case-specific, and, with another set of data, these particular evolutions may change. However, the fact remains that mass and heat integration are resolutely correlated, and it is essential to optimize both of them simultaneously.

2.3.2 Multi-properties case: Phenol Production Process

The second case study presented by Kheireddine et al. [68] concerns the reuse of wastewater in phenol production process. Phenol is produced from cumene hydroperoxide (CHP) (Fig. 2.18). The purpose of this case is to validate the interest of simultaneous over sequential optimization on a more complex case than the previous one. It also demonstrates the use and influence of technical constraints on the optimal targets.

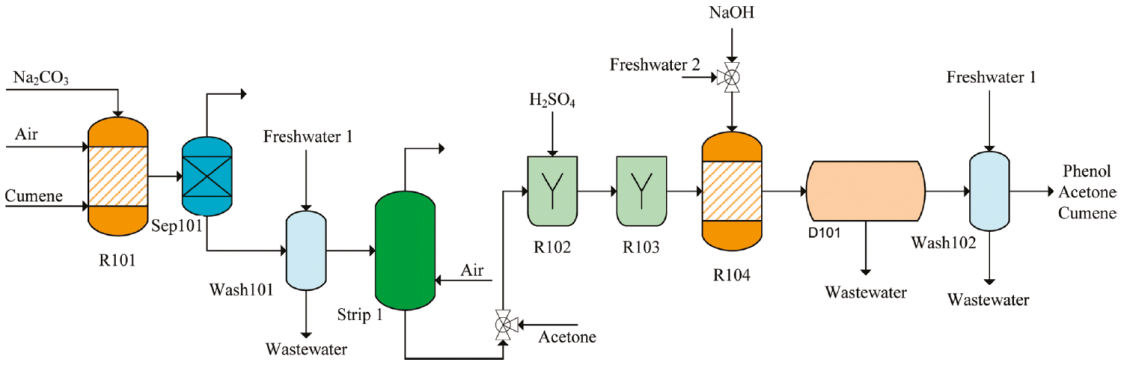

Figure 2.18: Phenol production flow sheet

Only one contaminant is considered, which phenol is. Streams are characterized by two properties in addition to temperature: pH and the vapor pressure in phenol. The economic data and chosen parameters for this study are shown in Table 2.7 and Table 2.8, respectively. In this case, two fresh sources with different features (temperature, properties, composition and cost) are used.

	Flow rate ($kg.h^{-1}$)	Comp. in Phenol (mass fraction)	p_v (kPa)	pH	Temperature ($°C$)
Sink					
Washer 101	2718	0.0 - 0.013	20.0 - 47.0	4.5 - 7.0	60
Washer 102	1993	0.0 - 0.013	4.0 - 38.0	4.0 - 8.0	78
R104	1127	0.0 - 0.100	3.0 - 25.0	4.5 - 7.0	40
Waste		0.0 - 0.150		5.0 - 9.0	30
Source					
Washer 101	3661	0.016	38.0	5.4	85
Decanter 101	1766	0.024	25.0	5.1	65
Washer 102	1485	0.220	7.0	4.8	40
Freshwater 1		0.000	3.0	7.0	25
Freshwater 2		0.012	6.0	6.8	35

Heat capacity $= 4.2kJ.kg^{-1}.K^{-1}$;
Temperature of cold utility $= 10 - 10.1°C$; Temperature of hot utility $= 100 - 99.9°C$

Table 2.7: Phenol production case - Process Data

Economic data		*Parameters*	
C_{fresh1}	$3.0\ €.ton^{-1}$	h_{op}	8000 hrs
C_{fresh2}	$1.0\ €.ton^{-1}$	ΔL^{max}_{fresh}	900 %
C_{waste}	$0.0\ €.ton^{-1}$	ΔT_{min}	$10\ °C$
C_{hot}	$0.01\ €.kWh^{-1}$	ΔT^{max}_{step}	$5\ °C$
C_{cold}	$0.0025\ €.kWh^{-1}$	N^{max}_{split}	3

Table 2.8: Phenol production case - Economic Data and Calculation Parameters

For this case study, the properties characterizing the streams are pH and the vapor pressure (p_v). Their respective mixing rules are defined by the functions (Φ_{pH}) and (Φ_{p_v}): $\Phi_{pH}(p) = 10^p$ and $\Phi_{p_v}(p) = p$.

2.3.2.1 Influence of on-site constraints on the minimum fresh consumption

Several possible on-site constraints are tested to show their impact on the results of the M1 model which are the minimum global fresh resource consumption and waste generation (Table 2.9). The theoretical minimum global fresh resource consumption and waste to be treated is obtained when no constraints are set (case 1). The results are $973.0 kg.h^{-1}$ and $2047.0 kg.h^{-1}$ respectively.

If one tries to limit the use of the fresh resource $Fresh1$ by limiting the maximum flow rate that can be allocated from this source to each sink to $300 kg.h^{-1}$ (case 2), the resulting global consumption and waste production will increase to $1733.3 kg.h^{-1}$ and $2807.3 kg.h^{-1}$. Note that a solution still exists.

Limiting the use of one fresh resource can be done in other way. For instance, if the total use of the fresh resource $Fresh2$ is limited to $200.0 kg.h^{-1}$ (case 3), one can observe that this particular constraint has no influence on the optimal global fresh resource consumption because this source is not used in case 1.

Case $n°$	Constraints	Solution Exists	L_{Fresh1} $(kg.h^{-1})$	L_{Fresh2} $(kg.h^{-1})$	L^{min}_{fresh} $(kg.h^{-1})$	G^{min}_{waste} $(kg.h^{-1})$
1	No constraints	Yes	973.0	0.0	973.0	2 047.0
2	$L_{Fresh1} = 300 kg.h^{-1}$	Yes	600.0	1 133.3	1 733.3	2 807.3
3	$L_{i,Fresh1} \leq 200 kg.h^{-1}$	Yes	973.0	0.0	973.0	2 047.0
4	$L^{exist}_{R104,Fresh2} = 500 kg.h^{-1}$	Yes	938.9	500.0	1 438.9	2 512.9
5	$L^{exist}_{Washer2,Fresh1} = 0 kg.h^{-1}$	Yes	509.6	1 494.8	2 004.4	3 078.4
6	$G_{Waste} \leq 2000 kg.h^{-1}$	No	-	-	-	-
7	$N_{Decanter} \leq 2$	Yes	1 100.4	0.0	1 100.4	2 174.4

Table 2.9: Minimum Fresh Resources and Waste for different technical constraints

The process flow sheet shows that the fresh resource $Fresh2$ is used to feed the reactor $R104$. A pipeline connecting those two points of the process may exist already. Therefore, one may want to keep using this line. If one imposes that $Fresh2$ sends $500.0 kg.h^{-1}$ to $R104$ (case 4), then the optimization results in an increase of the global fresh resource consumption ($1\ 438.9 kg.h^{-1}$).

The process flow sheet also shows that the fresh resource $Fresh1$ is used to feed the sink $Washer2$. If this allocation is forbidden (case 5), it causes a strong increase in fresh resource consumption ($2\ 004.4 kg.h^{-1}$) and a strong increase in waste generation ($3\ 078.4 kg.h^{-1}$).

One can face specific limitations on site, such as limited capacity of the waste treatment unit (for instance, limited to $2\ 000.0 kg.h^{-1}$ (case 6)), or limitations on the number of pipes that can be installed at one place in the process (for instance, the number of allocations of the source $Decanter1$ cannot exceed 2 (case 7)). In case 6, the limitation cannot comply with the mass balances; therefore there are no feasible solutions. In case 7, the limitation generates an increase in fresh resource use compared to the initial case.

The results of this study show the influence of technical constraints on the optimal solution and the necessity to consider them at an early stage of the network design. Certain constraints result in doubling the fresh resource consumption, which can direct the user towards other solutions early on in the design process.

2.3.2.2 Influence of on-site constraints on the annual operating cost, resource consumption and utility requirements

The model M2 that optimizes the AOC of the HIRAN will show the influence of heat integration and the technical constraints on the performances of the optimal solution. The previous technical are used again. The M2 model formulation allows comparing two strategies of optimization: sequential and simultaneous. Table 2.10 and Table 2.11 show the results of these two strategies.

By setting $\Delta L_{fresh}^{max} = 0\%$, Eq.2.16 forces the global fresh resource to be equal to its minimum found with the M1 model. The cost optimization targets the minimum energy consumption, as the global fresh resource target is fixed and set to its minimum value.

By setting $\Delta L_{fresh}^{max} = 900\%$, the global fresh resource mass flow rate can go up to 10 times its minimum value. The model calculates the optimal mass and energy targets simultaneously, within the defined search space for the global fresh resource consumption.

The first thing to note is that simultaneous optimization always gives better, or at least similar, results than sequential optimization in terms of AOC.

Case n°	L_{Fresh1} $(kg.h^{-1})$	L_{Fresh2} $(kg.h^{-1})$	L_{fresh} $(kg.h^{-1})$	G_{waste} $(kg.h^{-1})$	Q_h (kW)	Q_c (kW)	AOC $(\times 10^3 €)$
1	973.0	0.0	973.0	2 047.0	0.0	98.8	43.1
2	600.0	1 133.3	1 733.3	2 807.3	0.0	107.6	45.0
3	973.0	0.0	973.0	2 047.0	0.0	98.8	43.1
4	938.9	500.0	1 438.9	2 512.9	0.0	101.9	46.9
5	509.6	1 494.8	2 004.4	3 078.4	1.2	111.4	47.4
6	-	-	-	-	-	-	-
7	1 100.4	0.0	1 100.4	2 174.4	0.0	98.0	46.0

Table 2.10: Results for different technical constraints - (sequential strategy)

Case n°	L_{Fresh1} $(kg.h^{-1})$	L_{Fresh2} $(kg.h^{-1})$	L_{fresh} $(kg.h^{-1})$	G_{waste} $(kg.h^{-1})$	Q_h (kW)	Q_c (kW)	AOC $(\times 10^3 €)$
1	803.9	317.6	1 121.5	2 195.5	0.0	101.6	**42.2**
2	600.0	1 133.3	1 733.3	2 807.3	0.0	107.6	45.0
3	866.5	200.0	1 066.5	2 140.5	0.0	100.6	42.5
4	827.8	722.7	1 550.0	2 624.0	0.0	103.8	46.4
5	509.6	1 494.8	2 004.4	3 078.4	**1.2**	111.4	**47.4**
6	-	-	-	-	-	-	-
7	803.9	317.6	1 121.5	2 195.5	0.0	101.6	**42.2**

Table 2.11: Results for different technical constraints - (simultaneous strategy)

In the cases where the results are better (cases 1, 3, 4 and 6), the global fresh resource consumption increases compared to its minimum value found with the first model. It highlights the coupling between mass and heat integration. Optimal mass integration can lead to poor heat integration. Therefore, their optimization should be considered simultaneously.

Moreover, the technical constraints for mass integration can result, but not all the time, in constraints for heat integration (for instance in cases 2 and 6). Note that in case 5, the minimum of heating requirement is not equal to $0.0kW$ contrary to the other cases. In this case, the constraint limits the possibilities for optimal heat integration, because not enough heat (at the right temperature) can be found within the process. If a subsequent analysis is led on the capital investments, the solution may not be deemed profitable enough. Thus, another solution needs to be found.

Overall, the optimization of the mass allocation network requires considering the influence of heat integration and technical constraints early in the design process. The proposed methodology allows testing several sets of constraints and several optimization strategies. The set of solutions found can then be analyzed more precisely to determine its economic and technical feasibility on-site.

2.4 Conclusion

In this chapter, two linear models (M1 and M2) are presented for targeting minimal total operating cost of an heat-integrated resource allocation network. The M1 model determines the minimum fresh resource flow rate. Then, the M2 model (that includes M1) targets the minimum annual operating cost of the HIRAN considering, in one objective function, the fresh resource consumption, waste discharge treatment and thermal utilities costs. The result of the M1 model is used to bind the global resource consumption of the problem in the M2 problem.

The proposed models allow characterizing more precisely the industrial process (multiple properties) and design several optimized heat integrated mass allocation network taking into account real on-site constraints. Even if the M2 model is able to solve on its own the HIRAN problem by optimizing the TAC, using the M1 model via the two steps methodology allows having a better understanding of the material reuse potentials of the studied case before considering the influence of the bargain between the mass and heat requirements on the HIRAN design.

The two case studies presented in this work provided some interesting results about the proposed models:

First of all, in comparison with existing methodologies found in the literature, the proposed linear models can achieve similar or in some cases better results. This is due to the fact that they allow targeting minimal total operating cost of a heat integrated mass allocation network while taking into account mass/energy targets simultaneously, and the possibility of non-isothermal mixing of mass streams helps reducing further the heat requirements of the studied case. Simultaneous optimization of mass and heat requirements yields better results than sequential strategies.

Then, several sensitivity analyses have been led to have a better understanding of the influence of parameters on the optimal solution. The main results of these analyses are:

- The studies on ΔL_{fresh}^{max} and the cost associated with the fresh source showed that they can have a considerable influence on the optimal solution. The optimal configurations, depending on the cost structure of the problem, are not necessarily obtained when L_{fresh} is set at its minimum amount. Therefore, it is fundamental to optimize fresh resource and thermal utilities simultaneously.

- The heating and cooling part of annual operating cost decreases with ΔT_{min} because the opportunities of internal heat recovery are more important. However, decreasing implies the use of larger heat exchange areas to realize the heat transfers between mass streams which will consequently increase the capital costs. Therefore, the optimal structure of the HIRAN must take into account the capital investments

required to realize the heat exchanges within the process and properly assess the costs and benefits of heat recovery.

- ΔT_{step}^{max} and N_{split}^{max} have affected the number of variables and slightly the computation time but not really the solution found at this step. They will have a stronger impact on the optimal solution (and computational features of the problem) when the heat exchanger network capital costs will be taken into account in the objective function with the operation costs simultaneously. Indeed, they will strongly influence the number and features of heat exchangers required for the actual implementation of the HIRAN.

Finally, real on-site constraints can be addressed by the models formulation and have been taken into account in the second case study. It shows that considering them is essential because they can have a strong impact on the feasibility and performances of the solution.

After optimizing the operating costs and evaluating the potential savings that can be gained from the heat and mass recovery, the evaluation of the capital investments necessary to implement the networks will decide whether if the proposed solution is economically viable or not. The next chapter presents the following step of the methodology: the MILP model M3 which optimizes the mass allocation and heat exchanger networks (MAHEN) operating and capital costs simultaneously.

Chapter 3

Simultaneous mass allocation and heat exchanger networks design

The model developed in the previous chapter was looking for ways to reuse or recycle waste effluents as mass and energy resources; hence, reducing operating costs. However, those solutions imply additional capital expenditures. Therefore, there is a need to design economically interesting solutions that realize a compromise between reducing energy and resources consumption, waste generation and investing in extra capital costs related to mass and heat recovery networks.

In this chapter, a new mixed integer linear programming model (M3) is established to optimize the total annualized cost of an heat-integrated mass allocation network and its heat exchanger network. The model takes into account operating costs as previously detailed and capital costs (heat exchanger costs related to their existence and exchange area) simultaneously. This work has been published in an article [52].

Additional opportunities to minimize the HEN costs are included in the problem structure by reducing the number of heat exchangers. Indeed, these possibilities are based on numerical objects called mixer and splitter units that allows taking advantage of the capacity of mass streams to mix before being interacting with the HEN and split in between allocations. Their purpose is to reduce the number of streams participating in the HEN. A methodology is developed to assist in their selection based on a modified M2 model (M2'). This methodology has been presented in a published article [51]

First, in this chapter, the problem definition and the new objects useful to obtain an optimal solution are presented. Then, the additional equations to the first two models (M1 and M2) regarding the HEN design are detailed. And finally, the performances of the M3 model are demonstrated thanks to the two case studies previously mentioned in Chapter II. The first case study illustrates the performances of the proposed model compared to literature results. The second case study shows the capacity of the methodology to reduce the HEN costs and improve the solution by using and selecting proper mixer units.

3.1 Problem Statement

The models M1 and M2 described in the previous chapter were able to find an optimal way to reuse waste effluents within the process, recovering heat and matter from them while minimizing the operating costs. For this purpose, the model M2 characterized the heat requirements of the mass streams generated to design the optimal HIRAN. However, implementing the proper solution requires an evaluation of the capital investments; that is the costs of the heat exchanger networks associated with the mass allocation network (Fig.3.5).

Depending on the actual cost of setting up of the heat exchanger network, it may be necessary to deviate from the optimal solution of the M2 model with minimum operating costs. That is why the objective of the new model (M3) is to optimize the total annualized cost of both the mass allocation and heat exchange networks, taking into account capital and operating costs over a time period time at a given actualization rate simultaneously.

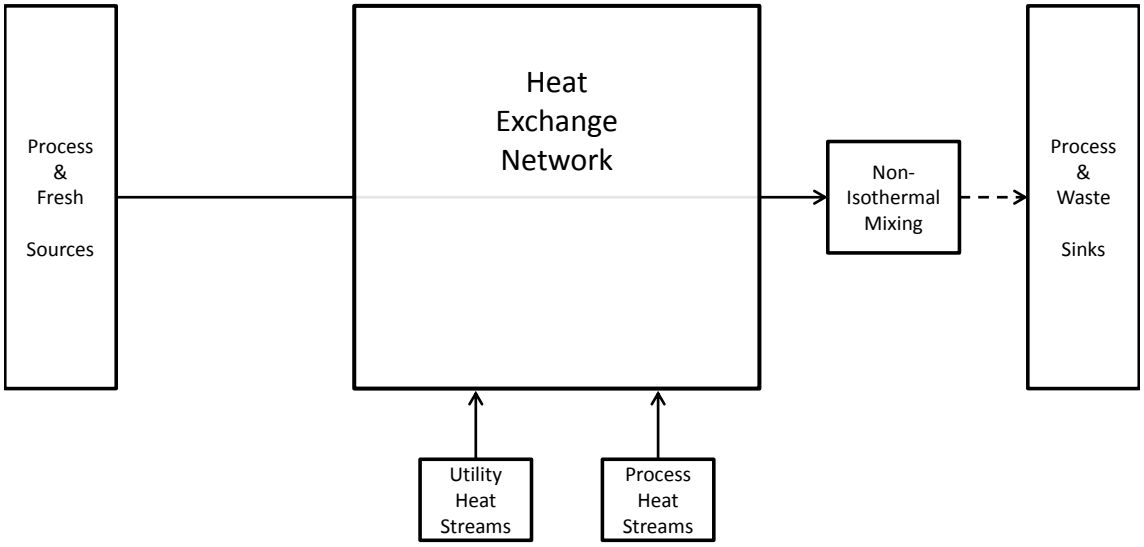

Figure 3.1: Schematic representation of interactions between the MAN and HEN

However, in the current formulation of the model, each mass stream allocated to a given sink is considered individually in the heat exchanger network. This can result in an important number of heat exchange units (Fig.3.2).

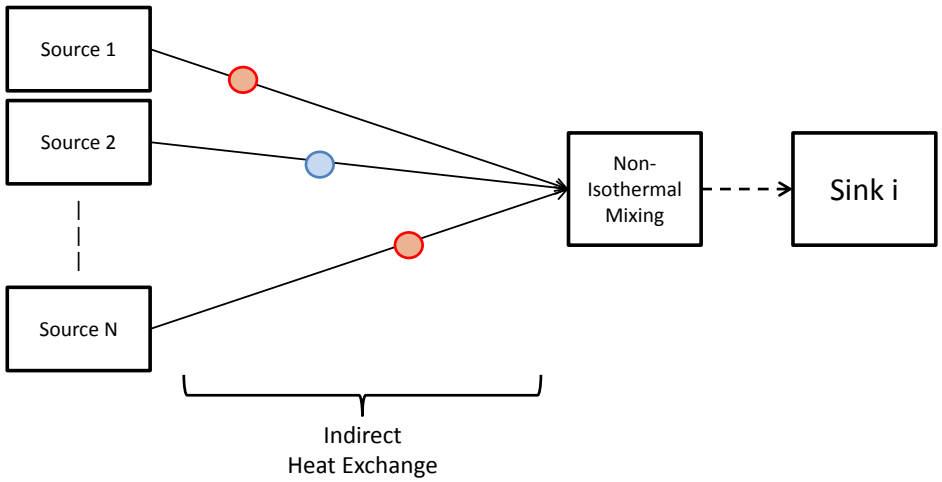

Figure 3.2: Problematic regarding the number of heat exchangers with the current model formulation

In reality, mass streams allocated to a given sink can potentially mix before exchanging heat in the HEN (Fig.3.3); thus, reducing the number of heat exchangers.

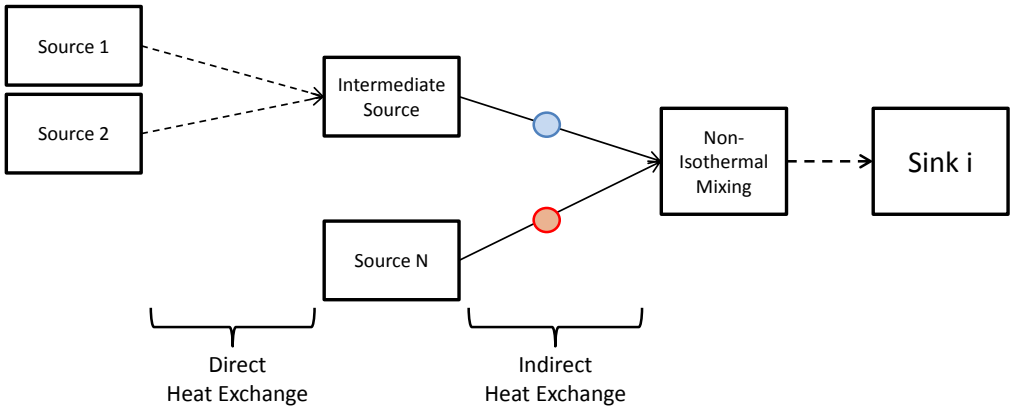

Figure 3.3: Possibility of mass streams mixing before the HEN

Similarly, in reality, one mass stream provided by a given source can also be split after the HEN and then be allocated to a given sink, which can also reduce the number of heat exchangers required to implement the recovery networks. These possibilities are described by non-linear equations because flow rates and temperatures are variables. Consequently, numerical objects must be added to the available elements of the new model formulation (Fig.3.4) to keep it linear: **mixer units** ($mu \in MU(i)$) and **splitter units** ($su \in SU(j)$).

Their purposes and characteristics are described in more details in following paragraphs 3.1.1 - 3.1.2.

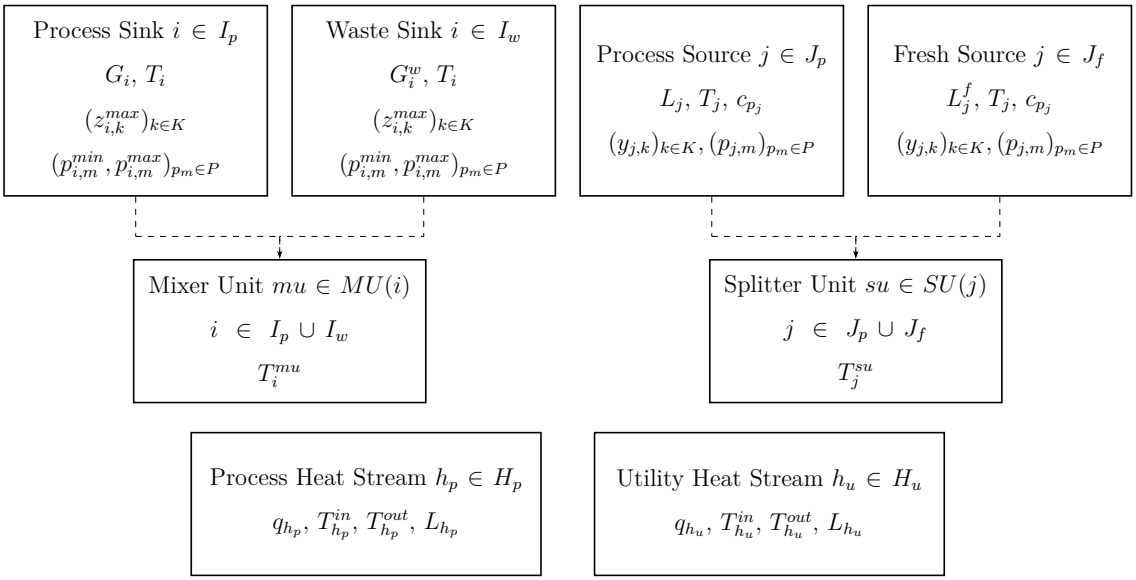

Figure 3.4: Elements and notations of the M3 model

Fig.3.5 presents the new superstructure of the problem with its elements and their interactions:

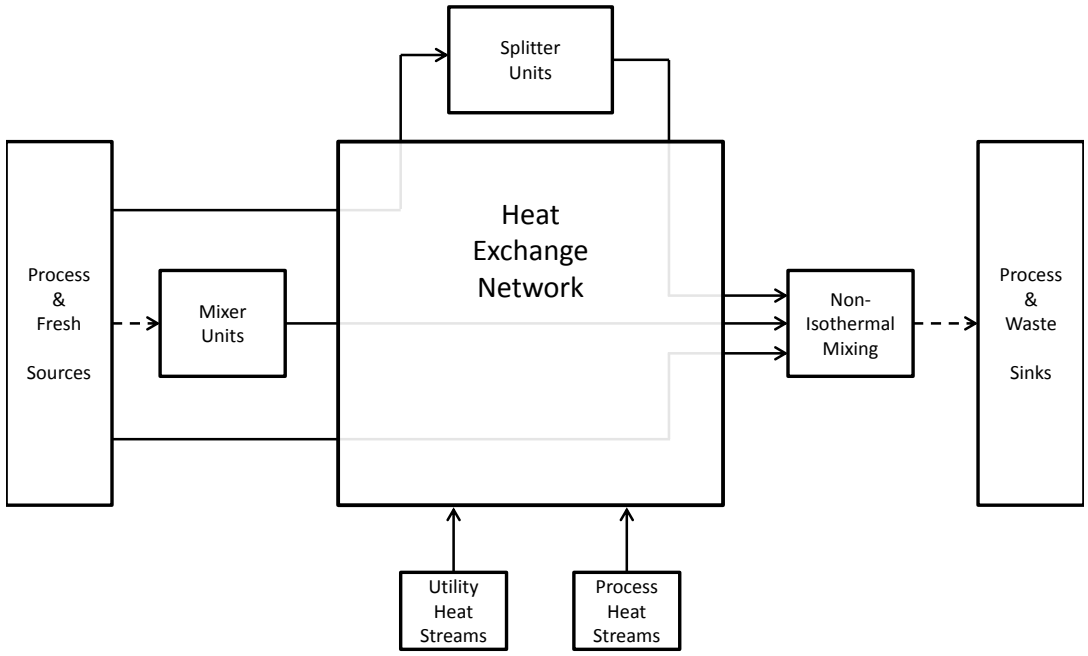

Figure 3.5: New schematic representation of interactions between the MAN and HEN

3.1.1 Mixer unit representation

A mixer unit model is proposed to represent mass streams mixing before heat integration. Its purpose is to reduce the number of heat exchangers if it has an economic interest. It is characterized by a fixed temperature and is associated with a specific sink. The resulting stream must have a temperature equal to the mixer unit temperature. A sink (process or waste) can have any number of mixer units. Mass streams created between sources and mixer units do not take part in the HEN.

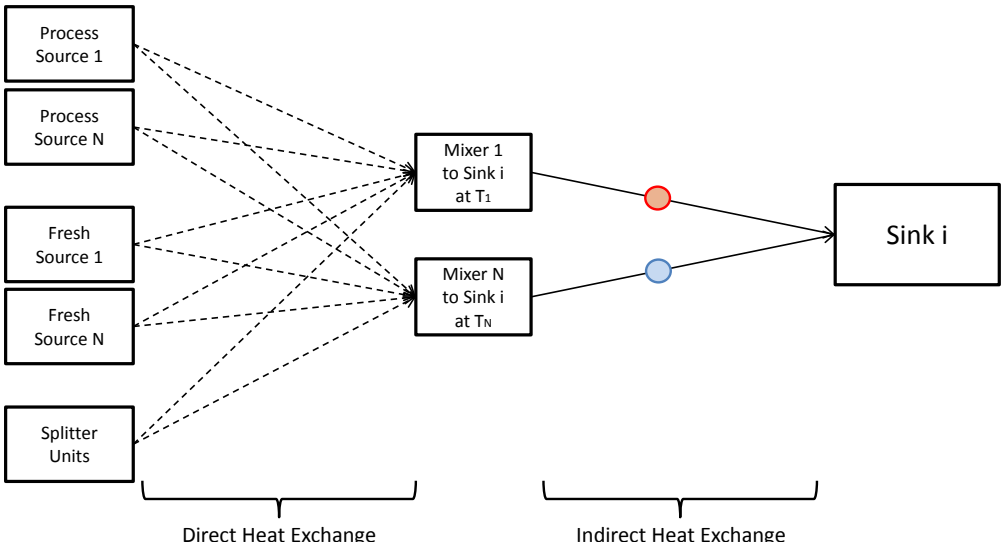

Figure 3.6: Mixer Units

A methodology for searching a proper mixer unit's temperature has been developed and presented by Ghazouani et al. [51]. The objective is to select in advance the mixer unit temperature to avoid using multiple mixer units which can increase significantly the size of the problem.

The idea is to calculate what could be the MAHEN total annualized cost by estimating the HEN costs without designing it. This model enables testing multiple mixer units at different temperatures with a simpler and faster model and selecting a suitable temperature, thus limiting the problem size of the full MAHEN design model presented in the following section 3.2. This methodology is presented in paragraph 3.2.5. However, using fixed temperatures limits the search space for the optimal solution because resulting mixing temperature belongs to a discrete set of temperatures. Therefore, a new parameter ΔT_{mu}^{max}, specific to each mixer unit, is introduced to characterize a temperature range around its given temperature: $[T_j^{mu} - \Delta T_{mu}^{max}; T_j^{mu} + \Delta T_{mu}^{max}]$.

The resulting temperature variation is associated with an excess or a shortage of heat which will be taken into account in the design of heat exchangers involving the mixer unit outlet stream.

3.1.2 Splitter unit representation

When a specific source is allocated to multiple sinks and if some of these mass streams must be heated up or cooled down, it could be economically interesting to realize the heat exchange for all of them at once instead of using a dedicated heat exchanger for each one (Fig.3.7). That is why splitter units are introduced in the superstructure. To describe them with linear equations, each splitter unit is characterized by a fixed temperature and is related to a specific source. A source can have multiple splitter units.

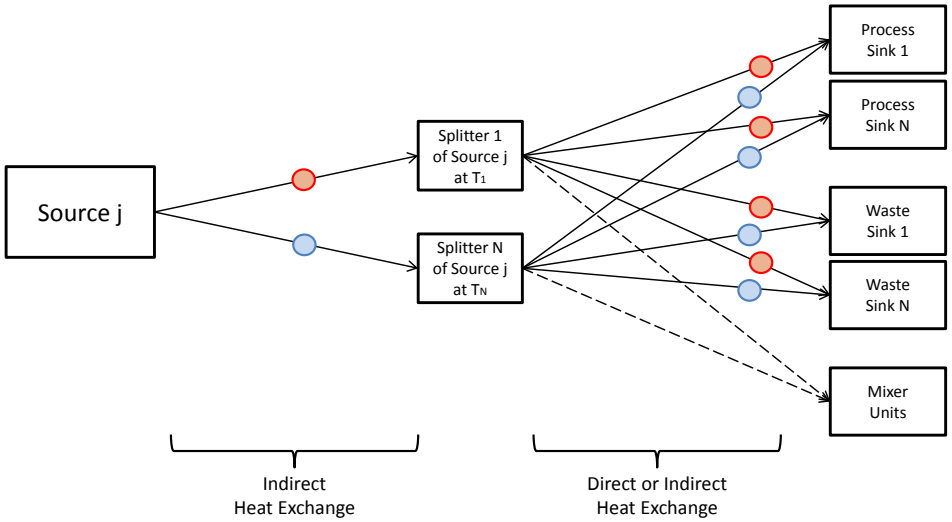

Figure 3.7: Splitter Units

Splitter and mixer units have very comparable behaviors. Therefore, similar principles of selection and relaxation of their temperature developed for the mixer units can be applied to splitter units to overcome the limitation of the search space due to predefined fixed temperature. Indeed, the integration of heat surplus or shortage related to this possible splitter unit temperature variation has to be included in the design of heat exchangers located before and after the splitter unit. This is very similar to the theoretical developments done for the mixer units.

3.2 Model Formulation - 3^{rd} MILP: MAHEN optimal design (M3)

The equations of the models M1 and M2 presented in Chapter II are included in the new model (M3) formulation. Some of them are modified to include mixer and splitter units. New specific equations concerning the ones characterizing the design of the HEN as well as the properties of mixer and splitter units are presented.

3.2.1 Mass Balance

The mass balance equations presented in the section 2.2.1.1 are modified to include the mixer and splitter units. For each process sink $i \in I_p$, the mass flow rate requirement (G_i) has to be met by a linear combination of all sources (L_{ij}), splitter units (L_{ij}^{su}) and associated mixer units (L_{ij}^{mu}) mass flow rates, while never exceeding the maximum allowable mass load ($z_{i,k}^{max}$) for each contaminant $k \in K$:

$$\forall i \in I_p, \sum_{j \in J_p \cup J_f} L_{ij} + \sum_{su \in SU(j)} \sum_{j \in J_p \cup J_f} L_{ij}^{su} + \sum_{mu \in MU(i)} \sum_{j \in J_p \cup J_f} L_{ij}^{mu} = G_i \tag{3.1}$$

$$\begin{aligned} &\forall i \in I_p, \forall k \in K, \\ &\sum_{j \in J_p \cup J_f} L_{ij} \times y_{j,k} + \sum_{su \in SU(j)} \sum_{j \in J_p \cup J_f} L_{ij}^{su} \times y_{j,k} \\ &\qquad + \sum_{mu \in MU(i)} \sum_{j \in J_p \cup J_f} L_{ij}^{mu} \times y_{j,k} \leq G_i \times z_{i,k}^{max} \end{aligned} \tag{3.2}$$

For each waste sink $i \in I_w$, the total mass flow rate (G_i^w) treated by the sink, which is a result of the optimization, is equal to a linear combination of all sources and associated mixer units mass flow rates:

$$\forall i \in I_w, \sum_{j \in J_p \cup J_f} L_{ij} + \sum_{su \in SU(j)} \sum_{j \in J_p \cup J_f} L_{ij}^{su} + \sum_{mu \in MU(i)} \sum_{j \in J_p \cup J_f} L_{ij}^{mu} = G_i^w \tag{3.3}$$

$$\begin{aligned} &\forall i \in I_w, \forall k \in K, \\ &\sum_{j \in J_p \cup J_f} L_{ij} \times y_{j,k} + \sum_{su \in SU(j)} \sum_{j \in J_p \cup J_f} L_{ij}^{su} \times y_{j,k} \\ &\qquad + \sum_{mu \in MU(i)} \sum_{j \in J_p \cup J_f} L_{ij}^{mu} \times y_{j,k} \leq G_i^w \times z_{i,k}^{max} \end{aligned} \tag{3.4}$$

Similar equations are used for properties. Each property $p_m \in P$ is characterized by a mixing rule defined by a function ϕ_m. The resulting value of the property p_m must be within the range defined for each sink. Assuming that ϕ_m is an increasing function:

$$\begin{aligned}
&\forall i \in I_p, \forall p_m \in P, \\
&G_i \times \phi_m(p_{i,m}^{min}) \leq \sum_{j \in J_p \cup J_f} L_{ij} \times \phi_m(p_{j,m}) + \sum_{su \in SU(j)} \sum_{j \in J_p \cup J_f} L_{ij}^{su} \times \phi_m(p_{j,m}) \\
&\qquad + \sum_{mu \in MU(i)} \sum_{j \in J_p \cup J_f} L_{ij}^{mu} \times \phi_m(p_{j,m}) \leq G_i \times \phi_m(p_{i,m}^{max})
\end{aligned} \tag{3.5}$$

$$\begin{aligned}
&\forall i \in I_w, \forall p_m \in P, \\
&G_i^w \times \phi_m(p_{i,m}^{min}) \leq \sum_{j \in J_p \cup J_f} L_{ij} \times \phi_m(p_{j,m}) + \sum_{su \in SU(j)} \sum_{j \in J_p \cup J_f} L_{ij}^{su} \times \phi_m(p_{j,m}) \\
&\qquad + \sum_{mu \in MU(i)} \sum_{j \in J_p \cup J_f} L_{ij}^{mu} \times \phi_m(p_{j,m}) \leq G_i^w \times \phi_m(p_{i,m}^{max})
\end{aligned} \tag{3.6}$$

Moreover, for each process source $j \in J_p$, the sum of stream mass flow rates allocated to each sink (process and waste), splitter and mixer units must be equal to its total mass flow rate (L_j):

$$\forall j \in J_p, \sum_{i \in I_p \cup I_w} L_{ij} + \sum_{i \in I_p \cup I_w} \sum_{mu \in MU(i)} L_{ij}^{mu} + \sum_{su \in SU(j)} L_j^{su} = L_j \tag{3.7}$$

Similarly, for each fresh source $j \in J_f$, the total mass flow rate (L_j^f) provided by j, which is a result of the optimization, must be:

$$\forall j \in J_f, \sum_{i \in I_p \cup I_w} L_{ij} + \sum_{i \in I_p \cup I_w} \sum_{mu \in MU(i)} L_{ij}^{mu} + \sum_{su \in SU(j)} L_j^{su} = L_j^f \tag{3.8}$$

For a splitter unit associated with a source, let L_j^{su} representing the mass flow rate between them. Therefore,

$$\forall j \in J_p \cup J_f, \forall su \in SU(j), \sum_{i \in I_p \cup I_w} L_{ij}^{su} + \sum_{i \in I_p \cup I_w} L_{ij}^{su/mu} = L_j^{su} \tag{3.9}$$

where $L_{ij}^{su/mu}$ is the mass flow rate from a splitter unit su associated with a source j to a mixer unit mu associated with a sink i.

A mixer unit associated with a sink i can be fed by all sources and other mixer units related to the same sink (Fig.3.6). Let L_i^{mu} be the variable representing mass flow rate from mixer unit mu to its sink i. Therefore,

$$\forall i \in I_p \cup I_w, \forall mu \in MU(i), \sum_{j \in J_p \cup J_f} L_{ij}^{mu} + \sum_{j \in J_p \cup J_f} \sum_{su \in SU(j)} L_{ij}^{su} = L_i^{mu} \tag{3.10}$$

Note that streams entering a mixer unit from sources or splitter units do not take part in the HEN.

As mentioned in Chapter II (paragraph 2.2.1.2), binary variables (γ_L) are introduced to indicate the existence of a stream including a mixer or a splitter unit.

$$\forall i \in I_p \cup I_w, \forall mu \in MU(i), L_i^{mu} - L_{i,mu}^{max} \times \gamma_{L_i^{mu}} \leq 0 \tag{3.11}$$

$$\forall i \in I_p \cup I_w, \forall j \in J_p \cup J_f, \forall mu \in MU(i), L_{ij}^{mu} - L_{ij,mu}^{max} \times \gamma_{L_{ij}^{mu}} \leq 0 \tag{3.12}$$

$$\forall j \in J_p \cup J_f, \forall su \in SU(j), L_j^{su} - L_{j,su}^{max} \times \gamma_{L_j^{su}} \leq 0 \tag{3.13}$$

$$\forall i \in I_p \cup I_w, \forall j \in J_p \cup J_f, \forall su \in SU(j), L_{ij}^{su} - L_{ij,su}^{max} \times \gamma_{L_{ij}^{su}} \leq 0 \tag{3.14}$$

$$\forall i \in I_p \cup I_w, \forall mu \in MU(i), \forall j \in J_p \cup J_f, \forall su \in SU(j), L_{ij}^{su/mu} - L_{ij,su,mu}^{max} \times \gamma_{L_{ij}^{su/mu}} \leq 0 \tag{3.15}$$

3.2.2 Heat balance

The transshipment model and the related equations presented in Chapter II (paragraph 2.2.2.2) are still used in the M3 model.

Variables are added to account for the extracted mass flow rate at a given temperature level on the scale and the mass flow rate going through the HEN when mass streams are related to a mixer or a splitter unit; the variables ($L_{i,n}^{mu}$, $\widetilde{L}_{i,n}^{mu}$) and ($L_{ij,n}^{su}$, $\widetilde{L}_{ij,n}^{su}$) are defined for these types of mass stream interacting in the HEN as explained in Chapter II.

Note that for a mass stream going from a source to a splitter unit, there are no possible extractions as there is only one source able to feed the splitter unit. Thus, the same mass flow rate goes through each temperature interval unit reaching the splitter unit temperature. For this type of stream, variables ($\widetilde{L}_{j,n}^{su}$) are used.

Fig.3.8 shows the new heat/mass integration superstructure. In this figure, the sources can represent process or fresh sources, splitter unit or mixer units indifferently.

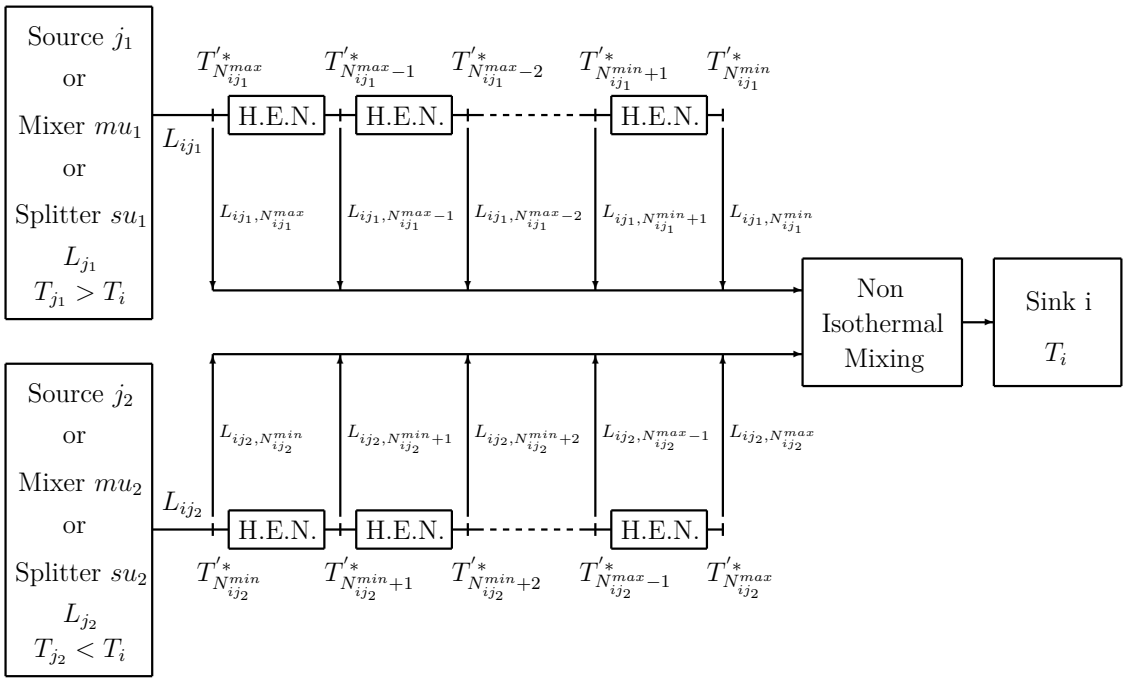

Figure 3.8: Superstructure for mass/heat integration through non-isothermal mixing

The following equations are similar to the ones presented in Chapter II (Eq.2.26 to Eq.2.35) and adapted for mass streams concerning mixer or splitter unit.

The extracted mass flow rate at each temperature level cannot exceed the allocation mass flow rate:

$$\forall i \in I_p \cup I_w, \forall mu \in MU(i), \forall n \in [N^{min}_{i,mu}; N^{max}_{i,mu}], L^{mu}_{i,n} \leq L^{mu}_i \tag{3.16}$$

$$\forall i \in I_p \cup I_w, \forall j \in J_p \cup J_f, \forall su \in SU(i), \forall n \in [N^{min}_{i,su}; N^{max}_{i,su}], L^{su}_{ij,n} \leq L^{su}_{ij} \tag{3.17}$$

The sum of all extractions mass flow rates is equal to the allocation mass flow rate:

$$\forall i \in I_p \cup I_w, \forall mu \in MU(i), \sum_n L^{mu}_{i,n} = L^{mu}_i \tag{3.18}$$

$$\forall i \in I_p \cup I_w, \forall j \in J_p \cup J_f, \forall su \in SU(i), \sum_n L^{su}_{ij,n} = L^{su}_{ij} \tag{3.19}$$

The existence of an extraction at a given temperature level is identified with a binary variable (γ_L):

$$\forall i \in I_p \cup I_w, \forall mu \in MU(i), \forall n \in [N_{i,mu}^{min}; N_{i,mu}^{max}], L_{i,n}^{mu} - \gamma_{L_{i,n}^{mu}} \times L_{i,mu}^{max} \leq 0 \tag{3.20}$$

$$\forall i \in I_p \cup I_w, \forall j \in J_p \cup J_f, \forall su \in SU(i), \forall n \in [N_{i,su}^{min}; N_{i,su}^{max}], \quad L_{ij,n}^{su} - \gamma_{L_{ij,n}^{su}} \times L_{ij,su}^{max} \leq 0 \tag{3.21}$$

Note that the stream from a source to its associated splitter cannot be split because it is the only stream entering the splitter unit.

The remaining part of the stream after each extraction, going through the HEN, is:
For hot mass streams:

$$\forall i \in I_p \cup I_w, \forall mu \in MU(i), \forall n \in [N_{i,mu}^{min}; N_{i,mu}^{max} - 1], L_i^{mu} - \sum_{k=n+1}^{N_{i,mu}^{max}} L_{i,k}^{mu} = \widetilde{L}_{i,n}^{mu} \tag{3.22}$$

$$\forall i \in I_p \cup I_w, \forall j \in J_p \cup J_f, \forall su \in SU(i), \forall n \in [N_{i,su}^{min}; N_{i,su}^{max}], \quad L_{ij}^{su} - \sum_{k=n+1}^{N_{i,su}^{max}} L_{ij,k}^{su} = \widetilde{L}_{ij,n}^{su} \tag{3.23}$$

$$\forall j \in J_p \cup J_f, \forall su \in SU(i), \forall n \in [N_{j,su}^{min}; N_{j,su}^{max}], L_j^{su} = \widetilde{L}_{j,n}^{su} \tag{3.24}$$

For cold mass streams:

$$\forall i \in I_p \cup I_w, \forall mu \in MU(i), \forall n \in [N_{i,mu}^{min}; N_{i,mu}^{max}], L_i^{mu} - \sum_{k=N_{i,mu}^{min}}^{n} L_{i,k}^{mu} = \widetilde{L}_{i,n}^{mu} \tag{3.25}$$

$$\forall i \in I_p \cup I_w, \forall j \in J_p \cup J_f, \forall su \in SU(i), \forall n \in [N_{i,su}^{min}; N_{i,su}^{max}], \quad L_{ij}^{su} - \sum_{k=N_{i,su}^{min}}^{n} L_{ij,k}^{su} = \widetilde{L}_{ij,n}^{su} \tag{3.26}$$

$$\forall j \in J_p \cup J_f, \forall su \in SU(i), \forall n \in [N_{j,su}^{min}; N_{j,su}^{max}], L_j^{su} = \widetilde{L}_{j,n}^{su} \tag{3.27}$$

Each extraction at a temperature level n is sent to the sink i. Let's note N_{ij}^{out}, $N_{i,mu}^{out}$ and $N_{ij,su}^{out}$, the index on the temperature scale of the sink temperature (which is different depending on whether the mass stream is hot or cold).

The resulting mixing temperature must be equal to the sink temperature. Therefore, the heat balance for the mix after the HEN is:

$$\begin{aligned}
&\forall i \in I_p \cup I_w, \\
&\sum_{j \in J_p \cup J_f} \sum_{n=N_{ij}^{min}}^{N_{ij}^{max}} L_{ij,n} \times cp_j \times (T'^{*}_{N_{ij}^{out}} - T'^{*}_{n}) \\
&+ \sum_{mu \in MU(i)} \sum_{n=N_{i,mu}^{min}}^{N_{i,mu}^{max}} L_{i,n}^{mu} \times cp_{mu} \times (T'^{*}_{N_{i,mu}^{out}} - T'^{*}_{n}) \\
&+ \sum_{j \in J_p \cup J_f} \sum_{su \in SU(j)} \sum_{n=N_{ij,su}^{min}}^{N_{ij,su}^{max}} L_{ij,n}^{su} \times cp_{su} \times (T'^{*}_{N_{ij,su}^{out}} - T'^{*}_{n}) = 0
\end{aligned} \tag{3.28}$$

As previously mentioned, streams allocated to a sink through a mixer unit reach a temperature within a range around a characteristic temperature T_i^{mu}. For each mixer unit, this range is defined by a parameter ΔT_{mu}^{max}. Variables q_{mu}^{+} and q_{mu}^{-} are introduced to quantify the excess heat or the heat shortage necessary to reach the optimal mixer unit temperature. If q_{mu}^{+} is not null, it indicates a reduction of its temperature whereas if q_{mu}^{-} is not null, it indicates an increase of its temperature. Therefore, the mass and heat balances of a mixer unit are defined by the following equations:

$$\begin{aligned}
&\forall i \in I_p \cup I_w, \forall mu \in MU(i), \\
&\sum_{j \in J_p \cup J_f} L_{ij}^{mu} \times cp_j \times (T_i^{mu} - T_j) \\
&+ \sum_{j \in J_p \cup J_f} \sum_{su \in SU(j)} L_{ij}^{mu/su} \times cp_{su} \times (T_i^{mu} - T_{su}) + q_{mu}^{+} + q_{mu}^{-} = 0
\end{aligned} \tag{3.29}$$

With ΔT_{mu}^{max}, it is possible to define the boundaries for q_{mu}^{+} and q_{mu}^{-}:

$$\forall i \in I_p \cup I_w, \forall mu \in MU(i),$$
$$\Bigg(\sum_{j \in J_p \cup J_f} L_{ij}^{mu} \times cp_j + \sum_{j \in J_p \cup J_f} \sum_{su \in SU(j)} L_{ij}^{mu/su} \times cp_{su} + \sum_{mu' \in MU(i)} \sum_{n=N_{mu',mu}^{min}}^{N_{mu',mu}^{max}} L_{mu',n}^{mu} \times cp_{mu'} \Bigg) \times (-\Delta T_{mu}^{max}) \leq q_{mu}^{-} \leq 0 \tag{3.30}$$

$$\forall i \in I_p \cup I_w, \forall mu \in MU(i),$$
$$\Bigg(\sum_{j \in J_p \cup J_f} L_{ij}^{mu} \times cp_j + \sum_{j \in J_p \cup J_f} \sum_{su \in SU(j)} L_{ij}^{mu/su} \times cp_{su} + \sum_{mu' \in MU(i)} \sum_{n=N_{mu',mu}^{min}}^{N_{mu',mu}^{max}} L_{mu',n}^{mu} \times cp_{mu'} \Bigg) \times \Delta T_{mu}^{max} \geq q_{mu}^{+} \geq 0 \tag{3.31}$$

Binary variables are also introduced to indicate which variable is used between q_{mu}^{+} and q_{mu}^{-}, knowing that one of them has to be null:
$\forall i \in I_p \cup I_w, \forall mu \in MU(i),$

$$-q_{mu}^{-} - \gamma_{q_{mu}^{-}} \times Q_{mu}^{max} \leq 0 \tag{3.32}$$
$$q_{mu}^{+} - \gamma_{q_{mu}^{+}} \times Q_{mu}^{max} \leq 0 \tag{3.33}$$
$$\gamma_{q_{mu}^{+}} + \gamma_{q_{mu}^{-}} \leq 1 \tag{3.34}$$

where Q_{mu}^{max} is a big number.

The heat transferred in the HEN, in each temperature interval, is defined as follows:

$$\forall i \in I_p \cup I_w, \forall j \in J_p \cup J_f, \forall su \in SU(i), \forall n \in [N_{i,su}^{min}; N_{i,su}^{max}], \widetilde{L}_{ij,n}^{su} \times cp_{su} \times (T_{n+1}^{'*} - T_n^{'*}) = q_{ij,n}^{su} \geq 0 \tag{3.35}$$

$$\forall j \in J_p \cup J_f, \forall su \in SU(i), \forall n \in [N_{j,su}^{min}; N_{j,su}^{max}], \widetilde{L}_{j,n}^{su} \times cp_j \times (T_{n+1}^{'*} - T_n^{'*}) = q_{j,n}^{su} \geq 0 \tag{3.36}$$

For mixer units, the previous equations are modified to account for the temperature variation from T_i^{mu}. The heat transferred by a stream going from a mixer unit to its associated sink i can be changed in its first temperature interval with q_{mu}^{+} or q_{mu}^{-}. Consequently,

$$\begin{gathered}\forall i \in I_p \cup I_w, \forall mu \in MU(i),\ if\ n = \left\{ \begin{array}{ll} N_{i,mu}^{max} - 1 & \text{for hot streams} \\ N_{i,mu}^{min} & \text{for cold streams} \end{array} \right. , \\ \widetilde{L}_{i,n}^{mu} \times cp_{mu} \times (T_{n+1}^{'*} - T_n^{'*}) - q_{mu}^{+} - q_{mu}^{-} = q_{i,n}^{mu} \geq 0 \end{gathered} \tag{3.37}$$

Thus, the total heat provided (q_n^h) or required (q_n^c) at the n^{th} temperature interval is slightly modified compared to Eq.2.41:

$$\begin{gathered}\forall n \in [0, N^{'} - 1], \\ \sum_{i \in I_p \cup I_w} \sum_{j \in J_p \cup J_f} q_{ij,n} + \sum_{j \in J_p \cup J_f} \sum_{su \in SU(j)} q_{j,n}^{su} \\ + \sum_{i \in I_p \cup I_w} \sum_{mu \in MU(i)} q_{i,n}^{mu} + \sum_{i \in I_p \cup I_w} \sum_{j \in J_p \cup J_f} \sum_{su \in SU(j)} q_{ij,n}^{su} \\ + \sum_{h_p \in H_p} q_{h_p,n} + \sum_{h_u \in H_u} q_{h_u,n} = \left\{ \begin{array}{ll} q_n^h \geq 0 & \text{for all hot mass and heat streams} \\ q_n^c \leq 0 & \text{for all cold mass and heat streams} \end{array} \right. \end{gathered} \tag{3.38}$$

The calculations of the global heating and cooling requirements through heat cascade obey to the same equations introduced in the Chapter II (Eq.2.42 to Eq.2.44).

3.2.3 Heat Exchanger Network

In this part, the model for designing the HEN is presented. Note that it is assumed that a pair of hot and cold streams can be connected by one heat exchanger at most.

3.2.3.1 Notations

The following equations present how to define and characterize a heat exchanger between a hot stream h_1 and a cold stream h_2 (Fig.3.9). h_1 and h_2 can represent either a heat or mass stream.

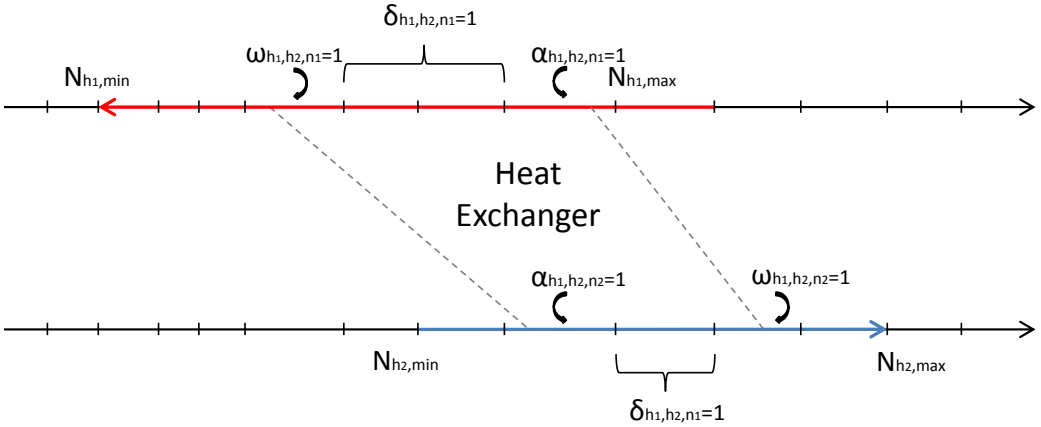

Figure 3.9: Heat exchanger

The heat load transferred from hot stream h_1 in interval n_1 to cold stream h_2 in interval n_2 is represented by q_{h_1,n_1,h_2,n_2}. Let's note q_{h_1,h_2,n_1} the heat load transferred from hot stream h_1 to cold stream h_2 in interval n_1 on the hot side, and q_{h_1,h_2,n_2} the heat load transferred from hot stream h_1 to cold stream h_2 in interval n_2 on the cold side.

Similarly, L_{h_1,h_2,n_1} is the flow rate going through the entire interval n_1 to transfer the heat load from hot stream h_1 to cold stream h_2 in interval n_1 on the hot side, and L_{h_1,h_2,n_2} is the flow rate going through the entire interval n_1 to transfer the heat load transferred from hot stream h_1 to cold stream h_2 in interval n_2 on the cold side.

Binary variables $\gamma_{q_{h_1,h_2,n_1}}$ and $\gamma_{q_{h_1,h_2,n_2}}$are used to indicate whether q_{h_1,h_2,n_1} and q_{h_1,h_2,n_2} are strictly positive, respectively. In the same way, α_{h_1,h_2,n_1}, ω_{h_1,h_2,n_1}, δ_{h_1,h_2,n_1} are binary variables to indicate the beginning, the end or an intermediate part of the heat exchanger between h_1 and h_2 on the hot side in interval n_1. For the cold side, α_{h_1,h_2,n_2}, ω_{h_1,h_2,n_2}, δ_{h_1,h_2,n_2} are introduced.

Finally, n_{h_1,h_2} indicates the number of exchangers between h_1 and h_2, which can be 0 or 1.

3.2.3.2 Heat Balance

Since the temperature scale is defined with shifted temperatures, to ensure that the minimum temperature difference is respected, the heat from the hot side in interval n_1 must be transferred to the cold side in a lower interval n_2, i.e. $n_1 \geq n_2$.

The heat balance must be respected within each interval and on each side of the heat exchanger. Therefore, the heat available from one stream, in a given interval, must be entirely distributed between all heat exchangers connected to it:
For hot streams:

$$\forall h_1 \in H_{hot}, \forall n_1 \in [N_{h_1}^{min}, N_{h_1}^{max} - 1], q_{h_1,n_1} = \sum_{h_2 \in H_{cold}} \sum_{\substack{n_1 = N_{h_1}^{min} \\ n_1 \geq n_2}}^{N_{h_1}^{max}-1} q_{h_1,n_1,h_2,n_2} \tag{3.39}$$

For cold streams:

$$\forall h_2 \in H_{cold}, \forall n_2 \in [N_{h_2}^{min}, N_{h_2}^{max} - 1], q_{h_2,n_2} = \sum_{h_1 \in H_{hot}} \sum_{\substack{n_2 = N_{h_2}^{min} \\ n_1 \geq n_2}}^{N_{h_2}^{max}-1} q_{h_1,n_1,h_2,n_2} \tag{3.40}$$

On the cold side, the heat load transferred from hot stream h_1 to cold stream h_2 in interval n_2 is:

$$\forall n_2 \in [N_{h_2}^{min}, N_{h_2}^{max} - 1], q_{h_1,h_2,n_2} = \sum_{\substack{n_1 = N_{h_1}^{min} \\ n_1 \geq n_2}}^{N_{h_1}^{max}-1} q_{h_1,n_1,h_2,n_2} \tag{3.41}$$

Thus, the mass flow rate that goes through the interval n_2 to transfer the heat load from hot stream h_1 to cold stream h_2 is:

$$\forall n_2 \in [N_{h_2}^{min}, N_{h_2}^{max} - 1], L_{h_1,h_2,n_2} = \frac{q_{h_1,h_2,n_2}}{(cp_{h_2} \times (T'^{*}_{n_2+1} - T'^{*}_{n_2}))} \tag{3.42}$$

where

$$cp_h = \begin{cases} cp_j & \text{if } h \textit{ is a mass stream from source } j \textit{ to sink } i \\ cp_j & \text{if } h \textit{ is a mass stream from source } j \textit{ to splitter } su \\ cp_{mu} & \text{if } h \textit{ is a mass stream from mixer unit } mu \textit{ to sink } i \\ cp_{su} & \text{if } h \textit{ is a mass stream from splitter unit } su \textit{ to sink } i \\ CP_h/L_h & \text{if } h \textit{ is a heat stream} \end{cases}$$

Binary variables ($\gamma_{q_{h_1,h_2,n_2}}$) are introduced to indicate if there is a heat transfer from hot stream h_1 to cold stream h_2 in the interval n_2:

$$\forall n_2 \in [N_{h_2}^{min}, N_{h_2}^{max} - 1], q_{h_1,h_2,n_2} - \gamma_{q_{h_1,h_2,n_2}} \times Q_{h_1,h_2}^{max} \leq 0 \tag{3.43}$$

where $Q^{max}_{h_1,h_2}$ is the maximum heat load that can be transferred between h_1 and h_2.

Similar equations are defined to characterize the heat transfer between h_1 and h_2 on the hot side:
$\forall n_1 \in [N^{min}_{h_1}, N^{max}_{h_1} - 1]$,

$$q_{h_1,h_2,n_1} = \sum_{\substack{n_2=N^{min}_{h_2} \\ n_1 \geq n_2}}^{N^{max}_{h_2}-1} q_{h_1,n_1,h_2,n_2} \tag{3.44}$$

$$L_{h_1,h_2,n_1} = q_{h_1,h_2,n_1}/(cp_{h_1} \times (T'^{*}_{n_1+1} - T'^{*}_{n_1})) \tag{3.45}$$

$$q_{h_1,h_2,n_1} - \gamma_{q_{h_1,h_2,n_1}} \times Q^{max}_{h_1,h_2} \leq 0 \tag{3.46}$$

The overall heat load exchanged between h_1 and h_2 is:

$$Q_{h_1,h_2} = \sum_{n_2=N^{min}_{h_2}}^{N^{max}_{h_2}-1} q_{h_1,h_2,n_2} = \sum_{n_1=N^{min}_{h_1}}^{N^{max}_{h_1}-1} q_{h_1,h_2,n_1} \tag{3.47}$$

3.2.3.3 Beginning of an heat exchanger

On the cold side, a heat exchange begins in the interval n_2 when there is heat transferred in it and none in the previous interval $n_2 - 1$: $\forall n_2 \in [N^{min}_{h_2}, N^{max}_{h_2} - 1]$,

$$\gamma_{q_{h_1,h_2,n_2}} - \alpha_{h_1,h_2,n_2} \geq 0 \tag{3.48}$$

$$\gamma_{q_{h_1,h_2,n_2}} - \alpha_{h_1,h_2,n_2} \leq \begin{cases} 0 & \text{if} \quad n_2 = N^{min}_{h_2} \\ \gamma_{q_{h_1,h_2,n_2-1}} & \text{if} \quad n_2 > N^{min}_{h_2} \end{cases} \tag{3.49}$$

The flow rate going through the interval n_2 (where the heat exchange begins) should be less than the real flow rate (that is the flow rate going through the entire interval $n_2 + 1$). Indeed, L_{h_1,h_2,n_2} is calculated with a larger temperature difference than the real one in the interval n_2:

$$\forall n_2 \in [N^{min}_{h_2}, N^{max}_{h_2} - 2], L_{h_1,h_2,n_2+1} - L_{h_1,h_2,n_2} \geq (\alpha_{h_1,h_2,n_2} - 1) \times L_{h_2} \tag{3.50}$$

On the hot side, a heat exchange begins in the interval n_1 when there is heat transferred in it and none in the following interval $n_1 + 1$: $\forall n_1 \in [N^{min}_{h_1}, N^{max}_{h_1} - 1]$,4

$$\gamma_{q_{h_1,h_2,n_1}} - \alpha_{h_1,h_2,n_1} \geq 0 \tag{3.51}$$

$$\gamma_{q_{h_1,h_2,n_1}} - \alpha_{h_1,h_2,n_1} \leq \begin{cases} 0 & \text{if} \quad n_1 = N^{max}_{h_1} - 1 \\ \gamma_{q_{h_1,h_2,n_1+1}} & \text{if} \quad n_1 < N^{max}_{h_1} - 1 \end{cases} \tag{3.52}$$

Similarly to the cold side, the flow rate going through the interval n_1 (where the heat

exchange begins) should be less than the real flow rate (that is the flow rate going through the entire interval $n_1 - 1$):

$$\forall n_1 \in [N_{h_1}^{min} + 1, N_{h_1}^{max} - 1], L_{h_1,h_2,n_1-1} - L_{h_1,h_2,n_1} \geq (\alpha_{h_1,h_2,n_1} - 1) \times L_{h_1} \tag{3.53}$$

3.2.3.4 End of an heat exchanger

On the cold side, a heat exchange ends in the interval n_2 when there heat transferred in it and none in the following interval $n_2 + 1$ $\forall n_2 \in [N_{h_2}^{min}, N_{h_2}^{max} - 1]$,

$$\gamma_{q_{h_1,h_2,n_2}} - \omega_{h_1,h_2,n_2} \geq 0 \tag{3.54}$$

$$\gamma_{q_{h_1,h_2,n_2}} - \omega_{h_1,h_2,n_2} \leq \begin{cases} 0 & \text{if} \quad n_2 = N_{h_2}^{max} - 1 \\ \gamma_{q_{h_1,h_2,n_2+1}} & \text{if} \quad n_2 < N_{h_2}^{max} - 1 \end{cases} \tag{3.55}$$

The flow rate going through the entire interval n_2 (where the heat exchange ends) should be less than the real flow rate (that is the flow rate going through the entire interval $n_2 - 1$). Indeed, L_{h_1,h_2,n_2} is calculated with a larger temperature difference than the real one in the interval n_2:

$$\forall n_2 \in [N_{h_2}^{min} + 1, N_{h_2}^{max} - 1], L_{h_1,h_2,n_2-1} - L_{h_1,h_2,n_2} \geq (\omega_{h_1,h_2,n_2} - 1) \times L_{h_2} \tag{3.56}$$

On the hot side, a heat exchange ends in the interval n_1 when there is heat transferred in it and none in the previous interval $n_1 - 1$: $\forall n_1 \in [N_{h_1}^{min}, N_{h_1}^{max} - 1]$,

$$\gamma_{q_{h_1,h_2,n_1}} - \omega_{h_1,h_2,n_1} \geq 0 \tag{3.57}$$

$$\gamma_{q_{h_1,h_2,n_1}} - \omega_{h_1,h_2,n_1} \leq \begin{cases} 0 & \text{if} \quad n_1 = N_{h_1}^{min} \\ \gamma_{q_{h_1,h_2,n_1-1}} & \text{if} \quad n_1 > N_{h_1}^{min} \end{cases} \tag{3.58}$$

Similarly to the cold side, the flow rate going through the interval n_1 (where the heat exchange ends) should be less than the real flow rate (that is the flow rate going through the entire interval $n_1 + 1$):

$$\forall n_1 \in [N_{h_1}^{min}, N_{h_1}^{max} - 2], L_{h_1,h_2,n_1+1} - L_{h_1,h_2,n_1} \geq (\omega_{h_1,h_2,n_1} - 1) \times L_{h_1} \tag{3.59}$$

The number of heat exchanger n_{h_1,h_2} between h_1 and h_2 is:

$$\begin{aligned} n_{h_1,h_2} &= \sum_{n_1=N_{h_1}^{min}}^{N_{h_1}^{max}-1} \alpha_{h_1,h_2,n_1} = \sum_{n_1=N_{h_1}^{min}}^{N_{h_1}^{max}-1} \omega_{h_1,h_2,n_1} \\ n_{h_1,h_2} &= \sum_{n_2=N_{h_2}^{min}}^{N_{h_2}^{max}-1} \alpha_{h_1,h_2,n_2} = \sum_{n_2=N_{h_2}^{min}}^{N_{h_2}^{max}-1} \omega_{h_1,h_2,n_2} \end{aligned} \tag{3.60}$$

3.2.3.5 Intermediate parts of an heat exchanger

The intermediate parts of an heat exchanger are characterized by the consistency of the mass flow rate throughout these parts.

On the cold side, the flow rate in n_2 is equal to the flow rate in $n_2 - 1$, except for the interval just before the beginning because the value of L_{h_1,h_2,n_2} in it should be inferior to the real flow rate: $\forall n_2 \in [N_{h_2}^{min} + 1, N_{h_2}^{max} - 1]$,

$$L_{h_1,h_2,n_2} - L_{h_1,h_2,n_2-1} \leq (1 - \delta_{h_1,h_2,n_2} + \alpha_{h_1,h_2,n_2-1}) \times L_{h_2} \tag{3.61}$$

$$L_{h_1,h_2,n_2} - L_{h_1,h_2,n_2-1} \geq -(1 - \delta_{h_1,h_2,n_2} + \alpha_{h_1,h_2,n_2-1}) \times L_{h_2} \tag{3.62}$$

On the hot side, the flow rate in n_1 is equal to the flow rate in $n_1 + 1$, except for the interval just after the beginning because the value of L_{h_1,h_2,n_1} in it should be inferior to the real flow rate: $\forall n_1 \in [N_{h_1}^{min} + 1, N_{h_1}^{max} - 1]$,

$$L_{h_1,h_2,n_1} - L_{h_1,h_2,n_1+1} \leq (1 - \delta_{h_1,h_2,n_1} + \alpha_{h_1,h_2,n_1+1}) \times L_{h_1} \tag{3.63}$$

$$L_{h_1,h_2,n_1} - L_{h_1,h_2,n_1+1} \geq -(1 - \delta_{h_1,h_2,n_1} + \alpha_{h_1,h_2,n_1+1}) \times L_{h_1} \tag{3.64}$$

3.2.3.6 Heat transfer consistency and minimum temperature enforcing

When there is a heat transfer in a given interval, it must be either a beginning, an end or an intermediate part of the heat exchanger:
On the cold side,$\forall n_2 \in [N_{h_2}^{min} + 1, N_{h_2}^{max} - 1]$,

$$\gamma_{q_{h_1,h_2,n_2}} = \alpha_{h_1,h_2,n_2} + \omega_{h_1,h_2,n_2} + \delta_{h_1,h_2,n_2} \tag{3.65}$$

On the hot side,$\forall n_1 \in [N_{h_1}^{min} + 1, N_{h_1}^{max} - 1]$,

$$\gamma_{q_{h_1,h_2,n_1}} = \alpha_{h_1,h_2,n_1} + \omega_{h_1,h_2,n_1} + \delta_{h_1,h_2,n_1} \tag{3.66}$$

Moreover, the beginning on the hot side must be located after the end on the cold side. Similarly, the end on the hot side must be before the beginning on the cold side:
$\forall n \in [min(N_{h_1}^{min}; N_{h_2}^{min}), max(N_{h_1}^{max} - 1; N_{h_2}^{max} - 1)]$,

$$\sum_{n_1=n}^{N_{h_1}^{max}-1} \alpha_{h_1,h_2,n_1} \geq \sum_{n_2=n}^{N_{h_2}^{max}-1} \omega_{h_1,h_2,n_2} \tag{3.67}$$

$$\sum_{n_1=n}^{N_{h_1}^{max}-1} \omega_{h_1,h_2,n_1} \geq \sum_{n_2=n}^{N_{h_2}^{max}-1} \alpha_{h_1,h_2,n_2} \tag{3.68}$$

Finally, to ensure the minimum temperature difference, it has been shown that $n_1 \geq n_2$.

However, in the case where $n_1 = n_2$, other conditions must be verified. If the beginning on the hot side is located in the same interval as the end on the cold, then to the temperature of the hot side must be superior to the one on the cold side:

$$T'^{*}_{n_1} + \frac{q_{h_1,h_2,n_1}}{L_{h_1,h_2,n_1-1} \times cp_{h_1}} \geq T'^{*}_{n_2} + \frac{q_{h_1,h_2,n_2}}{L_{h_1,h_2,n_2-1} \times cp_{h_2}}$$

Knowing that $n_1 = n_2$ and with definition of L_{h_1,h_2,n_1-1} and L_{h_1,h_2,n_2-1}, the previous condition can be reduced to:

$$\frac{q_{h_1,h_2,n_1}}{q_{h_1,h_2,n_1-1}} \geq \frac{q_{h_1,h_2,n_2}}{q_{h_1,h_2,n_2-1}}$$

It is also reasonable to assume that q_{h_1,h_2,n_1}, q_{h_1,h_2,n_2} and q_{h_1,h_2,n_1-1}, q_{h_1,h_2,n_2-1} are of the same order of magnitude, respectively. Therefore, the condition becomes:
$\forall n_1 \in [N^{min}_{h_1}, N^{max}_{h_1} - 1], \forall n_2 \in [N^{min}_{h_2}, N^{max}_{h_2} - 1], n_1 = n_2,$

$$q_{h_1,h_2,n_1} - q_{h_1,h_2,n_2} \geq -(2 - \alpha_{h_1,h_2,n_1} - \omega_{h_1,h_2,n_2}) \times Q^{max}_{h_1,h_2} \tag{3.69}$$

$\forall n_1 \in [N^{min}_{h_1} + 1, N^{max}_{h_1} - 1], \forall n_2 \in [N^{min}_{h_2} + 1, N^{max}_{h_2} - 1], n_1 = n_2,$

$$q_{h_1,h_2,n_1-1} - q_{h_1,h_2,n_2-1} \leq (2 - \alpha_{h_1,h_2,n_1} - \omega_{h_1,h_2,n_2}) \times Q^{max}_{h_1,h_2} \tag{3.70}$$

In the same way, if the end on the hot side is located in the same interval as the beginning on the cold, then to the temperature of the hot side must be superior to the one on the cold side.
This lead to:
$\forall n_1 \in [N^{min}_{h_1}, N^{max}_{h_1} - 1], \forall n_2 \in [N^{min}_{h_2}, N^{max}_{h_2} - 1], n_1 = n_2,$

$$q_{h_1,h_2,n_1} - q_{h_1,h_2,n_2} \leq (2 - \alpha_{h_1,h_2,n_1} - \omega_{h_1,h_2,n_2}) \times Q^{max}_{h_1,h_2} \tag{3.71}$$

$\forall n_1 \in [N^{min}_{h_1}, N^{max}_{h_1} - 2], \forall n_2 \in [N^{min}_{h_2}, N^{max}_{h_2} - 2], n_1 = n_2,$

$$q_{h_1,h_2,n_1+1} - q_{h_1,h_2,n_2+1} \geq -(2 - \alpha_{h_1,h_2,n_1} - \omega_{h_1,h_2,n_2}) \times Q^{max}_{h_1,h_2} \tag{3.72}$$

3.2.3.7 Mixer unit specific equations for heat exchangers within its beginning interval

For a mixer unit, the heat load transferred by the stream in its first interval depends on its flow rate and also on its variable temperature. Therefore, equations relative to the beginning of heat exchangers with this part of the stream are adapted to take into account this particularity. The equations Eq.3.50 and Eq.3.62 for cold streams, and Eq.3.53 and Eq.3.64 for hot streams are modified.

For cold streams, if h_2 is a stream from a mixer unit mu to its associated sink i:

$$\begin{aligned} &for\ n_2 = N_{h_2}^{min}, \\ &L_{h_1,h_2,n_2+1} - L_{h_1,h_2,n_2} \geq (\alpha_{h_1,h_2,n_2} - 1) \times L_{h_2} - q_{mu}^{+}/(cp_{mu} \times (T_{n_2+1}^{'*} - T_{n_2}^{'*}) \end{aligned} \tag{3.73}$$

$$\begin{aligned} &for\ n_2 = N_{h_2}^{min} + 1, \\ &L_{h_1,h_2,n_2} - L_{h_1,h_2,n_2-1} \geq -(1 - \delta_{h_1,h_2,n_2} + \alpha_{h_1,h_2,n_2-1}) \times L_{h_2} - q_{mu}^{+}/(cp_{mu} \times (T_{n_2}^{'*} - T_{n_2-1}^{'*}) \end{aligned} \tag{3.74}$$

For hot streams, if h_1 is a stream from a mixer unit mu to its associated sink i:

$$\begin{aligned} &for\ n_1 = N_{h_1}^{max} - 1, \\ &L_{h_1,h_2,n_1-1} - L_{h_1,h_2,n_1} \geq (\alpha_{h_1,h_2,n_1} - 1) \times L_{h_1} - q_{mu}^{-}/(cp_{mu} \times (T_{n_1+1}^{'*} - T_{n_1}^{'*}) \end{aligned} \tag{3.75}$$

$$\begin{aligned} &for\ n_1 = N_{h_1}^{max} - 2, \\ &L_{h_1,h_2,n_1} - L_{h_1,h_2,n_1+1} \geq -(1 - \delta_{h_1,h_2,n_1} + \alpha_{h_1,h_2,n_1+1}) \times L_{h_1} - q_{mu}^{-}/(cp_{mu} \times (T_{n_1+2}^{'*} - T_{n_1+1}^{'*}) \end{aligned} \tag{3.76}$$

3.2.3.8 Heat exchange area

The real heat exchange area needed to realize the heat transfer between h_1 and h_2 is approximated as the sum of all S_{h_1,n_1,h_2,n_2}, which is the heat exchange area for the heat transfer between h_1 in n_1 and h_2 in n_2:

$$S_{h_1,n_1,h_2,n_2} = \frac{q_{h_1,n_1,h_2,n_2}}{U_{h_1,h_2} \times \Delta T_{n_1,n_2}^{LMTD}} \tag{3.77}$$

$$S_{h_1,h_2}^{real} \simeq S_{h_1,h_2} = \sum_{n_1=N_{h_1}^{min}}^{N_{h_1}^{max}-1} \sum_{\substack{n_2=N_{h_2}^{min} \\ n_1 \geq n_2}}^{N_{h_2}^{max}-1} S_{h_1,n_1,h_2,n_2} \tag{3.78}$$

where

$$\Delta T_{n_1,n_2}^{LMTD} = \begin{cases} T_{n_1}^{'*} - T_{n_2}^{'*} + \Delta T_{min} & \text{if} \quad (T_{n_1}^{'*} - T_{n_2}^{'*}) = (T_{n_1+1}^{'*} - T_{n_2+1}^{'*}) \\ \frac{(T_{n_1+1}^{'*} - T_{n_2+1}^{'*}) - (T_{n_1}^{'*} - T_{n_2}^{'*})}{log((T_{n_1+1}^{'*} - T_{n_2+1}^{'*} + \Delta T_{min})/(T_{n_1}^{'*} - T_{n_2}^{'*} + \Delta T_{min}))} & \text{if} \quad (T_{n_1}^{'*} - T_{n_2}^{'*}) \neq (T_{n_1+1}^{'*} - T_{n_2+1}^{'*}) \end{cases}$$

and

$$\frac{1}{U_{h_1,h_2}} = \frac{1}{htc_{h_1}} + \frac{1}{htc_{h_2}}$$

Each heat exchanger area is corrected afterwards using the accurate ΔT_{LMTD} formula and recalculated. The capital costs and total annualized costs are also recalculated.

3.2.4 Objective function

The objective function represents the total annualized cost (TAC) including the annual operating cost (AOC) and the capital cost (CC). This function is minimized to obtain an economically optimal MAHEN design.

Assuming a nominal cost of fresh source j (C_j^f), waste sink i (C_i^w) and utility heat stream h_u (C_{h_u}), the AOC for a given total of operating hours (h_{op}) is expressed as follows:

$$AOC = h_{op} \times \left(\sum_{j \in J_f} C_j^f \times L_j^f + \sum_{i \in I_w} C_i^w \times G_i^w + \sum_{h_u \in H_u} C_{h_u} \times q_{h_u} \right) \tag{3.79}$$

Capital costs of the HEN are calculated depending on the required number of heat exchangers and the total heat exchange area; assuming a unit cost for each item (C_{he}^{cap} and C_S^{cap} respectively). The total capital cost is formulated as follows:

$$CC = \sum_{h_1 \in H_{hot}} \sum_{h_2 \in H_{cold}} (C_{he}^{cap} \times n_{h_1,h_2} + C_S^{cap} \times S_{h_1,h_2}) \tag{3.80}$$

Finally, assuming an actualization ratio (r_a) and a number of operating years (N_{op}), the total annualized cost of both networks is defined as follow:

$$TAC = \frac{1}{N_{op}} \times \left(CC + \sum_{n=1}^{N_{op}} \frac{AOC}{(1+r_a)^n} \right) \tag{3.81}$$

3.2.5 Mixer Unit screening

The selection of the most appropriate mixer unit for a given sink relies on the evaluation of the associated HEN costs which include a fixed part related to the existence of a heat exchanger and variable part related to heat exchange area. To this end, an alternate model based on the M2 model presented in Chapter II is introduced optimizing the estimation of the TAC (M2'). The objective is to select in advance the mixer unit temperature to avoid using multiple mixer units which can increase significantly the size of the problem. Since the computation time of the M2 model is a few seconds, it is appropriate to use it for this purpose. A few equations used to estimate the HEN capital costs are added to the M2 model which otherwise remains unchanged.

The first item of the HEN cost is related to the minimum number of heat exchangers required. The assumption made is that the minimum heat exchangers number is equal to the maximum number between hot and cold streams requiring cooling or heating:

$$n_{he}^{min} = max(n_{hot}; n_{cold}) \tag{3.82}$$

These numbers can be quantified using binary variables to count mass extractions at temperature levels different from its source (or mixer unit) temperature. Utilities are also counted as one if there output is not null. To comply with linear modeling and to avoid using the *max* function, integer variables are introduced (n_{hot}^{extra} and n_{cold}^{extra}) to fill the gap between n_{hot} and n_{cold}:

$$n_{he}^{min} = n_{hot} + n_{hot}^{extra} = n_{cold} + n_{cold}^{extra} \tag{3.83}$$

The total fixed part of HEN cost is:

$$C_{HEN}^{fixed} = c_{he}^{fixed} \times n_{he}^{min} + k_{fixed} \times (n_{hot} + n_{cold}) \tag{3.84}$$

The second part of C_{HEN}^{fixed} is added to guarantee minimizing the number of actual streams in mass allocation network (i.e. n_{hot} and n_{cold}) while remaining marginal (with k_{fixed} chosen very small).

The second item of the HEN cost is related to the estimation of the required heat exchange area. This cost is calculated by estimating what could the area for each mass stream (and utility). Since the matching between hot and cold streams is not done at this stage, an average temperature difference $k_{area}.\Delta T_{pinch}$ and a heat transfer coefficient (htc) are assumed for every stream, which can be modulated by the parameter k_{area} to give more importance to this cost in the objective function. The variable part of HEN costs is:

$$C_{HEN}^{variable} = c_{he}^{area} \times \left(\sum_{n} \sum_{ms} \frac{q_{ms,n}}{htc_{ms} \times k_{area}.\Delta T_{pinch}} + \sum_{u} \frac{q_u}{htc_u \times k_{area}.\Delta T_{pinch}} \right) \tag{3.85}$$

The new objective function is formulated as an estimation of the objective function of the M3 model (TAC_{esti}):

$$TAC_{esti} = \frac{1}{N_{op}} \times \left(C_{HEN}^{fixed} + C_{HEN}^{variable} + \sum_{n=1}^{N_{op}} \frac{AOC}{(1+r_a)^n} \right) \tag{3.86}$$

3.3 Case Study

The relevance of the MAHEN design presented model is discussed in two case studies. All cases are solved using Cplex (Cplex version: 12.6.1.0 - Processor: Intel© CORE™ i7 - 2760QM CPU @ 2.40GHz - RAM: 8Go - OS: Windows© 7). The ammonia recovery and phenol production case studies introduced in Chapter II serve as illustration for the MAHEN design.

3.3.1 Mono-contaminant case: Ammonia Recovery

The process data and calculation parameters are recalled in Table 3.1. Since ammonia cost outweighs all others, the global fresh consumption is set to its minimum (654.9 $kg.s^{-1}$). And its cost is not taken into account ($C_{fresh} = 0€.t^{-1}$) to study more precisely the influence of the other ones. The objective is now to find the most economical mass allocation network using minimum fresh resources and optimizing the heat requirements and HEN costs.

	Flow rate ($kg.s^{-1}$)	Comp. in impurities (ppm)	Temperature ($°C$)
Sink			
Sink1	350	0 - 0	30
Sink2	677	0 - 40	187
Sink3	126	0 - 75	55
Sink4	202	0 - 100	98
Waste		0 - 500	40
Source			
Source1	530	30	21
Source2	68	150	43
Source3	1130	300	130
Source4	36	500	35
Fresh		0	30

Temperature of fresh resource = $30°C$; Temperature of waste effluent = $40°C$;
Heat capacity = $2.19kJ.kg^{-1}.K^{-1}$;
Temperature of cold utility = $5 - 5.1°C$; Temperature of hot utility = $230 - 229.9°C$

Table 3.1: Ammonia recovery case - Process Data

The economic data and selected parameters are given in Table 3.2:

Economic data		*Parameters*			
C_{fresh}	500.0 €$.ton^{-1}$	h_{op}	8000 hrs	htc_{NH_3}	50 $W.K^{-1}.m^{-2}$
C_{waste}	0.0 €$.ton^{-1}$	N_{op}	1 year	htc_{hot}	1000 $W.K^{-1}.m^{-2}$
C_{hot}	0.01 €$.kWh^{-1}$	r_a	5 %	htc_{cold}	1000 $W.K^{-1}.m^{-2}$
C_{cold}	0.0025 €$.kWh^{-1}$	ΔT_{pinch}	35 °C		
C_{he}^{cap}	5291.9 €	ΔT_{step}	5 °C		
C_S^{cap}	77.79 €$.m^{-2}$	N_{split}	3		

Table 3.2: Ammonia recovery case - Economic Data and Calculation Parameters

3.3.1.1 Comparison with literature results - Analysis on N_{op}

This case was treated by Sahu et al. [100] and Tan et al. [110]. They both optimized mass allocation network first with a specific objective function (hot utility load and operating cost, respectively) and then applied the pinch design method [76] to provide a HEN structure sequentially. (Note that Sahu et al. [100] proposed a solution considering non-isothermal mixing; however, the HEN structure seems to have incorrect heat balances. Therefore, these results were not considered for comparison purposes). A sensitivity analysis is led on the number of operating years N_{op} (from 2 to 20 years). Balancing capital and operating costs may vary depending on the time horizon one is expecting a return on its investments. The comparison between results is shown in Table 3.3:

	Sahu et al. (2012)	Tan et al. (2014)	Model M3	
			$N_{op} = 1$	$N_{op} \geq 2$
L_{fresh} $(kg.s^{-1})$	655	654.9	654.9	654.9
Q_h (kW)	132 925.5	132 927.0	145 593.5	131 883.3
Q_c (kW)	79 224.5	79 228.0	91 895.7	78 184.5
n_{he}	12	12	10	10
S_{he} (m^2)	187 662	199 213	160 311	181 767
S_{he}^{real} (m^2)	-	-	160 178	181 481
Op. Cost $(MM€)$	12.22	12.22	13.49	12.11
Cap. Cost $(MM€)$	14.76	15.56	12.51	14.17

Table 3.3: Ammonia recovery case - Results

For $N_{op} = 1$ *year*, the solution found with the proposed methodology requires an increase in heat consumption (+9.5% for Q_h; +16.0% for Q_c) compared to the literature's solutions; however, the number of heat exchangers is down to 10 units and the overall heat exchange area decreases by 15 %. Over one year of operations, the global cost is reduced in comparison with the solutions found in the literature.

By increasing N_{op}, one is seeking a more long-term solution i.e. finding a structure

with lower operating costs. Given that operating and capital costs are of the same order of magnitude for $N_{op} = 1$, the model tends to decrease the operating costs rapidly when N_{op} is superior to 1. Consequently, the optimal MAHEN (Fig.3.10) for $N_{op} = 2$ *years* consumes the minimum energy requirements (MER) and operating costs reached their minimum. Capital cost increases (+13.2%) compared to the first solution; with a larger heat exchange area but the same heat exchangers number.

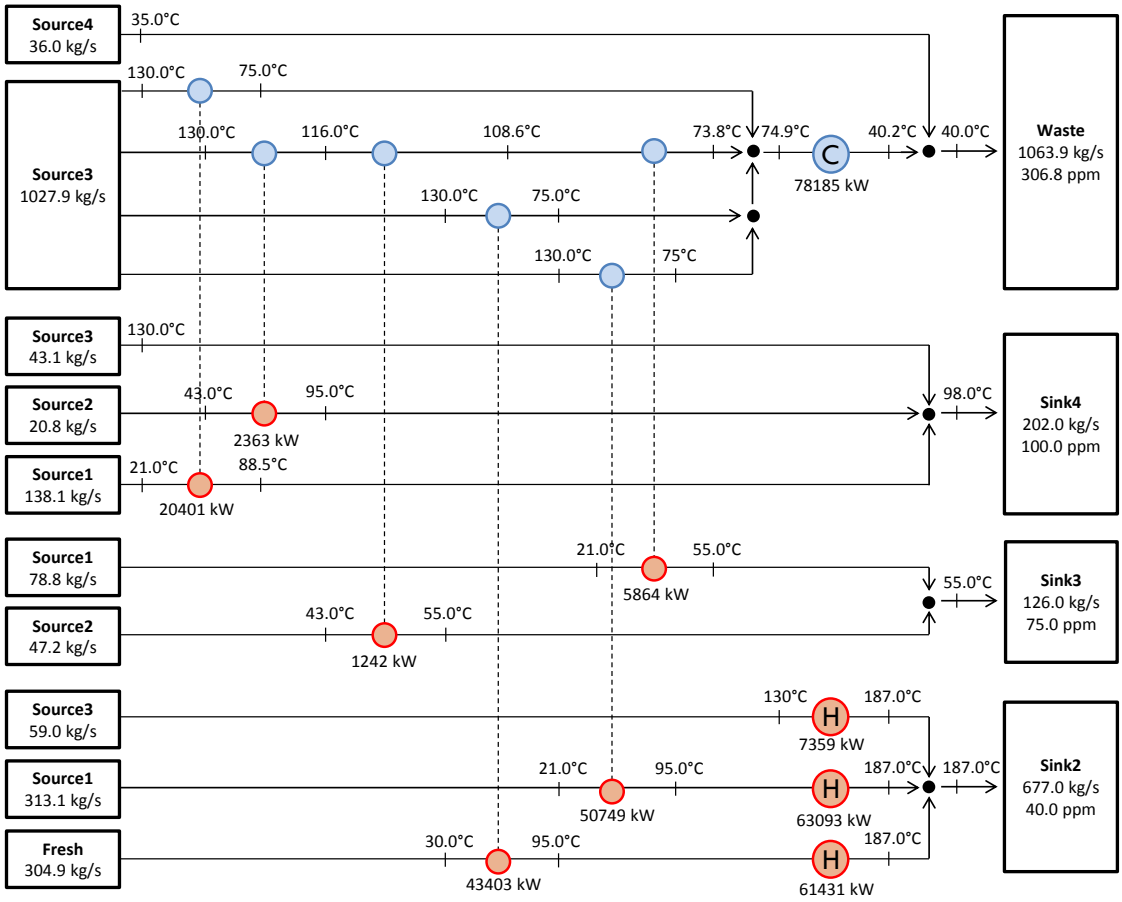

Figure 3.10: Optimal MAHEN for phenol production case ($N_{op} = 2$ year)

Moreover, the optimal solutions found for N_{op} from 2 to 20 years have the same structure with few differences. Indeed, temperatures at which the stream Source3-Waste (the internal heating source) and the flow rate of each split change slightly. Nonetheless, the heat exchangers and their heat loads remain the same. Only the total exchange area is affected, but it is negligible. So it can be assumed that the optimal structure remains identical as the one presented in (Fig.3.10). In any case, simultaneous optimization of the operating and capital costs allows designing better MAHEN structures because mass streams characteristics (flow rate and temperatures) can still be modified while conceiving HEN structure.

Finally, since the overall heat exchange area cost is greater than the cost related to the heat exchangers existence by a large amount ($14MM€$vs. $53k€$), the use of mixer or splitter units is not relevant in this case. In fact, the possible economic gain to reduce the number of heat exchangers cannot outweigh the resulting surplus of heat exchange area.

3.3.1.2 Sensitivity analysis on temperature intervals number (ΔT^{max}_{step})

The model presented relies on the discretization of the set of temperature values ($N^{'}$) at which mass streams can be split and heat exchanger are designed. The parameter ΔT^{max}_{step} defines the number of temperature intervals. In Table 3.4, the statistics of this problem resolution are shown for several values of ΔT^{max}_{step}. The initial data indicated in Table 3.2 are used.

ΔT^{max}_{step} $(°C)$	3	4	5	10	15	20	25
$N^{'}$	77	63	57	42	38	35	35
t_{comp} (s)	3 464,9	190,2	784,9	18,4	73,7	30,8	31,5
$N_{constraints}$	18 964	14 644	13 628	9 452	9 382	8 399	8 399
$N_{continuous}$	11 153	7 540	6 767	4 093	4 031	3 455	3 455
$N_{binaries}$	6 853	5 281	4 921	3 398	3 363	3 014	3 014
$N_{non-zeros}$	126 117	87 979	80 104	50 214	49 507	43 378	43 379
$Obj.func.(MM€)$	25,361	25,368	25,367	25,393	25,399	25,526	25,526
$\Delta Obj.func.$ (%)	0,000	0,030	0,024	0,128	0,150	0,651	0,651
Q_h (kW)	147 142.6	146 863.6	145 593.5	144 415.3	147 702.1	154 477.6	154 477.6
Q_c (kW)	93 443.6	93 164.8	91 895.7	90 716.5	94 003.3	100 778.8	100 778.8
n_{he}	10	10	10	10	10	11	11
S_{he} (m^2)	158 336.2	158 774.7	160 311.5	162 091.7	158 141.4	151 408.4	151 408.4
S^{real}_{he} (m^2)	158 267.7	158 622.2	160 178.4	161 625.9	157 698.4	150 749.9	150 749.9
Op. Cost $(MM€)$	12.370	12.404	12.524	12.662	12.355	11.836	11.836
Cap. Cost $(MM€)$	13.640	13.612	13.485	13.368	13.696	14.374	14.374

Table 3.4: Sensitivity analysis on ΔT^{max}_{step} - Main results and statistics

The selection of ΔT_{step}^{max} resides in the balance between computation time and optimality of the solution. The size of the problem increases when ΔT_{step}^{max} decreases. However, if the computation time is likely to decrease with ΔT_{step}^{max} increasing, it sometimes converge more rapidly (for instance when $\Delta T_{step}^{max} = 10$ or 4). This happens because opportunities of mass splits change depending on the temperature scale (knowing that one temperature level may not remain on the scale when ΔT_{step}^{max} decreases) which changes the structure of heat exchangers. Also, the way the solver browses the search space changes from one value to another; thus, there is not a linear and monotonous relation between ΔT_{step}^{max} and the computation time.

In this case, the structure of the optimal solution remains mostly the same when $\Delta T_{step}^{max} \leq 15$. The heat exchangers remain the same but their definition (i.e. inlet and outlet temperatures) change slightly. Consequently, their area and related costs change; thus, there is a tradeoff between energy cost and variable heat exchanger cost. When $\Delta T_{step}^{max} \geq 20$, one heat exchanger is added to the HEN structure while the MAN remains relatively similar to the previous one. This happens because some heat exchangers can no longer be designed as precisely as before; therefore, their selection is not optimal anymore.

Overall, the relative variation of the objective function compared to the minimum value obtained with $\Delta T_{step}^{max} = 3$ is inferior to 0.7%. More precisely, the difference is at most 0.15% between the best and the worst cases when a sufficient number of temperature values are on the scale ($\Delta T_{step}^{max} \leq 15$). Even though the value of the objective changes with ΔT_{step}^{max}, this variation can be considered negligible. A quasi-optimal solution can be found balancing optimality and speed when the number of temperature levels on the scale is in the range of 40 and 60 for this case. Note that the difference between S_{he}^{real} and S_{he} is fairly small and that S_{he}^{real} is always inferior to S_{he} .

3.3.2 Multi-properties case: Phenol Production Process

This second case study follows the water use in phenol production process as in chapter paragraph x. This time the interest of mixer units is explained and illustrated in this case. All data and parameters are given in Table 3.5 and Table 3.6.

	Flow rate ($kg.h^{-1}$)	Comp. in Phenol (mass fraction)	p_v (kPa)	pH	Temperature ($°C$)
Sink					
Washer 101	2718	0.0 - 0.013	20.0 - 47.0	4.5 - 7.0	60
Washer 102	1993	0.0 - 0.013	4.0 - 38.0	4.0 - 8.0	78
R104	1127	0.0 - 0.100	3.0 - 25.0	4.5 - 7.0	40
Waste		0.0 - 0.150		5.0 - 9.0	30
Source					
Washer 101	3661	0.016	38.0	5.4	85
Decanter 101	1766	0.024	25.0	5.1	65
Washer 102	1485	0.220	7.0	4.8	40
Freshwater 1		0.000	3.0	7.0	25
Freshwater 2		0.012	6.0	6.8	35

Heat capacity $= 4.2kJ.kg^{-1}.K^{-1}$;
Temperature of cold utility $= 10 - 10.1°C$; Temperature of hot utility $= 100 - 99.9°C$

Table 3.5: Phenol production case - Process Data

Economic data		*Parameters*			
C_{fresh1}	3.0 €$.ton^{-1}$	h_{op}	8000 hrs	htc_{water}	1000 $W.K^{-1}.m^{-2}$
C_{fresh2}	1.0 €$.ton^{-1}$	N_{op}	1 year	htc_{hot}	1000 $W.K^{-1}.m^{-2}$
C_{hot}	0.01 €$.kWh^{-1}$	r_a	5 %	htc_{cold}	1000 $W.K^{-1}.m^{-2}$
C_{cold}	0.0025 €$.kWh^{-1}$	ΔT_{pinch}	10 $°C$	k_{fixed}	1
C_{he}^{cap}	5291.9 €	ΔT_{step}	5 $°C$	k_{area}	0.001
C_S^{cap}	77.79 €$.m^{-2}$	N_{split}	3		

Table 3.6: Phenol production case - Economic Data and Calculation Parameters

The simultaneous approach considered in the M3 model formulation enables designing mass streams efficiently; limiting the need for fresh resources, external heat utilities and indirect heat exchange.

The solution obtained with the proposed methodology is shown in Fig.3.11. Thanks to non-isothermal mixing, there are no external heating requirements. The only heating need that remains ($Fresh1$-$Washer2$ stream) is met internally (using $Washer1$-$Neutralizer$ stream). Hence, only a cold utility is needed; minimizing the MAHEN cost.

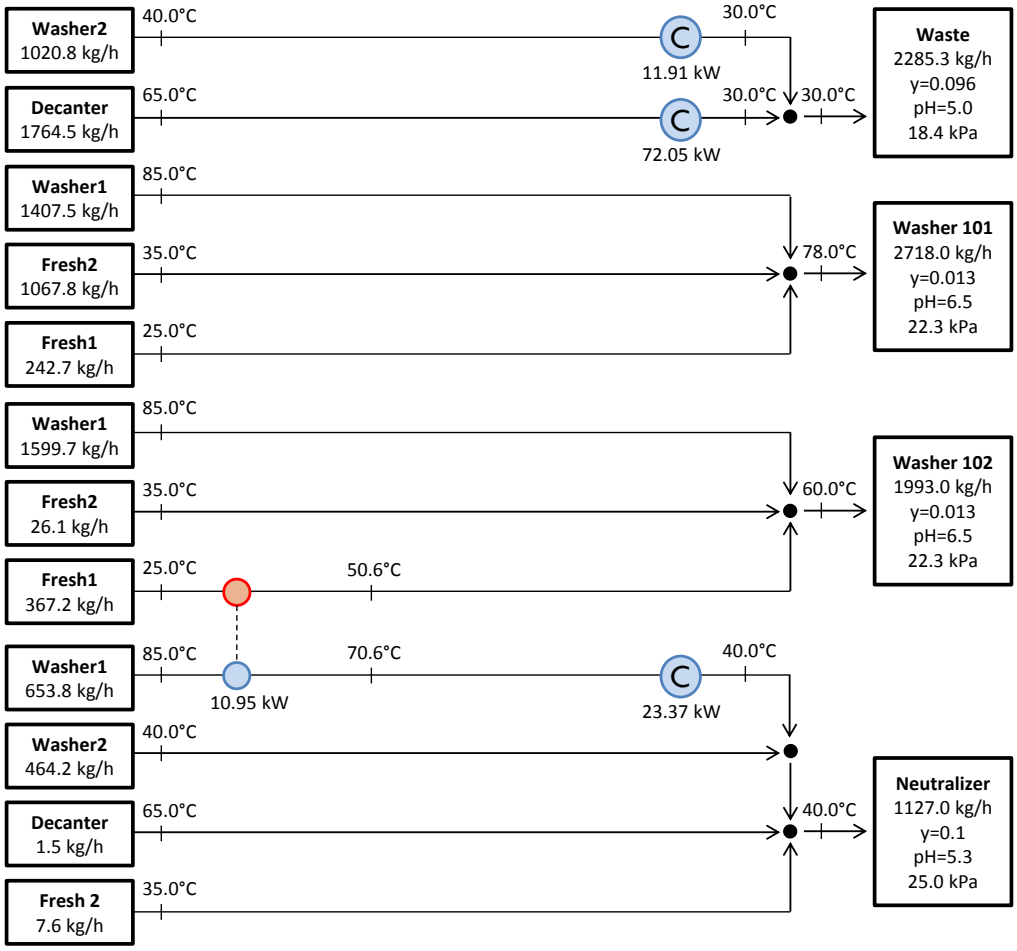

Figure 3.11: Optimal MAHEN for the phenol production case ($N_{op} = 1$ year)

However, mass streams going to the waste discharge sink are not exchanging with other ones. Rather, they are both cooled down by an external utility; each one requiring its own heat exchanger. This suggests that a mixer unit should be considered for this sink to potentially reduce the heat exchangers number and capital costs.

For this case, the selection of mixer units had been carried out using the M2' model introduced previously. Multiple mixer units' temperatures have been evaluated individually. First, a series of test using mixer units with every sink show that only mixers associated with the waste sink have a significant influence on the results of the M2' model. Therefore, the focus was made on the selection of mixer units for this only sink which has a temperature of $40°C$. Note that the highest source temperature is $85°C$.

A first series of mixer units was tested on range from 45 to 80°C with a 5°C step (Fig.3.12). The results show an optimum around 60°C. To refine the results, a second series was tested on range from 55 to 65°C with a 1°C step.

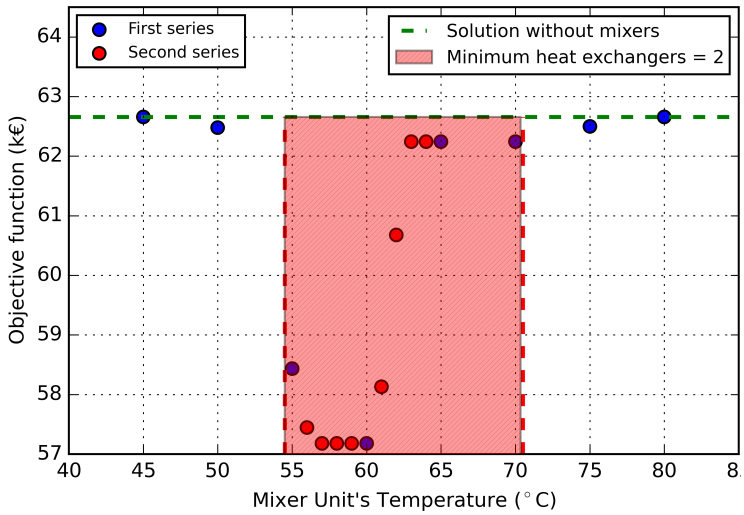

Figure 3.12: Selection of mixer units for the phenol production case (N_{op} = 1 year)

First, mixer units with a temperature between 55 and 70°C affect the number of streams that goes into the HEN, reducing the estimation of the heat exchangers number to 2. The difference between those solutions is mostly between the cooling requirements and the total heat exchanger area. The mass allocation structure is also slightly different.

In order to spot the optimal temperature more accurately, a sensitivity analysis is led on the waste sink mixer unit temperature. A range from 55°C to 65°C is tested with a 1°C-step and a relaxation margin ($\Delta T^{mu}_{error} = 2°C$) is set for each test (Fig.3.13).

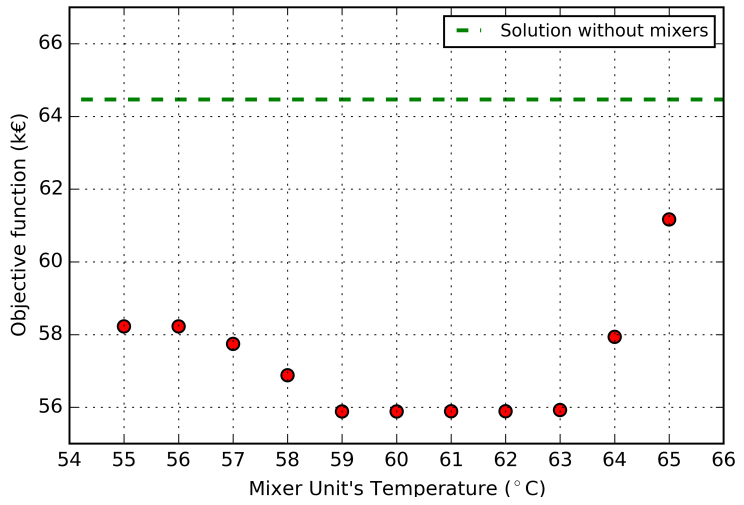

Figure 3.13: Mixer unit influence on TAC for the phenol production case (N_{op} = 1 year)

In this case, adding the possibility to have a mixer unit always reduces the TAC compared to the solution without mixer units. Moreover, the same optimal mixing temperature is obtained at $60.9°C$ for T_i^{mu} ranging from 59 to $62°C$, with the same MAHEN structure (Fig.3.14).

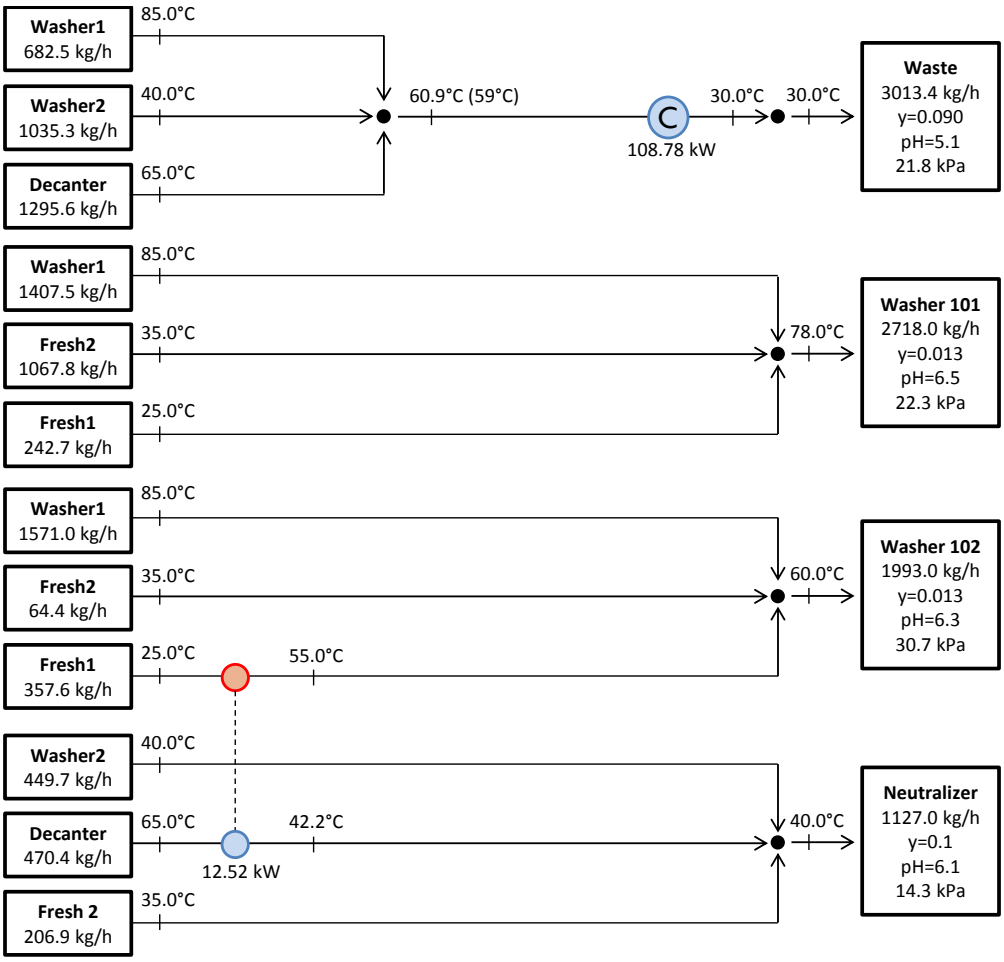

Figure 3.14: Optimal MAHEN for the phenol production case with mixer unit ($N_{op} = 1$ year)

The number of heat exchangers is reduced to 2 (as opposed to 4 in the initial solution). The main differences with the first solution concern fresh sources. As the mass flow rate of $Fresh1$ decreases a little, the one of Fresh 2 increases by 21.6% resulting in a small surge of waste (8.2%). The cold utility consumption is almost the same ($+1.5kW$).

For other mixer units, when $60.9°C$ cannot be reached within their $2°C$ margin of error, either the cold utility consumption or the number of heat exchanger ($n_{he} = 3$) increase in the optimal solution. This demonstrates the advantage of the simultaneous approach. Indeed, the possibility to mix stream prior to entering the HEN influenced both the mass allocation structure and the heat exchanger network. This would have been less efficient using a sequential approach or heuristics afterward.

A similar analysis is led for a more long-term solution ($N_{op} = 20$ years). This time, the optimal solution reached the minimum operating costs ([54]) with an optimal mixing temperature of $53.7°C$ for the mixer unit of the waste sink. This solution is shown in Fig.3.15. The capital costs are higher than the ones for the two previous structures; increasing the number of heat exchangers (but with a smaller overall heat exchange surface).

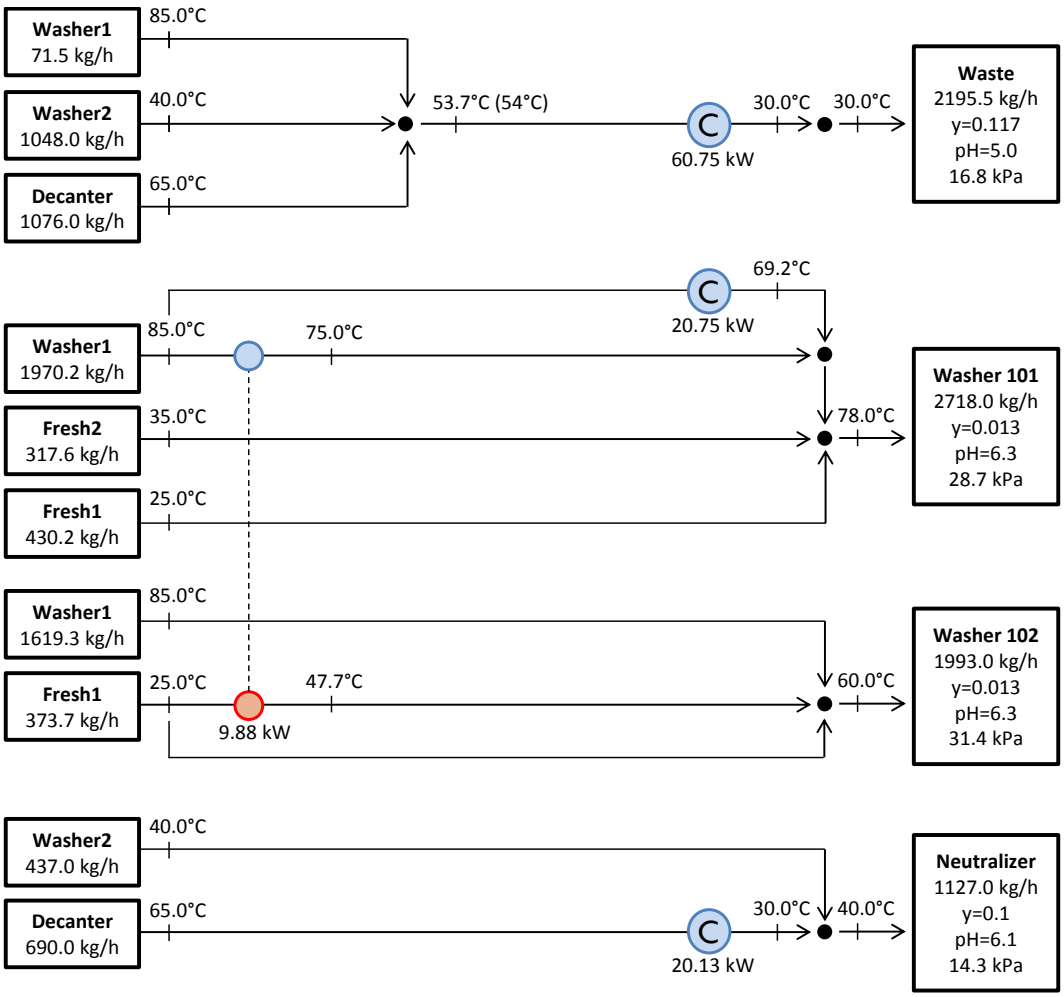

Figure 3.15: Optimal MAHEN for the phenol production case with optimal mixer unit ($N_{op} = 20$ years)

In Table 3.7, the results indicate that the decrease in operating cost is smaller than the increase in capital costs. However, this solution is more profitable over a 20-year period. The fresh resources consumption is completely different. Fresh 1 is far more used than Fresh 2. Therefore, the waste generation is reduced, which leads to a decrease in the cooling utility load. Overall, operating costs decreased. The selected MAHEN structure will depend strongly on over what time horizon should the investments be profitable.

Solution	1	2	3
N_{op} (years)	1	1	20
T_{waste}^{mu} $(°C)$	-	60.9	53.7
L_{fresh1} $(kg.h^{-1})$	609.8	600.2	803.9
L_{fresh2} $(kg.h^{-1})$	1 101.5	1 339.1	317.6
Q_h (kW)	107.3	108.8	101.6
Q_c (kW)	0.0	0.0	0.0
n_{he}	4	2	4
S_{he} (m^2)	6.76	8.51	6.07
S_{he}^{real} (m^2)	6.76	8.47	6.07
Op. Cost (k€)	44.9	46.9	42.2
Cap. Cost (k€)	21.7	11.2	21.6

Table 3.7: Comparison between results for different operating period of time

As a point of comparison with the previous case study, Table 3.8 shows the problem statistics of the three cases presented in Table 3.7.

Solution	1	2	3
ΔT_{step}^{max} $(°C)$	5	5	5
$N^{'}$	29	33	32
t_{comp} (s)	42.8	41.1	79.0
$N_{constraints}$	9 970	13 572	13 231
$N_{continuous}$	4 156	6 106	5 844
$N_{binaries}$	3 578	4 880	4 755
$N_{non-zeros}$	50 676	73 560	70 877

Table 3.8: Phenol production case - Problem statistics

Note that in this case the computation time is quite similar whether mixer units are used or not.

3.4 Conclusion

In this chapter, a new linear model M3 is presented to address the synthesis of heat-integrated mass allocation network and associated heat exchange network simultaneously; optimizing not only the operating costs (as the model M2 introduced in Chapter II), but also the capital costs related to the HEN associated with the MAN. Both quantities are taken into account in the objective function and optimized simultaneously.

Based on the models M1 and M2 introduced in Chapter II, a combined superstructure is presented considering direct and indirect heat exchanges. The non-linear equations modeling the design of heat exchanger are linearized thanks to the use of discrete values of temperature. The number of elements on the temperature scale must be chosen by balancing an acceptable computation time and accuracy on the optimal solution because it can restrict the search space of the optimal solution while limiting the problem size.

Two case studies (ammonia recovery and phenol production cases) are presented and used to illustrate the performances of the proposed model as well as the influence of some parameters on the optimal solution, such as the number of temperature levels on the scale (ΔT_{step}^{max}) and the number of operating years (N_{op}).

The results presented in the first case study show that the influence of the temperature scale on the objective function is relatively limited. The performances regarding the computation time are promising and within an acceptable range which can be further improved by carrying out a specific work on the problem size reduction by selecting more precisely the values on the temperature scale. Overall, the first case has shown the improvement of the solution compared to the ones presented in other publications.

Mixer and splitter units are introduced to reduce further the number of heat exchangers in the HEN and its cost. Their characterization with a fixed temperature tends to also limit the search space of the problem; however, a methodology has been developed and a relaxation parameter has been introduced to target promising test values. The second case study has illustrated the benefit of using mixer units, applying a selection method previously introduced to achieve a more economical MAHEN design.

Both case studies show that external fresh sources consumptions remain necessary and the waste effluents cannot be recovered completely because of property constraints or lack of use. However, chemical and physical treatments can be implemented in the process to modify their properties so they can either become alternate fresh sources or be discharged to the environment complying with current regulations. The mass and energy requirements, as well as their costs, can be integrated in the formulation of the previous problem and generate additional opportunities of resources and economic savings. The following chapter will introduce a generic model for such entities and described the way they can be used in specific cases.

Chapter 4

Simultaneous Heat and Mass integration with Regeneration Units

The two previous chapters presented models used to design networks allowing reusing waste effluents directly to feed process units while optimizing the heat requirements of the resulting streams and the structure of the heat exchanger network. The purpose of this fourth chapter is to add the opportunity of recycling waste effluents to the models M1, M2 and M3 using regeneration units to modify their properties; thus, easing their recovery within the process.

The content of the chapter focuses on how to design an economically optimal MAHEN taking advantage of regeneration technologies, whether it is for production or treatment purposes, and to evaluate how the mass and heat integration is influenced by adding the opportunity of recycling waste effluents. In this regard, a simple model is introduced to represent any type of regeneration units with generic parameters. The model of such units is based on objects already introduced in the problem and it includes a linear representation of their cost functions.

First of all, the interest of regeneration units within industrial processes is explained. Then, a model is detailed how such units are incorporated to the model structure and how the objective function is modified to include their operating and capital costs. Finally, the study of the integration of two different technologies (a thermal membrane distillation unit to produce fresh water from salted water and available excess heat, and a liquid-liquid extraction unit to comply with environmental regulations) in the phenol production case, studied in previous chapters, is presented illustrating the possibilities offered by this regeneration unit model and evaluating the influence on the MAHEN design.

4.1 Regeneration units within the Industry

Environmental standards impose more and more strict specifications for waste treatments to be able to discharge them back to the surroundings. These regulations are more and more constraining because sustainability and pollution prevention place high in political agendas. Consequently, waste management can represent a considerable and unavoidable financial burden for companies. It can require heavy investments and account for a significant part of annual operating costs. Therefore, selecting and designing properly and efficiently the processes to treat generated waste effluents are key decisions that will influence the company profitability and sustainability.

In the same perspective, making the decision of investing in systems capable of producing fresh resources instead of obtaining them from external suppliers can be complex. The balance between economic performances of each solution and additional benefits such as independence from external perturbations must be assessed to take a sound decision.

Finally, as seen in the case studies presented in Chapter III, even though direct reuse can improve substantially the fresh resources requirements, external fresh sources still may be necessary and waste effluents may remain to be treated. This is due to composition and property limitations that can prevent reusing a larger quantity of waste effluents. That is why being able to modify these limitations through process units (i.e. regeneration units) can allow improving further waste recycling and replacing external needs at a moderate cost.

Overall, the issues previously mentioned bring to light the need for integrating treatment units to the initial problem of heat and mass integration. Extending the possibilities of integration to the model can result in improving the economic and environmental performances of the MAHEN design.
Furthermore, one company (or group of companies) can address more realistic and relevant questions such as:

- What are the best investments to make to comply with environmental regulations?
- How recycling technologies can potentially help reducing the resources consumption?
- Is it more profitable to regenerate/treat effluents or produce its own fresh resources?
- How waste heat may be exploited through mass conversion systems?
- What is the optimal design of such units?

The proposed model is able to answer these questions with the addition of a generic representation of the regeneration units and their related costs.

4.1.1 Characterization of regeneration units

There are many different types of regeneration/treatment technologies available based on various physical and chemical principles. For instance, wastewater regeneration could imply treatments such as pH adjustment or physical removal of unwanted impurities e.g. by filters, membrane separators, sour water strippers, ion exchange resins. These treatments are often characterized by a ratio between inlet and outlet property (including concentration). It creates non-linearities in the equations representing the units operating conditions since the inlet flow rate and properties are variables [2, 59, 93].

Therefore, regeneration units need to be characterized in another way if the model is to remain linear. As a result, the performances of such units are set in advance by specifying the properties of its outlet stream; thus decoupling the characteristics of its entry and exit points. This can be seen as a limitation of the model; but, it can be overcome with the proper understanding of the technology as it will be shown in the first case study in the paragraph 4.3.1.

4.2 Model of regeneration units

The model for regeneration units is based on existing objects of the problem. In this model, a regeneration unit is represented by associating a waste sink (entry) and a fresh source (exit) (Fig.4.1). All process sources (and possibly fresh sources) can be allocated to the waste sink symbolizing the entrance of the unit whose treated flow rate is not specified in advance; but rather a variable to be optimized. A new fresh source is then generated which can feed process sinks (and possibly waste sinks), and whose mass flow rate is constrained by a specific relation with the flow rate collected by the waste sink.

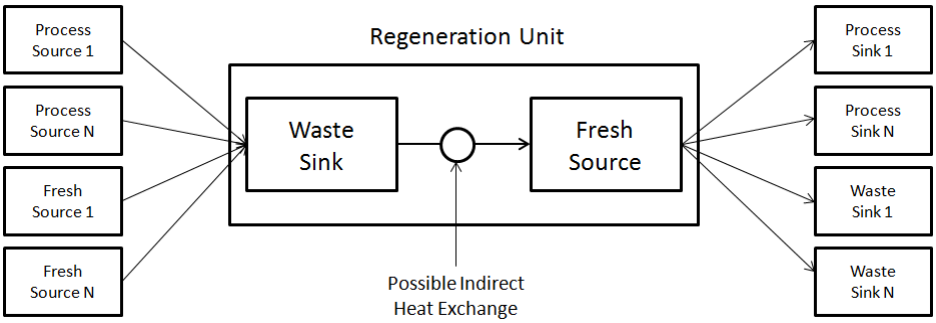

Figure 4.1: Generic representation of a regeneration unit

This model can be used to address different types of treatments for different means of applications (production of fresh resources, compliance with environmental regulations or regeneration for internal use). Note that the mass stream created within the regeneration unit may take part in the HEN.

4.2.1 Mass balance

Production and treatment units are represented as an association between a waste sink and a fresh source. These particular waste sink and fresh source are bound by the same equations as regular ones (section 2.2.1). A proportional relation defines the link between their mass flow rates. The relative mass flow rate variation between the input and output of the unit is characterized by a parameter ΔL_{ij}^{ru}.

- if $\Delta L_{ij}^{ru} \geq 0$, the mass flow rate of the output has increased (for instance, adding chemicals to react with some pollutants)
- if $\Delta L_{ij}^{ru} \leq 0$, the mass flow rate of the output has decreased (for instance, membrane treatment)

Therefore, the treatment/production unit characteristic equation is:

$$\forall i \in I_w, \forall j \in J_f, ru(i,j) \in RU,\ G_i^w \times (1 + \Delta L_{ij}^{ru}) = L_j^f = L_{ij}^{ru} \tag{4.1}$$

where $ru(i,j)$ is the regeneration unit defined by a waste sink $i \in I_w$ and a fresh source $j \in J_f$, and L_{ij}^{ru} is the total mass flow rate treated by the unit and available afterwards.

A binary variable ($\gamma_{L_{ij}^{ru}}$) is introduced to indicate the existence of the regeneration unit:

$$\forall i \in I_w, \forall j \in J_f,\ ru(i,j) \in RU, L_{ij}^{ru} - L_{ij,ru}^{max} \times \gamma_{L_{ij}^{ru}} \leq 0 \tag{4.2}$$

The extracted mass within the regeneration unit is defined by the variables $\dot{m}_{ij,k}^{ru}$ for each pollutant $k \in K$:

$$\begin{aligned} &\forall i \in I_w, \forall j \in J_f, ru(i,j) \in RU, \forall k \in K, \\ &\sum_{j' \in J_p \cup J_f} L_{ij'} \times y_{j',k} + \sum_{mu \in MU(i)} \sum_{j' \in J_p \cup J_f} L_{ij'}^{mu} \times y_{j',k} - L_{ij}^{ru} \times y_{j,k} = \dot{m}_{ij,k}^{ru} \end{aligned} \tag{4.3}$$

4.2.2 Heat requirement of the inner stream

The mass stream treated by a regeneration unit is particular in the sense that it goes from a waste sink to a fresh source (Fig.4.1). If it is relevant and feasible, the heat required or provided within the regeneration unit can be considered for the whole process heat integration. It can reduce the energy needs of such treatments; therefore, making them more economically attractive.

Since there are no other mass streams that can be mixed with it, this stream cannot be split as opposed to regular mass stream. Therefore, the heat transferred through the HEN is:

$$\forall i \in I_w, \forall j \in J_f, ru(i,j) \in RU, \forall n \in [N_{ij,ru}^{min}; N_{ij,ru}^{max} - 1], \\ L_{ij}^{ru} \times cp_j \times (T_{n+1}^{'*} - T_n^{'*}) = q_{ij,n}^{ru} \geq 0 \tag{4.4}$$

Depending on its nature (hot or cold), the variables $q_{ij,n}^{ru}$ associated with this stream are added to Eq.2.41 introduced in Chapter II (paragraph 2.2.2.2). The design of the heat exchangers involving this stream is realized in the exact same way as it is presented in the Chapter III (section 3.2.3).

4.2.3 Operating and Capital costs

The decision of selecting a regeneration unit and its design depend on the necessary cost to purchase and operate the technology in regards to its benefits. The cost function for a regeneration unit includes its operating and capital costs.

The operating costs are associated with the mass flow rate treated by the regeneration unit and the pollutant loads extracted by it. A nominal cost is defined for each item: $C_{ij,ru}^{flow}$ and $C_{ij,ru,k}^{load}$ respectively. Therefore, the operating cost function for this unit is:

$$C_{ij,ru}^{op} = C_{ij,ru}^{flow} \times L_{ij}^{ru} + \sum_{k \in K} C_{ij,ru,k}^{load} \times \dot{m}_{ij,k}^{ru} \tag{4.5}$$

Note that the operating costs normally associated with the fresh source and waste sink cost are considered as null.

The capital costs are related to the existence of the regeneration unit and its treatment capacity in terms of treated mass flow rate. A nominal cost is defined for each item: $C_{ij,ru}^{fixed}$ and $C_{ij,ru}^{variable}$ respectively. Therefore, the capital cost function for this regeneration unit is:

$$C_{ij,ru}^{cap} = C_{ij,ru}^{fixed} \times \gamma_{L_{ij}^{ru}} + C_{ij,ru}^{variable} \times L_{ij}^{ru} \tag{4.6}$$

4.3 Case Study

The phenol process case study presented in previous chapters is further developed to illustrate the selection and design of production and treatment units. First, a thermal membrane distillation (TMD) technology is designed to try replacing part of external fresh sources by taking advantage of the available excess heat from waste streams. Second, a sensitivity analysis is realized on certain costs (cold utility and heat exchangers) to evaluate the robustness of the solution. Finally, a phenol treatment unit is added to the problem

with the purpose of treating waste effluents to meet the environmental specifications before discharging them back to the environment. The mass and heat integration of the recycled wastewater into the phenol process will modify the MAHEN design in a way that remains to be evaluated.

4.3.1 Production unit: Thermal Membrane Distillation

4.3.1.1 Problem statement

The objective of this work is to achieve a minimum of fresh resources and energy consumption cost-effectively while complying with process specifications. As shown previously, it is possible to achieve substantial consumption reduction by designing cost-effective direct waste reuse and heat exchanger networks. However, in this case study, the need for external fresh resources and cooling utility remain. In this situation, the TMD technology may be useful because it is driven primarily by heat at low temperature which creates a vapor-pressure difference across a porous hydrophobic membrane. Therefore, if it is profitable, the excess heat from waste stream can be used to desalinate sea water to produce fresh water. A notable reduction in cooling and fresh resources requirements can be achieved at the same time resulting in savings in operating costs. The final decision to make use of a TMD unit depends on the balance between the savings and the added operating and capital costs.

4.3.1.2 TMD Model

The thermal membrane distillation is a separation process driven by the vapor pressure gradient which is generated by a temperature difference across a hydrophobic porous membrane. In case of a water treatment, the polluted water is heated up and evaporates through the membrane towards the cold side where the vapor phase is condensed.

Several TMD configurations exist and their difference come from how the vapor is condensed in the permeate side. There are four commonly used configurations [90] shown in Fig.4.2:

1. **Direct contact membrane distillation (DCMD)**:
   The treated water which is at a lower temperature than the feed is used as condensing fluid in the permeate side. In this configuration, the liquid in both sides of the membrane is in direct contact with the membrane.

2. **Air gap membrane distillation (AGMD)**:
   In this configuration, an air gap separates the membrane and a cold surface where the vapor is condensed. Compared to the previous configuration, the added air gap allows reducing the heat losses.

3. **Sweeping gas membrane distillation (SGMD)**:
   This configuration is similar to the DCMD configuration. The difference is that an inert gas is used as the cold collecting medium instead of the treated water.

4. **Vacuum membrane distillation (VMD)**:
   A vacuum is created on the permeate side to maintain the vapor pressure gradient towards it. The condensation takes place outside of the membrane module.

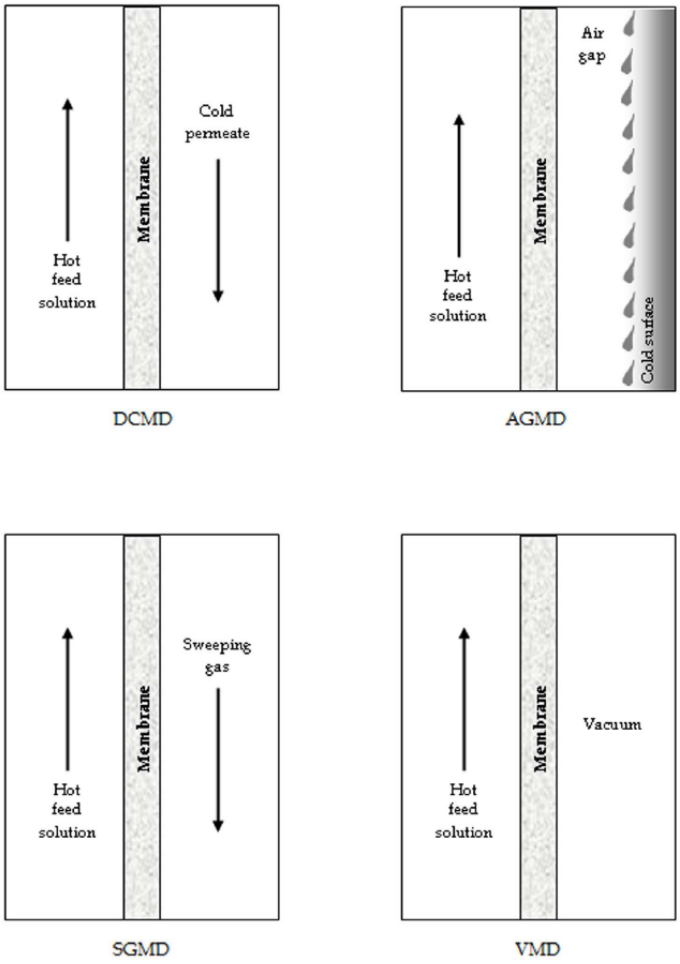

Figure 4.2: Common TMD configurations [90]

Water desalination can be achieved with a TMD unit and the DCMD configuration is the more commonly studied. This configuration has been studied in details by Elsayed et al. [44]. Experimental and numerical models have been developed and validated which will be used as a reference to formulate the specifications and cost functions of the TMD simplified model included in this case study.

The inlet salted stream is heated up from the ambient conditions to a selected temperature before being put in contact with the membrane inside the TMD. The recovery ratio (ξ) between the mass flow rates of the permeate streams ($\dot{m}_{vapor}$) and the raw stream ($\dot{m}_{seawater}$) characterizes how much water is ultimately recovered at the end. If it is assumed that the sensible heat provided ($cp_{seawater} \times \Delta T_{in}$) to the polluted stream to reach the operating temperature is roughly equal to the latent heat (h_{vapor}) required to vaporize some of the water contained in the contaminated stream water such as:

$$\dot{m}_{seawater} \times cp_{seawater} \times \Delta T_{in} \approx \dot{m}_{vapor} \times h_{vapor}$$

Therefore, the recovery ratio ξ is roughly equal to the ratio between these two heat loads:

$$\xi = \frac{\dot{m}_{vapor}}{\dot{m}_{seawater}} \approx \frac{cp_{seawater} \times \Delta T_{in}}{h_{vapor}}$$

In available studies, the raw stream is generally heated up to temperatures between $60°C$ and $90°C$ which is below the vaporization temperature in normal conditions. This range is selected to avoid membrane degradation. As a result, ξ would only be around 10% which is really low; rendering the TMD not really efficient.

This ratio can actually be increased by providing more sensible heat to the system to treat the same amount of polluted water. And since it cannot be done by increasing the TMD inlet temperature, a larger feed must be supplied to the system. This is achieved by recycling a part of the rejected stream and mixing it with the raw stream thus creating a larger feed. Let υ be the ratio of the recycled flow rate to the raw flow rate. This ratio depends on the selected inlet temperature. Fig.4.3 shows that it is the resulting stream with a mass flow rate equal to $\dot{m}_{seawater} \times (1 + \upsilon)$ that is heated up prior entering the TMD.

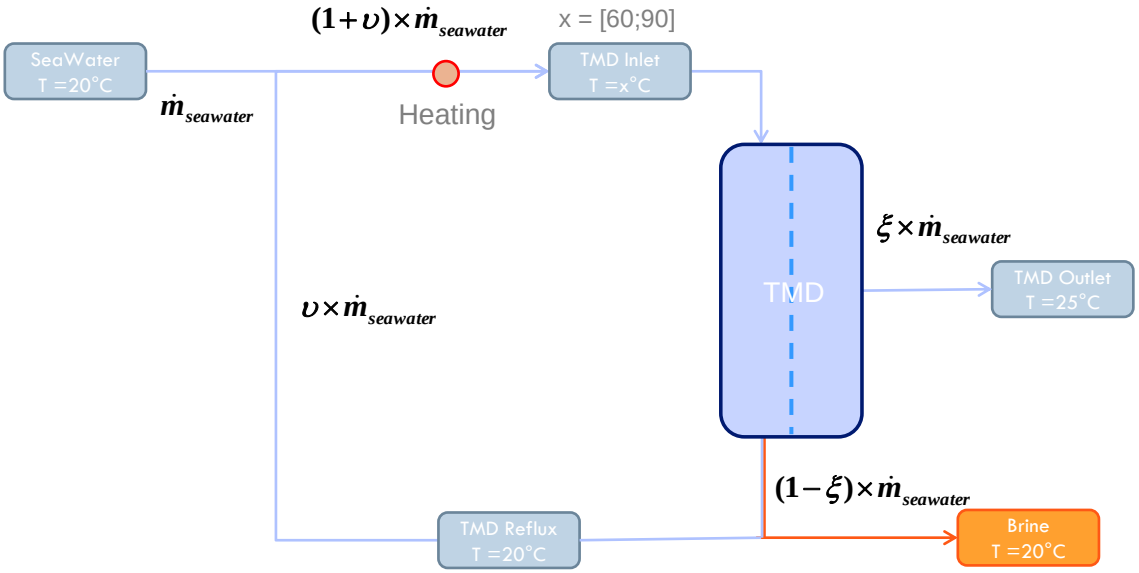

Figure 4.3: TMD configuration within the mass/heat integration problem

At the outlet of the TMD, a fraction of the inlet stream that has not been vaporized is called the *brine*. This stream is concentrated in salt and discarded back to the environment.

As previously mentioned, a detailed TMD model has been developed by Elsayed et al. [44] and validated based on experimental data for a direct-contact membrane distillation (DCMD). The cost functions for TMD capital and operating expenditures described in the article are modified in order to fit with the regeneration model presented previously:

- *Annual operating cost of TMD network excluding heating*:

$$C_{TMD}^{op} = c_{TMD}^{op} \times L_{ij}^{ru} = \frac{1411 + 43 \times (1-\xi) + 1613 \times (1+\upsilon)}{h_{op}} \times \frac{L_{ij}^{ru}}{\xi} \tag{4.7}$$

  It includes pretreatment, labor, brine disposal and pumping costs. h_{op} represents the annual operating hours.

- *TMD non-membrane capital cost*:

$$C_{non-membrane}^{capital} = c_{non-membrane}^{capital} \times L_{ij}^{ru} = (11150 \times (1+\upsilon)) \times \frac{L_{ij}^{ru}}{\xi} \tag{4.8}$$

  It includes the cost for internal heat exchangers, pumps, pipes, instrumentation, electrical subsystems and installation.

- *TMD membrane capital cost*:

$$C_{membrane}^{capital} = c_{membrane}^{capital} \times L_{ij}^{ru} = N_{op} \times (90/4 + 360/N_{op}) \times \frac{L_{ij}^{ru}}{J_w} \tag{4.9}$$

  The surface of the membrane depends on its geometry and the recovered flow rate. J_w represents the water flux per m^2 of membrane. The total membrane area is proportional to the ratio between the total recovered flow rate at the outlet of the TMD (L_{ij}^{ru}) and the unitary flux allowed by the selected membrane design (J_w).

  Elsayed et al. [44] assumed that the membrane lifetime is 4 years. Its annual replacement cost is equivalent to depreciating its cost ($90€.m^{-2}$) over this period with no salvage value. The rest of the fixed cost ($360€.m^{-2}$) is represents the costs required for the membrane installation assuming a typical value of 5.0 for the Lang factor. This part of the cost is depreciated over a N_{op}-year linear depreciation with no salvage value (where N_{op} represents the number of operating years of the system).

In this case study, a seawater fresh source is introduced as a supply for the TMD unit. In order to take into account the presence of salt into the seawater and its use to the TMD inlet, a new property is added to the sources and sinks of the case. Since the quantity of salt is supposed to be low and it is not taken into account in the TMD cost function, the salt concentration is only used as an indicator of its presence. Thus, for the seawater it is set to 1 as well as the for the acceptable range of the waste sink that represents the TMD inlet. This prevents other fresh sources to feed this particular sink. For the initial sources and sinks, this property is set to 0. With this property, only the seawater source can enter the TMD, and conversely the seawater can only interact with the waste sink used as the TMD entry.

Moreover, as shown in Fig.4.3, it is a stream with a mass flow rate equal to $(1 + \upsilon)$ times the inlet salted flow rate that is heated up before passing through the TMD. Thus to avoid the use of two fresh sources or modeling precisely the reflux mechanisms of TMD, the chosen assumption is that the reflux ratio of the TMD inlet is included in the formulation of the heat capacity of the seawater as follows (assuming $cp_{water} = 4.2kJ.(kg.K)^{-1}$:

$$cp_{seawater} = cp_{water} \times (1 + \upsilon) \tag{4.10}$$

In this way, the TMD consumes seawater from a unique fresh source with a linear and simple relationship to its outlet, and the heat requirement at the TMD inlet includes the necessary reflux. Note that the seawater source is supposed to be free.

The data regarding the TMD technology used in the phenol process case are shown in Table 4.1.

	Comp. in Phenol (mass fraction)	Salt (0 or 1)	p_v (kPa)	pH	Temperature ($°C$)
Fresh Source					
Seawater	0.0	1.0	0.0	7.0	20
Production Unit TMD					
TMD in	0.0-0.0	1.0-1.0		5.0 - 9.0	60 - 90
TMD out	0.0	0.0	0.0	7.0	25

Table 4.1: Phenol production case with TMD - Additional Process Data

In the first part of the case study, the objective is to find the best TMD inlet temperature to reach the most cost-effective design for the MAHEN over a 10-year period. The methodology established for the study is:

1. *Optimization of the TMD characteristic features (J_w,υ) for a given TMD inlet temperature using the NLP model developed by Elsayed et al. [44] under few assumptions*:

   An explicit multi-physics model has been developed by Elsayed et al. describing the relationship between the flux going through the membrane and the difference of chemical potentials across the membrane. In this article, the model is used to optimize the profits generated by the sell of the water produced by the TMD assuming different scenarios on the origin and cost of the heat provided as the entrance of the TMD. Moreover, the recovery ratio (ξ), characterizing the performances of the TMD technology, is fixed and set to 80%.

   However, in this present work, the water will not be sold and the heat required by the TMD inlet stream will be provided freely by the heat surplus found within the phenol process. Therefore, with these assumptions, the objective of the NLP model becomes the minimization of the TMD operating and capital costs. And, the analysis of their formulation shows that it comes down to maximizing the flux (J_w) and minimizing the reflux ratio (υ).

2. *Calculation of the TMD cost function coefficients introduced by Eq.4.7, Eq.4.8 and Eq.4.9.*

   Once the flux and the recovery ratio are determined, the coefficients of the TMD cost function can be evaluated. These coefficients are used to set up the TMD in the MAHEN design problem.

3. *Optimization of the MAHEN design for each TMD inlet temperature using mixer units:*

   In this step, the MAHEN design model developed in Chapter III is applied with the addition of a TMD unit. The features of the additional objects added to the problem structure are presented in Table 4.1.

   A sensitivity analysis is led on the TMD inlet temperature to determine the economically optimal MAHEN design including this water production unit. For each temperature between $60°C$ and $90°C$ with a $2°C$-step, the total annualized cost is calculated in order to determine the most suitable TMD operating conditions to be integrated with the phenol production process. Mixer units are used to further reduce the HEN costs in the solution; therefore, a selection of their temperature must be realized as explained in Chapter III.

4.3.1.3 Optimal TMD inlet temperature

The NLP model [44] is used to determine the maximum flux (J_w) and the minimum necessary reflux ratio (υ) assuming that the recovery ratio (ξ) is fixed and set to 0.8.The model is solved using GAMS solver for each temperature between $60°C$ and $90°C$ with a $2°C$-step. With the results of the first step of the methodology, the coefficients of the TMD cost function are calculated. The results are shown in Table 4.2.

T^{in}_{TMD} $°C$	J_w $kg.s^{-1}.m^{-2}$	υ -	q_{TMD} $kW.(kg.s^{-1})^{-1}$	c^{op}_{TMD} $€.(tons.h^{-1})^{-1}$	$c^{capital}_{membrane}$ $€.(kg.h^{-1})^{-1}$	$c^{capital}_{membrane}$ $€.(kg.h^{-1})^{-1}$
60	0.0021	14.36	2580.9	1.14	77.59	59.48
62	0.0023	13.41	2541.1	1.07	69.63	55.77
64	0.0026	12.55	2504.3	1.01	62.68	52.46
66	0.0029	11.79	2470.1	0.96	56.60	49.50
68	0.0032	11.09	2438.2	0.91	51.24	46.82
70	0.0035	10.47	2408.4	0.86	46.51	44.40
72	0.0038	9.90	2380.4	0.82	42.32	42.20
74	0.0042	9.38	2354.1	0.79	38.59	40.18
76	0.0046	8.90	2441.3	0.75	35.26	38.34
78	0.0050	8.47	2305.9	0.72	32.27	36.65
80	0.0055	8.06	2283.7	0.70	29.60	35.08
82	0.0060	7.69	2262.6	0.67	27.19	33.64
84	0.0065	7.34	2242.6	0.65	25.02	32.30
86	0.0070	7.02	2223.6	0.62	23.05	31.06
88	0.0076	6.72	2205.5	0.60	21.28	29.90
90	0.0083	6.44	2188.1	0.58	19.66	28.81

Table 4.2: TMD characteristic parameters and cost function coefficients

As shown in Table 4.2, the higher the TMD inlet temperature, the bigger the flux that can through the membrane because the temperature gets closer to the vaporisation temperature.

The heat requirements per unit of mass flow rate ($kg.s^{-1}$) is represented by q_{TMD} assuming that $T_{seawater} = 20°C$:

$$q_{TMD} = cp_{water} \times (1 + \upsilon) \times (T^{in}_{TMD} - T_{seawater})$$

This implies that the higher the TMD inlet temperature, the lower the heat requirements per unit of seawater treated and the lower the operating and capital costs for it. Therefore, substituting external fresh sources with the fresh water produced by the TMD at a lower cost requires finding available heat sources at the highest temperature possible and in sufficient quantities within the process; knowing that costly external heat utilities can be used to complete the missing part of the heat requirements. A balance must be found between the fresh water and cooling savings realized by using the TMD and the additional operating (including the use of external heating sources) and capital costs generated.

The phenol production process studied in Chapter III is an interesting example where the opportunity of using the TMD technology can be economically relevant. The optimal MAHEN structure found previously in Chapter III utilizes the cooling utility to extract around $100kW$ of heat from streams sent to the waste sink and around 1 $100kg.h^{-1}$ of external fresh sources are required to feed process sinks (Table 3.7). Therefore, this available heat can potentially be converted through the TMD to reduce the need for external fresh sources as well as cooling requirements.

In this case study, a sensitivity analysis on the TMD inlet temperature (from $60°C$ to $90°C$ with a $2°C$-step) is carried to evaluate the best operating parameter for the TMD to recover as much as it is economically profitable. The results regarding the mass and heat requirements of the process for each tested temperature are shown in Table 4.3.

T^{in}_{TMD} ($°C$)	Q_h (kW)	Q_c (kW)	Q_{TMD} (kW)	L_{Fresh1} ($kg.h^{-1}$)	L_{Fresh2} ($kg.h^{-1}$)	L_{TMD} ($kg.h^{-1}$)
60	0.0	0.0	101.1	725.4	253.2	112.8
62	0.0	1.9	99.8	690.8	317.6	113.1
64	0.0	3.3	98.4	690.8	317.6	113.1
66	0.0	4.5	97.1	690.7	317.6	113.2
68	0.0	5.6	96.0	690.5	317.6	113.4
70	0.0	6.6	95.0	690.3	317.6	113.6
72	0.0	7.8	94.1	690.1	317.6	113.8
74	0.0	8.3	93.3	689.8	317.6	114.1
76	5.9	7.9	99.7	677.5	329.9	123.3
78	9.5	7.9	103.3	671.8	329.9	129.0
80	8.4	8.7	101.4	676.1	317.6	127.8
82	11.8	8.7	104.7	670.6	317.6	133.3
84	15.2	8.7	108.1	665.1	317.6	138.8
86	18.6	8.7	111.5	659.5	317.6	144.4
88	22.0	8.7	114.9	653.5	317.6	150.0
90	0.0	98.0	-	803.9	317.6	-

Table 4.3: Phenol production case - Heat and mass requirements with the TMD

Fig.4.4 shows the evolution of the total annualized cost depending on T^{in}_{TMD}. With the cooling nominal cost fixed at $25€.MWh^{-1}$, the optimal structure is identified with a TMD operating at $60°C$. The TMD is not selected only when T^{in}_{TMD} reaches $90°C$

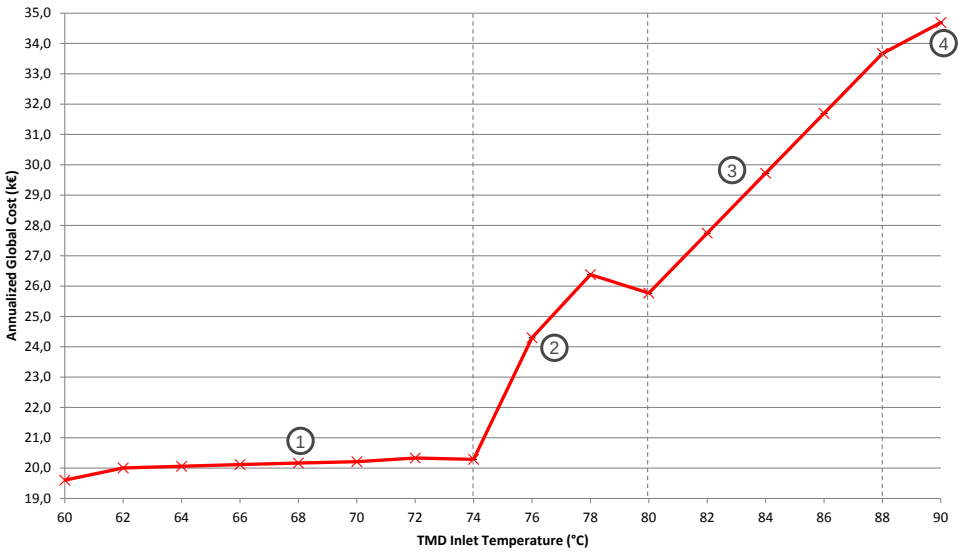

Figure 4.4: Total annualized cost

This evolution can be explained by evaluating the heat sources that be found and the constraints on the system that can restrict their use. There are three process sources and they have temperatures between $40°C$ and $85°C$. Moreover, the minimum approach

ΔT_{min} is equal to $10°C$; thus, the highest temperature at which the inlet stream of the TMD can be heated up by process sources is limited to $75°C$; otherwise, an external heating utility is necessary to reach the selected temperature.

For temperature higher than $75°C$, the use of an external source of heat created additional operating costs that lower the benefits of using the TMD; however, it can still be used, if the additional heating requirements are outweighed by the cooling and fresh source savings. That is why, the optimal solution is located be below $75°C$, and the total annualized cost increases rapidly when T^{in}_{TMD} is above it. Note that in a similar way as the study done in Chapter III, the optimal solutions are found using a mixer unit for the waste sink.

In Fig.4.4, five different zones indicating an evolution of the MAHEN structure are displayed. The proposed analysis of these zones is based on the MAHEN design displayed in Fig.4.5 to Fig.4.8 for four particular values of T^{in}_{TMD}: $62°C$, $74°C$, $78°C$ and $82°C$.

Zone 1: Below $75°C$ (Fig.4.5-Fig.4.6)

- The use of cold utility is necessary (except at $60°C$) but it is reduced to less than $9kW$ (less than 10% of the requirement without the TMD).
- The cooling demand is decreasing with T^{in}_{TMD} until it reaches $0kW$ at $60°C$
- The TMD output is relatively constant around $113kg.h^{-1}$
- Five heat exchangers are needed (except at $60°C$ because the unit used with the cooling utility disappears)

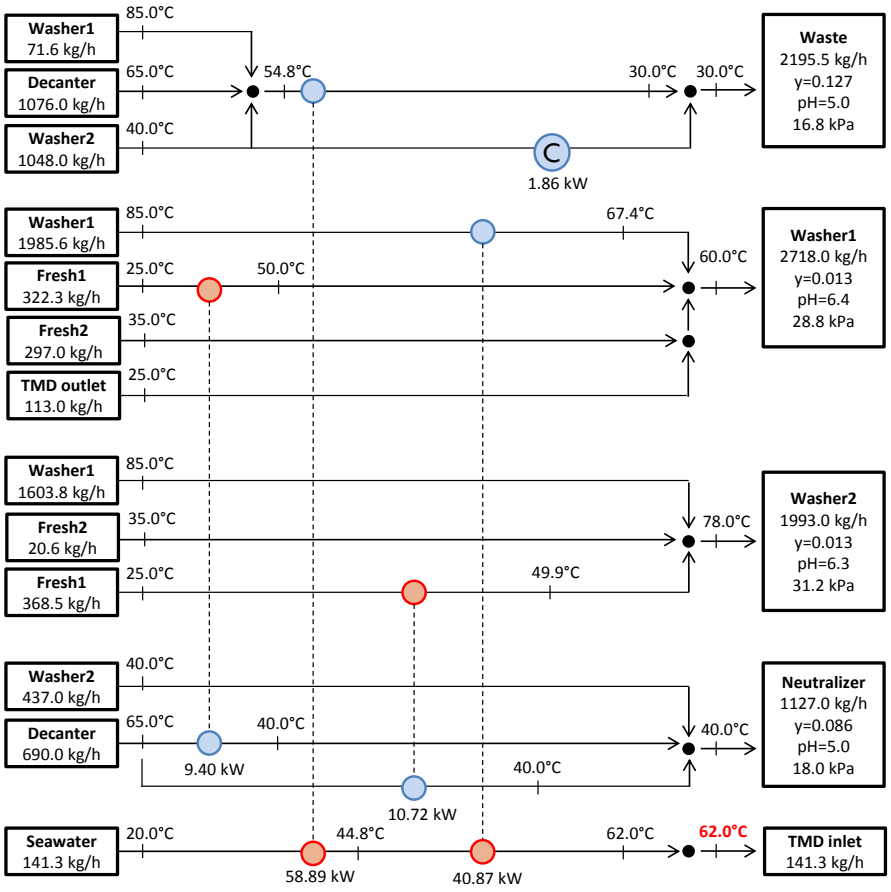

Figure 4.5: Optimal MAHEN structure for $T^{in}_{TMD} = 62°C$

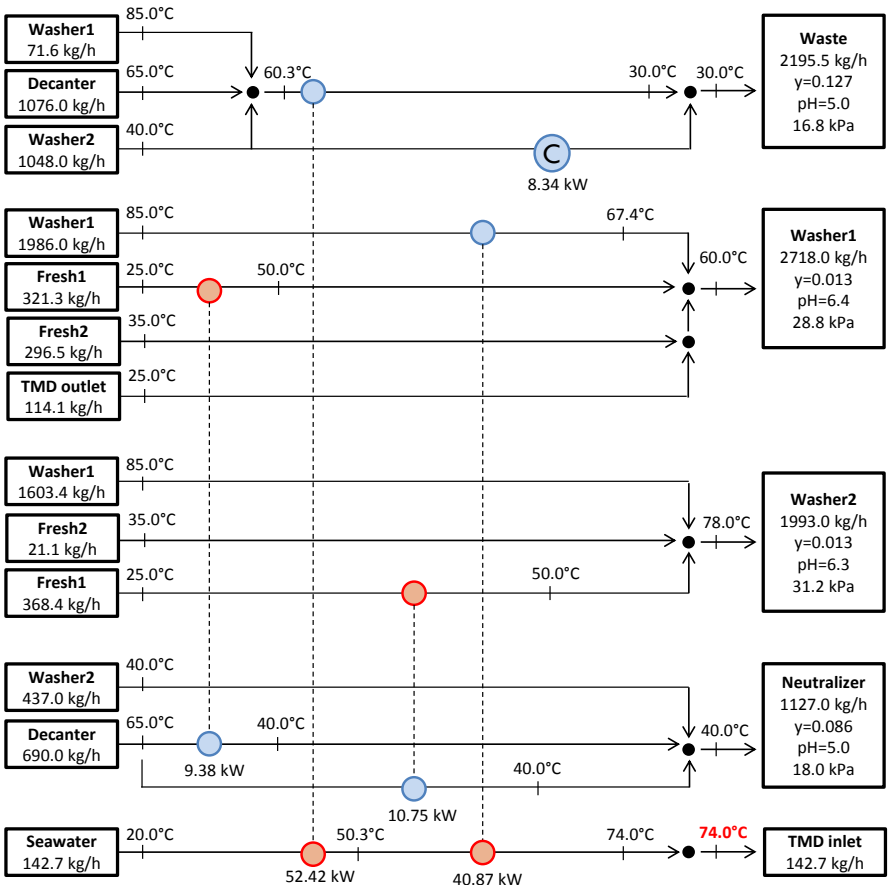

Figure 4.6: Optimal MAHEN structure for $T^{in}_{TMD} = 74°C$

When the MAHEN structures shown in Fig.4.5 and Fig.4.6, one can observe that structures remain the almost the same when the TMD inlet temperature varies in this zone. The mass allocation does not change. The two heat exchangers between process streams not involved with the seawater stream remain identical whatever the TMD inlet temperature.

The difference comes from the three other heat exchangers. When the TMD inlet temperature increases, the need to recover heat at higher temperature increases. This implies that the mixing temperature of the resulting mix stream going to the Waste needs to increase (from 53.8 to 60.3°C). Therefore, the portion of the coldest stream ($Washer2$ at 40°C) bypassing the mixer unit and sent to the waste sink is getting larger; thus, increasing the cooling requirements.

Zone 2: Between $76°C$ and $79°C$ (Fig.4.7)

- Heating requirements are no longer null ranging from $5.9kW$ to $9.5kW$
- The cooling demand is constant at $7.91kW$
- Reaching temperatures above $75°C$ creates additional and unavoidable costs; thus the TMD output is increasing (by $\approx 10.kg.h^{-1}$) to make them more cost-effective.
- An additional heat exchanger is required while the rest of the structure remains similar to the previous one. Although a slight difference appears. Indeed, to avoid a very small heat exchanger in regards with its fixed cost, the HEN structure is rearranged and deviated from the optimal structure, which explains the sudden change in this zone of the curve.

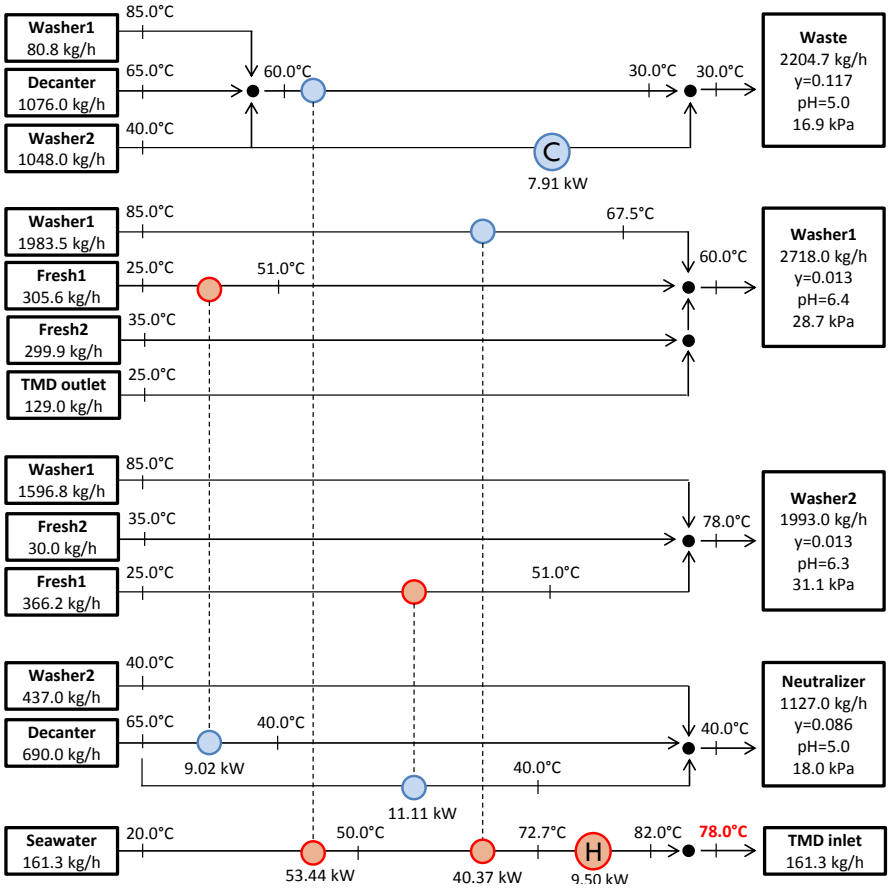

Figure 4.7: Optimal MAHEN structure for $T^{in}_{TMD} = 78°C$

Zone 3: Between $80°C$ and $88°C$ (Fig.4.8)

- The heat load provided by the external hot utility is increasing strongly with T^{in}_{TMD} reaching $22.0kW$ at $88°C$
- The TMD output is still increasing to optimize the use of additional and mandatory investments; reaching $150kg.h^{-1}$ at $88°C$, while the cooling demand remains constant at $8.72kW$
- The optimal structure comes back to the structure obtained when T^{in}_{TMD} was below $75°C$ with the additional heating utility exchanger. This time, in this configuration, the heat load of this exchanger is large enough to be economically viable (the TMD inlet stream would be heated up by more than $4°C$); thus, the return to a more linear evolution of the objective function with T^{in}_{TMD} can be observe on the curve.

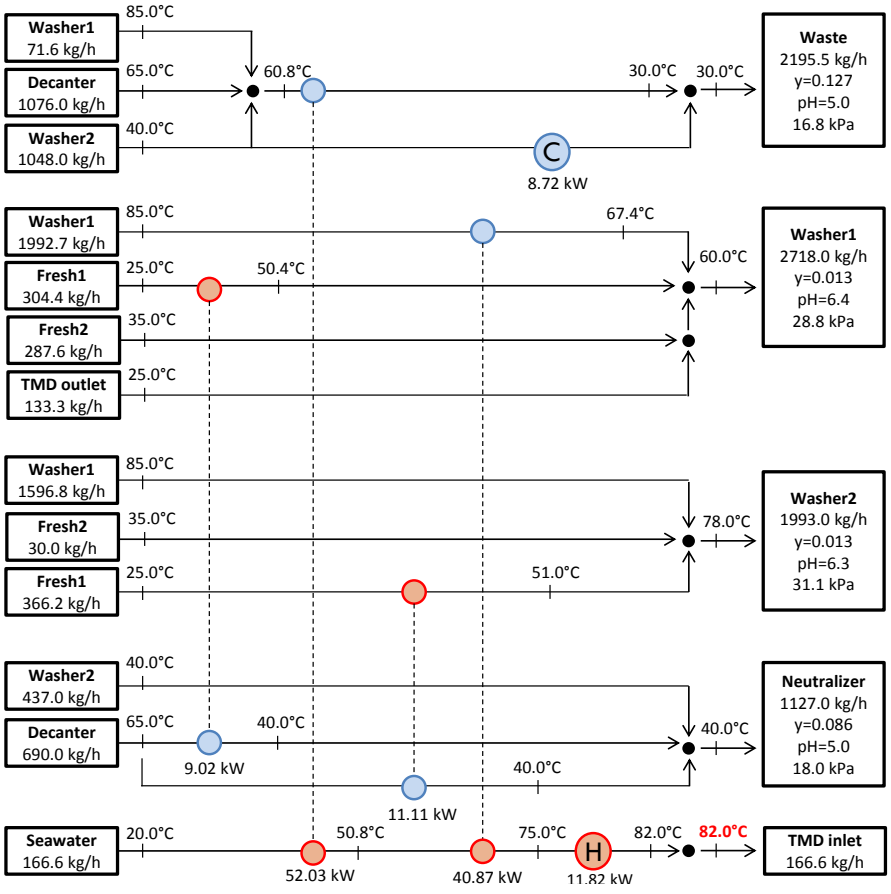

Figure 4.8: Optimal MAHEN structure for $T^{in}_{TMD} = 82°C$

Zone 4: Above $90°C$

- The TMD is no longer used
- The TMD heating cost is too substantial for it to be economically viable
- The optimal structure is the one obtained in Chapter III (Fig.3.15).

In order to compare the actual cost of the fresh water source produced by the TMD and the other external sources, the cost per unit of produced fresh water is calculated. Three different definitions are proposed to evaluate this cost:

- *TMD Gross cost without heat exchangers*
  It is the ratio between the annualized cost considering the TMD operating and capital costs (Eq.4.7 - 4.8 -4.9) and the annual fresh water produced with the TMD:

$$C_{TMD}^{gross\ without\ HE} = \frac{1}{N_{op}} \times \frac{(C_{membrane}^{capital} + C_{non-membrane}^{capital} + \sum_{n=1}^{N_{op}} \frac{AOC_{TMD}}{(1+r_a)^n})}{L_{ij}^{ru} \times h_{op}} \quad (4.11)$$

- *TMD Gross cost with heat exchangers*
  The capital cost of the heat exchangers used for providing heat to the TMD (C_{he}^{TMD}) is added to the previous cost.

$$C_{TMD}^{gross\ with\ HE} = \frac{1}{N_{op}} \times \frac{(C_{he}^{TMD} + C_{membrane}^{capital} + C_{non-membrane}^{capital} + \sum_{n=1}^{N_{op}} \frac{AOC_{TMD}}{(1+r_a)^n})}{L_{ij}^{ru} \times h_{op}} \quad (4.12)$$

- *TMD Net cost*
  It the difference between the global annualized cost of the solution (TAC_{TMD}) and the one of the reference without TMD (TAC_{ref}) divided by the annual fresh water production converted in TMD:

$$C_{TMD}^{Net} = \frac{TAC_{TMD} - TAC_{ref}}{L_{ij}^{ru} \times h_{op}} \quad (4.13)$$

The results are presented for each T_{TMD}^{in} in Fig.4.9.

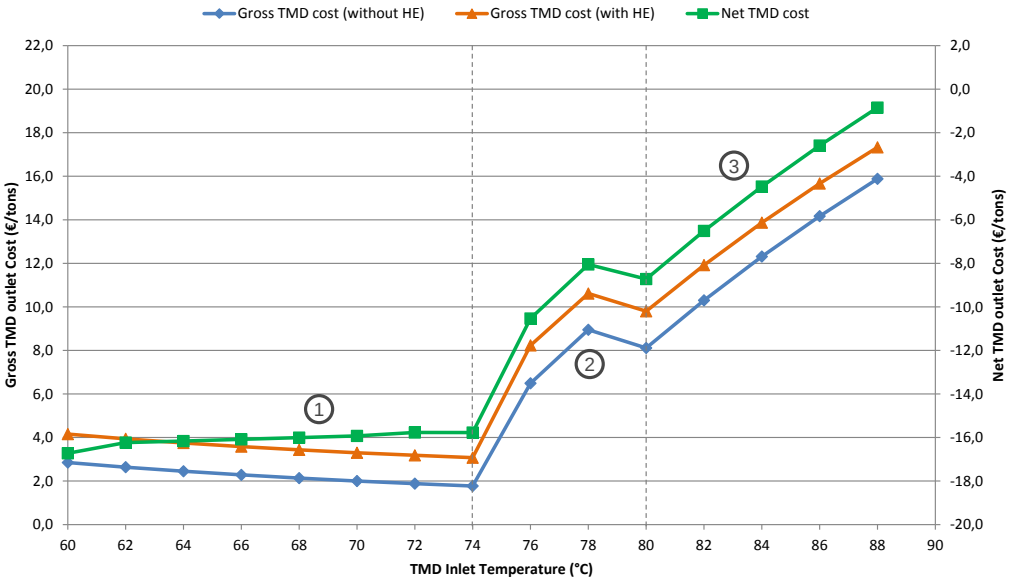

Figure 4.9: TMD fresh water production cost

Below $75°C$, the three curves evolves slightly differently. Similarly to the total annualized cost, the gross and net costs are almost a flat plateau with a variation between extreme points inferior to $1.0€.m^{-3}$. As T_{TMD}^{in} increases, this net cost increases while the gross cost decreases. The net cost increases following the same trajectory as the total annualized cost of the total MAHEN structure. But the gross cost which takes into account only the operating and capital cost related to the TMD are decreasing with T_{TMD}^{in}.

Above $75°C$, the three curves evolves in the exact same way. Note that the TMD is economically interesting as long as its net cost is negative. As T_{TMD}^{in} increases, this cost increases too, almost reaching the limit of $0.0€.m^{-3}$ at $88°C$. This explains why the TMD is not selected at $90°C$.

The gross TMD cost is growing very rapidly once the need for heating utility is unavoidable. The values reached are significantly above the usual order of magnitude for fresh water (from 1.0 to $3.0€.m^{-3}$), reaching values above $10.0€.m^{-3}$. Even though it will not be possible to sell this water at these prices, the implementation of the TMD still makes sense because of the important savings done in operating costs (mostly cooling savings).

Even though the optimum was found at $60°C$ for the global objective, the optimal operating point regarding the TMD alone is at $74°C$. Therefore, it may be interesting to evaluate the resilience of this optimal structure and verify if the optimal operating conditions for the TMD remain the same while the costs of what seems to be the driving factors in the TMD cost vary, i.e. the cold utility cost and the heat exchanger cost. A sensitivity analysis on these two parameters is led in the following paragraph.

4.3.1.4 Sensitivity Analyses

Two main parameters seem to drive the use of the TMD. These parameters are the cold utility and the heat exchanger costs. Therefore, the following results show the influence of these two parameters on the MAHEN and TMD designs for two values of T_{TMD}^{in}, $60°C$ and $74°C$. These two temperature values represent the extremities of the range in the previous results where the objective is a quasi flat plateau. There are three objectives for this study. First, check if the TMD is still used when the cooling savings are lower. Second, evaluate the resilience of the optimal structure found previously for each temperature against these two costs. Finally, determine how the optimal temperature evolves with these costs.

In this study, the nominal cooling utility cost ($C_{h_u}^{cold}$ in €$.MWh^{-1}$) and the nominal fixed part of an heat exchanger (C_{he}^{fixed} in €) take successively different values: (0.0 ; 2.5 ; 10.0 ; 25.0) and (1.0 ; 592.9 ; 2 500.0 ; 5 291.9), respectively. Figures 4.10 and 4.11 presented the variation of the objective function depending on the value of $C_{h_u}^{cold}$ and C_{he}^{fixed} for the two selected temperatures.

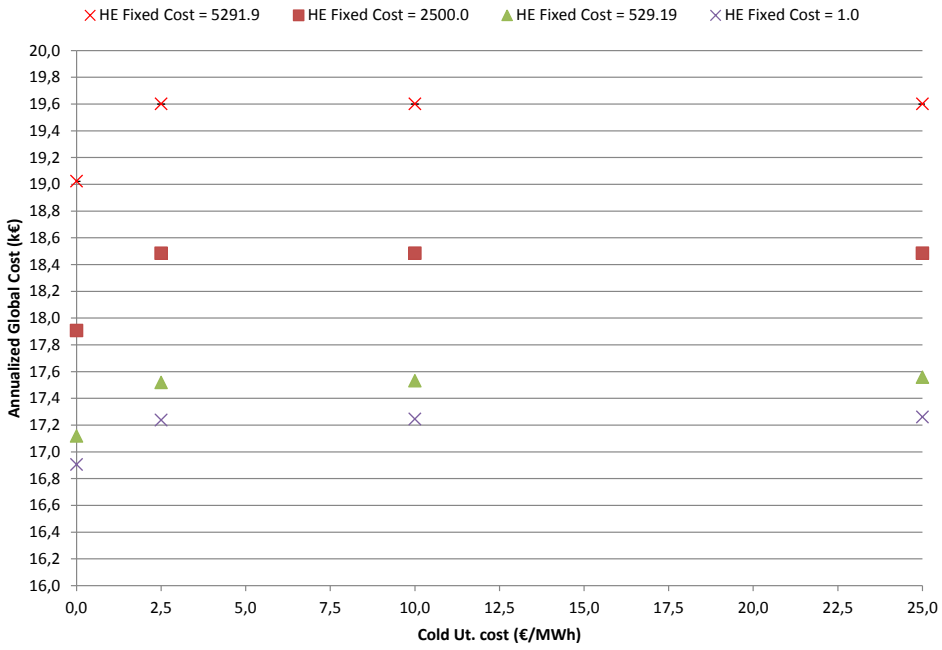

Figure 4.10: Sensitivity analysis results for $T_{TMD}^{in} = 60°C$

In Fig.4.10, for a given C_{he}^{fixed}, a plateau appears for values of $C_{h_u}^{cold}$ higher than 2.5€$.MWh^{-1}$. The optimal structure remains the same until the cooling savings are too modest to justify the implementation of the TMD. The TMD capital and operating costs are relatively substantial at this temperature because a higher internal reflux is required; therefore, using it must be compensated by a gain in operating costs. Limit values at which the TMD is not profitable anymore can be calculated for each couple of C_{he}^{fixed} and $C_{h_u}^{cold}$.

For each of the selected fixed heat exchanger cost, this limit value is located between 0.0 and 2.5€.MWh^{-1}, which at least 10 times lower than the initial nominal cooling cost. For $T^{in}_{TMD} = 60°C$, the cooling savings are significant enough to make the TMD profitable until they do not outweigh the additional costs required to use the TMD.

In Fig.4.11, for a given C^{fixed}_{he} when $T^{in}_{TMD} = 74°C$, it is not a plateau but a steady linear curve that appears to indicate that the structure of the MAHEN with the TMD evolves and adapts to the different costs but the TMD is still in place. Contrary to the previous case, at this temperature, the TMD operating and capital costs are less significant which means that the savings gain by recovering excess heat and limiting the external fresh purchases are significant enough for the TMD to be used.

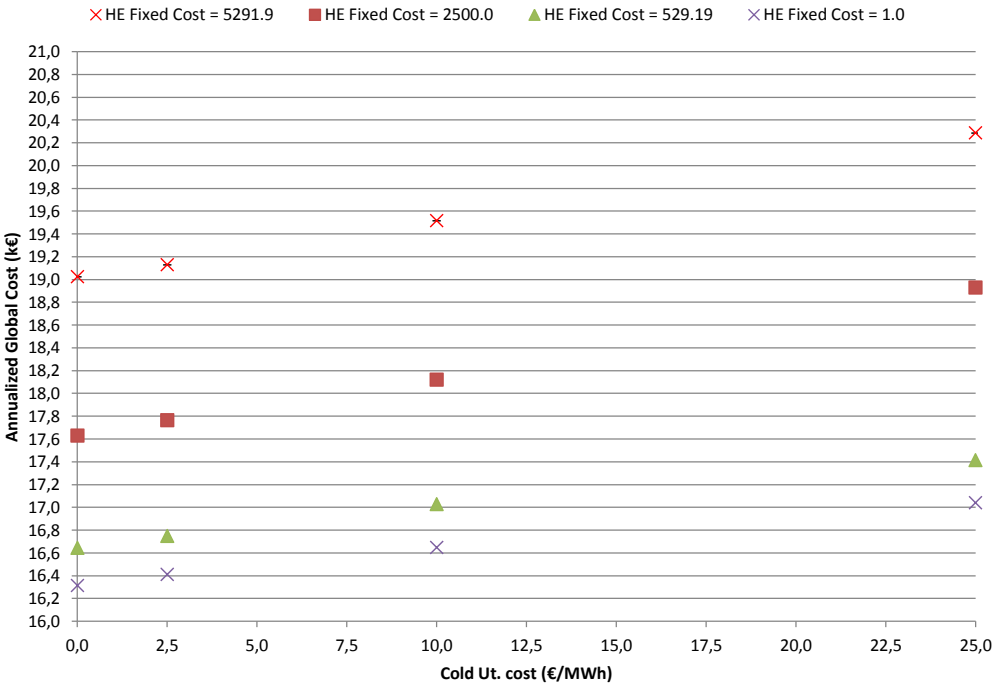

Figure 4.11: Sensitivity analysis results for $T^{in}_{TMD} = 74°C$

It appears that for this particular case, the TMD should operate at the highest available temperature to get the most cost effective design of the MAHEN when C^{fixed}_{he} and $C^{cold}_{h_u}$ are low. Even though the MAHEN structure is less complex at $60°C$ than the one at $74°C$, the reductions in fresh water consumption are quite similar while there is a small difference in cooling needs. Thus, the difference between the two structures comes mainly from the TMD costs and the slight gain in the HEN costs, in addition to the cooling savings. These last two items are not significant when C^{fixed}_{he} and $C^{cold}_{h_u}$ are low. This gives an advantage at working at the highest TMD inlet temperature reachable using free excess heat. The situation is reversed when these two costs are high for similar reasons.

Overall, it is interesting to note that in this case, the economic performance of the MAHEN is fairly identical whatever the TMD inlet temperature and the given nominal costs.

Table 4.4 shows the results of the sensitivity analyses for each proposed definition of the marginal cost of the water produced by the TMD.

T^{in}_{TMD} (°C)	C^{cap}_{he}	$C^{cold}_{h_u}$	$C^{gross\ without\ HE}_{TMD}$ 60	$C^{gross\ without\ HE}_{TMD}$ 74	$C^{gross\ with\ HE}_{TMD}$ 60	$C^{gross\ with\ HE}_{TMD}$ 74	C^{Net}_{TMD} 60	C^{Net}_{TMD} 74
	5 291.9	25.0	2.9	1.8	4.2	3.1	-16.7	-15.8
		10.0	2.9	1.8	4.2	3.1	-6.3	-6.3
		2.5	2.9	1.8	4.2	3.1	-1.1	-1.6
		0.0	-	1.8	-	3.1	-	**0.0**
	2 500.0	25.0	2.9	1.8	3.5	2.4	-16.8	-15.5
		10.0	2.9	1.8	3.5	2.5	-6.3	-6.6
		2.5	2.9	1.8	3.5	2.5	-1.1	-1.9
		0.0	-	1.8	-	2.5	-	-0.3
	529.2	25.0	2.9	1.8	3.1	2.5	-16.9	-15.7
		10.0	2.9	1.8	3.1	2.5	-6.5	-6.7
		2.5	2.9	1.8	3.1	2.5	-1.3	-2.1
		0.0	-	1.8	-	2.5	-	-0.5
	1.0	25.0	2.9	1.8	3.0	2.5	-16.9	-15.9
		10.0	2.9	1.8	3.0	2.5	-6.6	-6.9
		2.5	2.9	1.8	3.0	2.5	-1.4	-2.2
		0.0	-	1.8	-	2.5	-	-0.6

Table 4.4: TMD case - Sensitivity analyses results

The results in this table confirm the analysis above. Indeed, the marginal cost of the water produced by the TMD is lower when $T^{in}_{TMD} = 74°C$ for the first two definitions, while the third definition is more sensitive to the cold utility cost.

The gross water cost including the heat exchanger cost is decreasing when C^{cap}_{he} decreases because the TMD integration requires additional heat exchangers. Therefore, this cost is not the right one to be compared with the other fresh sources cost included in this case (i.e. $Fresh1$ and $Fresh2$ which nominal cost are 3 and 1 €$.tons^{-1}$ respectively). Actually, all the heat exchangers associated with the TMD, which are considered in the definition of this cost, are not additional. This explains why when $C^{gross\ with\ HE}_{TMD} = 3.1$€$.tons^{-1}$ the TMD is still cost-effective compared to the most expensive fresh source ($Fresh1$).

Regarding C^{Net}_{TMD}, the results show that, in the case where $C^{cap}_{he} = 5291.9$€ and $C^{cold}_{h_u} = 0.0$€$.MWh^{-1}$, the TMD integration is almost equivalent to the reference MAHEN; thus, the TMD is either not selected (at $60°C$ or not really profitable ($C^{Net}_{TMD} = 0.0$ at $74°C$). This is because the cost savings attributed to the TMD due to lower cooling requirements are null while the heat exchangers necessary for the MAHEN have still a significant influence on the total annualized cost. For the other values of C^{cap}_{he}, C^{Net}_{TMD} is always negative showing clear savings due to the TMD integration.

4.3.2 Treatment unit: Phenol removal

The following study focuses on how treatment units can help comply with the environmental regulations on phenol polluted wastewater being discharged to the environment. A quick literature review is realized on the existing phenol treatments of wastewater in order to model their capabilities as well as their cost function. The objective is to evaluate how the constraint on the phenol concentration of the ultimate waste effluents and the use of treatment units will influence the optimal design of the MAHEN.

4.3.2.1 Phenol environmental regulations

The phenol has high toxicity potential at very low concentrations and low biodegradability. Environmental standards are very strict concerning wastewater discharge back into the nature. The European Union fixes at $0.0005 mg.L^{-1}$ the phenol concentration in drinking waters and in France effluents must have a concentration lower than $0.3 mg.L^{-1}$ to be sent off to surroundings. It is a great topic of interest in the industry since this standard is very stringent and treatment costs can be substantial. Several other constraints are defined on the quality of wastewater effluents discharged to the environment. Most importantly, their pH must be ranging between 5.5 and 8.5 and their temperature must be lower than $30°C$.

The previous limitation, used in Chapter II and III, on phenol concentration (i.e. 150 000 $mg.L^{-1}$) characterizing the waste sinks were not appropriate to take into account the environmental standards regarding phenol concentration; therefore it must be adapted for this study knowing that the mass balance between sinks requirements and sources available flow rates shows that at least 1 $t.h^{-1}$ remain to be treated if all sinks requirements are met by process sources. Note that the resulting phenol concentration of the stream sent to the waste sink was around 100 000 $mg.L^{-1}$. Thus, despite the gain with direct reuse obtained on water and energy consumption, the remaining wastewater must be treated before its discharge to the environment. However, it can offer a new opportunity to further reduce the external fresh water consumption by recycling a portion of the treated water.

After a review of different technologies available to treat water polluted by phenol, selected regeneration units will be modeled in the phenol production problem and their use will be analyzed and discussed.

4.3.2.2 Review of existing treatments

There are many phenol removal treatments for industrial waste-waters available on the market. Depending on the initial concentration and the required performances for the treatment, the selected technology may vary. Several studies have reviewed the available technologies [19, 26, 83] and tried to evaluate them economically [28, 62].

When the concentration in phenol is high, that is over 3 000 $mg.L^{-1}$, recovery treatments are applied trying to harness most of the phenol from the wastewater without

degrading it since the quantity is sufficiently large to be economically valuable. The separation can be done thermally through a distillation column, chemically using a liquid-liquid extraction column or physically using membranes or adsorption. Their efficiency is generally above 90%.

When the phenol concentration is low, that is below 1000 $mg.L^{-1}$, phenol is transformed through oxidation reactions mostly into molecules with a lower toxicity. These degradation techniques include biological degradation, photocatalytic oxidation, ozonation, electrochemical treatments. Their efficiency depend strongly on the operating conditions such as pH, temperature, pressure. But generally they can reach a phenol removal ratio between 50 and 99.9%.

When the concentration are in between 1 000 $mg.L^{-1}$ and 3 000 $mg.L^{-1}$, the selected technology for this type of treatment depends on a more detailed cost/profit analysis.

According to Mohammadi et al. [83], the wastewater streams generated by the phenol production process can be treated by a liquid-liquid extraction (LLE) unit which can remove most of its phenol content. Cumene can be used as an extracting agent in a counter-current extraction column [19]. The phenol residual concentration in the exiting stream is between 20 and 500$mg.L^{-1}$. This stream is sent to a sewage treatment plant where the remaining phenol is removed in a biological purification stage. Unfortunately, there are very few economical data readily available on this type of treatment.

One study found in the literature tries to evaluate the cost of such technology. Instead of cumene, Jiang et al. [62] studied different extractants. Octanol was one of the most promising one with an efficiency of 99.6% using 0.5kg of octanol per m^3 of wastewater treated. The operating costs (including labor, electricity and extractant cost) related to this treatment was estimated to around 2€.t^{-1} of treated wastewater.

In the results presented in paragraph Chapter III (Fig.3.15), the phenol concentration of the final waste stream is around 100 000 $mg.L^{-1}$, which is very concentrated. Therefore, a separation technology is more likely to be implemented in a first stage to lower the concentration followed by a destructive treatment of the phenol to reach the standards value.

4.3.2.3 Selected treatment model

Since the purpose of this section is to show how the proposed model deals with the constraint of complying with the environmental standards through a treatment unit and how it affects the MAHEN structure and not to model precisely the phenol treatment unit, the remaining part of the treatment (which is biological and chemical treatments in a sewage treatment plant (STP)) will be modeled as a waste sink only without the possibility to use the treated water. The performances as well as the costs of the LLE are evaluated

using data and results provided by Jiang et al. [62] assuming the extraction of phenol is realized with octanol.

The former waste sink used since chapter II is replaced by the following data presented in Table 4.4:

	Comp. in Phenol (mass fraction)	p_v (kPa)	pH	Temperature ($^\circ C$)
Waste Sink				
Waste STP	0.0 - 0.005		5.0 - 9.0	30
Treatment Unit LLE				
LLE in	0.03 - 0.06		5.0 - 9.0	30
LLE out	0.00024	3.0	6.0	30

Heat capacity = $4.2kJ.kg^{-1}.K^{-1}$

Table 4.5: Process Data

All required economic and parametric data are the same as the ones presented in Chapter III are used. The flow cost for the LLE unit (C_{LLE}^{flow}) is set to $2€.tons^{-1}$ and the fixed capital cost (C_{LLE}^{fixed}) is assumed to be 100 000€ given that the mass flow rate to be treated will be around $1t.h^{-1}$. The waste sink STP cost (C_{STP}^{flow}) is set to $0€.tons^{-1}$. Given that all these costs have evaluated using more or less accurate assumptions, sensitivity analyses are performed to evaluate more precisely the influence of these costs on the optimal solution and the MAHEN design.

Note that given the previous results on this case, a mixer unit for the waste sink must be used to reduce the HEN costs. Previously, in the TMD case study, the selection of the mixer units was realized by a sensitivity analysis on the temperature range found in Fig x in Chapter III. This time, three mixer units associated with $LLEin$ waste sink are included simultaneously in the problem definition. Their temperature T_{mu} are set to $61, 57, 53^\circ C$ with $\Delta T_{error}^{max} = 2^\circ C$; covering a mixing temperature range going from 59 to $63^\circ C$. An additional constraint limiting the use of one mixer unit will force the model to select the most appropriated one.

4.3.2.4 Results

The optimized structure is presented in Fig.4.12 and the results are shown in Table 4.6.

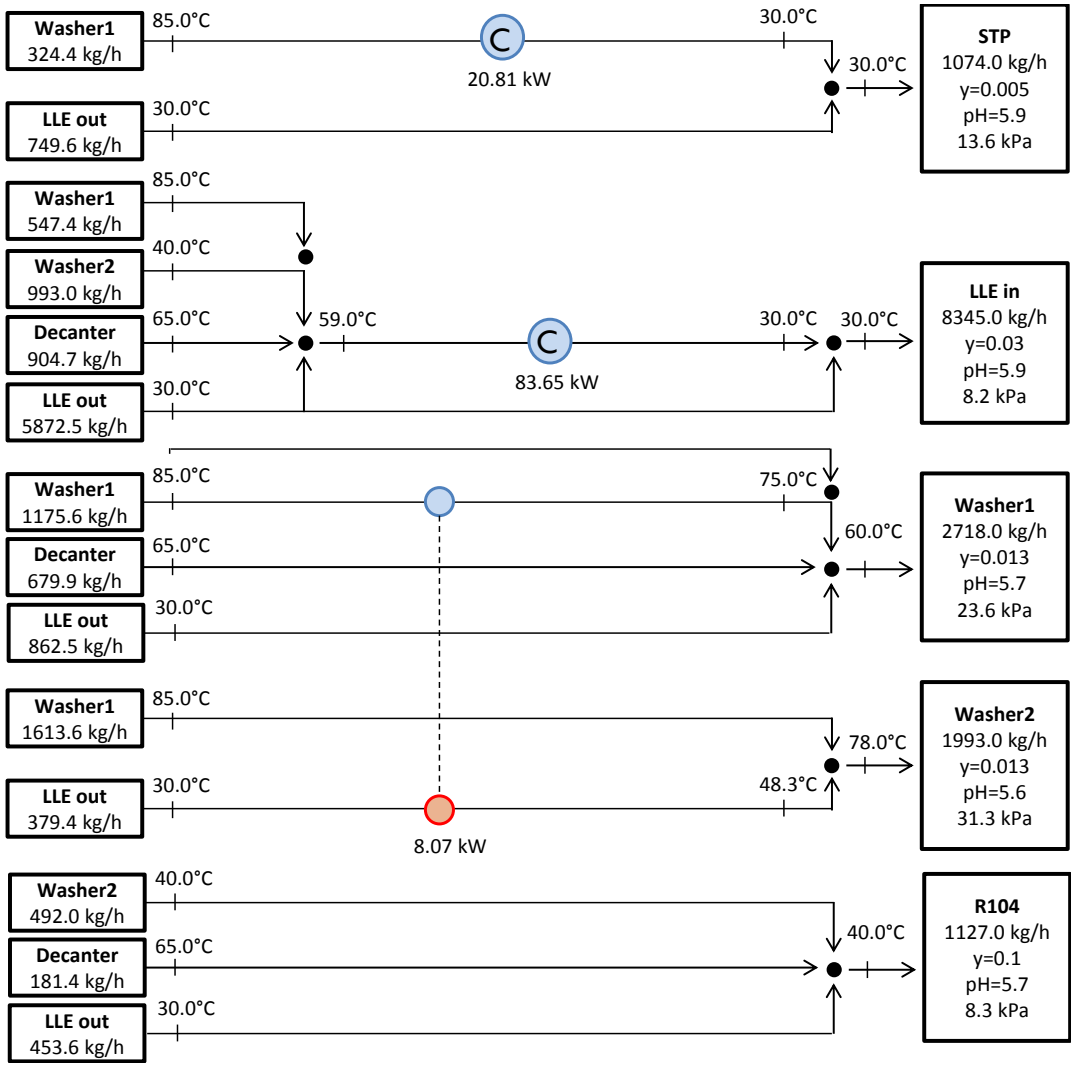

Figure 4.12: Optimal MAHEN with phenol treatment units and optimal mixer unit (N_{op} = 10 years)

The first and expected result is that both fresh external sources are no longer needed. Since there is the constraint to reach the low concentration of the ultimate waste sink (STP), part of the concentrated wastewater is forced to go through the LLE regeneration unit. The low concentration of the outlet stream allows the outlet stream to be used as a substitute to the other fresh sources. The high concentration of process sources, in particular the one coming from $Washer1$, and the relatively low limitation at the entrance of the LLE ($6000 mg.L^{-1}$) creates the need for an internal recycled stream to lower the inlet concentration; therefore, the resulting flow rate entering the LLE is significantly higher

T^{mu}_{LLEin} $(°C)$	59.0
G_{STP} $(kg.h^{-1})$	1 074.0
G_{LLEin} $(kg.h^{-1})$	8 345.0
L_{LLEout} $(kg.h^{-1})$	8 345.0 (7 271.0 for internal recycling)
Q_c (kW)	104.5
Q_h (kW)	0.0
n_{he}	3
S_{he} (m^2)	6.57
S^{real}_{he} (m^2)	6.56

Table 4.6: Phenol treatment results

than the part only coming from the process. In order to reduce the treatment cost, a part of the most concentrated process source ($Washer1$) is sent directly to the STP and a mixture between this stream and the outlet of the LLE is obtained to reached on overall concentration equal to the maximum allowed in the STP sink which is $500mg.L^{-1}$.

The overall energy consumption remains similar to one of the optimal structure found in Chapter III (cooling requirement are equal to 104.5 kW). Note that the mixer unit temperature selected is $59.0°C$. The new optimal structure succeeds to comply with new constraints, while avoiding the need for external sources. But its excess heat remains as a potential to be exploited but not on site since no fresh water is needed anymore.

Sensitivity analyses on C^{flow}_{LLE}, C^{fixed}_{LLE} and C^{flow}_{STP} are led to evaluate their influence on the resilience of the optimal solution structure presented inFig.4.12.

Case 1: C^{flow}_{LLE} varies from 10 to 0€$.tons^{-1}$ with a 1€$.tons^{-1}$ step.

Case 2: C^{fixed}_{LLE} varies from 1 000 000 to 0€ dividing by 10 at each step.

Case 3: C^{flow}_{STP} varies from 10 to 0€$.tons^{-1}$ with a 1€$.tons^{-1}$ step.

The optimal structure does not change except when $C^{flow}_{LLE} = 0$€$.tons^{-1}$. In this case, the amount of wastewater sent to the LLE unit does not impact the operating cost which means there is no need to optimize the amount of wastewater treated by the LLE unit. The flow rate from the Washer1 source sent directly to STP can now go through the LLE unit; thus, reducing the number of heat exchangers required to 2. Otherwise, the structure is exactly the same as the one presented in Fig.4.12.

All the statistics concerning this case are shown in Table 4.7. Note that the average computation time is 740sec ranging from 250 to 1765sec.

ΔT_{step}^{max} $(°C)$	10
$N^{'}$	36
t_{comp} (s)	665
$N_{constraints}$	36 990
$N_{continuous}$	17 547
$N_{binaries}$	13 627
$N_{non-zeros}$	215 458

Table 4.7: Problem statistics

The results of the sensitivity analyses show the resilience of the optimal solution even though the assumption of the phenol treatment cost function are not totally accurate. The constraint imposed by the environmental standard is the key factor in the design of the optimal MAHEN as long as the treatment cost is not too low (which in reality is not the case).

4.4 Conclusion

In this chapter, regeneration units are introduced to model processes that can modify the properties of waste streams in order to be recycled more easily into the process or directly produce fresh sources from free natural resources. The MILP model presented in the previous chapter is extended to take into account the opportunity to use regeneration units and recycle waste streams. The main limitation of the linear modeling of regeneration units comes from the decoupling between the inlet and outlet streams properties. However, this type of model allows understanding their influence on the mass and heat integration of processes with few assumptions. Two cases are presented to show how the design of regeneration units can be included to the simultaneous mass and heat integration of an industrial process and how these units can improve the optimal MAHEN design.

The first case study illustrated well how to use an accurate model of water desalination technology by modeling its cost as a function of few characteristic parameters. The simultaneous economic optimization and design of the MAHEN and TMD show how an industrial company can design optimal structures and technologies to exploit its internal potential to reduce its resources consumption and improve its economic performances.

The second case study illustrates how environmental standards can affect the structure of MAHEN. Indeed, making it compulsory to treat wastewater and reach a extremely low phenol concentration, the company had to invest on a technology that allows recovering most of its used process water. However, the excess heat recovered to produce part of the water needs of the process through the TMD can no longer be exploited in that way.

This potential which cannot be recovered locally within individual process creates an incentive to look for external ways to make the most of it. This train of thought leads to the idea of investigating potential synergies outside the process perimeter and find other companies that may benefit from these untapped sources of energy or matter. In the following chapter, the topic of designing eco-industrial parks (EIP) will be addressed. The applicability of the models M1, M2 and M3 is extended to be able to design an EIP including several industrial sites. The concepts of heat and mass networks used to share their resources are introduced. The structure of the EIP will depend on the economic balance between the cost of these networks related to the distance between connected sites and the savings that can be achieved using them.

Chapter 5

Eco-Industrial Parks design

After designing optimal recovery networks at a process level, the content of this chapter is focusing on ways to look for untapped synergies between industrial sites and create an optimal structure that allows a group of industrial sites to globally optimize their resources consumption and the cost associated with it. A few works on mass or heat integration of an eco-industrial park (EIP) have been published, and even fewer have studied these two aspects simultaneously at this scale.

In an EIP, resources can be shared either directly or indirectly. As the example of Kalundborg (c.f. section 1.2.2), companies sometimes choose to integrate into their process streams provided directly from neighboring industrial partners. However, for safety reasons or distance between companies, some exchanges must go through intermediate networks. In this chapter, a new MILP model (M4) is presented resulting from the extension of the applicability of the model M3 detailed in previous chapter to a larger scale allowing the design of recovery networks between industrial sites. New concepts are introduced enabling modeling direct and indirect exchanges between companies.

The objective of this work is to present what could be the most economical EIP structure considering a collaborative partnership between involved companies, regardless of individual economic strategy. The optimization is looking at collaborative partnership defined by a global economic objective without taking into account individual economic strategies. The purpose is to have a sense of what could be the most promising EIP structure in terms of resources and cost reductions without being restrained by individual objectives.

First, the new elements of the M4 model necessary to extend the applicability of the M1, M2 and especially M3 models for designing eco-industrial parks (sites, clusters, intermediate mass and heat networks) are introduced. Then, additional equations modeling the heat and mass transports through networks between industrial sites are presented. Finally, a case study is developed to illustrate the application of these new concepts and how the optimal design of a collaborative eco-industrial park can be obtained.

5.1 Model Formulation - 4^{th} MILP: Eco-industrial park optimal design (M4)

5.1.1 Clusters of sites

An eco-industrial park is a group of industrial companies that have decided to share their resources and wastes in order to reduce their environmental footprint and improve their cost-effectiveness. Therefore, to properly model all the possible interactions that can occur within and between industrial processes, it is necessary that each object (sources, sinks, heat streams,...) in the M4 model is assigned geographically to an entity. These entities can be industrial sites, urban networks, the environment... The term *site* is used as the prevailing term to identify these entities.

In an eco-industrial park, sites can exchange directly or indirectly mass and heat streams between them. A group of sites allowing direct exchanges is modeled as if it was a unique site. Their heat and mass balances must be realized independently of the other sites. Therefore, sites allowing direct interactions between their processes must be considered as a single entity. This idea is formalized in the concept of *cluster*. A cluster ($cl \in C$) is a group of sites that allows direct mass/heat integration as if they were a single site. Thus, by specifying to which site each element belongs to site and defining clusters of sites, the models M1, M2 and M3 developed earlier in previous chapter can be applied to each cluster within the same problem.

Connections between clusters are designed using intermediate objects called *mass and heat networks* (Fig.5.1).

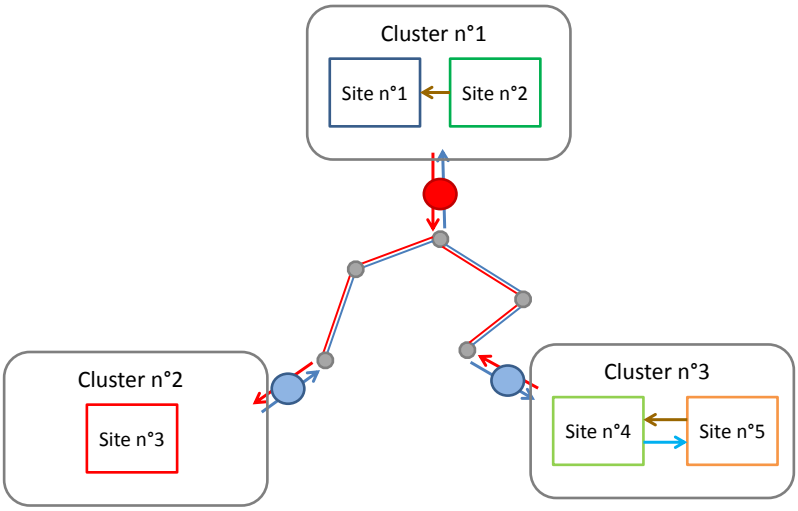

Figure 5.1: Schematic example of interactions between clusters

The following paragraphs explain how these objects are introduced in the M4 model without fundamentally modifying the structure of the previous models M1, M2 and M3.

5.1.2 Heat network

A heat network is represented as a stream going in loop between entities; some providing heat and others consuming it (Fig.5.2). Therefore, in this new model M4, a heat network is represented as an association between two utility heat streams related whose heat loads are equal; assuming that there are no heat losses.

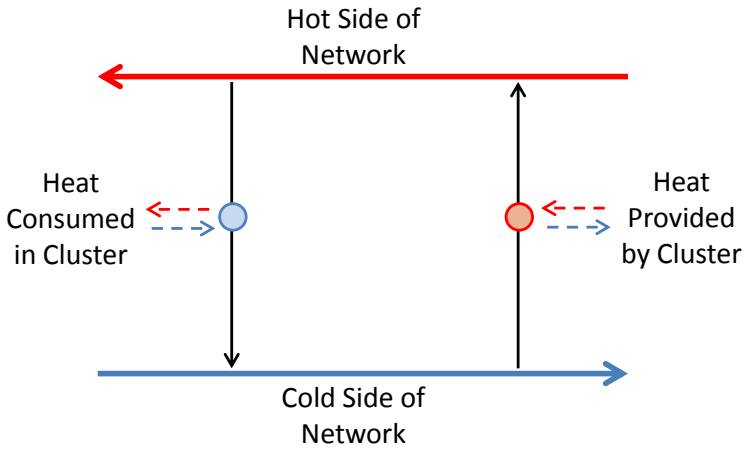

Figure 5.2: Schematic representation of a heat network

H_{net} is the set of all heat networks available in the examined case. An element of H_{net} is defined as a pair of two utilities $(h_u,\widetilde{h}_u) \in (H_u)^2$. The utility heat streams that are associated to form a network have symmetrical temperatures.

$$\forall(h_u,\widetilde{h}_u) \in H_{net},\ T^{in}_{h_u} = T^{out}_{\widetilde{h}_u}\ and\ T^{out}_{h_u} = T^{in}_{\widetilde{h}_u}$$

Each cluster has the opportunity of either providing or consuming heat through the network. If there is a heat surplus available in one cluster, it can be transferred to others having heat shortages. In terms of modeling, both utilities $(h_u,\widetilde{h}_u)$ representing a heat network are considered in the heat balance of each cluster using specific set of variables $(q^{cl}_{h_u})$.

For each heat network, a global heat balance accounts for all heat loads transferred to or from its two specific utilities such as all the heat provided to the network must be consumed:

$$\forall(h_u,\widetilde{h}_u) \in H_{net},\ \sum_{cl\in C} q^{cl}_{h_u} = \sum_{cl\in C} q^{cl}_{\widetilde{h}_u} \tag{5.1}$$

Regarding the cost of such network, no operating costs (i.e. $C_{h_u} = 0€.MWh^{-1}$ and $C_{\widetilde{h}_u} = 0€.MWh^{-1}$) are considered, neglecting the pumping and maintenance costs at this point. The capital costs are related to the piping necessary for connecting clusters with a given heat network as explained in section 5.1.4.

5.1.3 Mass network

A mass network is used to recover matter from one or several entities and provide it to others. Contrary to a heat network, it does not work in a loop; rather, it has one (or several) potential starting and ending points (Fig.5.3). The matter circulating in the network has particular specifications regarding temperature, composition and properties.

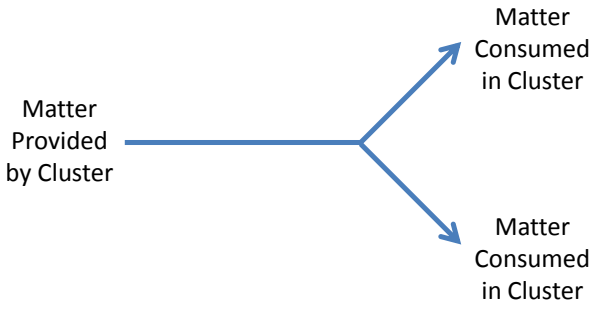

Figure 5.3: Mass Network

Similarly to the heat network, all the matter entering the mass network must be consumed within all clusters, assuming no mass losses. Modeling a mass network requires an object that can describe the actions of collecting and providing matter to each cluster. Waste sinks and fresh sources are used to represent the inlet and outlet points of the networks respectively.

M_{net} is the set of all mass networks available in the examined system. In the M4 model, an element of M_{net} is defined as a pair of a fresh source and a waste sink $(j,i) \in J_f \times I_w$. The interactions between a given cluster and a mass network $(j,i) \in M_{net}$ are considered in the cluster mass balance; therefore, fresh source j and waste sink i representing the mass network are duplicated and made available in each cluster. These copies are noted j_{cl} and i_{cl} for each $cl \in C$.

A mass network is represented similarly to a treatment unit; but in this case, multiple similar fresh sources and waste sinks are considered as follows:

$$\forall (j,i) \in M_{net}, \ \sum_{cl \in C} G^w_{i_{cl}} = \sum_{cl \in C} L^f_{j_{cl}} \tag{5.2}$$

The specifications of the mass network in terms of temperature, composition and properties are defined by the fresh source characteristics. The range of composition and properties of the inlet waste sinks must be centered on the chosen specifications of the network. It can more or less wide depending on the acceptable margins allowed around the specified value of the mass network. For instance, if the mass network pH value is set at 7, the inlet pH specification of the mass network can be strict and set to 7 or can be looser and allowed between 6.5 and 7.5.

The only costs related to the use of a mass network are the capital costs necessary for purchasing and installing the piping connecting clusters (including the trenching) as explained in 5.1.4.

5.1.4 Networks design

Designing a network aims at determining how to transfer a commodity (heat or mass) from suppliers to consumers. Straight line connections may be impossible due to geographical, urban or industrial obstacles. Therefore, a simplified layout of the industrial territory is introduced to establish the possible paths ($p \in P_{paths}$) by which pipes can be installed to connect clusters. The positions of clusters and intermediate points on a given map are symbolized by a set of *nodes* ($n \in N_{nodes}$) as shown in Fig.5.4.

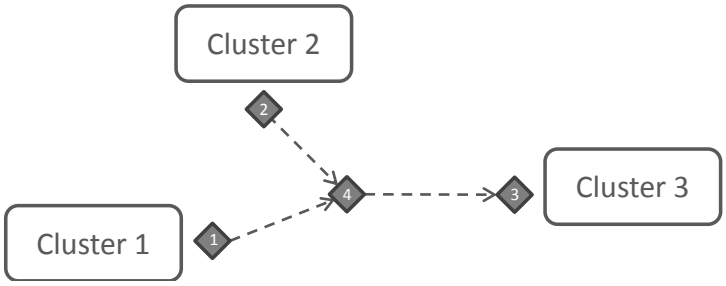

Figure 5.4: Example of clusters map

In Fig.5.4, the dotted lines represent the authorized paths. An authorized path $p \in P_{paths}$ connects two nodes $(n, m) \in N_{nodes}^2$. A random direction is assigned to each path p connecting the nodes n and m indicating whether the quantity passing through is counted positively from n to m or the other way around. For instance, considering the node 4 in Fig.5.4, incoming paths are $1-4$ and $1-2$, and outgoing path is $4-3$. Note that P_{paths}^n represents the sub-set of P_{paths} of paths including the node n. The direction for such path is provided by the parameter δ_{p_n}. Its value can be 1 or -1 depending on the selected positive direction for a given path p_n.

The design of mass and heat networks are governed by similar equations. For a heat network, q_p^{net} indicates the heat load traveling through a given $p \in P_{paths}$. A heat balance is realized for each node. Note that if a cluster cl is placed on a node n, the heat provided and consumed by it must be taken into account using the previously mentioned variables $q_{h_u}^{cl}$ and $q_{\widetilde{h}_u}^{cl}$. Thus, for a given heat network $(h_u, \widetilde{h}_u) \in H_{net}$:

$$\forall n \in N_{nodes}, \sum_{p_n \in P_{paths}^n} q_{p_n}^{net} \times \delta_{p_n} = \begin{cases} q_{h_u}^{cl} - q_{\widetilde{h}_u}^{cl} & \text{if cluster } cl \text{ is on node } n \\ 0 & \text{if cluster } cl \text{ is not on node } n \end{cases} \tag{5.3}$$

Note that $q_{p_n}^{net}$ can be positive or negative.

The heat loads traveling through each path cannot exceed the total amount provided and consumed by clusters in absolute value:

$$\forall p \in P_{paths},\ \sum_{cl \in C} q^{cl}_{h_u} = \sum_{cl \in C} q^{cl}_{\widetilde{h}_u} \geq q^{net}_{p} \tag{5.4}$$

$$\forall p \in P_{paths},\ -\sum_{cl \in C} q^{cl}_{h_u} = -\sum_{cl \in C} q^{cl}_{\widetilde{h}_u} \leq q^{net}_{p} \tag{5.5}$$

Binary variables ($\gamma_{q^{net}_p}$) are introduced to indicate whether a path p is used in the heat network $(h_u, \widetilde{h}_u) \in H_{net}$:

$$\forall p \in P_{paths},\ q^{net}_{p} - Q^{max}_{net} \times \gamma_{q^{net}_p} \leq 0 \tag{5.6}$$

$$\forall p \in P_{paths},\ q^{net}_{p} + Q^{max}_{net} \times \gamma_{q^{net}_p} \geq 0 \tag{5.7}$$

where Q^{max}_{net} is a big number.

Similarly for a mass network $(j, i) \in M_{net}$, $L^{net}_{p_n}$ indicates the mass flow rate traveling through a given $p_n \in P^n_{paths}$ and the mass balance realized for each node is:

$$\forall n \in N_{nodes},\ \sum_{p_n \in P^n_{paths}} L^{net}_{p_n} \times \delta_{p_n} = \begin{cases} G^w_{i_{cl}} - L^f_{j_{cl}} & \text{if cluster } cl \text{ is on node } n \\ 0 & \text{if cluster } cl \text{ is not on node } n \end{cases} \tag{5.8}$$

Note that $L^{net}_{p_n}$ can be positive or negative.

The mass flow rates traveling through each path cannot exceed the total amount provided and consumed by clusters in absolute value:

$$\forall p_n \in P^n_{paths},\ \sum_{cl \in C} G^w_{i_{cl}} = \sum_{cl \in C} L^f_{j_{cl}} \geq L^{net}_{p_n} \tag{5.9}$$

$$\forall p_n \in P^n_{paths},\ -\sum_{cl \in C} G^w_{i_{cl}} = -\sum_{cl \in C} L^f_{j_{cl}} \leq L^{net}_{p_n} \tag{5.10}$$

Binary variables ($\gamma_{L^{net}_{p_n}}$) are introduced to indicate whether a path p_n is used in the mass network $(j, i) \in M_{net}$:

$$\forall p_n \in P^n_{paths},\ L^{net}_{p_n} - L^{max}_{net} \times \gamma_{L^{net}_{p_n}} \leq 0 \tag{5.11}$$

$$\forall p_n \in P^n_{paths},\ L^{net}_{p_n} + L^{max}_{net} \times \gamma_{L^{net}_{p_n}} \geq 0 \tag{5.12}$$

where L^{max}_{net} is a big number.

5.1.5 Objective function

The capital costs for each network is related to the distance between nodes (d_p). The assumption is that this cost is independent of the mass flow rate and temperature.

Nominal costs per meter (c^{net}_{mass} and c^{net}_{heat}) are assigned to calculate the capital costs of mass and heat networks, respectively. These parameters include the pipes costs as well as the additional costs required to install them (like trenching). Hence, the definitions of the capital costs for each type of network are:

$$CC^{net}_{mass} = \left(\sum_{p \in P_{paths}} \gamma_{L^{net}_p} \times d_p \right) \times c^{net}_{mass} \tag{5.13}$$

$$CC^{net}_{heat} = \left(\sum_{p \in P_{paths}} \gamma_{q^{net}_p} \times d_p \right) \times c^{net}_{heat} \tag{5.14}$$

Note that the cost for a heat network must take into account that two pipes must be installed to create a loop to supply clusters in need for external heat sources and clusters providing heat to the network. Thus, using a heat network should be more expensive than a mass network.

The assumption for optimizing the structure of the EIP is that industrial sites are in a collaborative partnership; thus, the global objective is to optimize the overall total annualized cost (calculated using the equations presented in the M3 model) of all clusters at the same time and the capital costs of the required heat and mass networks:

$$TAC_{EIP} = \sum_{cl \in C} TAC_{cl} + \frac{1}{N_{op}} \times \left(\sum_{(h_u, \widetilde{h}_u) \in H_{net}} CC^{net}_{heat} + \sum_{(j,i) \in M_{net}} CC^{net}_{mass} \right) \tag{5.15}$$

5.2 Case study

The case study used to illustrate the presented model M4 has been built based on literature cases for each process included in this fictional EIP. This choice was made because, to the best of my knowledge, there are no case study in the literature that fit the modeling of processes used in the proposed model (i.e. *fixed flow rate*) and integrating mass and heat aspects simultaneously.

The EIP is formed by three industrial processes Fig.5.5. The first one is the phenol production process [68] which has been the main illustrative case of the three previous chapters. The second one is a wood to methane (CH_4) conversion process [1] where biomass is gasified with steam before going through the methanation reactor. The last one is a methanol production process from CH_4. Moreover, the possibility of providing fresh water and heat to urban networks is added to offer additional recovery opportunities.

Finally, the possibility of converting heat to water through the TMD technology is considered; thus, putting in competition the local use of heat or water and the transport of either of them to other potential users.

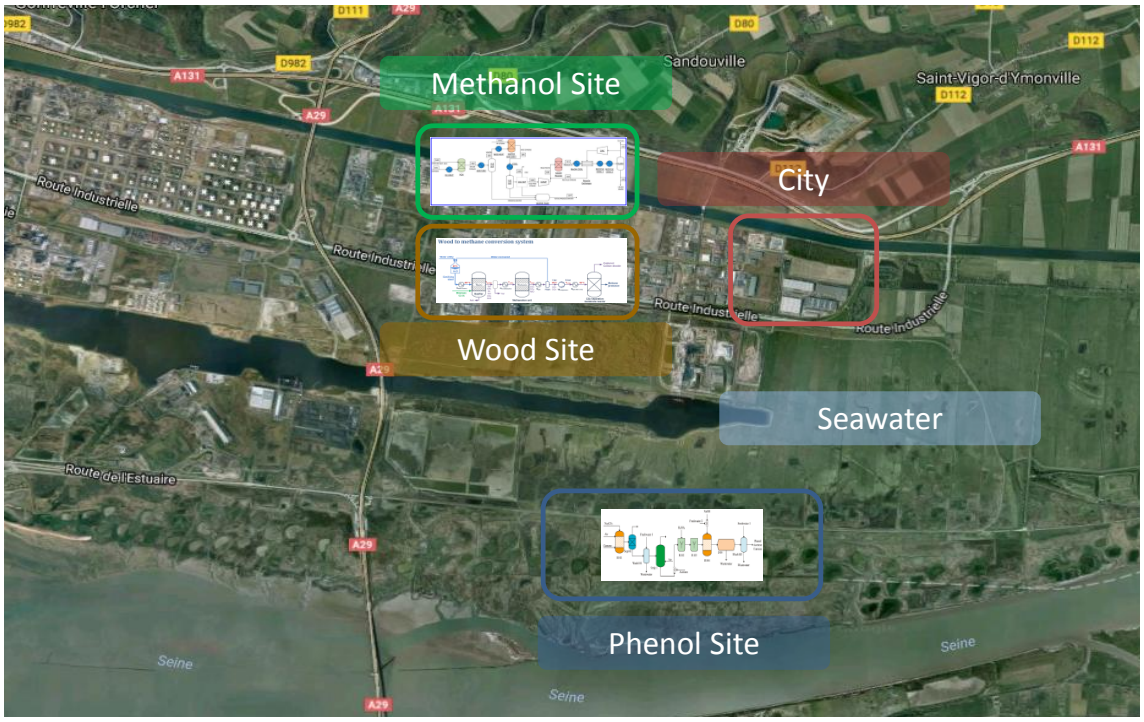

Figure 5.5: Geographical location of the industrial sites on a map[1]

The objective of the case study is to design the most economical EIP to recover heat and matter from some industrial sites and substitute external resource consumption by the use of heat and mass networks.

[1]Image taken from *Google Maps*

5.2.1 Sites and clusters definition

The description of the industrial sites and the definition of each cluster perimeter are presented in following paragraphs.

5.2.1.1 Site 1: Phenol production process

The case study used in previous chapters of the phenol process production is made part of the EIP. The process includes the phenol treatment unit (LLE) studied in Chapter IV. The results of the study (Table 4.6) have shown that the about $100kW$ of heat are discarded using a cold utility. This heat may be transferred to other partners as it is or transformed to produce water with the TMD technology.

In this case study, the process is scaled up by a factor of 10 in order to have similar and matching orders of magnitude regarding heat loads and flow rates of the other sites (Table 5.1).

	Flow rate ($kg.h^{-1}$)	Comp. in phenol (mass fraction)	p_v (kPa)	pH	Temperature ($°C$)
Sink					
Washer 101	27180	0.013	20.0 - 47.0	4.5 - 7.0	60
Washer 102	19930	0.013	4.0 - 38.0	4.0 - 8.0	78
R104	11270	0.100	3.0 - 25.0	4.5 - 7.0	40
Waste STP		0.0 - 0.150		5.0 - 9.0	30
Source					
Washer 101	36610	0.016	38.0	5.4	85
Decanter 101	17660	0.024	25.0	5.1	65
Washer 102	14850	0.220	7.0	4.8	40
Freshwater 1		0.000	3.0	7.0	25
Freshwater 2		0.012	6.0	6.8	35
Treatment Unit LLE					
LLE in		0.03 - 0.06		5.0 - 9.0	30
LLE out		0.00024	3.0	6.0	30

Heat capacity $= 4.2kJ.kg^{-1}.K^{-1}$; $htc = 1000W.m^{-2}.K^{-1}$

Table 5.1: Phenol production case - Process Data

Note that the LLE fixed capital cost is also multiplied by 10 with respect to the one used in Chapter IV (i.e. $C_{LLE}^{fixed} = 1\ 000\ 000$ €).

5.2.1.2 Site 2: CH_4 to methanol conversion process

The second process considered for the EIP is the production of methanol from methane [34] shown in Fig.5.6.

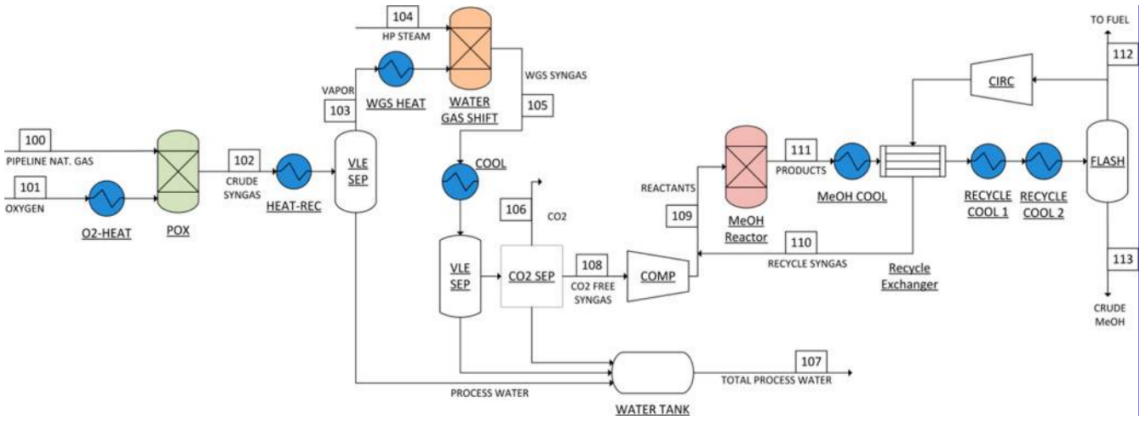

Figure 5.6: Methanol production process flow sheet [34]

Regarding the use of water in this process, steam is consumed in a water gas shift reaction and water is collected at various steps in a water tank. This process water is contaminated with CO and CO_2. Similarly to the phenol process, the mass flow rates are divided by 10 in order to have similar and matching orders of magnitude regarding heat loads and flow rates (Table 5.2 and Table 5.3) between sites.

	Flow rate ($kg.h^{-1}$)	Comp. in CO (mass fraction)	Comp. in CO_2 (mass fraction)	pH	Temperature ($°C$)
Sink					
Water Gas Shift	800	0.000	0.000	7.0 - 7.0	249.9
Environment		0.000 - 0.000	0.000 - 0.000	5.5 - 8.5	30
Source					
Process Source	4300	0.036	0.066	7.0	40
Freshwater 3		0.000	0.000	7.0	25
Degasser Unit					
Degasser in		0.000 - 0.04	0.000 - 0.07	5.5 - 8.5	40
Degasser out		0.000	0.000	7.0	80

Heat capacity $= 4.2kJ.kg^{-1}.K^{-1}$; $htc = 1000W.m^{-2}.K^{-1}$

Table 5.2: CH_4 to Methanol case - Process Data

The steam consumption is modeled by a process sink ($Water\ Gas\ Shift$) consuming water heated up until the boiling temperature which is 249.9° (the steam pressure is at 39.5 *bars* as described in the article). The actual phase change is modeled by a process heat stream (*Steam* in Table 5.3).

The process water collected is decontaminated through a *degasser* in which a steam flux (which is not modeled) bubbled in the contaminated water to strip the dissolved gases. Several assumptions are made for this treatment unit:

- 5% of the treated water is carried out with the steam
- The water treated by the degasser is considered free of any pollutant and heated up to $80°C$
- The capital costs for the unit are considered null

Finally all the heating and cooling requirements are represented by process heat streams (Table 5.3). Note that overall, an excess of heat is available from this process.

	q_h (kW)	T_h^{in} $(°C)$	T_h^{out} $(°C)$	C_h $(€.MWh^{-1})$
Hot Process Heat Stream				
Steam	382	249.9	250.0	
Heat-Rec	28 321	1271.0	40.0	
Cool	5 101	324.0	40.0	
MeOH Cool	4 239	240.0	150.0	
Recycle Cool	3 709	147.0	45.0	
Cold Process Heat Stream				
O2 Heat	761	26.0	200.0	
WGS Heat	4 513	40.0	300.0	
Utility Heat Stream				
Heater 2		320.0	319.9	200
Cooler 2		20.0	20.1	10

$$htc_h = 1000W.m^{-2}.K^{-1}$$

Table 5.3: Heat streams of methanol production process

5.2.1.3 Site 3: Wood to CH_4 conversion process

The last industrial process that takes part in the EIP is the production of methane made from biomass [1]; wood in this case. The need for fresh and pure water to produce steam is modeled by a process sink $Water\ to\ Gasifier$, knowing that part of the required water is recovered within the process. The steam generation is modeled by three process heat streams (*Steam Generator* 1 to 3 in Table 5.5 representing the water heating, the phase change at 1 bar and the vapor heating).

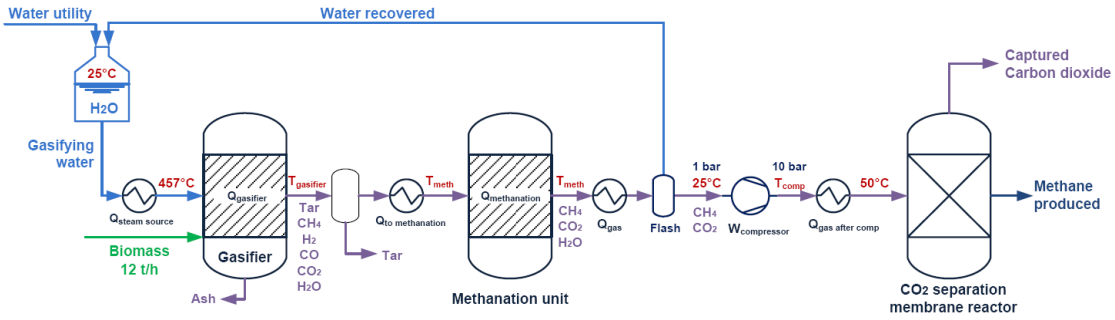

Figure 5.7: Wood to CH_4 conversion process flow sheet

	Flow rate ($kg.h^{-1}$)	Comp. in CO (mass fraction)	Comp. in CO_2 (mass fraction)	pH	Temperature ($°C$)
Sink					
Water to Gasifier	2232	0.000	0.000	7.0 - 7.0	25.0
Source					
Freshwater 4		0.000	0.000	7.0	25

Heat capacity $= 4.2kJ.kg^{-1}.K^{-1}$; $htc = 1000W.m^{-2}.K^{-1}$

Table 5.4: Wood to CH_4 case - Process Data

Similarly to the methanol production, an excess of heat is available from this process.

	q_h (kW)	T_h^{in} ($°C$)	T_h^{out} ($°C$)	C_h ($€.MWh^{-1}$)
Hot Process Heat Stream				
To Methanation	5 140	750.0	300.0	
Methanation	10 000	300.0	299.9	
Condenser	9 250	300.0	25.0	
Gas Cooler	950	215.0	50.0	
Cold Process Heat Stream				
Steam Generator 1	1 050	25.0	99.9	
Steam Generator 2	7 520	99.9	100.0	
Steam Generator 3	2 440	100.0	457.0	
Gasifier	13 430	457.0	750.0	
Utility Heat Stream				
Heater 3		770.0	769.9	300
Cooler 3		10.0	10.1	25

$htc_h = 1000W.m^{-2}.K^{-1}$

Table 5.5: Heat streams of methane production process

5.2.1.4 Site 4: Urban water and heat utilities

As shown in the description of the three industrial processes, they all have a heat surplus that must be discarded using a cooling utility. That is why a new site is introduced in this case study to represent a potential consumer. The heating need is modeled as a cooling utility representing the domestic hot water utility of the neighboring city. The incentive to provide heat to the city is created by assuming that its cost is negative ($-10€.MWh^{-1}$).

	T_h^{in} ($°C$)	T_h^{out} ($°C$)	C_h ($€.MWh^{-1}$)
Utility Heat Stream			
Hot Water urban utility	55.0	65.0	-10.0

$$htc_h = 1000W.m^{-2}.K^{-1}$$

Table 5.6: Domestic hot water network

In addition, the city is assumed to have potential needs for fresh and pure water, if any were to be produced by the industrial sites. In this case, it will be bought at a fixed nominal cost. This need is represented by a waste sink with a negative cost set at $-2€.t^{-1}$.

	pH	Temperature ($°C$)	C_i^w ($€.t^{-1}$)
Sink			
City Water Utility	7.0 - 7.0	25.0	-2.0

Table 5.7: Urban water network

5.2.1.5 Site 5: TMD

As demonstrated in Chapter IV (cf Table 4.3.1.2), the TMD technology can be used to convert heat surpluses into fresh water from seawater. Since there are important cooling requirements on the three industrial sites previously presented, the TMD gives the opportunity to recover them and either consume the newly produced fresh water on site or transport it at a lower cost to locations where it can be used.

To maximize the heat recovery within the three sites, the inlet TMD temperature is set at the lowest temperature possible, which is $60°C$. The specifications for the TMD are presented in Table 5.8 and Table 5.9.

	Salt (0 or 1)	pH	Temperature ($°C$)
Fresh Source			
Seawater	1.0	7.0	20
Production Unit TMD			
TMD in	1.0-1.0	5.0 - 9.0	60
TMD out	0.0	7.0	25

Table 5.8: TMD unit - Process Data

T^{in}_{TMD} $°C$	J_w $kg.s^{-1}.m^{-2}$	υ -	q_{TMD} $kW.(kg.s^{-1})^{-1}$	c^{op}_{TMD} $€.(tons.h^{-1})^{-1}$	$c^{capital}_{membrane}$ $€.(kg.h^{-1})^{-1}$	$c^{capital}_{membrane}$ $€.(kg.h^{-1})^{-1}$
60	0.0021	14.36	2580.9	1.14	77.59	59.48

Table 5.9: TMD characteristic parameters and cost function coefficients

5.2.2 Clusters definition and Territorial layout

The territorial layout of the industrial zone is shown in Fig.5.8 where the sites are grouped by *clusters*. Nodes located on the map represent the intermediate points by which mass and heat networks have to go through to connect clusters together.

Figure 5.8: Territorial layout for the EIP case study

As previously mentioned, some industrial sites may choose to share resources and effluents directly without intermediate means of transport. In this case study, it seems logical

that the process producing methane from wood is grouped with the process consuming methane and producing methanol. Therefore, they are located in the same cluster (on *node* 1 on the map).

The phenol production and the urban networks are set in their own cluster (on *node* 2 and 3 respectively). This means there are three main clusters considered in this case.

The TMD unit will be set in each cluster alternatively in order to find out what is its optimal position to improve the global annualized cost of the EIP. The seawater is provided by specific fresh sources settled in their own cluster. One seawater fresh source is positioned on a specific location close to each industrial cluster (on *node* 5, 6 and 7 respectively). Therefore, a seawater network can be designed and the cost of the pipe installed to supply the cluster requiring seawater for the TMD can be taken into account in the EIP annualized cost.

The *node* 4 is inserted in the map allowing avoiding the sea canal which represents a natural obstacle to connect clusters together more directly. Table 5.10 indicates the distance of allowed paths within the area. The other paths are forbidden.

Path p	1 - 3	1 - 4	1 - 5	2 - 4	2 - 6	3 - 4	3 - 7
Distance (m)	1 200	1 500	100	500	100	200	100

Table 5.10: Distances between nodes

5.2.3 Problematic and Solving strategy

The objective of this case study is to minimize the global consumption of fresh water sources and energy simultaneously of the studied industrial processes by finding economical ways to integrate them directly and indirectly. As explained in the previous paragraphs, three main clusters of industrial sites are defined and will be integrated together. The overall structure is optimized over a period of 10 years (i.e. $N_{op} = 10 years$).

The chosen methodology to obtain an optimal design for this EIP consists of first optimizing individual cluster using the M3 model described in the previous chapter. Then, the remaining requirements met by fresh sources or heating/cooling utilities as well as the wastes not recovered internally in each cluster are made available to others and represent the potential resources to be shared within the EIP. The use of heat and mass networks is put in competition with local costly external resources.

Moreover, to further encourage local and global mass and heat recovery, a TMD unit will be placed successively in each cluster. The purpose is to give an additional opportunity to use low grade heat locally via the TMD and to transform it into fresh water which is cheaper to transport than heat through intermediate networks. The objective is to find the best location for this unit to improve over all the cost-effectiveness of the EIP structure and to evaluate its influence on the EIP structure.

5.2.4 Individual Cluster optimization

The first step of the sequential methodology consists of optimizing each cluster separately.

The optimal MAHEN structure for the phenol process remains the same as the one found in Chapter IV (Fig.5.9). The fresh source requirements are met by the recycled stream within the liquid-liquid extraction unit (LLE) and the one sent to the sewage treatment plant (STP). The heating requirements are null whereas the cooling requirements created by the sources allocated to LLE unit amount to 1 045kW. There are divided into two heat exchangers among the three units in the HEN.

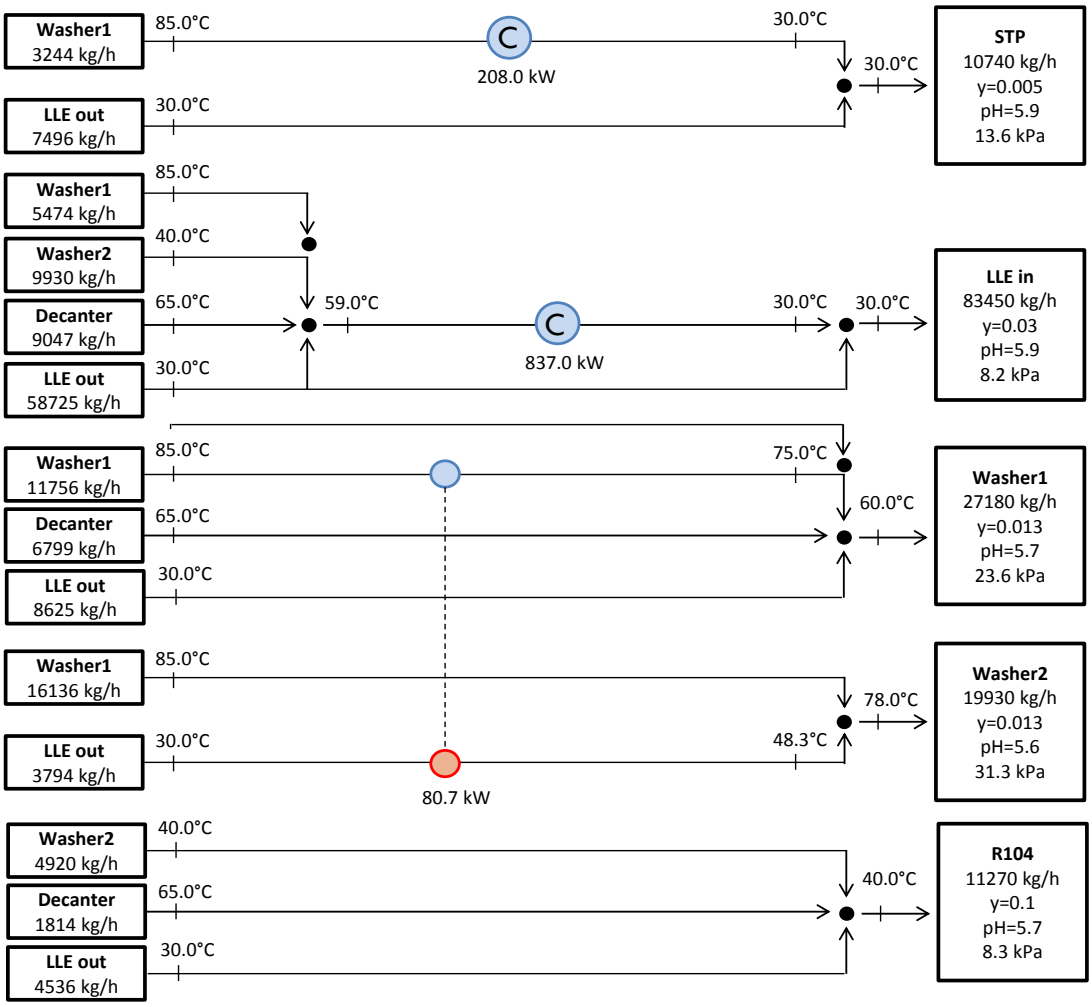

Figure 5.9: Initial optimal MAHEN structure for the phenol cluster

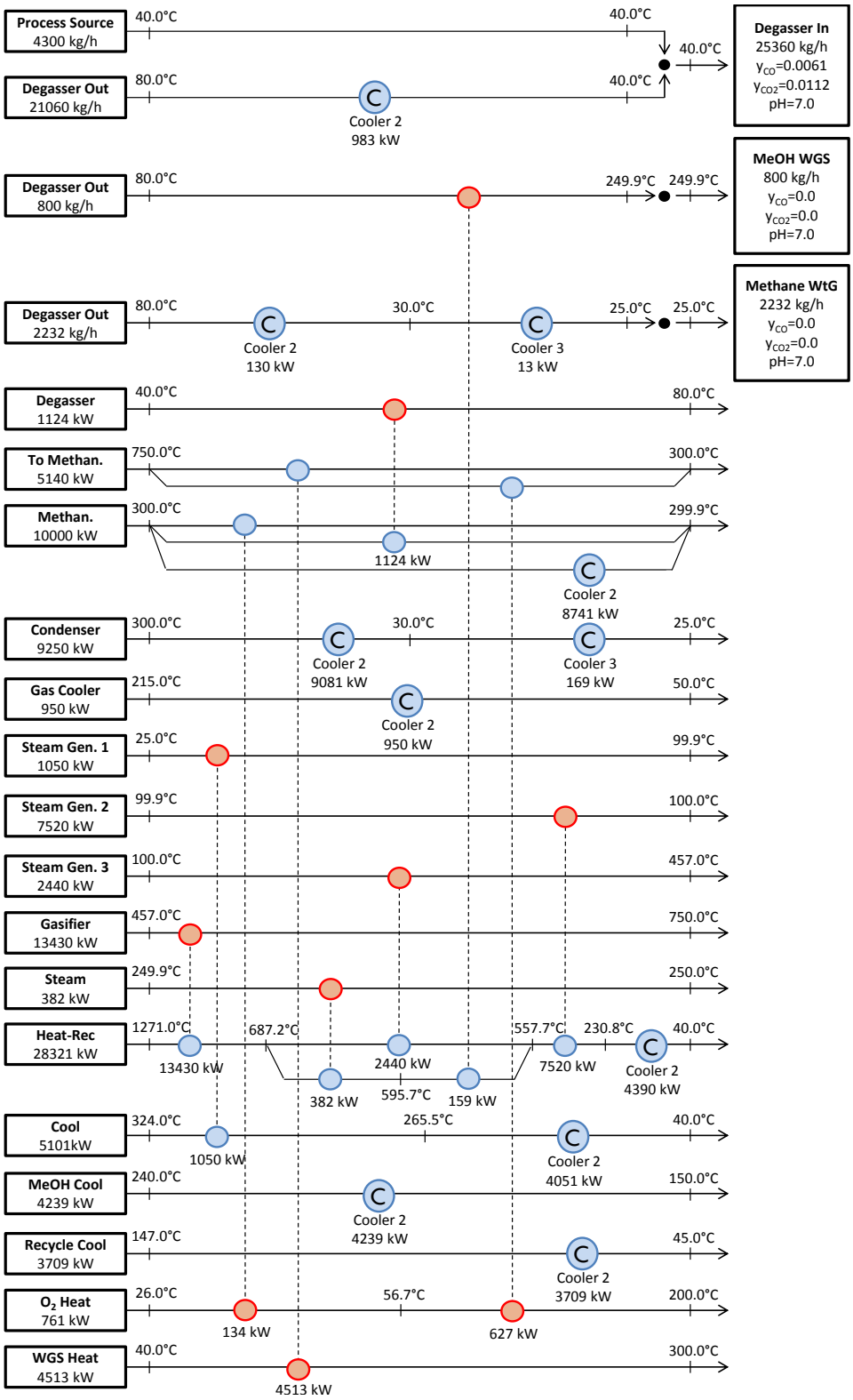

Figure 5.10: Initial optimal MAHEN structure for the methane cluster

Regarding the methane cluster, the process source from the methanol process is treated within the degasser. One part is used internally as a fresh source in the *Water Gas Shift* reactor and the other in the wood conversion process to produce steam. Therefore, there are no longer fresh source requirements as well as waste generated (Fig.5.10). Similarly to the phenol cluster, the heating requirements are met by internal heat integration. The remaining cooling needs are equal to 36 $457kW$. This heat is extracted from nine streams through eleven heat exchangers.

Therefore, as a result of the individual optimization of each cluster, heat surpluses remain to be extracted from each one. The heat loads as well as their quality in terms of temperature are different, but they still can be valued if the *City* cluster is considered as a possible outlet for this available heat. The question that remains is whether it should be recovered as it or transformed using the TMD technology and recovered as fresh water.

The results of the optimization of the two industrial clusters are shown in Table 5.11.

Cluster cl	Phenol	Methane
L_f $(kg.h^{-1})$	10 740.0	0.0
G_w $(kg.h^{-1})$	0.0	0.0
Q_c (kW)	1 045.0	36 457.0
Q_h (kW)	0.0	0.0
n_{he}	3	21
S_{he} (m^2)	65.7	958.4
S_{he}^{real} (m^2)	65.6	958.1

Table 5.11: Individual cluster results

5.2.5 Networks optimization

In this section, the objective is to find an optimal EIP structure. Three cases are considered where the TMD unit is placed in one cluster successively. The resulting data from the previous step for this step are shown in Table 5.12 and Table 5.13.

	q_h (kW)	T_h^{in} $(°C)$	T_h^{out} $(°C)$
Hot Process Heat Stream			
Washer1- STP	208	85.0	30.0
Mix - LLE in	837	59.0	30.0

$htc_h = 1000W.m^{-2}.K^{-1}$

Table 5.12: Remaining heat streams from the phenol cluster

	q_h (kW)	T_h^{in} $(^\circ C)$	T_h^{out} $(^\circ C)$
Hot Process Heat Stream			
Deg. Out - Deg. In	983	80.0	40.0
Deg. Out - Methane WtG	143	80.0	25.0
Methanation	8 741	300.0	299.9
Condenser	9 250	300.0	25.0
Gas Cooler	950	215.0	50.0
Heat-Rec	4 390	230.8	40.0
Cool	5 101	265.5	40.0
MeOH Cool	4 239	240.0	150.0
Recycle Cool	3 709	147.0	45.0
Utility Heat Stream			
Heater 2		320.0	319.9
Heater 3		770.0	769.9
Cooler 2		20.0	20.1
Cooler 3		10.0	10.1

$$htc_h = 1000 W.m^{-2}.K^{-1}$$

Table 5.13: Remaining heat streams from the methane cluster

Note that, at this point, the sum of the annualized cost of each individual cluster regarding the costs only associated with the use of external resources is equal to $2.44 MM€$ ($128k€$ for the capital costs and $3.14 MM€$ for the operating costs).

Given the results, two heat networks and two mass networks are proposed. Their features are presented in Table 5.14 and Table 5.15.

	T_h^{in} $(^\circ C)$	T_h^{out} $(^\circ C)$	C_h $(€.MWh^{-1})$
Heat Stream Network			
Low Temp. Network (LT)	65.0	75.0	0.0
High Temp. Network (HT)	99.9	100.0	0.0

$$htc_h = 1000 W.m^{-2}.K^{-1}$$

Table 5.14: Heat networks available for the EIP

	Comp. in salt (mass fraction)	pH ($^{\circ}C$)	Temperature
Seawater Network			
Seawater Net. in	1.0 - 1.0	7.0 - 7.0	20
Seawater Net. out	1.0	7.0	20
Freshwater Network			
Freshwater Net. in	0.0 - 0.0	7.0 - 7.0	25
Freshwater Net. out	0.0	7.0	25

$$htc = 1000 W.m^{-2}.K^{-1}$$

Table 5.15: Mass Networks available for the EIP

The nominal costs for the piping of heat and mass networks are set at $c_{net}^{heat} = 900€.m^{-1}$ and $c_{net}^{mass} = 500€.m^{-1}$ respectively.

The main results, comparing the three cases studied to the reference case where there are no connections between industrial clusters, are shown in Table 5.16.

Case TMD in Cluster cl	Reference None	Case 1 Phenol	Case 2 Methane	Case 3 City
$Q_{cooler1}$ (kW)	1 045	0	1 045	1 045
$Q_{cooler2}$ (kW)	36 274	5 294	3 301	5 294
$Q_{cooler3}$ (kW)	182	185	182	182
L_{TMD} $(kg.h^{-1})$	0.0	1 477.9	2 222.2	0.0
G_{city} $(kg.h^{-1})$	0.0	1 477.9	2 222.2	0.0
Q_{city} (kW)	0	30 700	30 979	30 979
n_{he}	13	22	19	19
S_{he} (m^2)	765.7	7 575.4	7 561.1	7 448.4
S_{he}^{real} (m^2)				
Op. Cost $(k€)$	3 147	473	530	669
Op. Gain $(k€)$	0	2 480	2 514	2 478
Cap. Cost $(k€)$	128	3 018	2 723	1 760
$TAC(k€)$	2 443	- 1 247	-1 259	-1 221

Table 5.16: EIP results

The optimal structures of the EIP for each case are shown in Fig.5.11, Fig.5.14 and Fig.5.16. The detailed heat exchange networks are shown in Fig.5.12, Fig.5.15 and Fig.5.17.

In Case 1 (Fig.5.12), when the TMD is set in the phenol cluster, the LT heat network and the freshwater network are used. All the heat available at a temperature superior to $75°C$ in the methane cluster is recovered with the LT network (36 $274kW$). The biggest portion of this heat is transported to the city cluster (30 $700kW$) and the remaining part ($278kW$) is sent to the phenol cluster to be converted into fresh water through the TMD. The production of the TMD is 1 $477.9kg.h^{-1}$ which represents 11 823 tons per year of fresh water.

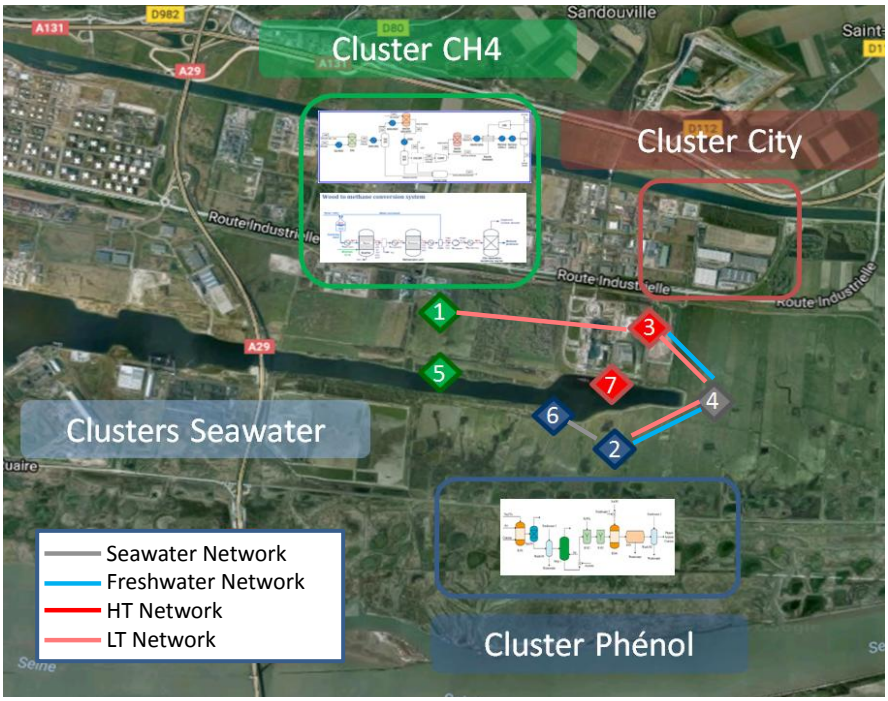

Figure 5.11: Case 1: EIP network when TMD is in the phenol cluster

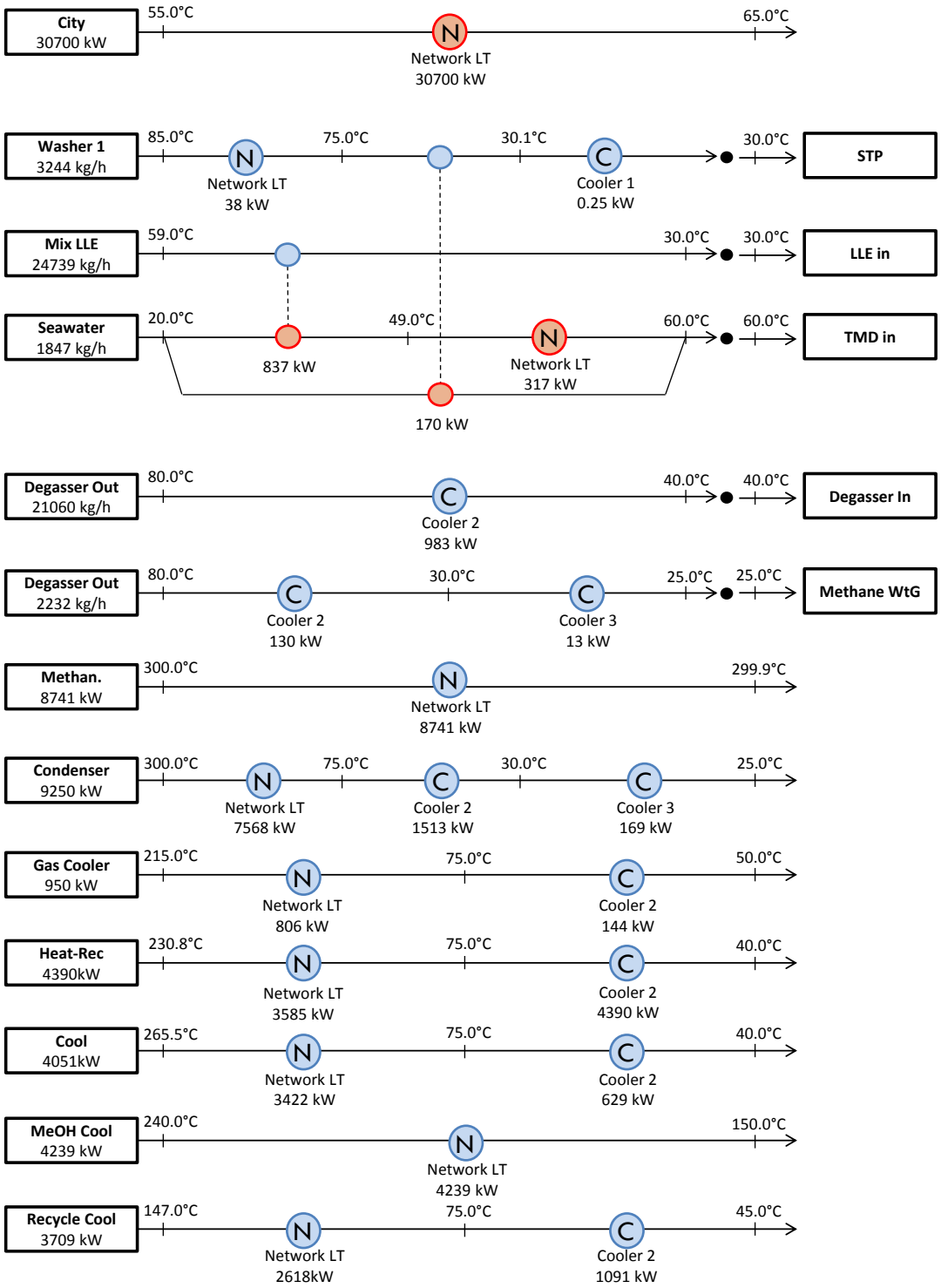

Figure 5.12: Case 1: EIP optimal structure when TMD is in the phenol cluster

A particularity is to be noted in this case. In the phenol cluster, the LT network is used to provide and consume heat locally. A small part of the $Washer1 - STP$ stream ($38kW$) is transferred on the cold end of the network, while the hot end is used to heat up the seawater entering the TMD. The heat load transferred indirectly from the process stream to the seawater results from the limitation imposed by the model that only one heat exchanger per pair of streams. If it were not the case, the $Washer1 - STP$ stream would have two heat exchanger with the inlet stream of the TMD as shown in Fig.5.13.

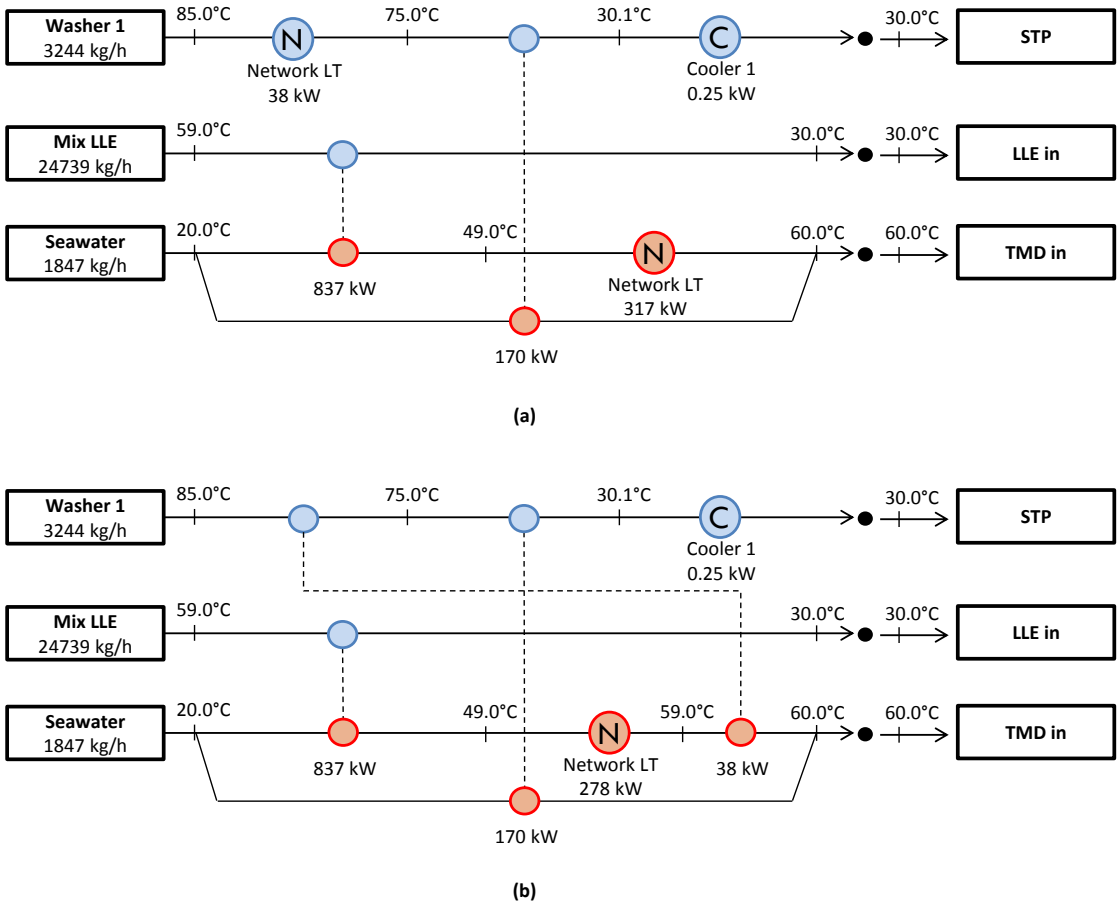

Figure 5.13: (a) Limitation imposed - (b) Limitation lifted

Both structures are feasible and equivalent in terms of energy balance. The only difference between the two cases would be the exchange area which would amount at around $10m^2$. In terms of total cost, it is negligible compared to the several millions in capital costs required by this solution.

In Case 2 (Fig.5.15), when the TMD is set in the methane cluster, the LT heat network and the freshwater network are also used. However, this time the heat provided to the TMD is only coming from the methane cluster. The phenol cluster is not connected to the EIP. The heat and the water produced are directly sold to the City.

By comparing the two HEN structures represented in Fig.5.12 and Fig.5.15 regarding the heat streams in the methane cluster, one can see that the heat exchangers involving the LT network are practically the same. But contrary to the case where the TMD was set in the phenol cluster, the available heat below $75°C$ that could not be recovered, and had to be discharged, is now usable by the TMD and available in relatively large proportions (Fig.5.10). Indeed, the output of the TMD is 50% more important than in the previous case (2 222.2$kg.h^{-1}$ against 1 477.9$kg.h^{-1}$ in Case1 as shown in Table 5.16).

Finally, contrary to Case 1, the phenol cluster is not connected to the EIP because the available heat in the phenol cluster cannot be recovered neither by transporting it to the city cluster to be consumed as it nor to the methane cluster to be used in the TMD. Indeed, the costs for transporting this heat from the phenol cluster to one of the other clusters outweigh the profits that can be made from it.

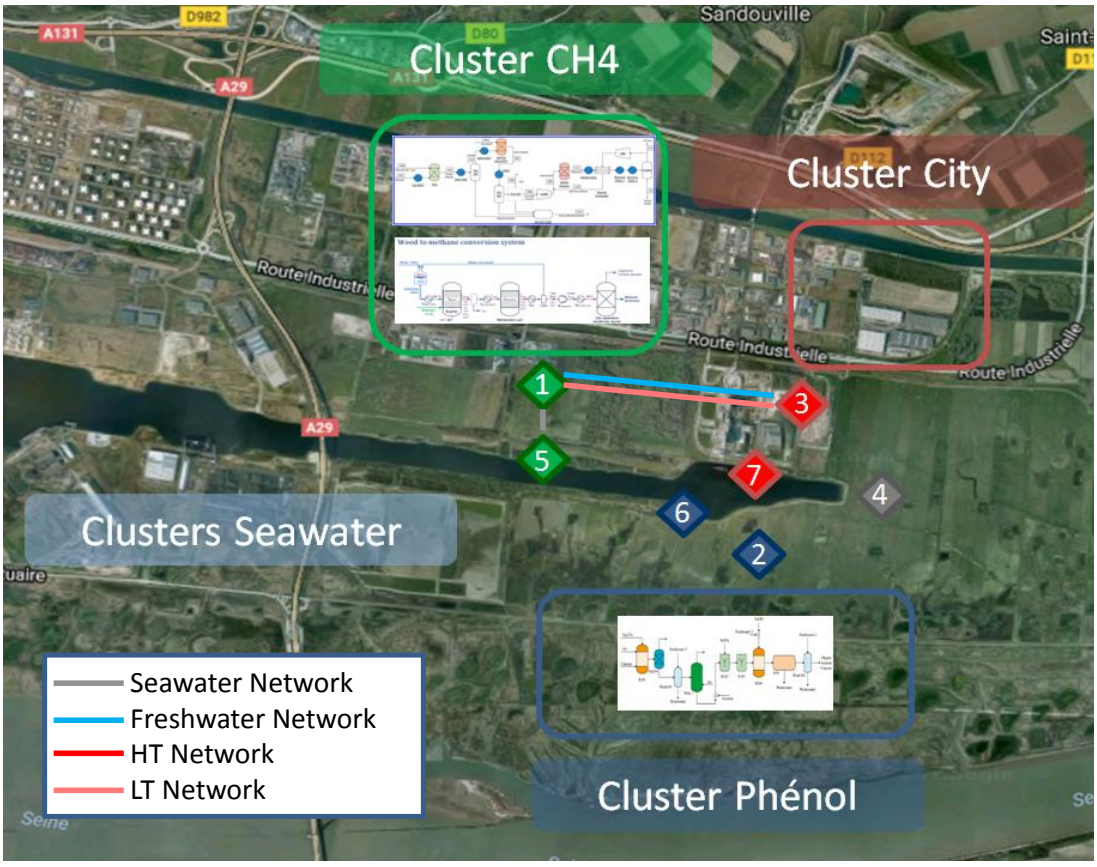

Figure 5.14: Case 2: EIP network when TMD is in the methane cluster

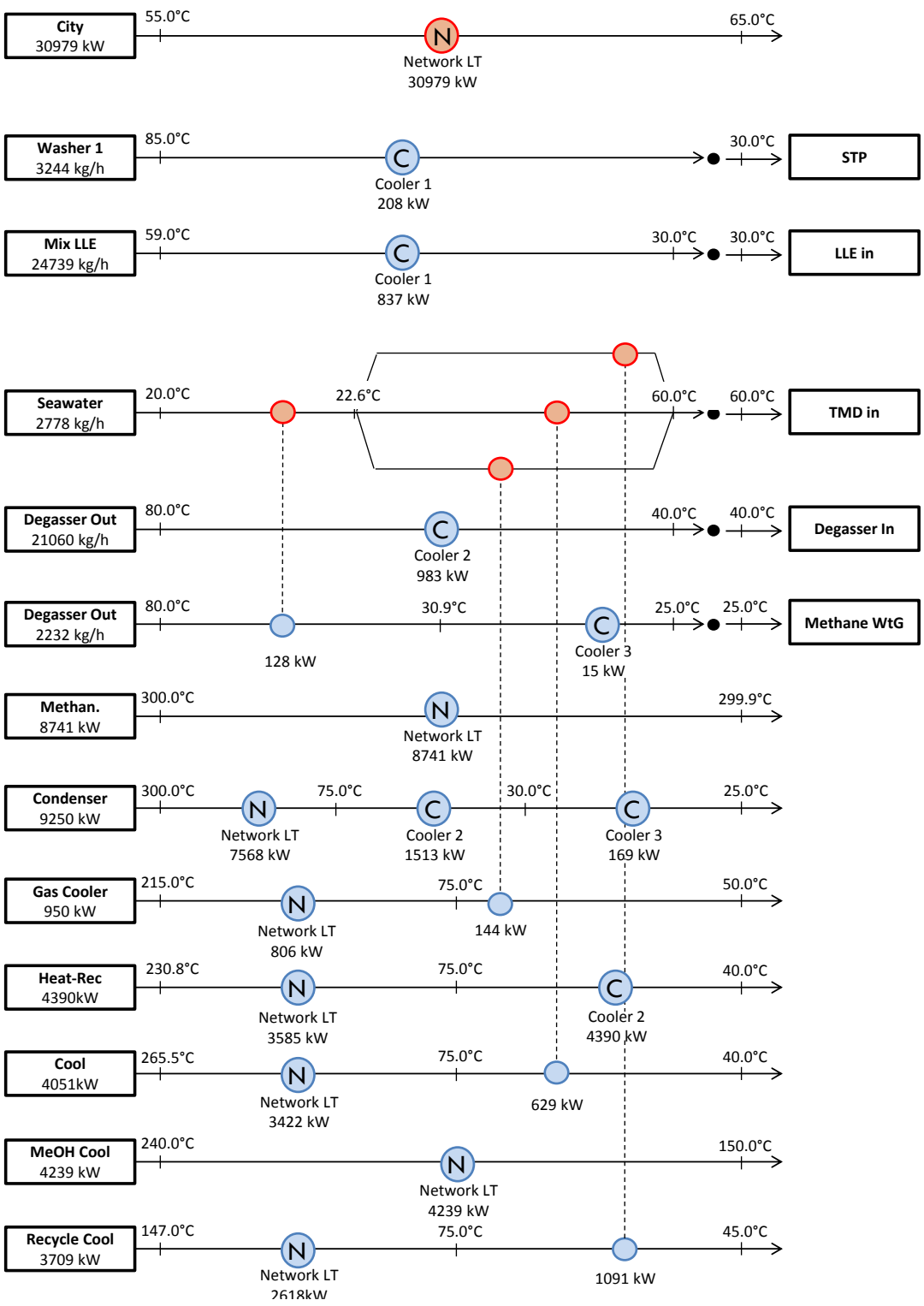

Figure 5.15: Case 2: EIP optimal structure when TMD is in the methane cluster

In Case 3 (Fig.5.17), when the TMD is set in the city cluster, only the LT heat network is used. All the available heat in the methane cluster is sent to the city cluster through the LT network in the same proportion as the previous case. This heat is then consumed via the local urban network because transforming part of this heat through the TMD is not profitable in this case. Indeed, using the TMD would generate operating and capital cost too important to be compensated by selling the produced freshwater.

Similarly to the previous case, the phenol is not connected to the EIP.

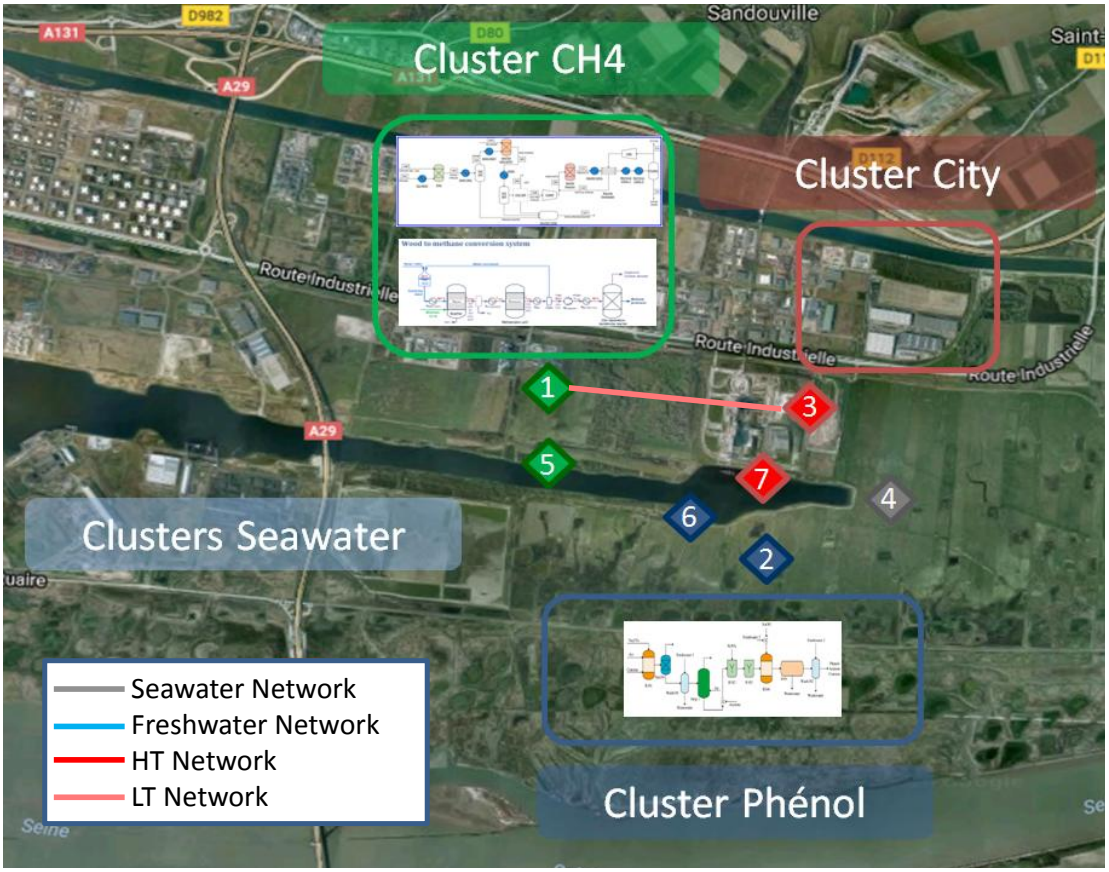

Figure 5.16: Case3: EIP network when TMD is in the city cluster

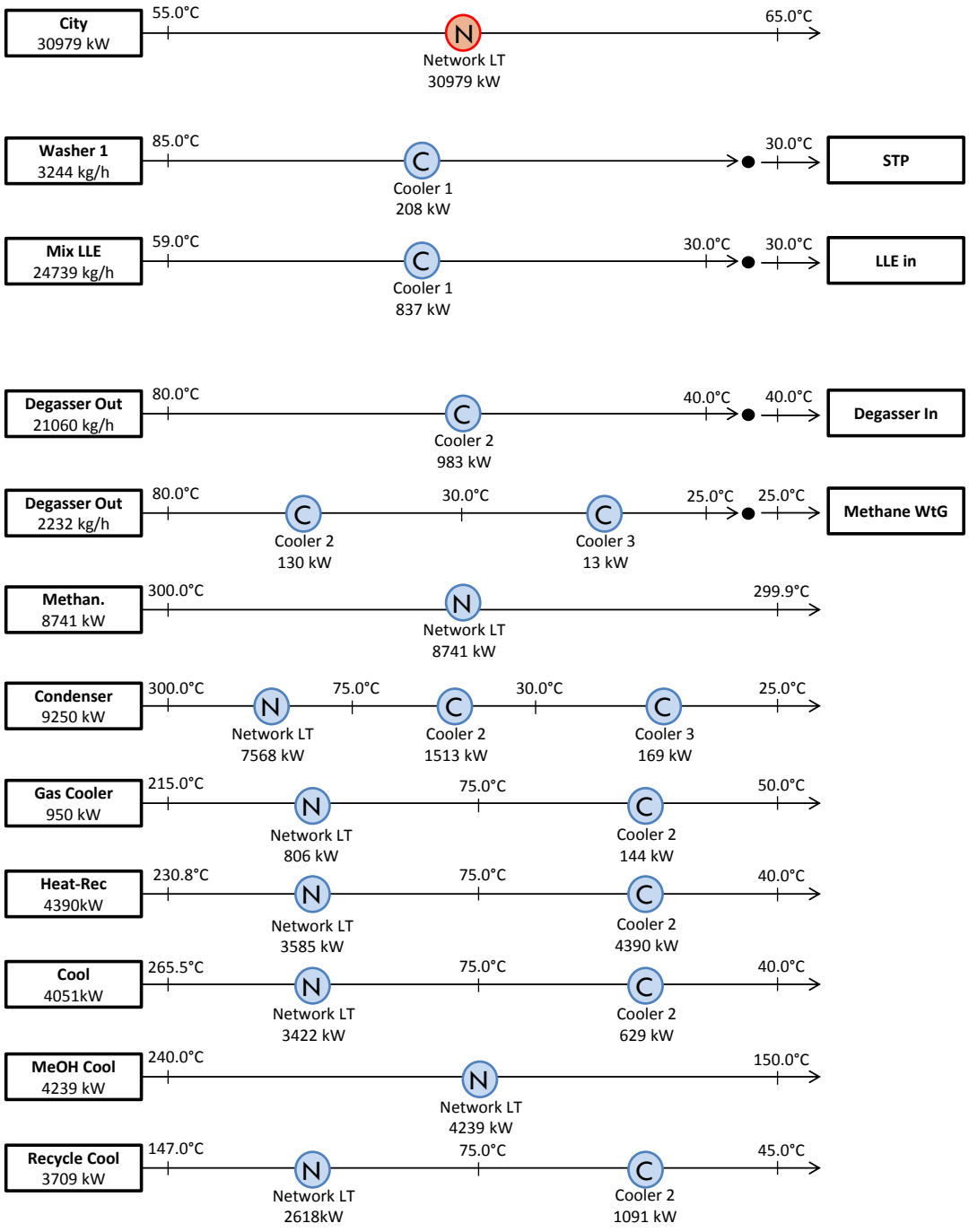

Figure 5.17: Case 3: EIP optimal structure when TMD is in the city cluster

Despite the sharp increase in capital costs, the optimal EIP manages to be profitable in the three cases. The most profitable situation is when the TMD is installed in cluster methane (Table 5.16). In this case, the low-grade heat that cannot be recovered in the two other cases via the LT network, and which is available in relative large quantity, can be transformed locally and transported at a lesser cost as fresh water. However, the relative difference between the best case (Case 2) and the others in terms of total annualized cost is relatively small (between 1 and 3%). This suggests that, in this case of cooperative relationship between industrial sites, the sharing and selling of resources and wastes is profitable.

Note that in case, the selling prices of the freshwater and the heat are null, the EIP structures found for the three cases remain the same. Moreover, the reduction in operating costs is mainly due to the decrease in cooling requirements in the two main industrial clusters. The cooling utility reductions are substantial in all three cases (more than 80% of the operating costs). It may be relevant to study the impact of the nominal cost of certain cooling utility heat streams that are more preeminent in the case (for instance $Cooler1$ and $Cooler2$) to evaluate the robustness of the optimal EIP structure.

5.2.6 Sensitivity analysis

As observed in the previous study, the cooling costs are substantial and drive the solution towards a collaborative EIP. To observe a better trade-off, the methane cluster is optimized again with a new nominal cost for the cold utility $Cooler2$ set at $1€.MWh^{-1}$. In this new structure, the amount of available energy is still quite important. Therefore, it will remain interesting to transfer some of it to the city cluster. To this extent, the nominal cost for the urban network remains fixed at $-10€.MWh^{-1}$. This is because the amount of heat transferred may vary depending on this cost but the connection will always be there.

The objective is to evaluate the city buying price of fresh water ($C^{limit}_{waste\ city}$) and to carry out a sensitivity analysis on it to determine, in the best case found previously (Case 2) when the TMD is placed in the methane cluster, at which price it becomes interesting to use part of the recoverable heat, to transform it into fresh water and to implement a fresh water network.

The new data obtained after the local optimization of the methane cluster in the sequential approach for the EIP design are shown in Table 5.17 and Table 5.18.

	q_h (kW)	T_h^{in} $(^\circ C)$	T_h^{out} $(^\circ C)$
Hot Process Heat Stream			
Deg. Out - Methane WtG	143	80.0	25.0
Methanation	2 289	300.0	299.9
Condenser	9 250	300.0	25.0
Heat-Rec	11 969	563.8	40.0
Cool	4 808	307.7	40.0
MeOH Cool	4 239	240.0	150.0
Recycle Cool	3 709	147.0	45.0
Utility Heat Stream			
Heater 2		320.0	319.9
Heater 3		770.0	769.9
Cooler 2		20.0	20.1
Cooler 3		10.0	10.1

$$htc_h = 1000W.m^{-2}.K^{-1}$$

Table 5.17: New remaining heat streams from the methane cluster

	Flow rate $(kg.h^{-1})$	Comp. in CO (mass fraction)	Comp. in CO_2 (mass fraction)	pH	Temperature $(^\circ C)$
Sink					
Environment		0.000 - 0.000	0.000 - 0.000	5.5 - 8.5	30
Source					
Degasser out	1053	0.000	0.000	7.0	80

Heat capacity $= 4.2kJ.kg^{-1}.K^{-1}$; $htc = 1000W.m^{-2}.K^{-1}$

Table 5.18: Remaining sources and sinks from the methane cluster

Note that part of the water treated by the degasser that was previously recycled to the entry of this unit is now sent to the environment ($1\ 053kg.h^{-1}$). This means that potentially there is fresh water already treated and unused readily available in the methane cluster. And as expected, the overall heat available has increased compared to the previous case because cooling requirements are cheaper. Note that the data from the phenol cluster remain the same as they were before. The buying price ranges from 1 to 15€$.tons^{-1}$. The results are shown in Table 5.19.

When the TMD is set on the methane cluster, there is a trade-off between investing in the desalination technology, transforming the low grade heat into fresh water and transporting it to the city or implementing heat exchangers to discard this heat with a low cost cooling medium. As long as the incentive is too low (Case 2a), when the buying price is lower than a critical value $C^{limit}_{waste\ city} = 4€.tons^{-1}$), it is understandable that the economical solution is to use the cooling utility (Fig.5.18).

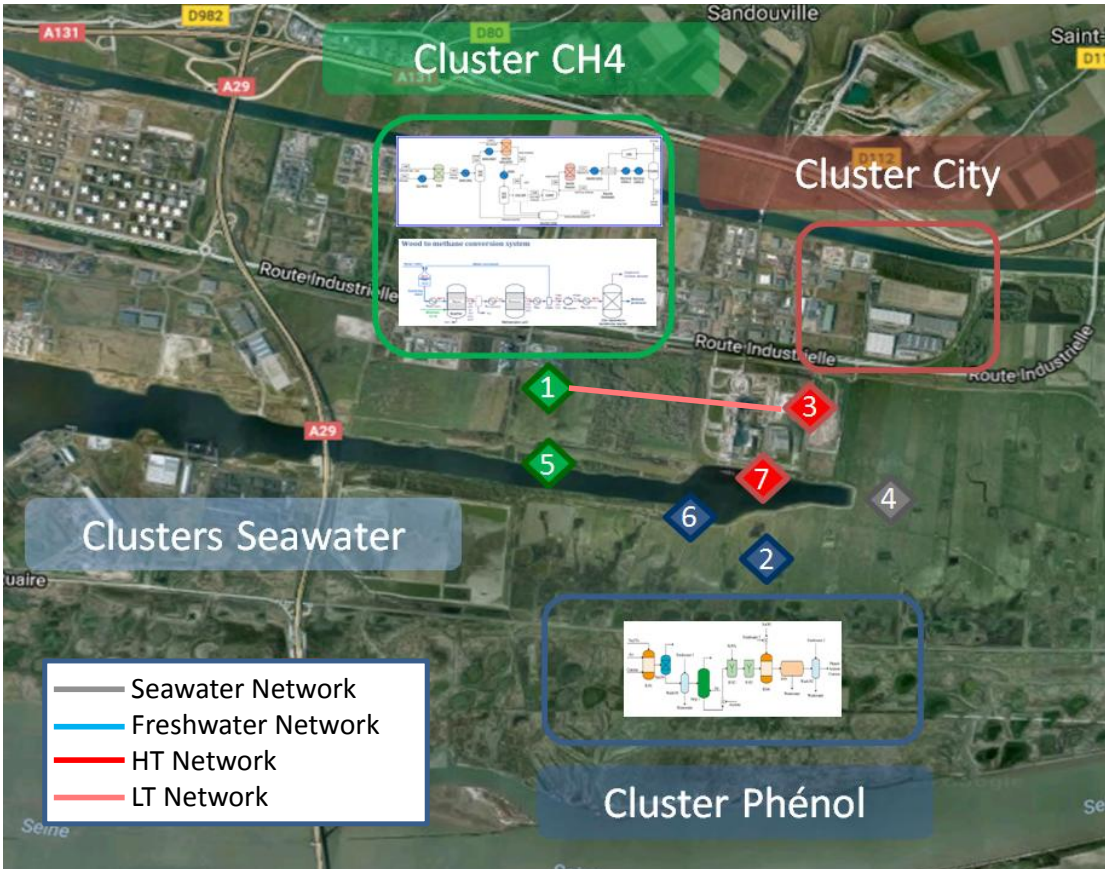

Figure 5.18: EIP network when TMD is in the methane cluster - $C_{city} < 4€.tons^{-1}$

However, when the buying price is high enough (Case 2b), when the buying price is higher than $C^{limit}_{waste\ city} = 4€.tons^{-1}$), the fresh water production with the TMD is maximized. The fresh water produced by the degasser treatment that was previously discharged to the environment is now recovered and transported also to the city cluster. It takes advantage of the opportunity that the fresh water produced by the TMD is profitable enough to justify the investments in the mass network.

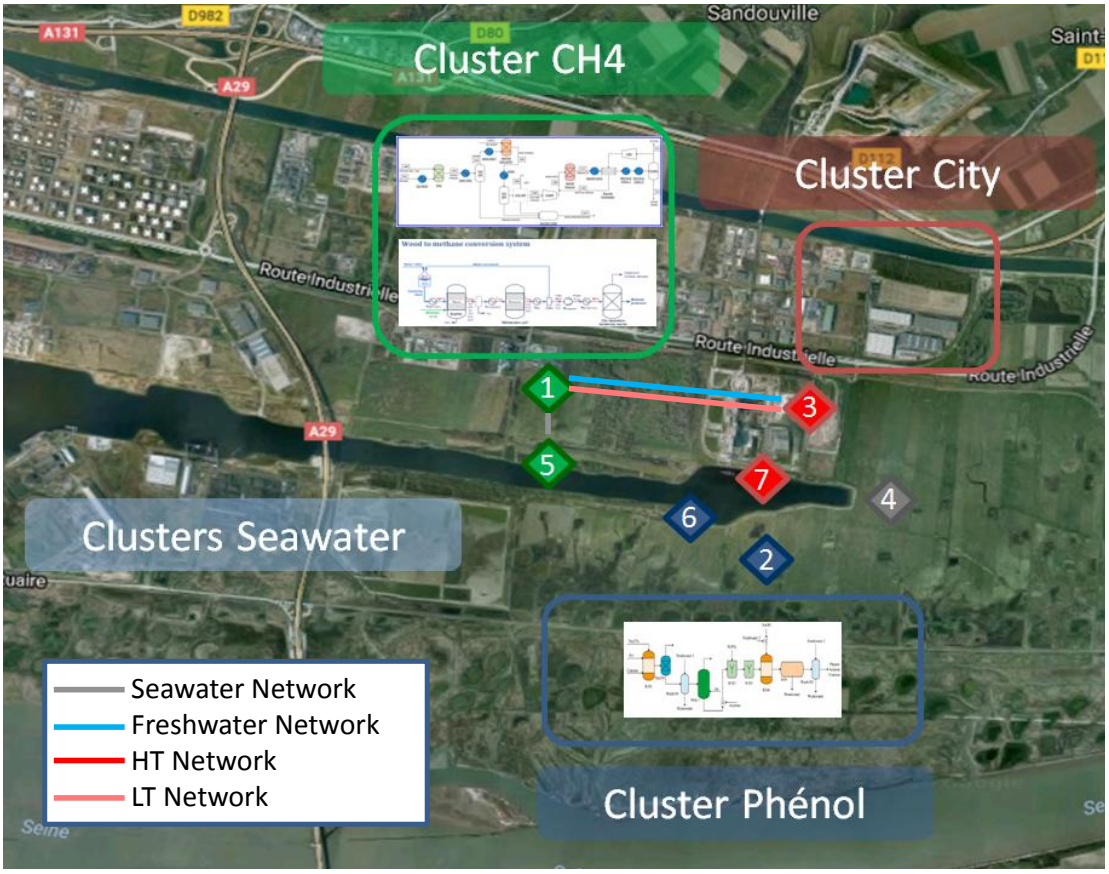

Figure 5.19: EIP network when TMD is in the city cluster - $C_{city} \geq 4€.tons^{-1}$

Case	New Reference	Case 2a	Case 2b
TMD in Cluster cl	None	Methane	
$C^{limit}_{waste\ city}$ ($€.tons^{-1}$)	-	< 4.0	≥ 4.0
$Q_{cooler1}$ (kW)	1 045	1 045	1 045
$Q_{cooler2}$ (kW)	36 287	4 223	3 301
$Q_{cooler3}$ (kW)	182	182	182
L_{TMD} ($kg.h^{-1}$)	0.0	0.0	4712.5
$G_{environment}$ ($kg.h^{-1}$)	1 053.0	1 053.0	0.0
G_{city} ($kg.h^{-1}$)	0.0	0.0	5 765.6
Q_{city} (kW)	0	32 063	32 063
n_{he}	12	18	18
S_{he} (m^2)	696.7	7573.3	7574.0
S^{real}_{he} (m^2)	695.9	7539.5	7827.0
Op. Cost ($k€$)	536	530	669
Cap. Cost ($k€$)	118	1 764	3 085

Table 5.19: Results of the sensitivity analysis of the EIP design to $C^{limit}_{waste\ city}$

Note that both structures are resilient when you are on each side on the critical price. This shows that the optimality of the found structures is stable when the buying price is set in one of the ranges.

This sensitivity analysis on the buying price introduced the notion of bargain between industrial partners. In reality, each company would try to maximize their profits under certain assumptions and constraints. In the proposed methodology, the main assumption is that the partners will share the costs and profits generated by their collaboration in the eco-industrial park. However, the modeling of the decision-making of each individual entity should be taken into account to design a more realistic EIP.

5.3 Conclusion

In this chapter, a new MILP model (M4) has been developed to design an optimal collaborative eco-industrial park. The direct exchanges of matter and heat are possible thanks to the notion of clusters, which regroup industrial sites allowing direct exchange to form the equivalent of a single site. The indirect exchanges between clusters are realized through heat and mass networks. A heat network is modeled like a pair of symmetrical hot and cold utility heat streams. A mass network is modeled as a network of particular treatment units. A global heat or mass balance is realized to ensure that the networks are feasible.

Due to the novelty of the topic, a case study has been built based on data of individual processes found in the literature or simulated. The study has shown how local and global heat and mass network can be designed illustrating the use of the new notions and objects (sites, clusters and intermediate networks) introduced in the M4 model.

The use of the TMD as a heat/mass conversion technology has shown interesting results in the context of the EIP as it can sometimes be more economical to transport matter instead of heat. And it opens a whole new realm of possibilities to integrate other conversion technologies realizing mass/heat, mass/mass or heat/mass transformations that can add new opportunities to further broaden the integration between industrial sites.

Conclusions and Perspectives

Industrial companies are facing new challenges as low-cost energy supplies and high quality natural resources, such as clean water, are getting scarcer and scarcer and environmental and quality regulations are getting more restrictive. Therefore, they are looking for innovative ways to maintain or gain a competitive edge while reducing their consumption of resources and energy and limiting their environmental footprint. In this perspective, the work presented in this thesis proposes three linear models for designing optimal mass and heat recovery networks simultaneously based on economic criteria at a local scale (process). A fourth model is introduced to extend the applicability of the three previous models to a larger scale including several industrial processes in order to design an optimal collaborative eco-industrial park.

Designing an optimal mass allocation and heat exchanger networks at a process scale is complex and involves multiple aspects at once. Therefore, the proposed methodology in this work consists of solving three consecutive MILP problems of increasing difficulty to have a better understanding of the influence of different parameters on the optimal solution. Moreover, once processes are optimized locally, the following step of the methodology is to look at a larger scale for synergy potentials between several industrial companies located on the same territorial area. Thus; applying the M4 model to design an optimal collaborative eco-industrial park.

The first chapter exposes the demographic, economic and environmental factors that make relevant the interest of industrial companies in reducing their consumption of natural resources and limiting their overall environmental footprint while improving their economic performances and complying with more and more stringent environmental regulations.

Afterwards, a literature review is realized on process integration methodologies that aim at reducing heat and mass consumption of industrial process. It shows that two approaches to the mass integration problem are possible: **fixed pollutant load** and **fixed flow rate**. The reference configuration selected to model the mass requirements in this work is the **fixed flow rate formulation** as it interferes less with the process units design and it is more easily applicable to the territorial scale.

Furthermore, this review allows establishing that relatively few methodologies are proposed to address the mass/heat integration problem and take into account these two dimensions simultaneously. Two main types of resolution techniques are used to tackle this problem: graphical and mathematical. Graphical approaches give useful insight on performances that can be expected but they are limited in their application and do not consider economical aspects. Mathematical programming techniques are used to tackle more complex problems in a more systematic way. The deterministic approach is divided into linear (LP/MILP) and non-linear (NLP/MINLP) formulations. Even though non-linear approaches are the most studied optimization techniques because their set up is really easy; however most of them require an initial guess and can be stuck in a local optimum, if they converge at all. Linear formulation requires simplifying assumptions to linearize the equations representing the physics of the problem; however, their resolution is more reliable, which is why the methodology proposed is based on a linear formulation.

Finally, a literature review on the design of eco-industrial parks show that the subject is gaining momentum in the scientific community; however, very few works were realized on this new topic and none consider heat and mass aspects simultaneously.

The second chapter introduces the core of the model in which mass and energy aspects are considered simultaneously.

First, the basic concepts of mass integration are presented. Industrial processes, which are a succession of unitary operations, are decomposed into sources and sinks characterized by several features such as mass flow rate, composition, properties and temperature. Several fresh sources and waste sinks can be included in the problem. The objective of this first MILP model (M1) is to determine the minimum global consumption of fresh resources by reusing directly process sources into process sinks in order to limit the need for external fresh sources and the waste generation.

Then, a second MILP model (M2) is introduced to design an heat-integrated mass allocation network with the minimum operating cost. This model aims at optimizing direct reuse of process sources while considering the heat requirements generated by these streams. The equations of M1 are included in M2 formulation. The result of the first model can be used to limit the search space of the global fresh consumption.

A transshipment model is adapted to calculate the overall heat requirements of the networks. Non-isothermal mixing of mass streams is enabled in order to further reduce the heating and cooling needs of the process, which is characterized by non-linear equations. However, the model formulation is linear thanks to these equations are discretized on a temperature scale which is defined for each specific case which is the main novelty proposed with this model. The temperature levels on the scale define temperatures at which mass streams can be split. Process heat streams representing available heating or cooling in the process can be included in the study. Several utility heat streams can be

considered in the problem at once. Moreover, various constraints that model real on site limitations or obstacles such as forbidden allocation can be considered. The objective function is to minimize the annual operating costs which include costs related to fresh source consumption, waste generation and heating and cooling requirements.

After the evaluation of the potential operating cost savings that can be achieved through the heat integrated mass allocation network, it is necessary to assess the investments that are required to implement such network.

The chapter III focuses on the simultaneous design of the mass allocation and heat exchangers networks. The introduced linear model (M3) adds equations necessary to design each heat exchanger between two given streams in the problem, knowing that a pair of streams can only interact through a unique heat exchanger. The proposed MILP model minimizes the total annualized cost of both networks. It takes into account investments and operating costs over a time period time at a given actualization rate. The model is the main innovation proposed in this thesis.

Mixer and splitter units have been introduced to reduce further the HEN cost. Their characterization with a fixed temperature tend to also limit the search space of the problem; however, a methodology has been developed and a relaxation parameter has been introduced to keep the model linear while targeting promising test values and partially remove this limitation.

Two case studies are presented and used to illustrate the performances of the proposed model compared to results found in the literature which are better or at least similar. Moreover, the influence of some parameters on the optimal solution, such as the number of temperature levels on the scale (ΔT_{step}^{max}) and the number of operating years (N_{op}) is tested. The first case study shows that the influence of the temperature scale on the objective function is relatively limited. The performances regarding the computation time are promising and within an acceptable range. The second case study has illustrated the benefit of using mixer units, applying a selection method previously introduced to achieve a more economical MAHEN design.

At this point, only direct reuse of process sources have been considered and the results of the case studies used to illustrate the methodology show that external fresh sources consumption remain necessary and the waste effluents cannot be recovered completely often because of property constraints. These restrictions can partially or totally be lifted using chemical and physical treatments to modify streams properties so they become alternate fresh sources. In order to further improve the performances.

The fourth chapter introduces in the three models described previously the opportunity of recycling waste effluents using regeneration units which can generate additional opportunities of resources and economic savings. The problem addressed in this chapter

is the economical design of the MAHEN taking advantage of regeneration technologies, whether it is for production or treatment purposes. In this regard, a simple model is introduced to represent any type of regeneration units with the generic parameters.

In the proposed formulation, a regeneration unit is represented as an association between a waste sink (the unit inlet) and a fresh source (the unit outlet). These two objects are governed by similar equations already included in the model with the addition of proportional relationship between the mass flow rate sent to the waste sink and the one provided by the fresh source. The model of such unit is based on objects already introduced in the problem and it includes a linear representation of their operating and capital cost functions. The mass and energy requirements, as well as their costs, can be integrated in the formulation of the previous problem and generate additional opportunities of resources and economic savings.

In this chapter, two types of regeneration unit are tested. The first one, the Thermal Membrane Distillation (TMD) unit, is used as a desalination unit to produce fresh water. It is driven primarily by heat at low temperature which creates a vapor-pressure difference across a porous hydrophobic membrane. The heat requirements of this unit can be provided by heat surplus discarded within the process. The operating and capital costs are related to the output of the TMD unit which allows balancing the savings earned from replacing external fresh sources and recovering heating surplus, and the costs to produce. A detailed study shows how the optimal parameters of the TMD can be found in order to be the most relevant in the design of the MAHEN of phenol production process. The cooling requirements as the cost savings found are quite significant, and makes this technology relevant when trying to improve the cost-effectiveness and overall performances of the process.

The second unit is a treatment unit specific to the phenol process case study used throughout this work. The phenol removal unit is used to comply with accurate environmental standard on phenol contaminated effluents discharged back in the environment. As opposed to the first regeneration unit, the liquid-liquid extraction unit does not use available heat to function. However, by reducing substantially the concentration of phenol, it allows recycling a large amount of wastewater, sufficient enough to lower the need for external fresh resources to zero.

These two case studies illustrate well how regeneration units can be modeled based on data provided by a detailed and accurate model (TMD) or by publications in the literature (LLE). It shows how taking into account heat and mass aspects of the problem simultaneously as well as operating and capital costs can be crucial to design a relevant structure for the MAHEN. The results prove that realistic results can be obtained with this representation of regeneration units.

The last chapter explains how the models developed at the process scale can be extended to consider multiple industrial sites and design an eco-industrial park. The new MILP model (M4) is developed based on the extension of the applicability of the three previous models (M1, M2 and above all M3) to design a collaborative eco-industrial park between multiple industrial sites. The direct exchange of matter and heat is possible thanks to the notion of clusters, which regroup industrial sites allowing direct exchange to form the equivalent of a single site. The indirect exchanges between clusters are realized through heat and mass networks. A territorial layout is set to define in advance the possible paths between clusters; taking into account potential obstacles due to geographical, urban or industrial obstacles. The cost of the intermediate networks related to their length is added to the objective function.

A case study is built based on several processes; each one found in the literature. The study shows how local and global heat and mass networks can be designed illustrating the use of the new notions and objects introduced in this chapter. One of the issues addressed in this case study was to determine the optimal location of a TMD unit to obtain the most economical design of the EIP. The use of the TMD as a converting technology of heat to mass has shown interesting results in the context of the EIP as it can sometimes be more economical to transport matter instead of heat. And it opens a whole new realm of possibilities to integrate other converting technologies realizing mass/heat, mass/mass or heat/mass transformations that can add new opportunities to further broaden the integration between industrial sites.

The models developed in this work are innovative compared to the existing literature regarding process integration and they have been implemented in an operational decision support tool. They manage to find quasi-optimal solution for the mass/heat integration problem from the process scale to the territorial scale. Their potential has been demonstrated on various case studies addressing several types of issues and obtaining realistic solutions. However, a few limitations remain to be addressed concerning either the performances or the applicability of the methodology:

- The computational time of a complex problem may become considerable if a significant number of objects (sources, sinks, heat streams,...) were included in the case perimeter. For instance, in the case of an EIP design, if the simultaneous optimization of clusters and intermediate networks was addressed, obtaining an optimal solution may become take a long time because a lot of variables are generated by the problem. A specific work must be led to either simplify the problem prior to its resolution or finding ways to limit the number of variables while considering the entire problem. For instance, finding the most appropriate levels on the temperature scale can be help reducing significantly the variables number.

- A strong assumption made throughout this work is that processes operate in a continuous mode. If it is true for industries such as oil refineries, lots of industrials processes works in batch. Therefore, adding a time dimension to the MAHEN design model would be necessary but complex and could increase the size of the problem substantially.

- The selection of the characteristics of elements such as treatments units or utilities have a strong influence on the solution. Therefore, as the model remain linear and to avoid increasing the problem size, a methodology must be developed to properly select their features according to criteria that remain to be defined.

- The notion of piping has been introduced in the EIP design. Its modeling and cost evaluation is quite simplistic in the proposed model. These investments can be quite significant even at the process scale. Therefore, a better understanding and representation could be realized and added to the current formulation.

- Non-cooperative behavior between industrial partners in the EIP is the more likely to happen in reality. The decision to participate to the EIP based on costs/benefits analysis of each individual partner can be included in the methodology to have a better understanding of their behavior within the context of the industrial symbiosis. This could help make recommendations to favor the emergence of integrated industrial territory.

Works on simultaneous mass and heat recovery networks design are relatively new, especially the ones addressing the territorial scale. The work presented in this thesis is the first step towards designing a realistic solution. Several new developments may be interesting to work on to reach this objective.

- The resilience of the obtained solution remain to be proved in actual operating conditions. The decision of implementing it will be done after evaluating its behavior while testing several cases of operating failure that could happen in real life, especially regarding eco-industrial parks where each company relies on others. The economic evaluation of these cases may lead to additional constraint on the problem or additional costs (such as equipment redundancy) to be considered in the economic performances of the solution.

- In an industrial process, different types of materials are transported between unitary operations. Each one can be the object of a mass integration study. Similarly, in an eco-industrial park, as shown in the first chapter, different kinds of streams are exchanged between companies. Therefore, it could be interesting to enable the model to treat several mass problems which can be heat integrated simultaneously.

- Along the same idea, the possibility of transforming matter and heat into other types of matter, heat or energy would add new opportunities to make the MAHEN design more efficient in terms of resource recovery.

The aforementioned aspects are particularly important if one of the solutions found applying these methodologies is meant to be implemented in reality; the methodology presented in this thesis can help evaluating the recovery potentials that can be found within one or several processes, and have a relatively accurate idea of the costs and benefits that can be expected from the solution.

Nomenclature

Acronyms

HEN	Heat Exchanger Network
$HIRAN$	Heat Integrated Resource Allocation Network
LP	Linear Programming
$MILP$	Mixed Integer Linear Programming
$MINLP$	Mixed Integer Non Linear Programming
$MAHEN$	Mass Allocation and Heat Exchanger Networks
RAN	Resource Allocation Network
AOC	Annual Operating Cost
CC	Capital Cost
TAC	Total Annualized Cost
$WAHEN$	Water Allocation and Heat Exchanger Networks
WAN	Water Allocation Network

Parameters

C_i^w	Nominal cost for mass flow rate sent to waste sink i ($€.kg^{-1}.s$)
C_j^f	Nominal cost for mass flow rate provided by fresh source j ($€.kg^{-1}.s$)
C_{h_u}	Nominal cost for utility heat stream h_u ($€.kWh^{-1}$)
$C_{h_u}^{cap}$	Nominal fixed cost for a utility heat stream h_u (€)
C_{he}^{cap}	Nominal fixed cost for a heat exchanger (€)
C_S^{cap}	Nominal cost for heat exchange area ($€.m^{-2}$)
$C_{ij,ru}^{fixed}$	Fixed cost for a regeneration unit $ru(i,j)$ (€)
$C_{ij,ru}^{variable}$	Variable part of the fixed cost for a regeneration unit $ru(i,j)$ related to L_{ij}^{ru} ($€.(kg.s^{-1})^{-1}$)
c_{heat}^{net}	Nominal fixed cost of piping for a heat network ($€.m^{-1}$)
c_{mass}^{net}	Nominal fixed cost of piping for a mass network ($€.m^{-1}$)
$C_{ij,ru}^{flow}$	Nominal operating cost for a regeneration unit $ru(i,j)$ related to L_{ij}^{ru} ($€.(kg.s^{-1})^{-1}$)
$C_{ij,ru,k}^{load}$	Nominal operating cost for a regeneration unit $ru(i,j)$ related to $\dot{m}_{ij,k}^{ru}$ ($€.(kg.s^{-1})^{-1}$)
CP_{h_p}	Heat capacity of process heat stream h_p ($kW.K^{-1}$)
cp_h	Specific heat capacity of stream h (mass or heat) (depends on the tem-

	perature) ($kJ.kg^{-1}.K^{-1}$)
cp_j	Specific heat capacity of source j (depends on the temperature) ($kJ.kg^{-1}.K^{-1}$)
cp_{mu}	Specific heat capacity of mass stream provided by mixer unit mu (depends on the temperature) ($kJ.kg^{-1}.K^{-1}$)
cp_{su}	Specific heat capacity of mass stream provided by splitter unit su (depends on the temperature) ($kJ.kg^{-1}.K^{-1}$)
$cp_{j,n}$	Specific heat capacity of source j within the n^{th} temperature interval ($kJ.kg^{-1}.K^{-1}$)
ΔT_{step}^{max}	Maximum temperature interval length for the temperature scale $\{T_n^{'*}\}_{n\in[1,N']}$ ($^\circ C$)
ΔT_{min}	Minimum approach temperature ($^\circ C$)
ΔL_{ru}^{ij}	Relative mass flow rate variation going through a regeneration unit $ru(i,j)$
ΔT_{mu}^{max}	Relative temperature range around the fixed mixer unit temperature ($^\circ C$)
δ_{pn}	Parameter indicating the direction of the path p_n (1 or -1)
d_p	Length of the path p (m)
h_{op}	Operating hours ($h.year^{-1}$)
N_{op}	Number of operating years ($year$)
r_a	Actualization ratio
G_i	Mass flow rate required by sink i ($kg.s^{-1}$)
L_j	Mass flow rate of source j ($kg.s^{-1}$)
L_{h_p}	Mass flow rate of process heat stream h_p ($kg.s^{-1}$)
L_{h_u}	Mass flow rate of utility heat stream h_u ($kg.s^{-1}$)
ϕ_m	Mixing function associated to the m^{th} property in P
$p_{i,m}^{max}$	Maximum allowable value of m^{th} property for sink i
$p_{i,m}^{min}$	Minimum allowable value of m^{th} property for sink i
$p_{j,m}$	Value of m^{th} property for source j
p_m	m^{th} property in P
q_{h_p}	Heat required or provided by process heat stream h_p (kW)
N	Number of temperature intervals on the initial temperature scale $\{T_n^*\}_{n\in[0,N]}$
$N^{'}$	Number of temperature intervals on the final temperature scale $\{T_n^{'*}\}_{n\in[0,N']}$
$N_{i,mu}^{out}$	Index of sink i temperature level for a mass stream from mixer unit mu
$N_{ij,su}^{max}$	Index of maximum temperature level at which a mass stream from splitter unit su associated to source j to sink i exists
$N_{ij,su}^{min}$	Index of minimum temperature level at which a mass stream from splitter unit su associated to source j to sink i exists
$N_{ij,su}^{out}$	Index of sink i temperature level for a mass stream from splitter unit

	su associated to source j
N_{ij}^{max}	Index of maximum temperature level at which a mass stream from source j to sink i exists
N_{ij}^{min}	Index of minimum temperature level at which a mass stream from source j to sink i exists
N_{ij}^{out}	Index of sink i temperature level for a mass stream from source j
$N_{j,su}^{max}$	Index of maximum temperature level at which a mass stream from source j to splitter unit su exists
$N_{j,su}^{min}$	Index of minimum temperature level at which a mass stream from source j to splitter unit su exists
$N_{j,su}^{out}$	Index of splitter unit su temperature level for a mass stream from source j
$N_{i,mu}^{max}$	Index of maximum temperature level at which a mass stream from mixer unit mu to sink i exists
$N_{i,mu}^{min}$	Index of minimum temperature level at which a mass stream from mixer unit mu to sink i exists
$N_{h_p}^{max}$	Index of maximum temperature level at which a process heat stream h_p exists
$N_{h_p}^{min}$	Index of minimum temperature level at which a process heat stream h_p exists
$N_{h_u}^{max}$	Index of maximum temperature level at which an utility heat stream h_u exists
$N_{h_u}^{min}$	Index of minimum temperature level at which an utility heat stream h_u exists
N_{h}^{max}	Index of maximum temperature level at which a stream h (mass or heat) exists
N_{h}^{min}	Index of minimum temperature level at which a stream h (mass or heat) exists
T_i	Temperature of sink i ($^\circ C$)
T_j	Temperature of source j ($^\circ C$)
T_j^f	Temperature of fresh source ($^\circ C$)
T_i^{mu}	Temperature of mixer unit mu associated to sink i ($^\circ C$)
T_i^w	Temperature of waste ($^\circ C$)
T_j^{su}	Temperature of splitter unit su associated to source j($^\circ C$)
$T_{h_p}^{in}$	Inlet temperature of process heat stream h_p ($^\circ C$)
$T_{h_p}^{out}$	Outlet temperature of process heat stream h_p ($^\circ C$)
$T_{h_u}^{in}$	Inlet temperature of utility heat stream h_u ($^\circ C$)
$T_{h_u}^{out}$	Outlet temperature of utility heat stream h_u ($^\circ C$)
$y_{j,k}$	Composition of source j for contaminant k (ppm)

$z_{i,k}^{max}$ Maximum allowable composition of sink i for contaminant k (ppm)

Continuous Variables

L_{ij} Mass flow rate from source j allocated to sink i ($kg.s^{-1}$)

$C_{ij,ru}^{cap}$ Total capital cost for a regeneration unit $ru(i,j)$ (€)

$C_{ij,ru}^{op}$ Total operating cost for a regeneration unit $ru(i,j)$ (€)

CC_{heat}^{net} Total capital cost of heat network $(h_u, \widetilde{h}_u) \in H_{net}$ (€)

CC_{mass}^{net} Total capital cost of mass network $(j,i) \in M_{net}$ (€)

$L_{ij}^{mu/su}$ Mass flow rate from splitter unit su associated to source j allocated to mixer unit mu associated to sink i ($kg.s^{-1}$)

L_{ij}^{mu} Mass flow rate from source j allocated to mixer unit mu associated to sink i ($kg.s^{-1}$)

L_{ij}^{ru} Mass flow rate treated by regeneration unit $ru(i,j)$ ($kg.s^{-1}$)

L_{ij}^{su} Mass flow rate from splitter unit su associated to source j allocated to sink i ($kg.s^{-1}$)

L_{i}^{mu} Mass flow rate from mixer unit i allocated to sink i ($kg.s^{-1}$)

L_{j}^{su} Mass flow rate from source j allocated to splitter unit su ($kg.s^{-1}$)

$\widetilde{L}_{i,n}^{mu}$ Mass flow rate of L_i^{mu} going through the HEN in the n^{th} interval of $\{T_n'^*\}_{n\in[1,N']}$ ($kg.s^{-1}$)

$\widetilde{L}_{ij,n}$ Mass flow rate of L_{ij} going through the HEN in the n^{th} interval of $\{T_n'^*\}_{n\in[1,N']}$ ($kg.s^{-1}$)

$\widetilde{L}_{ij,n}^{su}$ Mass flow rate of L_{ij}^{su} going through the HEN in the n^{th} interval of $\{T_n'^*\}_{n\in[1,N']}$ ($kg.s^{-1}$)

$\widetilde{L}_{j,n}^{su}$ Mass flow rate of L_{j}^{su} going through the HEN in the n^{th} interval of $\{T_n'^*\}_{n\in[1,N']}$ ($kg.s^{-1}$)

$L_{i,n}^{mu}$ Mass flow rate of L_i^{mu} extracted at $T_n'^*$ ($kg.s^{-1}$)

$L_{ij,n}$ Mass flow rate of L_{ij} extracted at $T_n'^*$ ($kg.s^{-1}$)

$L_{ij,n}^{su}$ Mass flow rate of L_{ij}^{su} extracted at $T_n'^*$ ($kg.s^{-1}$)

$L_{j,n}^{su}$ Mass flow rate of L_{j}^{su} extracted at $T_n'^*$ ($kg.s^{-1}$)

$L_{j_{cl}}^{f}$ Total mass flow rate provided by fresh source j in cluster cl ($kg.s^{-1}$)

L_{j}^{f} Total mass flow rate provided by fresh source j ($kg.s^{-1}$)

L_{p}^{net} Mass flow rate going through the path p via mass network $(j,i) \in M_{net}$ ($kg.s^{-1}$)

$G_{i_{cl}}^{w}$ Total mass flow rate sent to waste sink i in cluster cl ($kg.s^{-1}$)

G_{i}^{w} Total mass flow rate sent to waste sink i ($kg.s^{-1}$)

$Q_{cooling}$ Total cooling requirement (kW)

$Q_{heating}$ Total heating requirement (kW)

$\dot{m}_{ij,k}^{ru}$ Mass flow extracted in regeneration unit $ru(i,j)$ for contaminant k ($kg.s^{-1}$)

$N_{binaries}$ Number of binary variables

$N_{constraints}$	Number of constraints
$N_{continuous}$	Number of continuous variables
$N_{non-zeros}$	Number of non-zeros coefficients in the problem matrix
L_{h_1,h_2,n_1}	Mass flow rate going through the entire interval n_1 to transfer the heat load from hot stream h_1 to cold stream h_2 on the hot side $(kg.s^{-1})$
L_{h_1,h_2,n_2}	Mass flow rate going through the entire interval n_1 to transfer the heat load from hot stream h_1 to cold stream h_2 on the cold side $(kg.s^{-1})$
q_{h_1,h_2,n_1}	Heat load transferred from hot stream h_1 to cold stream h_2 in interval n_1 on the hot side (kW)
q_{h_1,h_2,n_2}	Heat load transferred from hot stream h_1 to cold stream h_2 in interval n_2 on the cold side (kW)
q_{h_1,n_1,h_2,n_2}	Heat load transferred from hot stream h_1 in interval n_1 to cold stream h_2 in interval n_2 (kW)
CP_{h_u}	Heat capacity of utility heat stream h_u $(kW.K^{-1})$
$q_{h,n}$	Heat required or provided by stream h (mass or heat) going through the n^{th} temperature interval (kW)
$q_{h_p,n}$	Heat required or provided by process heat stream h_p going through the n^{th} temperature interval (kW)
$q_{h_u,n}$	Heat required or provided by utility heat stream h_u going through the n^{th} temperature interval (kW)
q_{h_u}	Heat required or provided by utility heat stream h_u (kW)
$q_{h_u}^{cl}$	Heat required or provided by utility heat stream h_u in cluster cl (kW)
$q_{i,mu}^{+}$	Excess heat provided to decrease the mixer unit temperature for the stream going from mixer unit mu to sink i(kW)
$q_{i,mu}^{-}$	Shortage of heat required to increase the mixer unit temperature for the stream going from mixer unit mu to sink i(kW)
$q_{i,n}^{mu}$	Heat required or provided by mass stream from mixer unit mu to sink i going through the n^{th} temperature interval (kW)
$q_{ij,n}$	Heat required or provided by mass stream from source j to sink i going through the n^{th} temperature interval (kW)
$q_{ij,n}^{su}$	Heat required or provided by mass stream from splitter unit su associated to source j to sink i going through the n^{th} temperature interval (kW)
$q_{j,n}^{su}$	Heat required or provided by mass stream from source j to splitter unit su going through the n^{th} temperature interval (kW)
q_{mu}^{+}	Excess heat provided to decrease the mixer unit temperature(kW)
q_{mu}^{-}	Shortage of heat required to increase the mixer unit temperature(kW)
q_{n}^{cold}	Total heat provided at the n^{th} temperature interval (kW)
q_{n}^{hot}	Total heat required at the n^{th} temperature interval (kW)

$q_{p_n}^{net}$	Heat going through the path p_n via heat network $(h_u, \widetilde{h}_u) \in H_{net}$ (kW)
$\Delta T_{n_1,n_2}^{LMTD}$	Logarithmic mean temperature difference for temperature interval n_1 and n_2 $(^\circ C)$
htc_h	Heat transfer coefficient for stream h (mass or heat) $(W.m^{-2}.K^{-1})$
R_n	Residual heat entering the n^{th} temperature interval (kW)
S_{h_1,h_2}	Heat exchange area between hot stream h_1 and cold stream h_2 (m^2)
S_{h_1,h_2}^{real}	Real heat exchange area between hot stream h_1 and cold stream h_2 (m^2)
S_{h_1,n_1,h_2,n_2}	Heat exchange area between hot stream h_1 in n_1 and cold stream h_2 in n_2 (m^2)
U_{h_1,h_2}	Global heat transfer coefficient between hot stream h_1 and cold stream h_2 $(W.m^{-2}.K^{-1})$
n_{h_1,h_2}	Number of exchanger between h_1 and h_2, which can be 0 or 1
T_n^*	Temperature level on the initial temperature scale $(^\circ C)$
$T_n'^*$	Temperature level on the final temperature scale built from $\{T_n^*\}_{n\in[1,N]}$ $(^\circ C)$
t_{comp}	Computation time (seconds)
$ru(i,j)$	Regeneration unit defined by a waste sink i and a fresh source j

Binary Variables

$\gamma_{L_{ij}^{mu/su}}$	Binary variable indicating if $L_{ij}^{mu/su} > 0$
$\gamma_{L_{ij}^{mu}}$	Binary variable indicating if $L_{ij}^{mu} > 0$
$\gamma_{L_{ij}^{ru}}$	Binary variable indicating if $L_{ij}^{ru} > 0$
$\gamma_{L_{ij}^{su}}$	Binary variable indicating if $L_{ij}^{su} > 0$
$\gamma_{L_{ij}}$	Binary variable indicating if $L_{ij} > 0$
$\gamma_{L_i^{mu}}$	Binary variable indicating if $L_i^{mu} > 0$
$\gamma_{L_i^{ru}}$	Binary variable indicating if $L_i^{ru} > 0$
$\gamma_{L_j^{su}}$	Binary variable indicating if $L_j^{su} > 0$
$\gamma_{L_p^{net}}$	Binary variable indicating if $L_p^{net} \neq 0$
$\gamma_{L_{i,n}^{mu}}$	Binary variable indicating if $L_{i,n}^{mu} > 0$
$\gamma_{L_{ij,n}^{mu}}$	Binary variable indicating if $L_{ij,n}^{mu} > 0$
$\gamma_{L_{ij,n}^{su}}$	Binary variable indicating if $L_{ij,n}^{su} > 0$
$\gamma_{L_{ij,n}}$	Binary variable indicating if $L_{ij,n} > 0$
$\gamma_{L_{j,n}^{su}}$	Binary variable indicating if $L_{j,n}^{su} > 0$
$\gamma_{q_{h_u}^{cl}}$	Binary variable indicating if $q_{h_u}^{cl} > 0$
$\gamma_{q_{h_u}}$	Binary variable indicating if $q_{h_u} > 0$
$\gamma_{q_{p_n}^{net}}$	Binary variable indicating if $q_{p_n}^{net} \neq 0$
$\gamma_{q_{h_1,h_2,n_1}}$	Binary variable indicating if $q_{h_1,h_2,n_1} > 0$
$\gamma_{q_{h_1,h_2,n_2}}$	Binary variable indicating if $q_{h_1,h_2,n_2} > 0$
α_{h_1,h_2,n_1}	Binary variable indicating the beginning of the heat exchanger h_1 and

	h_2 on the hot side in interval n_1
α_{h_1,h_2,n_2}	Binary variable indicating the beginning of the heat exchanger h_1 and h_2 on the cold side in interval n_2
ω_{h_1,h_2,n_1}	Binary variable indicating the end of the heat exchanger h_1 and h_2 on the hot side in interval n_1
ω_{h_1,h_2,n_2}	Binary variable indicating the end of the heat exchanger h_1 and h_2 on the cold side in interval n_2
δ_{h_1,h_2,n_1}	Binary variable indicating the end of the heat exchanger h_1 and h_2 on the hot side in interval n_1
δ_{h_1,h_2,n_2}	Binary variable indicating the end of the heat exchanger h_1 and h_2 on the cold side in interval n_2

Subscripts and Superscripts

$'_*$	final temperature level
$*$	shifted temperature level
i	Sink index
$cold$	cold
j	Source index
h	Stream (mass or heat) index
h_p	Process heat stream index
h_u	Utility heat stream index
hot	hot
mu	Mixer unit index
su	Splitter unit index
in	inlet
out	outlet
cl	cluster
net	mass or heat network

Sets

I_p	Process Sinks
I_w	Waste Sinks
J_f	Fresh Sources
J_p	Process Sources
MU	Mixer Units
SU	Splitter Units
$MU(i)$	Mixer Units associated to a sink i
$SU(j)$	Splitter Units associated to a source j
MS	Mass Streams
K	Contaminants
P	Properties

H_p	Process Heat Streams
H_u	Utility Heat Streams
H_{hot}	Hot Streams
H_{cold}	Cold Streams
H_{net}	Heat Networks
C	Clusters
N_{nodes}	Set of available nodes n
P_{paths}	Set of possible paths p
P_{paths}^{n}	Set of possible paths p_n including the node n

Bibliography

[1] G. Abi Chahla, A. Zoughaib, C.T. Tran, and R. Farel. Is wood waste only for burning? A methodology for best pathway identification of waste recovery. *Comp. Aided Chem. Eng.*, 38:199–204, 2016.

[2] E. Ahmetović, N. Ibrìc, and Z. Kravanja. Optimal design for heat-integrated water-using and wastewater treatment networks. *App. Eng.*, 135:791–808, 2014.

[3] E. Ahmetović and Z. Kravanja. Simultaneous synthesis of process water and heat exchanger networks. *Energy*, 57:236–250, 2013.

[4] E. Ahmetović and Z. Kravanja. Simultaneous optimization of heat-integrated water networks involving process-to-process streams for heat integration. *App.Therm. Eng.*, 62:302–317, 2014.

[5] S.Y. Alnouri, P. Linke, and M.M. El Halwagi. A synthesis approach for industrial city water reuse networks considering central and distributed treatment systems. *J. Clean.Prod.*, 89:231–250, 2015.

[6] A. Alva-Argaéz, M. Vallianatos and A. Kokossis. A multi-contaminant transshipment model for mass exchange networks and wastewater minimization problems. *Comp. Chem. Eng.*, 23:1439–1453, 1999.

[7] J. Bagajewicz and H. Rodera. Energy savings in the total site heat integration across many plants. *Comp. Chem. Eng.*, 24:1237–1242, 2000.

[8] M. Bagajewicz, H. Rodera, and M. Savelski. Energy efficient water utilization sytems in process plants. *Comput. Chem. Eng.*, 26 (1):59–79, 2002.

[9] S. Bandyopadhyay and G. Sahu. Modified problem table algorithm for energy targeting. *Ind. Eng. Chem. Res.*, 49:11557–11563, 2010.

[10] A. Barbaro and M. J. Bagajewicz. New rigorous one-step milp formulation for heat exchanger network synthesis. *Comp. Chem. Eng.*, 29 (9):1945–1976, 2005.

[11] R. Bayard and R. Gourdon. Traitement biologique des déchets. *Techniques de l'Ingénieur*, j3966, 2007.

[12] S.K. Behera, J.H. Kim, S.Y. Lee, S. Suh, and H.S. Park. Evolution of 'designed' industrial symbiosis networks in the ulsan eco-industrial park: 'research and development into business' as the enabling framework. *J. Cle. Prod.*, 29-30:103–112, 2012.

[13] M. Bogataj and M. Bagajewicz. Synthesis of non-isothermal heat integrated water networks in chemical processes. *Comp. Chem. Eng.*, 32:3130–3142, 2008.

[14] M. Boix, L. Montastruc, C. Azzaro-Pantel, and S. Domenech. Optimization methods applied to the design of eco-industrial parks: a literature review. *J. Clean. Prod.*, 87:303–317, 2015.

[15] M. Boix, L. Montastruc, L. Pibouleau, C. Azzaro-Pantel, and S. Domenech. A multiobjective optimization framework for multicontaminant industrial water network design. *J. Env. Man.*, 92:1802–1808, 2011.

[16] M. Boix, L. Montastruc, L. Pibouleau, C. Azzaro-Pantel, and S. Domenech. Industrial water management by multiobjective optimization: from individual to collective solution through eco-industrial parks. *J. Clean. Prod.*, 22:85–97, 2012.

[17] M. Boix, L. Pibouleau, L. Montastruc, C. Azzaro-Pantel, and S. Domenech. Minimizing water and energy consumptions in water and heat exchange networks. *Appl. Therm. Eng.*, 36:442–455, 2012.

[18] F. Broust, P. Girard, and L. Van de steene. Biocarburants de seconde génération et bioraffinerie. *Techniques de l'ingénieur Innovations en énergie et environnement*, TIB503DUO (re110), 2008.

[19] G. Busca, S. Berardinelli, C. Resini, and L. Arrighi. Technologies for the removal of phenol from fluid streams: A short review of recent developments. *J. Haz. Mat.*, 160:265–288, 2008.

[20] CGEDD, CGEiet, IGF. Les certificats d'économies d'énergie : efficacité énergétique et analyse économique. Technical report, Ministères de l'écologie, du développement durable et de l'énergie; de l'économie, du redressement productif et du numérique; des finances et comptes publics, 2014.

[21] M.R. Chertow. Industrial symbiosis: literature and taxonomy. *Annu. Rev. energy Environ.*, 25:313–337, 2000.

[22] I.M.L. Chew and D.C.Y. Foo. Automated targeting for inter-plant water integration. *Chem. Eng. J.*, 153:23–36, 2009.

[23] I.M.L. Chew, D.C.Y. Foo, and A.S.F. Chiu. Game theory approach to the analysis of inter-plant water integration in an eco-industrial park. *J. Clean. Prod.*, 17:1611–1619, 2009.

[24] I.M.L. Chew, R. Tan, D.K.S. Ng, D.C.Y. Foo, T. Majozi, and J. Gouws. Synthesis of direct and indirect interplant water network. *Ind. Eng. Chem. Res.*, 47:9485–9496, 2009.

[25] I.M.L. Chew, S.L. Thillaivarrna, R.R. Tan, and D.C.Y. Foo. Analysis of inter-plant water integration with indirect integration schemes through game theory approach: Pareto optimal solution with interventions. *Clean. Technol. Environ. Policy*, 13:49–62, 2011.

[26] L.G. Cordova Villegas, N. Mashhadi, M. Chen, D. Mukherjee, K.E. Taylor, and N. Biswas. A short review of techniques for phenol removal from wastewater. *Curr. Pollution Rep.*, 2 (3):157–167, 2016.

[27] S. De-León Almaraz, M. Boix, L. Montastruc, C. Azzaro-Pantel, Z. Liao, and S. Domenech. Design of a water allocation and energy network for multi-contaminant problems using multi-objective optimization. *Proc. Saf. and Env. Prot.*, 16, 2016.

[28] A. De Lucas, P. Canizares, M.A. Rodrigo, and J. Garcia-Gomez. A short review of techniques for phenol removal from wastewater. *Waste Management and the Environment*, 56:161–179, 2002.

[29] V.R. Dhole and B. Linnhoff. Total site targets for fuel co-generation, emissions, and cooling. *Comput. Chem. Eng.*, 17:101–109, 1993.

[30] DOE. International energy outlook 2016. Technical report, U.S. Energy Information Administration, 2016.

[31] H.G. Dong, C.Y. Lin, and C.T. Chang. Simultaneous optimization approach for integrated water-allocation and heat-exchange networks. *Chem. Eng. Sci.*, 63:3664–3678, 2008.

[32] S. Doyle and R. Smith. Targeting water reuse with multiple contaminants. *Proc. Safe Env. Prot.*, 75(3):181–189, 1997.

[33] R.F. Dunn and M.M. El Halwagi. Process integration technology review: background and applications in the chemical process industry. *J. Chem. Technol. Biotechnol.*, 78:1011–1021, 2003.

[34] V.M. Ehlinger, K.J. Gabriel, M.M.B. Noureldin, and M.M. El Halwagi. Process design and integration of shale gas to methanol. *Sust. Chem. Eng.*, 2:30–37, 2014.

[35] EIA. Key world energy statistics. Technical report.

[36] EIA. Energy efficiency market report. Technical report, Directorate of Sustainable Energy Policy and Technology, 2015.

[37] EIA. Energy technology perspectives 2015. Technical report, EIA/OECD, 2015.

[38] EIA. World energy outlook special report: Energy climate and change. Technical report, Directorate of Global Energy Economics, 2015.

[39] M.M. El Halwagi. *Pollution prevention through process integration—Systematic design tools*. Academic Press, CA, USA, 1997.

[40] M.M. El Halwagi. *Process Integration*. Amsterdam, Academic Press/Elsevier, 2006.

[41] M.M. El Halwagi. *Sustainable Design Through Process Integration - Fundamentals and Applications to Industrial Pollution Prevention, Resouce Conservation, and Profitability Enhancement*. Elsevier, 2012.

[42] M.M. El Halwagi, F. Gabriel, and D. Harrel. Rigourous graphical targeting for resource conservation via material recycle/reuse networks. *Ind. Eng. Chem. Res.*, 42:4319–4328, 2003.

[43] M.M. El Halwagi, I. Glasgow, M. Eden, and X. Qin. Propriety integration: componentless design techniques and visualization tools. *AIChE J.*, 50 (8):1854–1869, 2004.

[44] N.A. Elsayed, M.A. Barrufet, and M.M. El Halwagi. Integration of thermal membrane distillation networks with processing facilities. *Ind. Eng. Chem. Res.*, 53 (13):5284–5298, 2014.

[45] A. Farhat, A. Zoughaib, and K. El Khourky. A new methodology combining total site analysis with exergy analysis. *Comp. Chem. Eng.*, 82:216–227, 2015.

[46] X. Feng, J. Bai, H.M. Wang, and X.S. Zheng. Grass-roots design of regeneration recycling water networks. *Comp. Chem. Eng.*, 32:1892–1907, 2008.

[47] D.C.Y. Foo. Flowrate targeting for threshold problems and plant-wide integration for water network synthesis. *J. Environ. Manag.*, 88:253–274, 2008.

[48] S. Frédéric and A. Lugardon. Méthanisation des effluents industriels liquides. *Techniques de l'ingénieur Génie des procédés et protection de l'environnement*, TIB327DUO (j3943)(j3943), 2007.

[49] F. Gabriel and M.M. El Halwagi. Simultaneous synthesis of waste interception and material reuse networks: Problem reformulation for global optimization. *Environmental Progress*, 24:171–180, 2005.

[50] J. George, G. Sahu, and S. Bandyopadhyay. Heat integration in process water networks. *Ind. Eng. Chem. Res.*, 50:3695–3704, 2011.

[51] S. Ghazouani, A. Zoughaib, and S. Le Bourdiec. Methodology for preselecting heat-integrated mass allocation networks likely to be associated with cost efficient hen. *Comp. Aided Chem. Eng.*, 38:109–1144, 2016a.

[52] S. Ghazouani, A. Zoughaib, and S. Le Bourdiec. An milp model for simultaneous mass allocation and heat exchange networks design. *Chem. Eng. Sci.*, In Publication, 2016b.

[53] S. Ghazouani, A. Zoughaib, and S. Pelloux-Prayer. Simultaneous heat integrated resource allocation network targeting for total annual cost considering non-isothermal mixing. *Chem. Eng. Sci.*, 134:385–398, 2015a.

[54] S. Ghazouani, A. Zoughaib, and S. Pelloux-Prayer. Coupled heat and resource allocation network design considering multi-contaminants, properties and non-isothermal mixing. In *Proceedings of ECOS 2015: 28th International Conference on Efficiency, Cost, Optimization, Simulation and Environmental Impact of Energy Systems*, 2015b.

[55] N. Hallale. A new graphical targeting method for water minimization. *Adv. Env. Res.*, 6:377–390, 2002.

[56] H. Haslenda and M.Z. Jamaludin. Industry-to-industry by-products exchange network towards the zero waste in palm oil refining processes. *Resour. Conserv. Recycl.*, 55:713–718, 2011.

[57] A. Hortua, M.M. El Halwagi, D. Ng, and D. Foo. Integrated approach for simultaneous mass and property integration for resource conservation. *ACS Sustain. Chem. Eng.*, 1:29–38, 2013.

[58] Y. Hou, J. Wang, Z. Chen, X. Li, and J. Zhang. Simultaneous integration of water and energy on conceptual methodology for both single- and multi- contaminant problems. *Chem. Eng. Sci.*, 117:436–444, 2014.

[59] C.H. Huang, C.T. Chang, and H.C. Ling. A mathematical programming model for water usage and treatment network design. *Ind. Eng. Chem. Res.*, 38:2666–2679, 1999.

[60] N. Ibrìc, E. Ahmetović, and Z. Kravanja. Two-step mathematical programming synthesis of pinched and threshold heat-integrated water networks. *J. Clean. Prod.*, 77:116–139, 2014.

[61] J. Jezowski, R. Bochenek, and A. Jezowska. Loop breaking in heat exchanger networks by mathematical programming. *Appl. Therm. Eng.*, 21:1429–1448, 2001.

[62] H. Jiang, Y. Fang, Y. Fu, and Q.X. Guo. Studies on the extraction of phenol in wastewater. *J. Haz. Mat.*, 101 (2):179–190, 2003.

[63] L. Jidong, H. Yanling, Z. Xudong, and W. Guodong. Pinch technology reduces wastewater at a paper mill. *Bioinfo. Biomed. Eng.*, pages 2753–2756, 2008.

[64] A. Jiménez-Gutiérrez, J. Lona-Ramírez, J. María Ponce-Ortega, and M.M. El Halwagi. An MINLP model for the simultaneous integration of energy, mass and properties in water networks. *Comp. Chem. Eng.*, 71:52–66, 2014.

[65] S. Karimkashi and M. Amidpour. Total site energy improvement using air-curve concept. *Energy*, 40:329–340, 2012.

[66] R. Karuppiah and I.E. Grossmann. Global optimization for the synthesis of integrated water systems in chemical processes. *Comp. Chem. Eng.*, 30:650–673, 2006.

[67] V. Kazantzi and M.M. El Halwagi. Targeting material reuse via property integration. *Chem. Eng. Prog.*, 101(8):28–37, 2005.

[68] H. Kheireddine, Y. Dadmohammadi, C. Deng, X. Feng, and M.M. El Halwagi. Optimization of direct recycle networks with simultaneous consideration of property mass, and thermal effects. *Ind. Eng. Chem. Res.*, 50:3754–3762, 2011.

[69] J. Klemeš, V. R. Dhole, K. Raissi, S. J. Perry, and L. Puigjaner. Targeting and design methodology for reduction of fuel, power and co2 on total sites. *Appl. Therm. Eng.*, 17 (8-10):993–1003, 1997.

[70] J. Klemes, N. Nenov, P. Kimenov, and M. Mintchev. Heat integration in food industry. *Int. Tech. Energ. Sav.*, 4:9–26, 1999.

[71] J. Klemes, P. Varbanov, and Z. Kravanja. Recent developments in process integration. *Chem. Eng. Res. Des.*, 91:2037–2053, 2013.

[72] A. Koppol, M. Bagajewicz, B. Dericks, and M. Savelski. On zero water discharge solutions in the process industry. *Adv. Env. Res.*, 8:151–171, 2003.

[73] B. Leewongtanawit and J. Kim. Synthesis and optimisation of heat integrated multiple-contaminant water systems. *Chem. Eng. Process*, 47:670–694, 2008.

[74] Z. Liao, G. Rong, J. Wang, and Y. Yang. Systematic optimization of heat-integrated water allocation networks. *Ind. Eng. Chem. Res.*, 50:6713–6727, 2011.

[75] J.S. Lim, Z.A. Manan, H. Hashim, and S.R. Wan Alwi. Optimal multi-site resource allocation and utility planning for integrated rice mill complex. *Ind. Eng. Chem. Res.*, 52:3816–3831, 2013.

[76] B. Linhoff and E. Hindmarsh. The pinch design method for heat exchanger networks. *Chem. Eng. Sci.*, 38:745–763, 1983.

[77] B. Linnhoff and J.R. Flower. Synthesis of heat exchanger networks: I. systematic generation of energy optimal networks. *AIChE J.*, 24 (4):633–642, 1978.

[78] E.M. Lovelady and M.M. El Halwagi. Design and integration of eco-industrial parks for managing water resources. *Energy*, 28:265–272, 2009.

[79] E. Lowe. Creating by-product resource exchanges: strategies for eco-industrial parks. *J. Clean. Prod.*, 5:57–65, 1997.

[80] Z. Manan, S. Tea, and S. Wan Alwi. A new technique for simultaneous water and energy minimisation in process plant. *Chem. Eng. Res. Des.*, 87:1509–1519, 2009.

[81] M. Martínez-Patiño, J.and Picón-Núñez, L. Serra, and V. Verda. Design of water and energy networks using temperature-concentration diagrams. *Energy*, 36:3888–3896, 2011.

[82] M. Martínez-Patiño, J.and Picón-Núñez, L. Serra, and V. Verda. Systematic approach for the synthesis of water and energy networks. *Appl. Therm. Eng.*, 48:458–464, 2012.

[83] S. Mohammadi, A. Kargaria, H. Sanaeepura, K. Abbassiana, A. Najafia, and E. Mofarrah. Phenol removal from industrial wastewaters: a short review. *Desalination and Water Treatment*, 53 (8):1–20, 2014.

[84] R. Moletta. Méthanisation de la biomasse. *Techniques de l'ingénieur Bioprocédés dans les domaines de l'énergie et de l'environnement*, TIB161DUO (bio5100), 2008.

[85] R. Moletta and M. Torrijos. Traitement des effluents de la filière laitière. *Techniques de l'ingénieur Agroalimentaire : risques, sécurité, qualité et environnement*, TIB427DUO (f1501), 1999.

[86] F. Nápoles-Riviera, J. Ponce-Ortega, M.M. El Halwagi, and A. Jimenez-Gutierrez. Global optimization of mass and property integration networks with in-plant property interceptors. *Chem. Eng. Sci.*, 65:4363–4377, 2010.

[87] OECD. Oecd environmental outlook to 2050: The consequences of inaction key facts and figures. Technical report, OECD and the PBL Netherlands Environmental Assessment Agency, 2014.

[88] S.G. Olesen and G.T. Polley. Dealing with plant geography and piping constraints in water network design. *Process Saf. Environ. Prot.*, 74:273–276, 1996.

[89] S.G. Olesen and G.T. Polley. A simple methodology for the design of water networks handling single contaminants. *Process Saf. Environ. Prot.*, 75:420–426, 1997.

[90] P. Onsekizoglu. *Membrane Distillation: Principle, Advances, Limitations and Future Prospects in Food Industry, Distillation - Advances from Modeling to Applications.* Dr. Sina Zereshki (Ed.), InTech, DOI: 10.5772/37625, 2012.

[91] M. Pan, J. Sikorski, J. Akroyd, S. Mosbach, R. Lau, and M. Kraft. Design technologies for eco-industrial parks: From unit operations to processes, plants and industrial networks. *Applied Energy*, 175:305–323, 2016.

[92] S.A. Papoulias and I.E. Grossmann. A structural optimization approach in process synthesis i: utility systems. *Comp. Chem. Eng.*, 7 (6):695–706, 1983.

[93] J.M. Ponce-Ortega, A.C. Hortua, M.M. El Halwagi, and A. Jimenez-Gutierrez. A property-based optimization of direct recycle networks and wastewater treatment processes. *AIChE Journal*, 55:2329–2344, 2009.

[94] J.M. Ponce-Ortega, M. Serna-Gonzalez, and A. Jimenez-Gutierrez. Synthesis of heat exchanger networks with optimal placement of multiple utilities. *Ind. Eng. Chem. Res*, 49 (6):2849–2856, 2010.

[95] PS2E. Eco-parcs industriels : évaluation de l'état de l'art. Technical report, PS2E, 2009.

[96] M.A. Ramos, M. Boix, D. Aussel, L. Montastruc, and S. Domenech. Water integration in eco-industrial parks using a multi-leader-follower approach. *Comp.Chem. Eng.*, 87:190–207, 2016.

[97] H. Rodera and J. Bagajewicz. Targeting procedures for energy savings by heat integration across plants. *AIChE J.*, 45(8):1721–1742, 1999.

[98] H. Rodera and J. Bagajewicz. On the use of heat belts for energy integration across many plants in the total site. *Can. J. Chem. Eng.*, 79(4):633–642, 2001.

[99] E. Rubio-Castro, J.M. Ponce-Ortega, M. Serna-González, and M.M. El Halwagi. Optimal reconfiguration of multi-plant water networks into an eco-industrial park. *Comp. Chem. Eng.*, 44:58–83, 2012.

[100] G. Sahu and S. Bandyopadhyay. Energy optimisation in heat integrated water allocation networks. *Chem. Eng. Sci.*, 69:352–364, 2012.

[101] M. Savelski and M. Bagajewicz. On the optimality conditions of water utilization systems in process plants with single contaminants. *Chem. Eng. Sci.*, 55:5035–5048, 2000.

[102] M. Savelski and M. Bagajewicz. On the necessary conditions of optimality of water utilizations systems in process plants with multiple contaminants. *Chem. Eng. Sci.*, 58:5349–5362, 2003.

[103] L. Savulescu, J. Kim, and R. Smith. Studies on simultaneous energy and water minimisation -part i: Systems with no water re-use. *Chem. Eng. Sci.*, 60:3279–3290, 2005a.

[104] L. Savulescu, J. Kim, and R. Smith. Studies on simultaneous energy and water minimisation -part ii: Systems with maximum re-use of water. *Chem. Eng. Sci.*, 60:3291–3308, 2005b.

[105] L. Savulescu, M. Sorin, and R. Smith. Direct and indirect heat transfer in water network system. *Appl. Therm. Eng.*, 22:981–988, 2002.

[106] L.J. Shiun, H. Hachim, Z.A. Manan, and S.R. Wan Alwi. Optimal design of a rice mill utility system with rice husk logistic network. *Ind. Eng. Chem. Res.*, 51:362–373, 2011.

[107] D. Spriggs, E. Lowe, J. Watz, M.M. El Halwagi, and E.M. Lovelady. Design and development of eco-industrial parks. *AIChE Spring Meeting 2004, New Orleans*, 2004.

[108] N. Takama, T. Kuriyama, K. Shiroko, and T. Umeda. Optimal water allocation in a petroleum refinery. *Comput.Chem.Eng.*, 4:251–258, 1980.

[109] Y. Tan, D.K.S. Ng, M.M. El Halwagi, D.C.Y. Foo, and Y. Samyudia. Floating pinch method utility targeting in heat exchanger network (hen). *Chem. Eng. Res. Des.*, 92:119–126, 2014.

[110] Y. Tan, D.K.S. Ng, M.M. El Halwagi, D.C.Y. Foo, and Y. Samyudia. Heat integrated resource conservation networks without mixing prior to heat exchanger networks. *J. Clean. Prod.*, 2014.

[111] UNESCO. Water for people, water for life - the united nations world water development report. Technical report, UNESCO, 2003.

[112] UNESCO. Water in a changing world - the united nations world water development report 3. Technical report, UNESCO, 2009.

[113] United Nations. World population prospects: The 2015 revision. Technical report, Department of Economic and Social Affairs - Population Division, 2015.

[114] P.S. Varbanov, Z. Fodor, and J.J. Klemes. Total site targeting with process specific minimum temperature difference (dtmin). *Energy*, 44:20e28, 2012.

[115] S. Wan Alwi, A. Ismail, Z. Manan, and Z. Handani. A new graphical approach for simultaneous mass and energy minimisation. *Appl. Therm. Eng.*, 1:1021–1030, 2011.

[116] Y. Wang and R. Smith. A new graphical approach for simultaneous mass and energy minimization. *Chem. Eng. Sci.*, 49(7):981–1006, 1994.

[117] T.F. Yee and I.E. Grossmann. Optimization models for heat integration—ii. heat exchanger network synthesis. *Comput. Chem. Eng.*, 14:1165–1184, 1990.

Résumé

La conception des procédés industriels doit s'adapter à la raréfaction des ressources naturelles à bas prix et au durcissement des réglementations visant à limiter leur impact environnemental. Ainsi, pour améliorer leur rentabilité économique et leur pérennité, leurs effluents doivent être considérés comme des ressources potentielles de matière et d'énergie qui peuvent être valorisées localement ou à un plus grande échelle en les partageant avec d'autres industries voisines en formant un écoparc industriel.

Cette thèse présente une nouvelle approche systémique et systématique pour concevoir des réseaux de valorisation d'énergie et de matière optimisés simultanément. Trois modèles linéaires de complexité croissante ont été développés pour concevoir ces réseaux à l'échelle locale. Le premier modèle (M1) détermine la consommation minimale nécessaire de ressources fraîches. Le second modèle (M2) introduit une nouvelle superstructure permettant l'optimisation simultanée des besoins énergétiques et matière pour atteindre le minimum de coûts de fonctionnement. Le troisième modèle (M3) conçoit les réseaux optimaux d'allocation de matière et d'échangeurs de chaleur simultanément. Sa fonction objective est le coût total annualisé incluant les coûts d'investissement et de fonctionnement.

L'utilisation des unités de régénération est rendu possible dans la structure des trois modèles précédents. Tous les types d'unités peuvent être représentés par un modèle simple avec des paramètres génériques utilisant des objets déjà définis dans la formulation du modèle M3.

Finalement, l'application du modèle M3 est étendue à la conception d'écoparcs industriels grâce à de nouvelles notions (sites, clusters, réseaux intermédiaires de matière et de chaleur), obtenant ainsi un nouveau modèle M4. Ce modèle inclut dans sa fonction objective les coûts d'investissements des réseaux liés à leur topologie.

Des cas d'études issus de la littérature sont utilisés pour valider la pertinence et les performances des modèles présentés.

Mots Clés

Ecologie industrielle; Ecoparc industriel; Intégration matière; Intégration énergétique; Programmation linéaire

Abstract

The design of industrial processes needs to be adapted as cheap natural resources are scarcer and environmental standards are more stringent to limit their environmental footprints. In order to improve their cost-effectiveness as well as their sustainability, industrial effluents must considered as potential heat and mass resources whether they are recycled locally or at a larger scale by sharing them with other industrial companies; thus forming an eco-industrial park (EIP).

This thesis presents a new systemic and systematic approach to design optimal mass allocation and heat exchanger networks simultaneously. Three linear models of incremental complexity have been developed to design optimal recovery networks at a local scale. The first linear model (M1) looks for the necessary minimum fresh resource consumption. The second linear model (M2) presents a new superstructure that allows optimizing mass and heat requirements simultaneously, targeting the minimum annual operating costs. The third linear model (M3) allows designing optimal mass allocation and heat exchanger networks simultaneously. Its objective function is the total annualized cost considering operating and capital costs.

The opportunity to use regeneration units is added to the structure of the three previous models. Any type of these units can be represented by a simple model with the generic parameters based on objects already existing in the previous models formulations.

Finally, the M3 model applicability is extended to the design of collaborative eco-industrial parks with additional concepts (sites, clusters, indirect heat and mass networks) to obtain a new M4 model. In this model, the capital costs related to the topology of the networks are taken into account in the objective function.

The relevance and performances of the proposed models are validated with several case studies taken from the literature.

Keywords

Industrial ecology; Eco-industrial park; Mass integration; Heat integration; MILP